UNIVERSITAT DE
BARCELONA

Exploration of sulfated polysaccharides as antimalarials and as targeting molecules for nanovector-mediated drug delivery to *Plasmodium*-infected cells

Joana Marques

ADVERTIMENT. La consulta d'aquesta tesi queda condicionada a l'acceptació de les següents condicions d'ús: La difusió d'aquesta tesi per mitjà del servei TDX (**www.tdx.cat**) i a través del Dipòsit Digital de la UB (**diposit.ub.edu**) ha estat autoritzada pels titulars dels drets de propietat intel·lectual únicament per a usos privats emmarcats en activitats d'investigació i docència. No s'autoritza la seva reproducció amb finalitats de lucre ni la seva difusió i posada a disposició des d'un lloc aliè al servei TDX ni al Dipòsit Digital de la UB. No s'autoritza la presentació del seu contingut en una finestra o marc aliè a TDX o al Dipòsit Digital de la UB (framing). Aquesta reserva de drets afecta tant al resum de presentació de la tesi com als seus continguts. En la utilització o cita de parts de la tesi és obligat indicar el nom de la persona autora.

ADVERTENCIA. La consulta de esta tesis queda condicionada a la aceptación de las siguientes condiciones de uso: La difusión de esta tesis por medio del servicio TDR (**www.tdx.cat**) y a través del Repositorio Digital de la UB (**diposit.ub.edu**) ha sido autorizada por los titulares de los derechos de propiedad intelectual únicamente para usos privados enmarcados en actividades de investigación y docencia. No se autoriza su reproducción con finalidades de lucro ni su difusión y puesta a disposición desde un sitio ajeno al servicio TDR o al Repositorio Digital de la UB. No se autoriza la presentación de su contenido en una ventana o marco ajeno a TDR o al Repositorio Digital de la UB (framing). Esta reserva de derechos afecta tanto al resumen de presentación de la tesis como a sus contenidos. En la utilización o cita de partes de la tesis es obligado indicar el nombre de la persona autora.

WARNING. On having consulted this thesis you're accepting the following use conditions: Spreading this thesis by the TDX (**www.tdx.cat**) service and by the UB Digital Repository (**diposit.ub.edu**) has been authorized by the titular of the intellectual property rights only for private uses placed in investigation and teaching activities. Reproduction with lucrative aims is not authorized nor its spreading and availability from a site foreign to the TDX service or to the UB Digital Repository. Introducing its content in a window or frame foreign to the TDX service or to the UB Digital Repository is not authorized (framing). Those rights affect to the presentation summary of the thesis as well as to its contents. In the using or citation of parts of the thesis it's obliged to indicate the name of the author.

Exploration of sulfated polysaccharides as antimalarials and as targeting molecules for nanovector-mediated drug delivery to *Plasmodium*-infected cells

Joana Marques

Director: Dr. Xavier Fernàndez Busquets

Tutor: Dr. Maria Antònia Busquets

Doctoral Program - Biotechnology

Universitat de Barcelona, Facultat de Farmàcia

Institut de bioenginyeria de Catalunya

ISGlobal Barcelona Institute for Global Health

Universitat de Barcelona

I dedicate this thesis to my grandmother, the one I missed the most during these years I have been apart, and the one who teaches me, every day, that human strength and love are unlimited.

“If you think you are too small to make a difference, try spending the night with a mosquito.” – African Proverb

TABLE OF CONTENTS

INTRODUCTION **13**

1. **Malaria** 15

    1.1 Epidemiology, clinical manifestations and general concepts 15

    1.2 Pathophysiology 17

        1.2.1 *Plasmodium falciparum* life cycle 17

        1.2.2 Erythrocyte invasion by *P. falciparum* merozoites.................... 21

        1.2.3 *P. falciparum* cytoadhesion & rosetting 23

    1.3 Diagnosis, treatment and prophylaxis 25

2. **Nanotechnology** 27

    2.1 Nanomedicine.. 27

        2.1.1 Role of nanomedicine in malaria treatment 29

    2.2 Liposomes 30

    2.3 Polymers.. 33

    2.4 Nanomedicine-based drug delivery systems as antimalarial vehicles 34

    2.5 Nanoparticles deliver their cargo to pRBCs 35

3. **Sulfated Polysaccharides** 37

    3.1 Sulfated glycosaminoglycans 37

    3.2 Marine polysaccharides.. 40

HYPOTHESIS & OBJECTIVES **43**

RESULTS **47**

1. **Article 1** 51

2. **Article 2** 69

3. **Article 3** 103

4. **Internship Project** 139

5. **Other Results – Article 4** 149

DISCUSSION **165**

CONCLUSIONS **179**

ANNEXES **183**

1. **Review** 187

2. **Patent** 205

3. **Report by the Director** 209

REFERENCES **215**

ACKNOWLEDGEMENTS **239**

LIST OF ABBREVIATIONS

ACTs	Artemisinin-based combination therapies
CHOL	Cholesterol
CSA	Chondroitin sulfate A
DBL	Duffy binding-like
DOPC	1,2-dioleoyl-sn-glycero-3-phosphatidylethanolcholine
DAPI	4,6-diamino-2-phenylindole
DOTAP	1,2-dioleoyl-3-trimethylammonium-propane, 18:1
FACS	Fluorescence-assisted cell sorting
FITC	Fluorescein
FucCS	Fucosylated chondroitin sulfate
GAG	Glycosaminoglycan
HS	Heparan sulfate
IV	Intravenous
LPs	Liposomes
MSP	Merozoite surface protein
NPPs	New permeability pathways
PAA	Poly(amidoamine)
PFA	Paraformaldehyde
PfEMP1	*Plasmodium falciparum* erythrocyte membrane protein 1
PHZ	Phenylhydrazine
PQ	Primaquine
pRBC	*Plasmodium*-infected red blood cell
PV	Parasitophorous vacuole
PVM	Parasitophorous vacuole membrane

LIST OF ABBREVIATIONS

RBC	Red blood cell
RT	Room temperature
SERA	Serine repeat antigen
SUV	Small unilamellar vesicle
TVN	Tubulovesicular network
WHO	World Health Organization

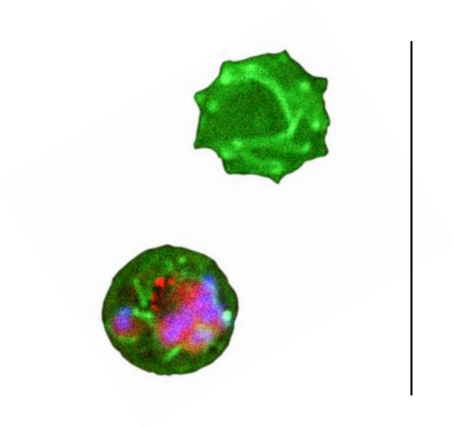

INTRODUCTION

INTRODUCTION

1. MALARIA

1.1. Epidemiology, clinical manifestations and general concepts

Malaria is an acute and/or chronic infection caused by protists of the genus *Plasmodium.* Parasites are transmitted from one human to another by female *Anopheles* mosquitoes. Five species of the parasite infect humans: *P. falciparum*, *P. vivax*, *P. ovale*, *P. malariae*, and *P. knowlesi*. During our recent evolution, malaria's influence has probably been greater than that of any other infectious agent in terms of global health impact[1].

Infectious diseases are prevalent in the developing world and are one of its major sources of morbidity and mortality[2]. According to the latest estimates, released in December 2014, there were about 198 million cases of malaria in 2013 and an estimated 584,000 deaths, most of them among children living in Africa, where a child dies every minute from the disease[3]. In regions presenting high transmission, children under the age of 5 years old and pregnant women expecting their first child are the most vulnerable. In regions of low transmission, all ages are at risk due mainly to low immunity. Finally, non-immune travelers visiting endemic areas are also a vulnerable group[4].

Nowadays, *P. vivax* and *P. falciparum* are the most commonly encountered malaria parasites. *P. vivax* is still found sporadically in some temperate regions, where it used to be widely prevalent. It remains, however, very common throughout much of the tropics and subtropics. Due to temperature limitations on its transmission, *P. falciparum* is usually present only in tropical, subtropical, and warm temperate regions. Today, *P. falciparum* remains extensively prevalent in the tropics[1], including much of Sub-Saharan Africa, Asia, and the Americas. Malaria is endemic in over 90 countries in which approximately 2400 million people live, corresponding to 40% of the world's population. Because transmission intensity varies geographically, maps that describe this variation are necessary to identify populations at different levels of risk, to compare and interpret malaria interventions conducted in different places, and to evaluate objectively the options for disease control[5] (**Figure 1**).

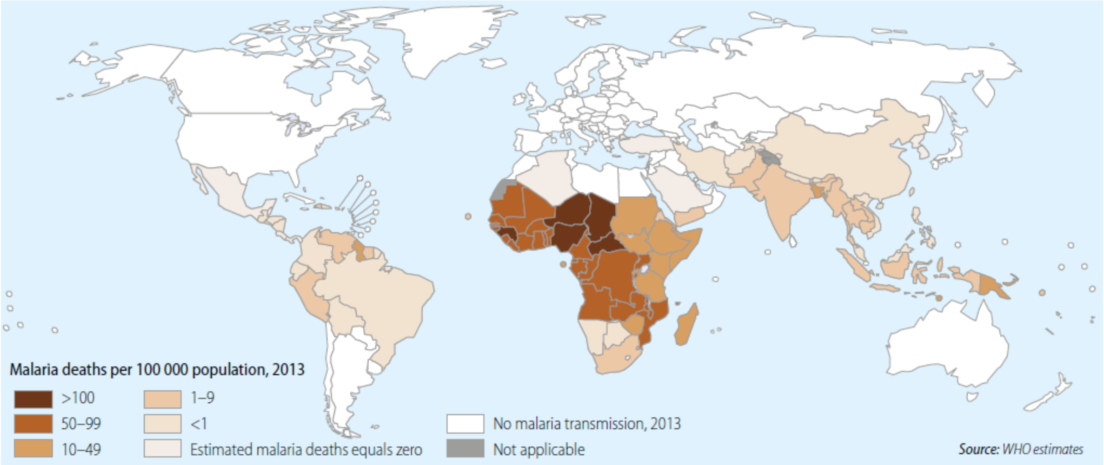
Malaria deaths per 100 000 population, 2013
>100
50–99
10–49
1–9
<1
Estimated malaria deaths equals zero
No malaria transmission, 2013
Not applicable

Source: *WHO estimates*

Figure 1. Estimated malaria deaths per 100,000 population, World Malaria Report 2014[3].

Generally, 10 to 15 days after the infective mosquito bite, first symptoms appear – fever, headache, chills and vomiting. If not treated within 24 hours, *P. falciparum* malaria can progress to severe illness often leading to death. Children with severe malaria frequently develop severe anemia, respiratory distress related to metabolic acidosis, and/or cerebral malaria[6]. In adults, multi-organ failure is also frequent. In malaria endemic areas, asymptomatic infections might also occur due to the development of partial immunity in some cases. Infection in pregnant women can cause spontaneous abortion, premature delivery, stillbirth, severe maternal anemia, low birth-weight, and neonatal death[7].

P. vivax and *P. ovale* may cause clinical relapses weeks to months after the first infection, even if the patient has left the malarious area. These new episodes arise from dormant liver forms known as hypnozoites. Although *P. malariae* and *P. falciparum* have no latent forms, they can remain asymptomatically in the blood for decades[8].

There are two major forms of acquired immunity to malaria: reduced susceptibility to clinical disease developed with age and exposure, and faster clearance of parasitemia which is acquired later in life and lasts longer[4].

1.2. Pathophysiology

1.2.1 *P. falciparum* life cycle

Malaria infection starts when a parasitized female *Anopheles* mosquito inoculates during a blood meal sporozoites of the malaria parasite, the protist *Plasmodium spp.*, which migrate through the skin into the circulation and then to the liver. In a few minutes sporozoites invade hepatocytes, where they will develop into merozoites[9] that enter the circulation to invade red blood cells (RBCs)[10], where they replicate asexually to produce daughter cells that invade new erythrocytes to perpetuate the blood-stage cycle. For *P. falciparum*, the intraerythrocytic parasite grows and divides for 48 hours from ring stages into a schizont stage containing up to 30 daughter merozoites (**Figure 2**).

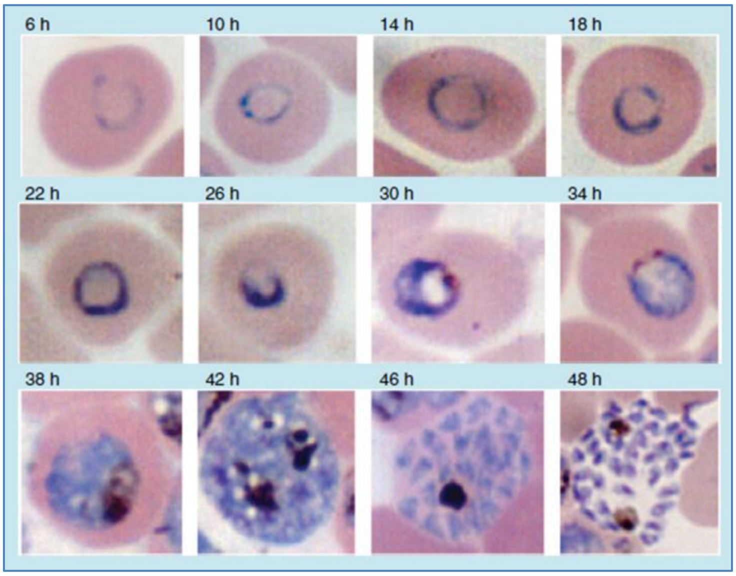

Figure 2. Intraerythrocytic development of *P. falciparum* in the human host. Ring stages are observed between 6 and 18 hours (first row). Trophozoites are present from 22 to 34 hours post-invasion (second row). Schizonts develop from 38 to 48 hours after invasion, and merozoites appear at 48 hours (third row)[11].

Some parasites eventually differentiate into sexual stages, female or male gametocytes that are ingested by a mosquito from peripheral blood, and reach the insects' midgut where micro- and macrogametocytes develop into male and female gametes. Following fertilization the zygote differentiates into a motile ookinete that moves through the midgut epithelium of the mosquito host and forms an oocyst from which sporozoites are released and migrate to the salivary glands to restart the cycle at the next bite[11] (**Figure 3**).

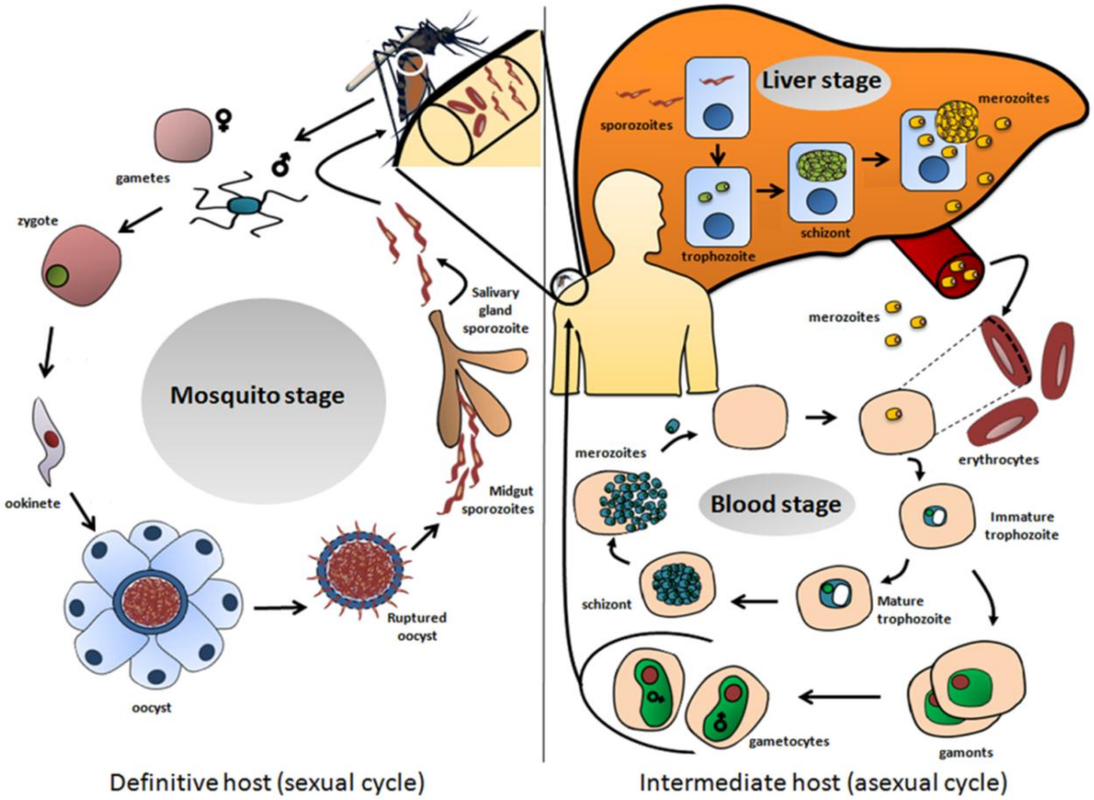
♀
gametes
♂
zygote
Mosquito stage
ookinete
oocyst
Ruptured oocyst
Midgut sporozoites
Salivary gland sporozoite
Liver stage
sporozoites
trophozoite
schizont
merozoites
merozoites
erythrocytes
Immature trophozoite
Blood stage
merozoites
schizont
Mature trophozoite
gametocytes
gamonts
Definitive host (sexual cycle)
Intermediate host (asexual cycle)

Figure 3. The life cycle of *Plasmodium* unfolds in two steps: an asexual stage that occurs in human liver and red blood cells (represented in the right side of the image) and a sexual stage in the vector, the female *Anopheles* mosquito (described in the left side of the picture)[12].

Asexual blood-stages are responsible for all symptoms and pathologies of malaria, and therefore resident parasites inside *Plasmodium*-infected RBCs (pRBCs) are the main target for current chemotherapeutic approaches[13]. As there can be several hundred billion pRBCs in the bloodstream of a malarious person it is nearly impossible to clear infections with single-dose administrations. Multiple doses are required instead and this continuous exposure to drugs increases the likelihood for resistance to develop, which will rapidly decrease treatment efficacy.

This fact is prompting research oriented to target bottlenecks in the parasite life cycle, i.e. the pathogen population consisting of a few individuals in certain transmission stages from the human host to the insect and vice versa[14-16], which will reduce the probability of resistance emergence[17]. The first bottleneck (**Figure 4**) is represented by sporozoites, of which a few thousands can be found inside the salivary glands of *Anopheles*, although only approximately 100 will be transferred to the human host when a mosquito bites. This figure is several orders of magnitude lower than the number of parasites found in an active blood-stage infection, but given the low *in vitro* invasion rates of hepatocytes by sporozoites, rarely above 4% and often below 1%[8], targeting the liver stage will be difficult. The short time that free sporozoites remain in the circulation is also a serious obstacle to target them before reaching the liver. The second bottleneck occurs during sexual development, when ca. 0.2–1% of the intraerythrocytic parasites may develop into gametocytes per round of schizogony. Although this still leaves an estimated 10^8–10^9 parasites to be cleared from the blood circulation, gametocyte targeting can offer interesting advantages, such as an ease of drug exposure[16].

Nevertheless, the largely untapped resource in antimalarial interventions is targeting *Plasmodium* stages in the mosquito itself, in what can be the first medicine designed to cure an insect with the highest prize in mind of, simultaneously, preventing new infections. Although the innate immune system of mosquitoes is capable of completely clearing a malaria infection[18], it is far from the sophisticated arsenal providing long-term protection in mammalian adaptive immunity. This might result in parasite stages with reduced defenses because they only need to survive for a few weeks inside the insect facing an immune surveillance not as demanding as in the human host. Drugs targeting early *Anopheles* stages must kill only ca. 5000 parasites to free a mosquito from *Plasmodium* infection[19], and the absolute low corresponds to oocysts, of which there are only 2–5 in a single insect[16] and which are around for over a week.

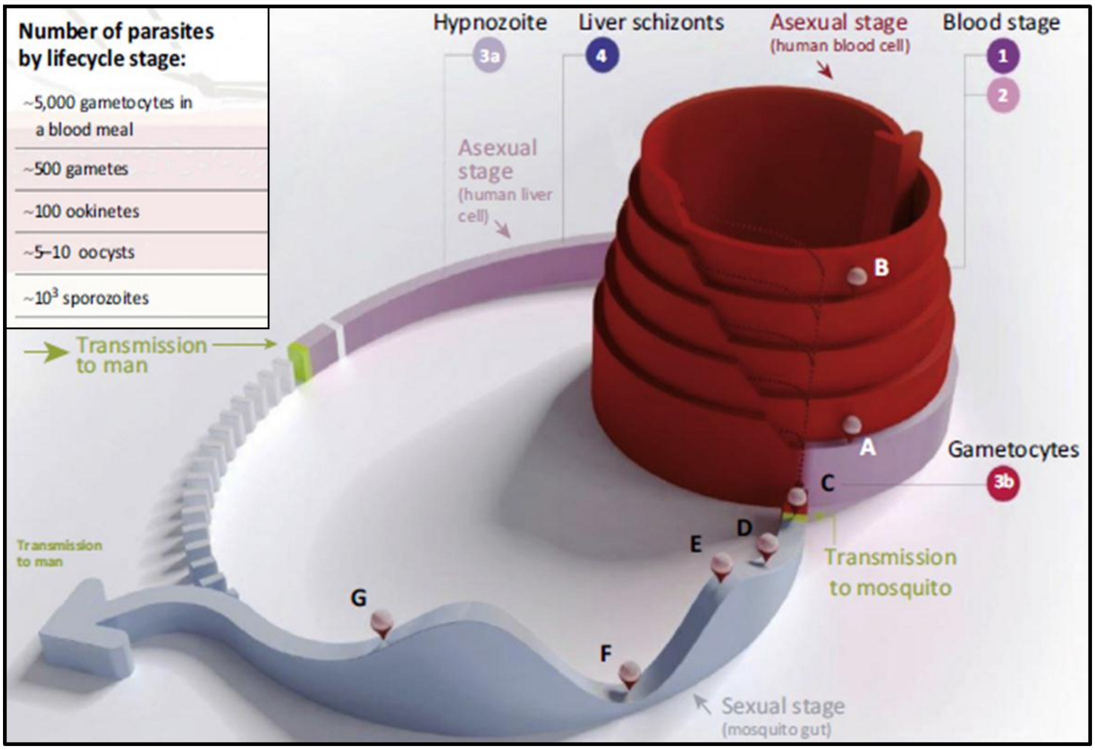
Number of parasites by lifecycle stage:
~5,000 gametocytes in a blood meal
~500 gametes
~100 ookinetes
~5-10 oocysts
~10³ sporozoites
Hypnozoite
3a
Liver schizonts
4
Asexual stage
(human blood cell)
Blood stage
1
2
Asexual stage
(human liver cell)
B
A
Gametocytes
3b
C
D
E
Transmission to man
Transmission to man
Transmission to mosquito
G
F
Sexual stage
(mosquito gut)

Figure 4. Parasite bottlenecks along the *Plasmodium* life cycle. In hepatocytes the parasite develops into schizonts (A) that will multiply and invade RBCs. pRBCs (B) are the most abundant forms and can be present in the bloodstream of an infected person up to 10^{12} parasites per individual. Some blood-stage parasites may develop into gametocytes (C) that are ingested by the mosquito vector. In the gut of the *Anopheles* these gametocytes become male and female gametes (D) that fertilize into an ookinete (E). Finally, the zygote grows into an oocyst (F) capable of producing sporozoites (G) that will migrate to the mosquito salivary glands. Adapted by MMV[20] from Burrows, J. *et al.*[21].

Blocking transmission implies different approaches such as the elimination of the vector mosquitoes, prevention of their bite through the use of insecticides and repellents, and killing *Plasmodium* during its development in *Anopheles*[22]. To reduce the global burden of malaria and achieve the long-term goal of malaria elimination, we must look beyond the blood-stage and pursue molecules able to eliminate all forms of the parasite, leading to the radical cure.

1.2.2. Erythrocyte invasion by *P. falciparum* merozoites

RBCs invasion by *P. falciparum* merozoites is a crucial step on the survival of the parasite. Several models have been proposed for this relevant process consisting of 5 major steps: initial contact, reorientation, commitment to invasion, tight-junction formation, and invasion (**Figure 5**)[10].

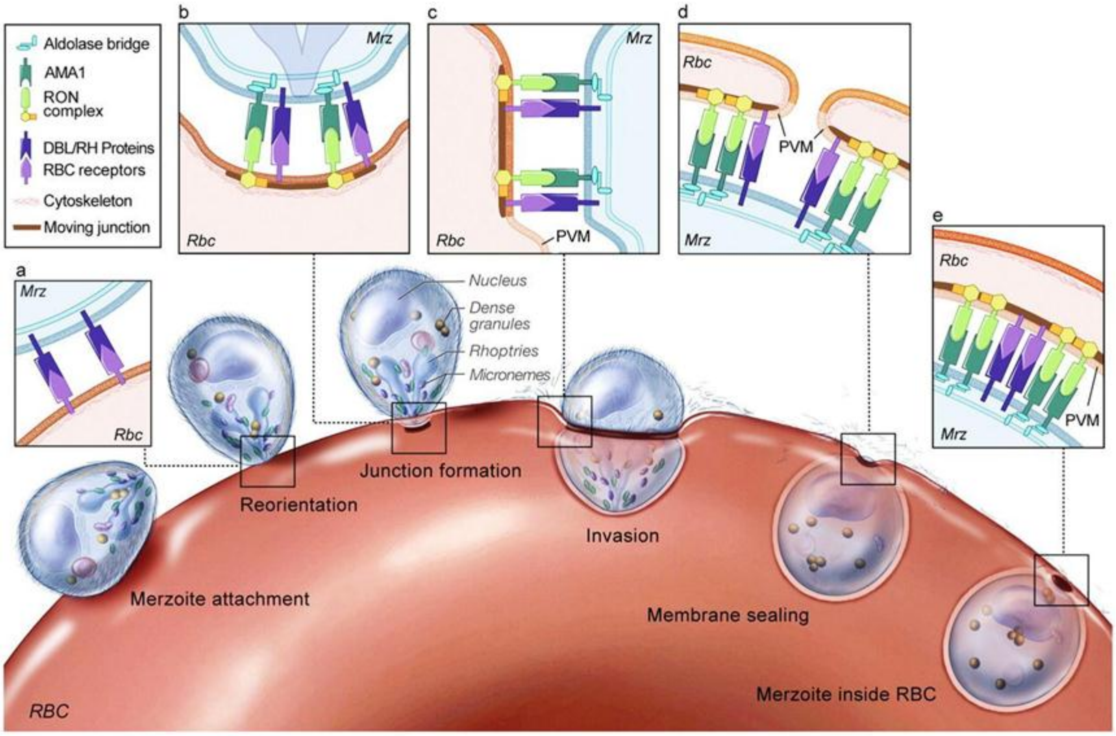
Aldolase bridge
AMA1
RON complex
DBL/RH Proteins
RBC receptors
Cytoskeleton
Moving junction
a
b
c
d
e
Mrz
Rbc
PVM
Nucleus
Dense granules
Rhoptries
Micronemes
Reorientation
Junction formation
Invasion
Merzoite attachment
Membrane sealing
Merzoite inside RBC
RBC

Figure 5. Schematic model of the complex series of events involved in *P. falciparum* merozoite (Mrz) invasion. The first step corresponds to the attachment of a *P. falciparum* merozoite to the RBC through interactions that are thought to be mediated by the ligands on the merozoite surface. Following attachment, a rapid reorientation takes place (a), and the parasite ligand families Duffy binding-like (DBL) and reticulocyte homology (RH) lead to a closer association between parasite and RBC. At this point, a junction between merozoite and target cell is formed (b) through the interaction of various proteins and receptors such as members of the rhoptry neck (RON) family and the apical membrane antigen 1 (AMA1). Thereafter, the actin-myosin motor allows the entry of the parasite inside the cell during the invasion step (c). Finally, the RBC membrane seals (d) and the invasion process is completed (e). Adapted from Srinivasan, P. *et al.*[23].

Because this complex process is essential for malaria pathogenesis, the parasite has evolved an extensive molecular machinery to ensure invasion through multiple pathways[24-26]. The merozoite is well adapted for erythrocytes invasion[27], it possesses the typical structure from members of the Apicomplexa phylum including an apical end, and with secretory organelles (micronemes, rhoptries, and dense granules)[28]. Both the morphology and kinetics of the invasion steps are remarkably conserved across evolutionary divergent *Plasmodium* species[29,30]. The most accepted model postulates that merozoites bind to erythrocyte surfaces in a reversible manner through numerous low affinity interactions between the parasite-expressed merozoite surface proteins (MSPs) and RBC surface proteins (such as Band 3) or heparin-like glycosaminoglycans (GAGs)[31-33]. Hence *P. falciparum* uses heparan sulfate as the receptor for initial binding of sporozoites to hepatocytes[34] and merozoites to host RBCs[31]. MSP1 is the largest and most abundant protein present in the merozoite surface coat and, even though its exact role remains unclear, it has been suggested as the main invasion blocking target of heparin[31,35].

Soon after invasion and once inside the host RBC, the primary amino acid nutrient source for the developing parasite is hemoglobin, which is degraded in the food vacuole. Merozoites and early ring stages are deprived of hemoglobin-derived amino acids for several hours; however organelle degradation by autophagy likely provides these parasite stages with some nutrient.

An accurate understanding of this stepwise mechanism is essential because merozoite proteins are top vaccine candidates[36] and targeting invasion stages may be an efficient approach in antimalarial drug development[37,38]. Of all merozoite proteins involved in this process, some are shed during invasion (e.g., N-terminal MSP1, MSP7, MSP3, SERA4, and SERA5), which suggests their engagement in initial invasion events; others are degraded rapidly after invasion (such as MSP2), implying that they might have a role on invasion but do not function in intraerythrocytic development. Finally, other proteins (e.g. MSP1-19) are internalized and remain present indicating a possible role in intraerythrocytic development of parasites[39].

1.2.3. *P. falciparum* cytoadhesion & rosetting

In severe malaria there are two events that contribute to the virulent activity of *P. falciparum*: sequestration of pRBCs in the microvascular endothelium of different tissues and organs, and the formation of small clusters between RBCs and pRBCs known as rosettes[40] (**Figure 6**). Multiple receptors, including both proteins and carbohydrates, are known to be involved in this process which is thought to play a major role in the fatal outcome of severe malaria[41] (**Figure 7**).

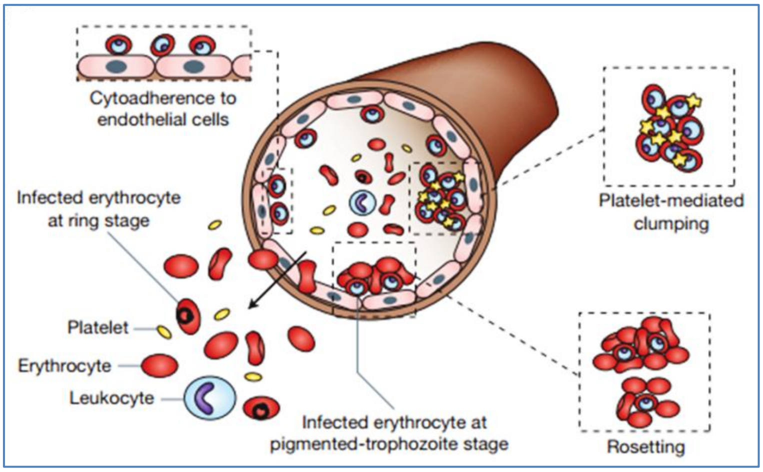

Cytoadherence to endothelial cells
Infected erythrocyte at ring stage
Platelet
Erythrocyte
Leukocyte
Infected erythrocyte at pigmented-trophozoite stage
Platelet-mediated clumping
Rosetting

Figure 6. Schematic representation of the different adhesion processes of *P. falciparum* to human cells. Adapted from Rowe, A. *et al.*[42].

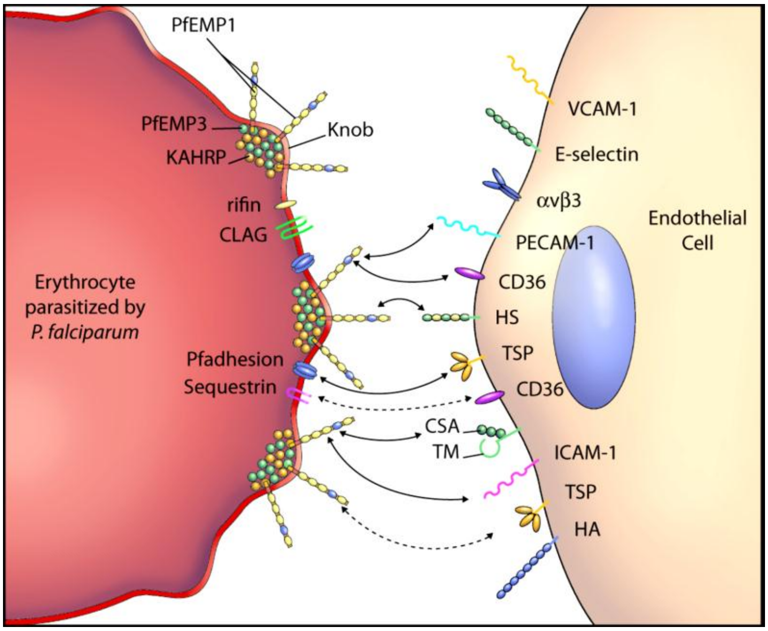

PfEMP1
PfEMP3
KAHRP
Knob
rifin
CLAG
Erythrocyte parasitized by P. falciparum
Pfadhesion
Sequestrin
CSA
TM
VCAM-1
E-selectin
αvβ3
PECAM-1
CD36
HS
TSP
CD36
ICAM-1
TSP
HA
Endothelial Cell

Figure 7. Schematic representation of the molecules implicated in the cytoadhesive interaction between RBCs infected with *P. falciparum* and vascular endothelial cells or placental syncytio-trophoblasts.

Adapted from Cooke, B. M. *et al.*[43].

Cytoadherence of pRBCs is suggested to be mediated by *P. falciparum* erythrocyte membrane protein 1 (PfEMP1) which is expressed on the surface of mature infected erythrocytes[44]. This multi-gene protein family is encoded by hypervariable genes known as *var*, each representing a different antigenic form. Moreover, the parasite is capable of changing its antigenic profile by switching expression between different *var* genes, which enables evasion of the human immune system[45,46] and avoids clearance by the host's spleen. By changing its surface variant antigens the parasite also changes its sequestration properties. This exported family of parasite-encoded immunovariant adhesins has been demonstrated to localize to specific regions on the RBC plasma membrane called knobs[47-49]. Previous studies have shown that knob associated histidine rich protein (KAHRP) is necessary for knob formation in pRBCs[50,51] and that the dynamic association between KAHRP and PfEMP1mediates cytoadherence during *Plasmodium* invasion[52]. Sequestration causes vascular blockage leading to cerebral and placental malaria[53,54] which contributes to the parasite pathogenicity. Sequestered erythrocytes undergo significant biomechanical modifications in their cytoskeleton and cell surface that are crucial for the parasite survival[55].

PfEMP1 proteins are proposed to be one of the main targets for naturally acquired immunity to malaria as well as being the main mediator for sequestration and rosetting. The fact that this protein family is unique to *P. falciparum* and taking into account that other *Plasmodium* species also evade host immunity, rosette and sequester to a lesser extent in its absence suggests evolvement of PfEMP1-independent mechanisms for immune evasion, sequestration and rosetting. The common feature for all *Plasmodium spp.* is the presence of small immunogenic variant surface antigens on pRBCs surface suggesting they could play a crucial role in these adhesion mechanisms[56]. The rosetting process is also related to the virulence of *P. falciparum* and, even though its role in pathogenesis is still ambiguous, it has been associated with different outcomes of severe disease, such as anemia and cerebral malaria[57]. This complex binding interaction resides in a promiscuous lectin-like interaction that depends on the parasite phenotype and whether the receptors are present on the host cell or not[58]. Rosetting has been observed in all human malaria species and has also been shown to occur in simian and rodent malaria parasites[59-63] but at different levels[60,64,65] consistent with this phenomenon being mediated by variant adhesins. The binding of uninfected RBCs to pRBCs is frequently observed in individuals with severe malaria and is mediated by the N-terminal sequence of the DBL1α domain (relatively conserved head) of PfEMP1 expressed at the surface of the infected erythrocyte[66-68].

1.3 Diagnosis, treatment and prophylaxis

Rapid and accurate diagnosis of malaria is crucial to define the appropriate treatment of affected individuals, thus decreasing resistance emergence, and to prevent further spread of infection in the community. Even though lately there have been major advances in diagnostic technologies, microscopy is still the gold standard[2]. The main drawbacks of this technique are a need for highly trained and experienced staff and difficulty of detecting parasite at low parasitemia. Besides the visualization of parasites in stained blood samples, rapid diagnostic tests[69,70] (detecting malaria antigens) and molecular techniques[71] (detecting parasite genetic material) are also available. Nevertheless, these methods have limitations such as the need for equipment and supplies, personnel expertise, high cost, long processing time, risk of false negatives, and/or applicability in acute infection.

Despite the fact that malaria is a curable (see **Table 1**) and preventable disease, there is no vaccine available yet, and resistance to artemisinin-based combination therapies (ACTs, currently the first-line treatment) is already emerging in Southeast Asia[72], a fact that threatens to reverse several decades of progress in decreasing malaria impact. At the moment the mainly used prophylactic drugs are atovaquone-proguanil, chloroquine, doxycycline, and mefloquine. It is also recommended to avoid mosquitoes' bites by using insecticide-treated mosquito nets and repellents. Insecticides such as dichlorodiphenyltrichloroethane, deltamethrin and lambdacyhalothrin are the major elements used in vector control and are still remarkably effective in malaria endemic regions where the parasites are sensitive to these chemical compounds[73].

The high variability of *Plasmodium* proteins has hampered vaccine approaches and is largely responsible for the appearance of strains resistant to new drugs which is a major threat to malaria control. Recent clinical trials involving a pre-erythrocytic *P. falciparum* vaccine, RTS-S, demonstrated partial efficacy[74,75], however, the need to explore other vaccine options remains, especially those having the potential of controlling blood-stage infection. Pre-erythrocytic vaccines should be paired with a blood-stage vaccine in order to, besides avoiding parasites from exiting the liver to infect blood, eliminate breakthrough parasites hence providing better protection from both clinical and more severe malarias. Several attempts of designing vaccines targeting the merozoite stages showed promising potential but their development has been hindered by limited functional knowledge of the molecular targets since the functions of many receptor-ligand associations involved in RBC invasion are not well established yet[76]. Drug resistance can develop through several mechanisms, including changes in drug permeability or transport, drug conversion to another form that becomes ineffective, increased expression of the drug target, or changes in the enzyme target that decrease the binding affinity of the inhibitor[77].

Table 1. Summary of the most frequently used antimalarial treatments, recommended by the WHO in 2010, for uncomplicated and severe *P. falciparum* malaria cases[78]

<table>
<tr><th colspan="4">Uncomplicated Malaria</th></tr>
<tr><td colspan="4"><i>1st Line Treatment: artemether plus lumefantrine, artesunate plus amodiaquine, artesunate plus mefloquine, artesunate plus sulfadoxine-pyrimethamine, and dihydroartemisinin plus piperaquine.
Single dose 0,75 mg/kg primaquine as an antigametocyte.</i></td></tr>
<tr><th>Pregnancy</th><th>Lactating Women</th><th>Infants & Young Children</th><th>Travellers</th></tr>
<tr><td>quinine plus clindamycin/ artesunate plus clindamycin (7 days)</td><td>ACTs except dapsone, primaquine and tetracyclines</td><td>ACTs</td><td>atovaquone-proguanil, artemether-lumefantrine, quinine plus doxycycline or clindamycin</td></tr>
<tr><th colspan="4">Severe Malaria</th></tr>
<tr><td colspan="4"><i>Considered a medical emergency, treatment should be started without delay.</i></td></tr>
<tr><th colspan="2">Adults</th><th colspan="2">Children</th></tr>
<tr><td colspan="2">artesunate IV or IM, artemether or quinine if parenteral artesunate is not available</td><td colspan="2">artesunate IV or IM, artemether or quinine if parenteral artesunate is not available</td></tr>
</table>

The current delivery method of antimalarials ends up with the free compound in the bloodstream, where it can be absorbed by all cells, and not only by pRBCs. Thus, an efficient treatment requires high doses that can trigger undesirable side effects. On the other hand, reduced specificity of toxic drugs demands low concentrations to minimize pernicious side effects, thus incurring the risk of delivering sublethal doses favouring the appearance of resistant parasite strains. There is a pressing need for new therapeutic strategies against malaria because the disease has to be fought from different fronts and the currently available treatments will not guarantee its eradication. This includes the necessity for a constant search of new antimalarial drugs and of improved methods for their efficient administration.

Malaria eradication faces a series of difficulties due to extrinsic factors such as technical and operational failures concerning the implementation of campaigns to fight the disease, the poor quality of antimalarials distributed in malaria endemic regions, drug interactions, unavailability of less toxic drugs, resistance of *Anopheles spp.* to insecticides, and socioeconomic circumstances of the affected populations[79]. The development of an effective vaccine is a world health priority and represents an important step toward the control and eventual elimination of this disease.

2. NANOTECHNOLOGY

2.1. Nanomedicine

Nanomedicine, the application of nanotechnology to medicine, is defined by the European Science Foundation as "*the science and technology of diagnosing, treating and preventing disease and traumatic injury of relieving pain, and of preserving and improving human health, using molecular tools and molecular knowledge of the human body*" [80]. Nanotechnology, i.e. the ability to assemble and study materials with nanoscale precision (**Figure 8**) enabled a wide range of research opportunities in many fields[81], for instance the improvement of diagnosis tools available for infectious diseases, the development of new biomedical technologies such as drug delivery systems, and imaging probes or devices, among many others[82].

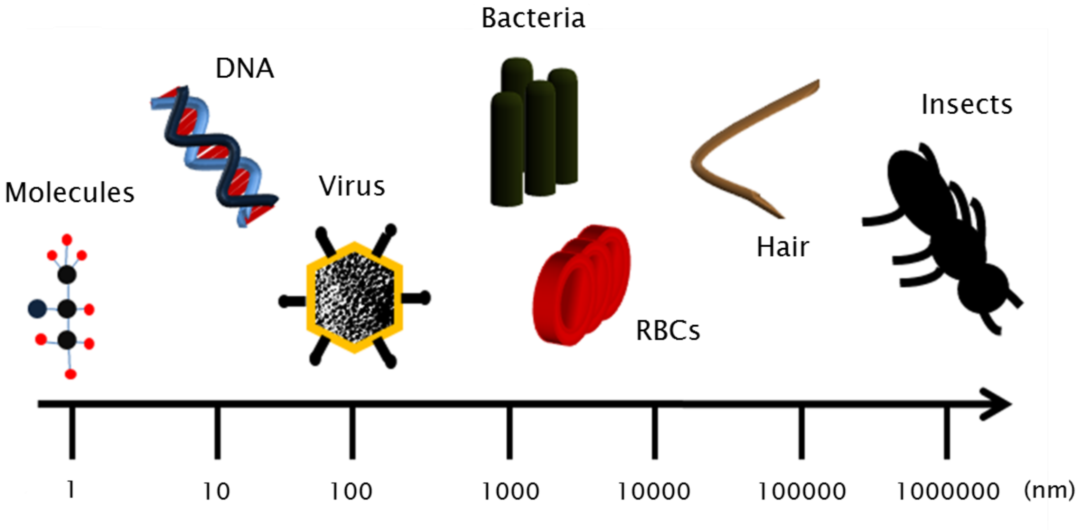

Figure 8. Relative sizes of naturally occurring structures. Adapted from Boisseau, P. *et al.*[82].

This promising evolving field allows the development of new materials and functional devices by designing their shape and size, enabling their manipulation and application in a wide range of scientific areas. Nanoparticulate systems consist of a heterogeneous family of submicron forms that can be liposomal, polymeric, and carbon nanotube-based[81]. Their surface can be modified with suitable molecules to target them to the appropriate sites of action which confers an outstanding advantage to these nanosystems (**Figure 9**). Their use as drug delivery systems constitute an advantage over conventional methods since these nanocarriers enhance drug absorption into diseased tissues/cells, they confer drug protection refraining degradation before reaching their specific site of action, allow for better control over the timing and distribution of drugs to the tissues, and prevent drugs from interacting with normal cells thus avoiding undesirable side effects. Some possible explanations for the slow clinical translation of these nanomedicines are the insufficient understanding of events at the nano-bio interface both *in vitro* and *in vivo*, inadequate knowledge of the fate of nanoparticles at the body, difficulty in achieving reproducible and controlled synthesis at scales suitable for clinical development and commercialization, and lack of technologies enabling screening of a large number of nanoparticle candidates under biologically relevant conditions that could be reliably correlated to clinical performance[83].

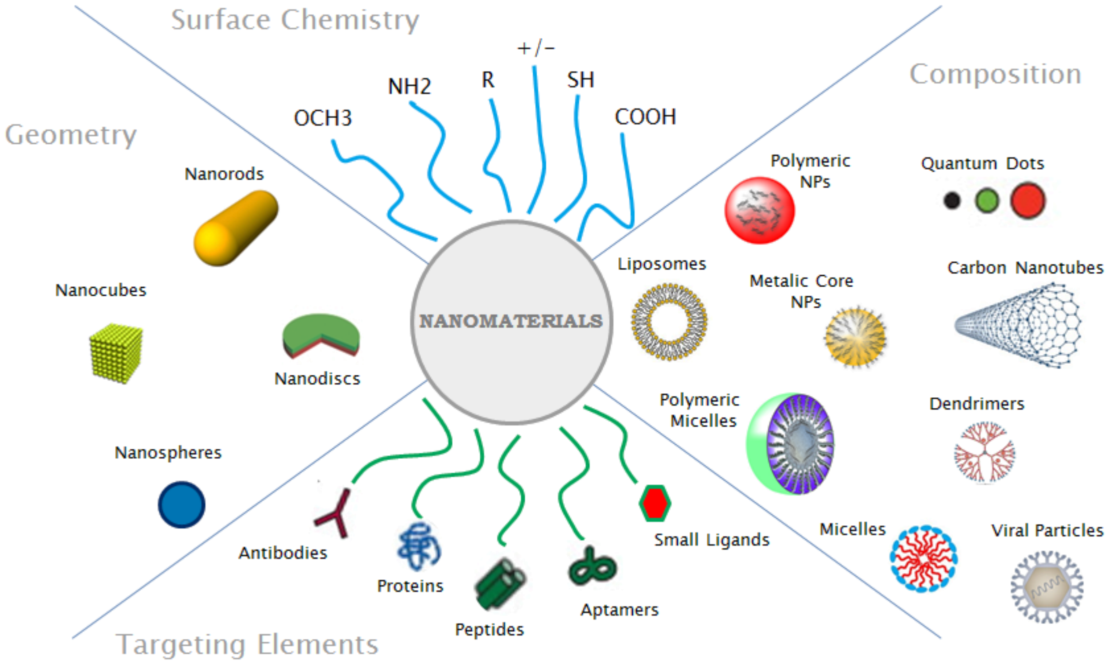
Surface Chemistry
+/-
NH2
R
SH
OCH3
COOH
Composition
Geometry
Nanorods
Polymeric NPs
Quantum Dots
Liposomes
Nanocubes
Metalic Core NPs
Carbon Nanotubes
NANOMATERIALS
Nanodiscs
Polymeric Micelles
Dendrimers
Nanospheres
Antibodies
Small Ligands
Micelles
Viral Particles
Proteins
Aptamers
Peptides
Targeting Elements

Figure 9. Composition and geometry of nanomaterials functionalized with targeting elements through surface chemistry, appropriate for therapeutics delivery and imaging labels. Adapted from Kamaly, N. *et al.*[83].

2.1.1. Role of nanomedicine in malaria treatment

Regarding malaria, the main drawbacks of current available chemotherapeutic approaches are the development of multiple drug resistance and the non-specific cell targeting, which inevitably results in an increase of required drug doses and subsequent toxicity for the human organism[84]. The challenge of drug delivery is the liberation of drug agents at the right time in a safe and reproducible manner, usually to a specific target site[85]. In the case of antimicrobial drugs it is essential to deliver sufficiently high local amounts to avoid stimulating the evolution of resistant parasite strains[86], a common risk when using sustained low doses to limit the toxicity of the drug for the patient.

In this context, nanocarriers have been suggested for malaria diagnosis[2], treatment[87] and vaccine formulation[88] because these nanotechnology-based delivery systems allow improving the pharmacokinetic profile of effective drugs and their therapeutic outcome by targeting antimalarials specifically to their site of action[89,90]. Likewise, nanotechnology is also a useful tool to recover the use of old and toxic drugs[91] by modifying their biodistribution and reducing toxicity, thus decreasing possible side effects. Many promising antimalarial compounds are charged and therefore require transportation into the parasite. The route of administration is also an important aspect to be considered in malaria. The oral route should be the first choice for clinically uncomplicated malaria; however, parenteral therapy is advocated in severe or complicated disease cases. Hence, it is more cost-efficient to develop new drug-delivery methods than new antimalarials[92].

Despite the significant development of nanotechnology and the current optimistic progress obtained both *in vitro* and *in vivo* by the application of these cutting edge technologies on malaria therapy and control, there is still the general misconception that nanomedicine relies only on complex and expensive devices that are not suitable for a poverty-related disease[93].

2.2. Liposomes

Liposomes (LPs) are biodegradable and biocompatible carriers containing an aqueous core entrapped by one or more lipid bilayers, generally formed by amphiphilic phospholipids and cholesterol (CHOL)[94]. These drug-delivery systems are characterized as first-generation liposomes (conventional vesicles) or as second-generation liposomes (when the lipid composition, size and/or charge are modified). LPs may be classified based on their structure, size (**Figure 10**), and preparation method (e.g. lipid film hydration method). Unilamellar vesicles are generally used to encapsulate water-soluble drugs whereas multilamellar vesicles permit the entrapment of lipid-soluble drugs on the lipid bilayer due to the high lipid content[95].

Water-soluble drugs may be encapsulated into the hydrophilic core or be present outside of the vesicles. The content of entrapped drug in the nanoparticles will depend on the bilayer composition and preparation method. On the other hand, lipophilic drugs are mainly entrapped in the lipid bilayer, which diminishes significantly the possible loss of drug content during storage[96].

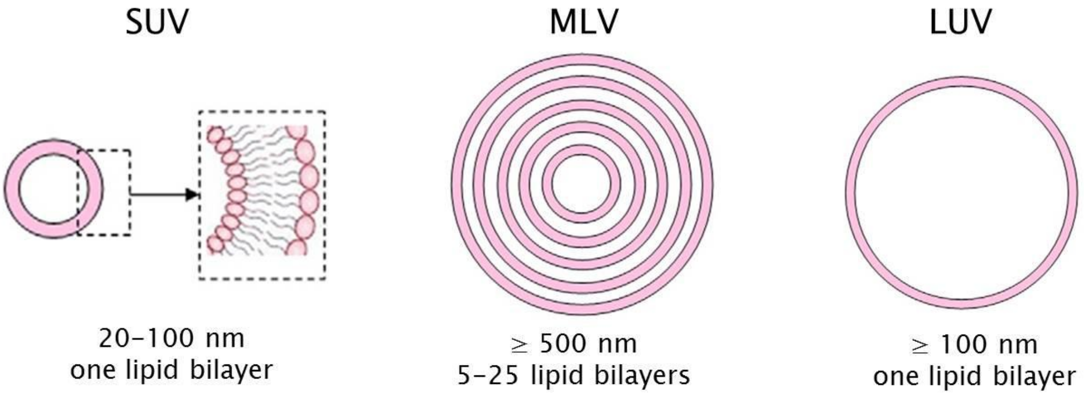

Figure 10. Main classification of liposomes based on lamellarity. Small unilamellar vesicles (SUV) range from 20 to 100 nm and are formed by a single bilayer; multilamellar vesicles (MLV) range from 500 to 5000 nm and consist of several concentric bilayers; large unilamellar vesicles (LUV) also consist on one lipid bilayer and are larger than 100 nm. Adapted from Yang, F. *et al.*[97].

The leading advantages of using these biphasic carriers are the low toxicity, good biocompatibility, reduced immune system activation, possibility of targeted delivery of bioactive drugs (hydrophilic and hydrophobic) directly to their site of action (**Figure 11**), protection of encapsulated compounds from chemical degradation, and considerable versatility[84,94,97]. However, some limitations are also present, namely the relatively short plasma half-life[98], stability issues, and poor control of cargo delivery along time[99].

In the last few years significant efforts have been undertaken to overcome these drawbacks, such as the incorporation of cholesterol (the "helper" lipid) in the LPs formulation that promotes stability and slows down the release of the encapsulated compound[100,101]. One of the most remarkable advances concerning the use of LPs for clinical applications consisted on the introduction of poly-(ethylene glycol), a synthetic polymer, on the surface of the liposomal carrier[96]. This modification allowed LPs to remain in circulation for a prolonged period of time and facilitated the escape from mononuclear phagocytosis[102]. Besides the incorporation of synthetic polymers, other moieties have also been described to increase liposomal drug accumulation in the desired tissues or organs, such as monoclonal antibodies[97] or their fragments, growth factors, peptides[81], carbohydrates[103], and receptor ligands[104], among others.

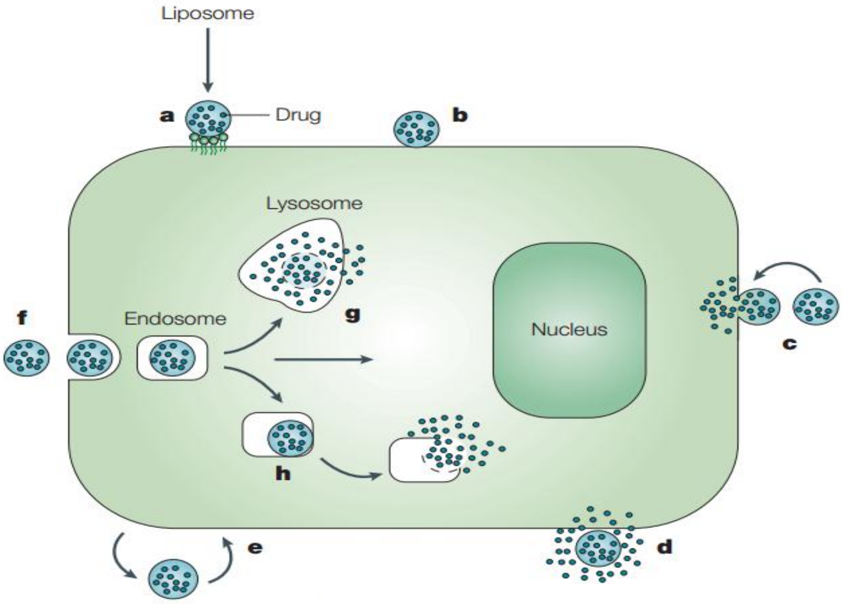

Figure 11. Delivery of liposome cargo to target cells. Drug-loaded LPs can be adsorbed onto the cell surface specifically (a) or nonspecifically (b). Fusion of LPs with the cell membrane may also occur (c) allowing the delivery of their content to the cytoplasm or, in case of destabilization by certain cell membrane components, releasing the drug extracellularly (d). LPs can undergo the direct or transfer protein-mediated exchange of lipid components with the cell membrane (e) or be internalized by endocytosis (f). Regarding endocytosis, these nanocarriers can be delivered by an endosome into the lysosome (g) or, in case of endosome destabilization (h), drug liberation occurs directly in the cell cytoplasm. Adapted from Torchilin, V. *et al.*[105].

More specifically, carbohydrates are considered versatile adhesion molecules due to the extraordinary plasticity of glycan chains, the low affinity and reversibility of individual binding sites, and the cluster effect[106]. Recognition of carbohydrates by proteins is central to many intra- and extracellular physiological and pathological processes[103], and thus carbohydrate-mediated targeted delivery of drugs is a promising new avenue.

Finally, it is important to underline that the liposomal surface charge plays a crucial role in the interaction with many biological membranes and on the prevention of aggregates formation[107]. Even though it has been reported that the use of cationic LPs in clinical fronts was hampered by their instability, toxicity at repeated administration, rapid clearance, and induction of immunostimulation and complement activation[94], other studies showed that positively-charged liposomes exhibited higher drug loading rates and faster drug release efficiency[107].

2.3. Polymers

Polymers display a broad spectrum of variable characteristics regarding dimension, topology and chemistry[108]. There are many fascinating benefits in using biodegradable polymers for biomedical applications as a result of their biocompatibility, high surface/volume proportion, and the possibility to control the rate of polymer degradation and encapsulated drug release[109].

Poly(amidoamine)s (PAA)s are a family of biodegradable synthetic polymers that deserve special attention considering their unique features such as an easy and potentially diverse synthesis (linear, cross-linked or grafted) and facile functionalization allowing the attachment of crucial moieties that make them suitable for a wide variety of applications[110]. PAAs in particular have been used to neutralize the anticoagulant activity of heparin in solution[111], as polymer drug carriers, as pH-responsive polymers, and in the design of polymeric drugs[110].

The therapeutic applications of polymers include polymeric drugs, polymer-drug conjugates, polymeric micelles and bio-responsive polymers used for intracellular delivery[112]. Polymeric nanoparticles consisting of polymer-drug conjugates have advantages in the nanoscale range (from 10 to 1000 nm) such as the increase of drug bioavailability, protection during its delivery towards the site of action and escape from a pronounced immune response, improved pharmacokinetics, among others. Also, polymer-based nanocarriers are suitable for oral administration which constitutes an advantage when comparing them to LPs[113]. For these reasons, they have been used as targeting agents for the delivery of drugs and imaging compounds in a controlled manner[114].

2.4. Nanomedicine-based drug delivery systems as antimalarial vehicles

Many efforts have been put forth aiming to demonstrate the potential of nanocarriers' application in antimalarial drug delivery. Results obtained by our group showed that an immunoliposomal prototype designed by us was able to deliver its contents exclusively to pRBCs containing the *P. falciparum* late forms trophozoites and schizonts[115], and improved on average tenfold the efficacy of the antimalarial drug chloroquine (CQ) *in vitro*[90]. Moreover, the delivery to pRBCs and non-infected RBCs of CQ-containing immunoliposomes was also explored as a dual therapeutic and prophylactic strategy. These immunoliposomes studded with monoclonal antibodies raised against the RBC surface protein glycophorin A showed complete targeting towards RBCs and pRBCs at low lipid concentration, exhibited the capacity of completely arresting early intraerythrocytic stages of *P. falciparum* growth *in vitro* at 50 nM CQ, and allowed the clearance of the pathogen below detectable levels *in vivo* at a CQ dose of 0.5 mg/kg in mice[116].

Others demonstrated that galactose-coated dendrimers loaded with CQ[117] (i) had a drastically reduced hemolytic toxicity, (ii) were less immunogenic, (iii) increased drug entrapment efficiency several fold depending upon generations, and (iv) extended the release period up to 3 times[106].

Because the antimalarial drug primaquine (PQ) is known to be hemolytic, especially in populations with glucose-6-phosphate dehydrogenase deficiency[118], previous studies by others hypothesized that this hemotoxicity could be avoided by encapsulating the drug within LPs. Moreover, the authors confirmed the effectiveness of the carrier system by the enhanced therapeutic activity and reduced toxicity achieved[119]. In another study, PQ encapsulated in solid lipid nanoparticles proved to be 20% more efficient than the conventional oral dose when tested in *P. berghei* infected mice indicating that this nanoformulation might be a promising drug delivery system[91]. As another example, to counteract the low oral bioavailability of the poorly water-soluble antimalarial agent artemether and the disadvantages of its currently available oily intramuscular injection, the potential of nanostructured lipid carriers for intravenous (IV) administration was tested. Briefly, artemether-containing carriers showed higher antimalarial activity when compared to the marketed intramuscular formulation, longer times in the treated animals blood circulation of *P. berghei* infected mice, and higher survival rates[120]. Furthermore, in a study conducted by us, we showed the efficacy of two PAA polymers entrapping CQ, AGMA-1 and ISA-23, in eliminating the parasite from *P. yoelii* infected-mice and clearing infection in comparison to the same amounts of free CQ injected intraperitoneally[121].

In conclusion, antimalarial drug nanocarriers must provide optimal drug half-lives in circulation, specific delivery to the correct tissue, and a timely initiation and termination of the therapeutic action[116].

2.5. Nanoparticles deliver their cargo to pRBCs

Soon after invasion, RBCs infected by *Plasmodium spp.* suffer deleterious rheological alterations (**Figure 12**) such as modified morphology (loss of the normal discoid shape), decreased deformability and increased cell adhesiveness[122]. Several anomalous parasite-induced protein-protein interactions in the erythrocyte membrane skeleton cause these alterations that have pathophysiological importance, especially in *P. falciparum* malaria. The RBC acquires a series of new characteristics and is converted from a relatively simple sack of hemoglobin that delivers oxygen to cells into a much more complex cell as a result of the appearance of new structures in its cytoplasm, and new proteins at its cytoskeleton and on the cell surface[123]. Mature human RBCs lack *de novo* protein synthesis and endogenous protein trafficking machinery[124]. For this reason, in order to survive inside the host cell, parasites induce new permeability pathways (NPPs) in the pRBC that increase plasma membrane permeability allowing for the uptake of nutrients and the elimination of waste products[125]. Infected RBCs become spherocytic and their surface evolves into a more rigid form, punctuated with numerous electron-dense elevations called knobs that are believed to participate in pRBC adhesiveness[126]. Additionally, novel membranous structures known as Maurer's clefts and tubulovesicular networks are established in the pRBC cytoplasm to enable protein traffic[127].

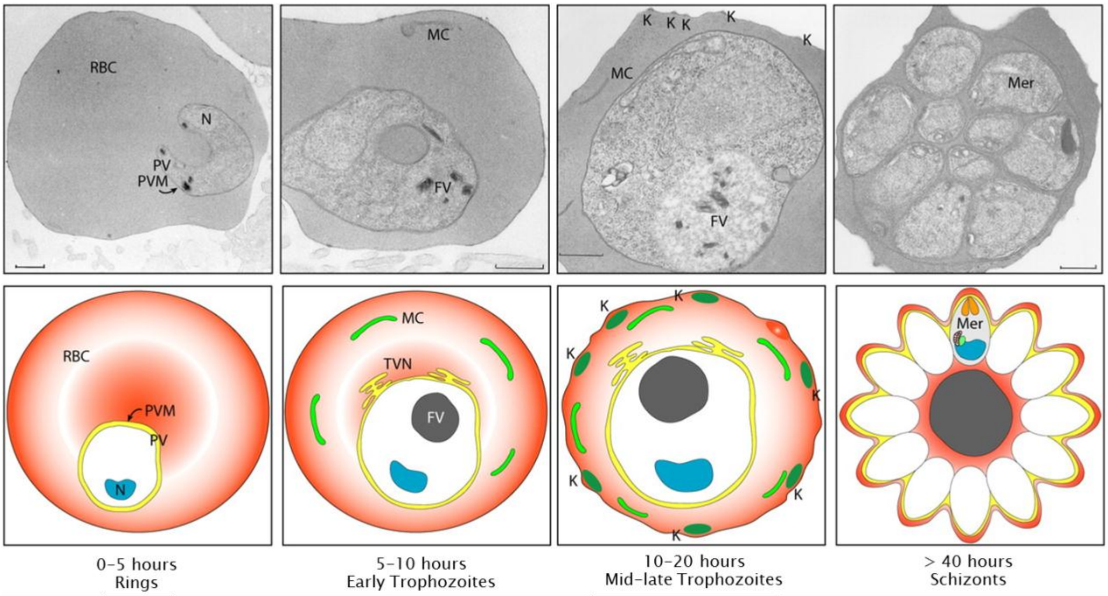

Figure 12. *Plasmodium*-infected RBCs. Between 0 and 5 hours the parasite acquires a ring-like form and is surrounded by the parasitophorous vacuole (PV). From 5 to 10 hours after invasion, the ring stages develop to early trophozoites and induce the extension of the parasitophorous vacuole membrane (PVM) into the host cell, forming a tubulovesicular network (TVN) and RBC membrane-tethered Maurer's clefts (MCs). Hemozoin crystals become visible in the food vacuole (FV). 10 to 20 hours after invasion, the parasite progresses to trophozoite stages increasing its volume and producing knobs (K) on the pRBC membrane. Finally, 40 hours post-invasion the parasite undergoes several rounds of asexual multiplication resulting in merozoite (Mer) stages. The nucleus is indicated by N and the size bars correspond to 0.5 μm. Adapted from Marti, M. *et al.*[128].

Despite the fact that parasitized erythrocytes lack endocytic capacity, it has been shown that particles up to 70 nm in diameter were able to access intracellular parasites[129]. Moreover, there is also evidence demonstrating that pRBCs become leaky prior to rupture[130], and that the membrane site of parasite entry never completely closes leaving a pore and a small duct extending into the PV[129]. These features contribute to an anomalous membrane that might explain the permeability of pRBCs to certain macromolecules[131]. Subsequently, several studies showed evidence on the ability of nanovectors to deliver their contents to pRBCs even though the delivery mechanism is still not completely established and understood[115,119,132,133].

3. SULFATED POLYSACCHARIDES

Sulfated polysaccharides consist of a complex group of macromolecules with a variable range of biological functions, such as anticoagulating, antiviral, antioxidant, antiprotozoal, and anti-inflammatory activities[134,135]. They are present in a vast variety of animals, including the sulfated glycosaminoglycans found in invertebrates and mammals[136]. Additionally, marine invertebrate species also represent an important source of sulfated polysaccharides with novel structures (e.g. sulfated fucans and galactans)[135]. The main reason why these compounds are becoming increasingly attractive in many scientific fields is their natural polyanionic feature that makes them suitable to interact with important functional proteins.

3.1. Sulfated glycosaminoglycans

All GAGs are long and linear polysaccharides composed of the same building blocks (glucosamine and glucuronic or iduronic acid) and the vast majority present negative charge due to the presence of sulfate groups[57,137,138]. More specifically, heparin is a polysaccharide formed by repeated disaccharide units of an uronic acid and a glucosamine, exhibiting the most highly negative charge in nature due to the presence of its numerous sulfate groups[139]. Moreover, heparin (**Figure 13A**) was also one of the first naturally occurring drugs applied to medicine, the main example of a carbohydrate-based therapy, and one of the oldest natural products that are still in use nowadays[140]. Heparin is still considered the gold standard in matters of anticoagulating action because of its rare pentasaccharide sequence which is responsible for the interaction and conformational activation of antithrombin III, the major plasma serpin. This high affinity interaction determines the inhibition of serpin-dependent proteases of the coagulation system, especially thrombin and factor Xa[136].

Chondroitin sulfate is composed by chains of alternating D-glucuronic acid and N-acetyl-D-galactosamine and their disaccharides might have different amounts and patterns of sulfation[141] (**Figure 13B**). Heparan sulfate (HS) is a linear polysaccharide with a disaccharide repeating unit of D-glucosamine and L-iduronic or D-glucuronic acid, which can be O- or N-sulfated or N-acetylated[142] (**Figure 13C**).

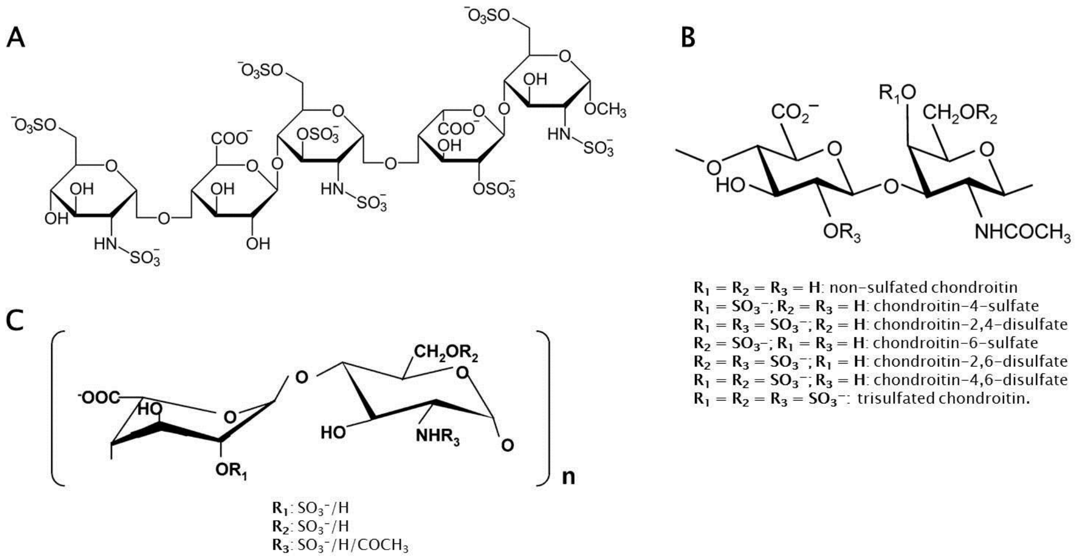
A
B
C
R1 = R2 = R3 = H: non-sulfated chondroitin
R1 = SO3−; R2 = R3 = H: chondroitin-4-sulfate
R1 = R3 = SO3−; R2 = H: chondroitin-2,4-disulfate
R2 = SO3−; R1 = R3 = H: chondroitin-6-sulfate
R2 = R3 = SO3−; R1 = H: chondroitin-2,6-disulfate
R1 = R2 = SO3−; R3 = H: chondroitin-4,6-disulfate
R1 = R2 = R3 = SO3−: trisulfated chondroitin.
R1: SO3−/H
R2: SO3−/H
R3: SO3−/H/COCH3

Figure 13. Chemical structures of heparin (A), chondroitin sulfate (B) and heparan sulfate (C).

During the blood-stage of infection, PfEMP1 interacts with various host receptors to avoid immune surveillance and splenic clearance. Lectin-like interactions of PfEMP1 have been described with heparin[6] and HS[138]. There are numerous studies demonstrating the involvement of various GAGs in several adhesive stages of *P. falciparum*. For instance, pRBCs present in the placenta during pregnancy adhere to chondroitin sulfate A (CSA)[143] through interactions with PfEMP1 domains prompting inflammation and blocking fetal blood circulation[144]. Furthermore, HS present on the surface of hepatocytes was shown to function as a ligand for the circumsporozoite protein[145] that covers the parasite sporozoites enabling the targeting of liver cells for infection. Additionally, sulfated glycoconjugates such as HS, CSA and heparin, presented an inhibitory effect on the merozoite invasion of RBCs *in vitro*[146] although the molecular mechanisms remain poorly understood[147]. Heparin, dextran sulfate, fucoidan, and fucosylated chondroitin sulfate (FucCS) have all been shown to prevent cytoadherence of pRBCs and to inhibit merozoite invasion of erythrocytes *in vitro*[148-150]. In addition, several studies have described the importance of the sulfate groups for the inhibitory activity of heparin and HS[31,149,151-153]. Besides inhibiting blood-stage growth, heparin binds to several members of the Duffy and reticulocyte binding-like families with different affinity rates. This fact suggests that this sulfated glycoconjugate masks the apical surface of merozoites[35], blocking the interaction with erythrocyte membrane after initial attachment[31]. These evidences, among many others, constitute the basis for GAG-based therapies against malaria.

Chemical structure plays an important role in the interaction between heparin and the DBL1α domain of PfEMP1[154]. Previous studies showed that an avid interaction depends, at least, on the presence of a 12-mer fragment of heparin as well as on N-sulfation and 6-*O*- and 2-*O*-sulfations, demonstrating that heparin binds to the rosetting domain in a size and sulfation-dependent manner[57]. Moreover, evidence on heparin's specific adhesion to *P. falciparum* schizonts *versus* RBCs revealed a binding strength matching that of an antibody-antigen interaction[40].

GAGs, including heparin, are promising molecules in the context of anti-adhesion therapies against malaria due to their ability of inhibiting *P. falciparum* pRBCs cytoadherence and growth[58,137,155]. Nevertheless, their use in malaria infections is hindered by short *in vivo* circulation half-lives[156,157], limited efficacy, and anticoagulant properties, which led to intracranial bleedings (in the case of heparin)[158]. Furthermore, depolymerized heparin lacking anticoagulant activity has been observed to disrupt rosette formation and pRBC cytoadherence both *in vitro* and *in vivo*, and in fresh parasite isolates[159]. There is also evidence of non-anticoagulant activity of heparin when covalently immobilized on a substrate[160], which opens up novel opportunities to overcome its pernicious side effects.

Transmission-blocking interventions foresee the great importance of inhibiting *Plasmodium* ookinete-to-oocyst transition in the midgut of *Anopheles* mosquitoes in a future scenario of malaria eradication. Hence, drugs presenting potential transmission-blocking activity have been receiving special attention in the last decade. Previous studies demonstrated that ookinete micronemal circumsporozoite thrombospondin-related protein and von Willebrand factor A domain-related protein (WARP) bind to sulfated GAGs *in vitro*[161]. Even though the exact function of these micronemal proteins is still unclear, it has been well established that both of them are essential for midgut epithelial cell invasion by *Plasmodium* ookinetes. Interestingly, CS is predominantly present on the apical side of the midgut epithelium and HS is mainly found in the basal side of it[162]. These facts stimulated efforts on finding new compounds that can interfere with ookinete-GAG interactions, therefore preventing midgut invasion and abolishing subsequent sporogony[163].

3.2. Marine polysaccharides

In the last decade, sulfated polysaccharides from marine organisms are gaining an enormous popularity due to their potential medical and therapeutic applications. Regarding GAG-related therapies, the risk of contamination with prions and viruses has hindered the use of these compounds because many of them arise from mammals. In this scenario, carbohydrates derived from marine organisms can offer a valuable alternative[164-166]. Sulfated fucans (or fucoidan when isolated from brown algae) and sulfated galactans (or carrageenans when isolated from red algae) are the most abundant sulfated polysaccharides found in algae and marine invertebrates[167]. Sulfated fucans are mostly constituted by α-L-fucopyranosyl units and can be extracted mainly from sea urchins, sea cucumbers, and brown algae. The latter (also known as fucoidans), besides containing α-L-fucopyranosyl, are also composed of other sugars such as xylose and uronic acids. Sulfated galactans consist of α-L-, α-D-, or β-D-galactopyranosyl units and can be isolated from green algae, red algae, sea urchins, and ascidians (also known as tunicates)[168]. As mentioned above, marine-derived polysaccharides exhibited a wide range of bioactivities, including antitumor[166], antiviral, anticoagulant[169], antioxidant[134], and anti-inflammatory effects[170]. A previous study conducted with well-defined sulfated polysaccharide structures from a sea cucumber showed that the pattern of sulfation, the position of the residues, and the type of constituent sugars influence the resultant anticoagulant and antithrombotic events[171].

There is evidence of a FucCS isolated from a sea cucumber that had inhibitory effects on *P. falciparum* cytoadhesion, invasion and rosette formation. Its effect seems to be very similar to that of heparin, i.e. through binding to PfEMP1 and MSP1 regions[150]. One of the FucCS main advantages is that it can be formulated for oral administration, contrary to other sulfated polysaccharides.

These results broaden new research directions concerning the use of sulfated glycoconjugates from marine organisms as an adjunct therapy in the treatment of severe malaria.

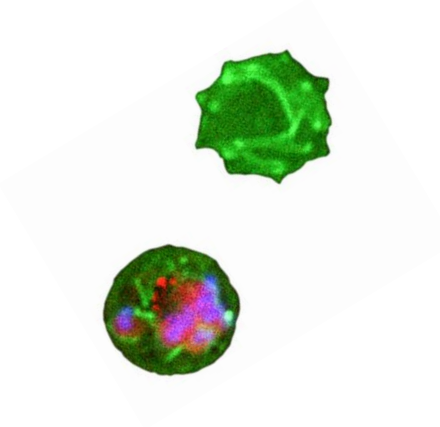

HYPOTHESIS
&
OBJECTIVES

HYPOTHESIS & OBJECTIVES

Antimalarial drug delivery currently relies on the administration of compounds with little or no specificity for the main target cell, namely the pRBC, and thus delivery approaches for most antimalarials require high overall doses. However, cellular unspecificity of drugs often demands low concentrations to minimize undesirable side effects, thus incurring the risk of sublethal doses favoring the appearance of resistant pathogen strains. Targeted nanovectors can fulfill the objective of achieving the intake of total doses sufficiently low to be innocuous for the patient but that locally are high enough to be lethal for the malaria parasite (**Figure 14**). In this PhD thesis we have explored the development of antimalarial nanocarriers incorporating sulfated polysaccharides as both antimalarial drugs and as specific targeting agents against pRBCs because (i) heparin had been described to possess antimalarial activity and (ii) *Plasmodium* uses host GAGs as receptors for erythrocyte invasion and intravascular sequestration.

Hypothesis:

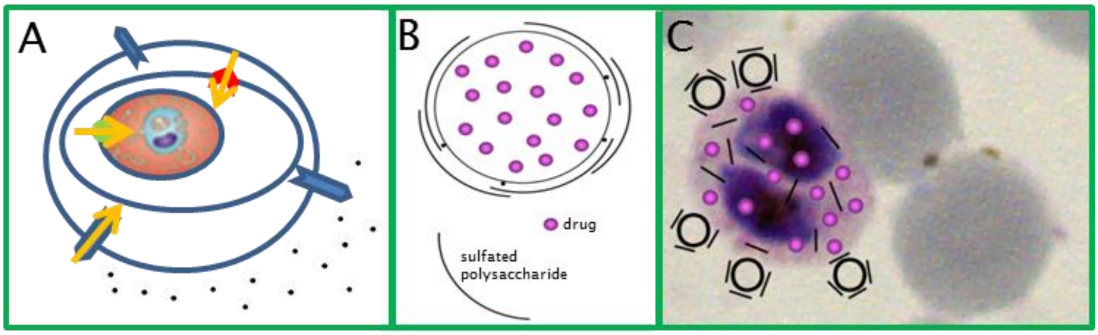

Figure 14. Contrary to the currently available antimalarial delivery strategies (A), we hypothesize that the use of sulfated polysaccharide-functionalized liposomes (B) might allow the delivery of drug doses that locally are high enough to be lethal for the malaria parasite but do not cause any damage to non-infected cells, thus decreasing resistance emergence and lowering the drug IC50 by adding to it the antimalarial activity of the polysaccharides themselves (C).

To explore this hypothesis, the detailed objectives of this PhD thesis are the following:

1. Quantitative exploration of the *in vitro* antimalarial activity of heparin and of novel sulfated polysaccharides derived from marine organisms.

2. Characterization of those sulfated polysaccharides having good antimalarial activity for their pRBC specific binding, low hemolysis, low unspecific cytotoxicity, and low anticoagulant activity both *in vitro* and *in vivo*.

3. Use of heparin as a targeting element of nanocapsules (liposomes and chitosan nanoparticles) to pRBCs.

4. Study of the possible synergistic antimalarial activity of drug-loaded liposomes targeted to pRBCs with heparin.

5. Investigation of the antimalarial mechanism of sulfated polysaccharides.

6. Exploration of heparin as specific targeting agent against gametocytes, ookinetes, oocysts, and sporozoites.

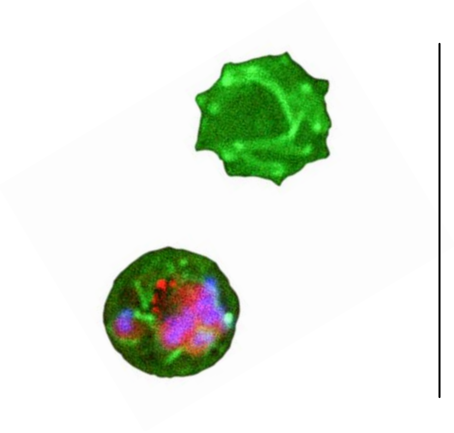

RESULTS

RESULTS

Article 1

Nanomedicine: Nanotechnology, Biology, and Medicine 10 (2014) 1719–1728

"Application of heparin as a dual agent with antimalarial and liposome targeting activities toward *Plasmodium*-infected red blood cells."

Joana Marques, Ernest Moles, Patricia Urbán, Rafael Prohens, Maria Antònia Busquets, Chantal Sevrin, Christian Grandfils, and Xavier Fernàndez-Busquets

Article 2

"Marine organism sulfated polysaccharides exhibiting significant antimalarial activity and inhibition of red blood cell invasion by *Plasmodium*."

Submitted to PLOS Pathogens

Joana Marques, Eduardo Vilanova, Paulo António de Souza Mourão, and Xavier Fernàndez-Busquets

Article 3

"Adaptation of nanocarriers to changing requirements in antimalarial drug delivery."

Preparing for submission to Journal of Controlled Release

Joana Marques, Juan José Valle-Delgado, Patricia Urbán, Elisabet Baró, Rafel Prohens, Alfredo Mayor, Pau Cisteró, Michael Delves, Robert Sinden, Christian Grandfils, Chantal Sevrin, José Luis de Paz, José Antonio García-Salcedo, and Xavier Fernàndez-Busquets

Internship Project

Targeting of *Plasmodium* transmission stages with heparin labeled with FITC for future antimalarial delivery strategies.

- performed at the Imperial College (London, UK), department of Life Sciences
- in collaboration with Professor Robert Sinden, Dr. Michael Delves, and Dr. Ursula Straschil
- funded by Xarxa Eurolife, Universitat de Barcelona

Other results - Article 4

Journal of Controlled Release 177 (2014) 84-95

"Use of poly(amidoamine) drug conjugates for the delivery of antimalarials to *Plasmodium*."

Patricia Urbán, Juan José Valle-Delgado, Nicolò Mauro, Joana Marques, Amedea Manfredi, Matthias Rottmann, Elisabetta Ranucci, Paolo Ferruti, Xavier Fernàndez-Busquets

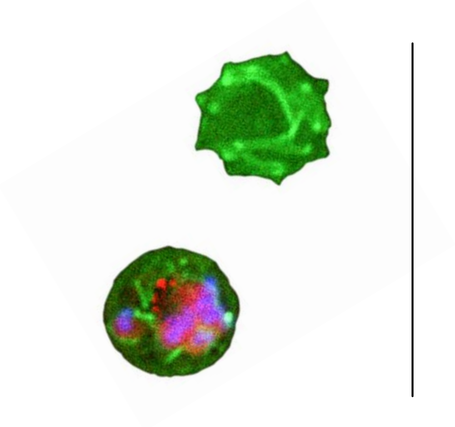

Article 1

ARTICLE 1

Article 1: Application of heparin as a dual agent with antimalarial and liposome targeting activities toward *Plasmodium*-infected red blood cells.

Current delivery methods for antimalarial drugs require high doses that can trigger undesirable side effects, a problem that can be averted with the use of targeted delivery strategies. Therefore, our main objective was the development of highly specific targeting agents for pRBCs adequate for the functionalization of nanovectors. Our group had previously shown that, provided the existence of a sufficiently good targeting molecule, nanocarriers can be designed to deliver their contents with complete discrimination only to pRBCs but not to non-infected RBCs, significantly increasing the efficacy of antimalarial drugs[115]. We had also demonstrated and characterized the high specificity of heparin binding to pRBCs by fluorescence microscopy, flow cytometry, and single molecule force spectroscopy[40].

In this work we have explored the potential ability of heparin as an antimalarial compound and as a targeting agent toward pRBCs when electrostatically conjugated to cationic liposomes.

The property of heparin to penetrate parasitized erythrocytes can be of use in the design of new cost-effective methods for the delivery of drugs to intracellular components of the pathogen. Our results represent a promising starting point in the context of the current malaria socioeconomic and pharmacotherapy scenario, which demands new delivery systems for current and future drugs exclusively to target cells. Achieving this degree of specificity would contribute to the administration of lower overall antimalarial doses reducing undesired side effects but maintaining high local drug concentrations capable of quickly eliminating the parasite and thus minimizing the risk of resistance induction. Heparin might be the spearhead of a new generation of GAG-related molecules exhibiting a synergistic activity as antimalarials and as targeting molecules for the localized delivery of drugs to *Plasmodium*-infected cells.

ARTICLE 1

ELSEVIER

Nanomedicine: Nanotechnology, Biology, and Medicine
10 (2014) 1719 – 1728

nanomedicine
Nanotechnology, Biology, and Medicine

nanomedjournal.com

Application of heparin as a dual agent with antimalarial and liposome targeting activities toward *Plasmodium*-infected red blood cells

Joana Marques, MS[a,b], Ernest Moles, MS[a,b], Patricia Urbán, PhD[a,b], Rafel Prohens, PhD[c],
Maria Antònia Busquets, PhD[d], Chantal Sevrin, BSc[e],
Christian Grandfils, PhD[e], Xavier Fernàndez-Busquets, PhD[a,b,*]

[a] *Nanomalaria Unit, Institute for Bioengineering of Catalonia (IBEC), Barcelona, Spain*
[b] *Nanomalaria Unit, Barcelona Centre for International Health Research (CRESIB, Hospital Clínic-Universitat de Barcelona), Barcelona, Spain*
[c] *Unitat de Polimorfisme i Calorimetria, Centres Científics i Tecnològics, Universitat de Barcelona, Barcelona, Spain*
[d] *Departament de Fisicoquímica, Facultat de Farmàcia, University of Barcelona, Barcelona, Spain*
[e] *Interfacultary Research Center of Biomaterials (CEIB), University of Liège, Chemistry Institute, Liège (Sart-Tilman), Belgium*

Received 7 January 2014; accepted 4 June 2014

Abstract

Heparin had been demonstrated to have antimalarial activity and specific binding affinity for *Plasmodium*-infected red blood cells (pRBCs) *vs.* non-infected erythrocytes. Here we have explored if both properties could be joined into a drug delivery strategy where heparin would have a dual role as antimalarial and as a targeting element of drug-loaded nanoparticles. Confocal fluorescence and transmission electron microscopy data show that after 30 min of being added to living pRBCs fluorescein-labeled heparin colocalizes with the intracellular parasites. Heparin electrostatically adsorbed onto positively charged liposomes containing the cationic lipid 1,2-dioleoyl-3-trimethylammonium-propane and loaded with the antimalarial drug primaquine was capable of increasing three-fold the activity of encapsulated drug in *Plasmodium falciparum* cultures. At concentrations below those inducing anticoagulation of mouse blood *in vivo*, parasiticidal activity was found to be the additive result of the separate activities of free heparin as antimalarial and of liposome-bound heparin as targeting element for encapsulated primaquine.
© 2014 Elsevier Inc.All rights reserved.

Key words: Heparin; Liposomes; Malaria; *Plasmodium*; Targeted drug delivery

---

Background

Malaria is a life-threatening infectious disease which remains a major cause of morbidity and mortality in tropical and subtropical regions of the world, caused by protists of the genus *Plasmodium* that are transmitted by infected *Anopheles* mosquitoes. Although increased prevention and control measures have led to a reduction in mortality rates by more than 42% globally since 2000, the World Health Organization has estimated 207 million episodes of malaria in 2012 that resulted in 627,000 deaths. People living in the poorest countries are the most vulnerable and approximately 90% of deaths were in Africa, of which 77% were children under 5 years of age.[1] The clinical, social and economic burden of malaria has led for the last 100 years to several waves of serious efforts to reach its control and eventual eradication, without success to this day. With the advent of nanoscience, renewed hopes have appeared of finally obtaining the long sought-after *magic bullet* against malaria in the form of a nanovector for the targeted delivery of antimalarial drugs exclusively to *Plasmodium*-infected cells.

In the life cycle of *Plasmodium* parasites,[2] the female *Anopheles* mosquito inoculates during a bite *Plasmodium* sporozoites that in the liver bind to and infect hepatocytes and proliferate into thousands of merozoites. Merozoites rupture from the hepatocytes and invade red

---

This work was supported by grant BIO2011-25039 from the *Ministerio de Economía y Competitividad*, Spain, which included FEDER funds, and by grant 2009SGR-760 from the *Generalitat de Catalunya*, Spain. A PFIS grant from *Instituto de Salud Carlos III* is acknowledged by P. Urbán. C. Sevrin has received the financial support of Interreg grant BioMimedics.

Patent application: Heparin-lipidic nanoparticle conjugates. Inventors: Fernàndez-Busquets, X., Marques, J., Moles, E. Institutions: IBEC, CRESIB. Application number: EP13152187.4; priority country: Europe; priority date: January 22, 2013.

*Corresponding author at: Nanomalaria Unit, Centre Esther Koplowitz, 1st floor, CRESIB, Rosselló 149-153, Barcelona ES-08036, Spain.
E-mail address: xfernandez_busquets@ub.edu (X. Fernàndez-Busquets).

http://dx.doi.org/10.1016/j.nano.2014.06.002
1549-9634/© 2014 Elsevier Inc.All rights reserved.

blood cells (RBCs), where they develop first into rings, and then into the late forms trophozoites and schizonts. Schizont-infected RBCs burst and release more merozoites, which start the blood cycle again. Because the blood-stage infection is responsible for all symptoms and pathologies of malaria, *Plasmodium*-infected RBCs (pRBCs) are a main chemotherapeutic target.[3] Thus, the future of malaria control requires efficacious drugs[4] acting on adequate therapeutic targets,[5] but also effective targeted drug delivery strategies.[6] The formulation and evaluation of novel delivery systems is less expensive than developing new drugs, and therapeutic failure has often been attributed in part to adverse drug effects and to the non-compliance of patients due to inconvenient dosing schedules.[7] At present, administration methods of antimalarials release the free compound in the blood stream, from where it can be significantly removed by many tissues and organs before entering pRBCs. As a result of this lack of specificity regarding the target cells, current oral or intravenous delivery approaches for most drugs require multiple doses. However, reduced specificity of toxic drugs demands low concentrations to minimize undesirable side effects, thus incurring the risk of sublethal levels favoring the appearance of resistant parasite strains. Targeted delivery systems can provide an increased drug bioavailability and selectivity to fulfill the objective of achieving the intake of total amounts sufficiently low to be innocuous for the patient but that locally are high enough to be lethal for the malaria parasite.

Antibody-functionalized liposomal nanovectors for the targeted delivery of drugs specifically to pRBCs have shown complete discrimination *in vitro* for pRBCs vs. non-infected erythrocytes,[8] but some properties of antibodies limit their role as targeting elements in antimalarial therapeutic strategies. They have a lengthy and relatively expensive production, are highly immunogenic unless genetically engineered humanized forms are used, and, as a result of the high variability of *Plasmodium* proteins exposed on pRBC surfaces, as the parasite switches to new antigenic repertoires any antibody will likely lose targeting efficacy and will have to be replaced. However, interesting alternatives to antibody-mediated targeting do exist.

One of the main pRBC-binding molecules are glycosaminoglycans (GAGs), a family of ubiquitous polysaccharides, some of whose members count among the most negatively charged natural polymers. Binding to the GAG chondroitin 4-sulfate (CSA) is thought to cause pRBC sequestration in the placenta, which has been linked to the severe disease outcome of pregnancy-associated malaria.[9] Heparan sulfate (HS), or a HS-like molecule exposed on RBCs is the ligand responsible for rosetting, the formation of small clusters (rosettes) between RBCs and pRBCs.[10] Heparin and HS are also targets for the circumsporozoite protein in the sporozoite attachment to hepatocytes during the primary stage of malaria infection in the liver. GAG-based therapies against malaria have been proposed in the wake of the results from different assays showing that soluble CSA, heparin, HS, heparin/HS derivatives and other sulfated glycoconjugates can inhibit pRBC sequestration, disrupt rosettes, and block sporozoite adhesion to hepatocytes. Direct antimalarial activity of heparin has been observed,[18] and suggested to proceed through a mechanism involving the inhibition of merozoite invasion. Heparin had actually been used in the treatment of severe malaria,[11–15] but it was abandoned because of its strong anticoagulant action, with side effects such as intracranial bleeding.[16] However, the formation of polyelectrolyte stable complexes between heparin and macromolecular structures such as polyamidoamines has been explored as a strategy to reduce the hemorrhagic activity of heparin.[17]

Single-molecule force spectroscopy data have revealed a complete specificity of adhesion of heparin to late-form pRBCs (schizonts) *vs.* RBCs,[19] with a binding strength matching that of antibody-antigen interactions.[20–22] We have explored here if the electrostatic binding of heparin to liposomes could offer good perspectives for a fast and cost-effective assembly of efficacious antimalarial targeted drug delivery nanovectors.[23]

Methods

Liposome preparation

Liposomes were prepared by the lipid film hydration method.[24] Different lipid combinations were tested in order to establish a liposomal formulation with low hemolytic activity and low general cytotoxicity. In a typical experiment, liposomes (10 mM total lipid) encapsulating the antimalarial drug primaquine were prepared by dissolving it in the hydration buffer (phosphate buffered saline, PBS) at a primaquine concentration of 6 mM, removing non-encapsulated drug by molecular exclusion chromatography. Heparin (13,000 kDa mean molecular mass) was electrostatically bound by addition of 1 vol of heparin solution in PBS to liposomes containing 4% 1,2-dioleoyl-3-trimethylammonium-propane,18:1 (DOTAP). In some samples, unbound heparin was removed by ultracentrifugation and the resulting liposome pellet was taken up in 10 pellet volumes of PBS immediately before addition to pRBC cultures whith a further 100-fold dilution (ca. 3 μM final primaquine concentration in the culture). For the quantification of encapsulated primaquine, a lipid extraction of the liposomes was performed. Briefly, following ultracentrifugation the liposome pellet was treated with methanol:chloroform:0.1 M HCl (1.8:2:1) and after phase separation primaquine content in the upper water–methanol phase was determined by measuring A_{320}.

Heparin determination, unspecific cytotoxicity and hemolysis assays

For the determination of heparin concentration the Alcian Blue method was used.[25] Shortly, 10 μL of heparin-containing solution was mixed with 10 μL of a solution containing 27 mM H_2SO_4, 0.375% Triton X-100, and 4 M guanidine-HCl. To the resulting 20 μL was added 100 μL of 1 mg/mL Alcian Blue 8GX solution in 0.25% Triton X-100, 18 mM H_2SO_4. Samples were centrifuged and the pellet was resuspended in 500 μL of 8 M guanidine-HCl. Finally, after spinning down debris, A_{600} of the supernatant was recorded and heparin content was determined from a standard linear regression of known concentrations. Unspecific cytotoxicity and hemolysis assays were performed as described previously.[8]

Isothermal titration calorimetry (ITC)

The working cell of a VP-ITC microcalorimeter was filled with a liposome suspension (containing 0.01 mM lipid) in PBS and the reference cell with liposome-free PBS. Ten-microliter aliquots of 0.05 mM heparin solution in PBS were injected stepwise into the working cell at 200 s intervals. The corresponding reference blank experiments were also performed, namely titration of the liposome suspension with PBS and titration of PBS with heparin solution.

Plasmodium falciparum cell culture and growth inhibition assays

The *P. falciparum* 3D7 strain was grown *in vitro* in group B human RBCs using previously described conditions.[26] Briefly, parasites (thawed from glycerol stocks) were cultured at 37 °C in Petri dishes containing RBCs in Roswell Park Memorial Institute (RPMI) complete medium under a gas mixture of 92% N_2, 5% CO_2, and 3% O_2. Synchronized cultures were obtained by 5% sorbitol lysis,[27] and the medium was changed every 2 days maintaining 3% hematocrit. For culture maintenance, parasitemias were kept below 5% late forms by dilution with washed RBCs prepared as described elsewhere.[8] For growth inhibition assays, parasitemia was adjusted to 1.5% with more than 90% of parasites at ring stage after sorbitol synchronization. One hundred fifty microliters of this *Plasmodium* culture was plated in 96-well plates and incubated in the presence of liposomes or heparin for 48 h in the conditions described above. Parasitemia was determined by flow cytometry, after staining pRBC DNA with the nucleic acid dye Syto 11, added 10 min before analysis without any further washing step. Samples were analyzed using a BD FACSCalibur™ flow cytometer and parasitemia was expressed as the number of parasitized cells per 100 erythrocytes.

Fluorescence microscopy

Living *P. falciparum* cultures with mature stages of the parasite were incubated in the presence of 10 μg/mL fluorescein-labeled heparin in PBS supplemented with 0.75% bovine serum albumin for the indicated times at 37 °C with gentle stirring. After PBS washing, blood smears were prepared and cells were fixed for 20 min with 1% (vol/vol) paraformaldehyde in PBS. For rodent malaria parasite assays, a *Plasmodium yoelii*-infected Balb/C mouse blood stock at 20% parasitemia was washed 3 × with PBS by centrifugation at 500 *g*. A 4-μL blood smear was fixed with 1% (vol/vol) paraformaldehyde for 15 min at room temperature in PBS, and after 2 additional PBS washes, cells were incubated with 10 μg/mL FITC-labeled heparin for 90 min at room temperature. Parasite nuclei were stained with 4′6-diamino-2-phenylindole (DAPI) and the RBC membrane was labeled with wheat germ agglutinin–tetramethylrhodamine conjugate. For Congo Red-stained samples, mouse blood infected with living mature stages of the rodent malaria parasite was incubated in the presence of 5 μg/mL Congo Red for 90 min at 37 °C with gentle stirring, and membrane staining was omitted. Slides were finally mounted with ProLong® Gold antifade reagent, and analyzed with a Leica TCS SP5 laser scanning confocal microscope.

Transmission electron microscopy

Knob-bearing erythrocytes infected with mature blood-stage *P. falciparum* parasites were enriched from *in vitro* cultures by Percoll gradient,[28] incubated in the presence of 20 μg/mL heparin-FITC for 90 min, and finally fixed at 4 °C for 2 h with a mixture of 4% paraformaldehyde and 0.1% glutaraldehyde in 0.1 M sodium phosphate buffer. Ultrathin cryosections were then obtained and processed as described elsewhere,[29] treating them with goat anti-FITC antibody followed by donkey anti-goat IgG coupled to 18 nm colloidal gold particles before finally mounting the sections on formvar-coated 200-hexagonal mesh nickel grids. The observations were done in a Tecnai Spirit electron microscope.

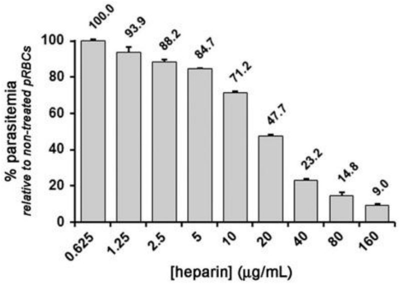

Figure 1. Inhibition by heparin of *P. falciparum in vitro* growth. Heparin was added to RBC/pRBC cocultures at early ring stage and incubated for 48 h before proceeding to parasitemia determination.

Determination of activated partial thromboplastin time (aPTT)

Balb/C female mice were anesthesized for 2–3 min with 1.5%–2% isoflurane vaporized in O_2 prior to intravenous administration via the tail vein of the different heparin formulations. Blood samples (0.5 mL) were subsequently collected terminally under deep isoflurane anesthesia in citrate-containing tubes and spun down, using the resulting plasma to determine aPTT with an S Tart® 4 equipment. Mice assays and humane care of the animals were approved and supervised by the corresponding animal experimentation committee (Laboratory Animal Applied Research Platform, Barcelona Science Park, www.pcb.ub.es/sea-pcb).

Statistical analysis

Data are presented as the mean ± standard deviation of three independent replicates and the corresponding standard errors in histograms are represented by error bars. The parametric T-Student test was used to compare two independent groups when data followed a Gaussian distribution. Differences were considered significant when the *P*-value was ≤ 0.05. Percentages of viability were obtained using non-treated cells as control of survival and IC_{50} values were calculated by nonlinear regression with an inhibitory dose–response model using GraphPad Prism5 software (95% confidence interval).

Results

Characterization of antimalarial and targeting activities of free heparin

In our *P. falciparum* growth inhibition assays commercial heparin from porcine intestinal mucosa showed antimalarial

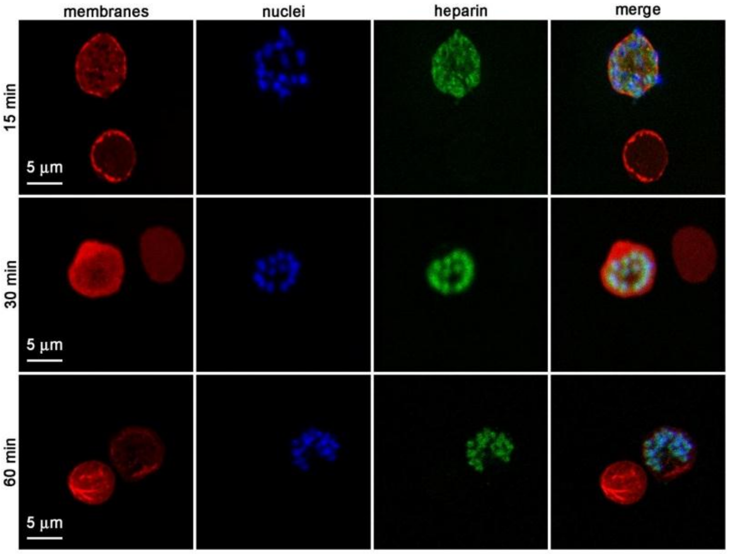

Figure 2. Specific targeting of heparin to pRBCs *vs.* RBCs. Heparin-FITC was added to living cocultures of *P. falciparum*-infected RBCs and non-infected RBCs and incubated for the indicated times before sample preparation for microscopic analysis. Each series shows a pRBC and a non-infected erythrocyte as a control of the specificty of heparin targeting. Free FITC used at the same concentration according to fluorescence intensity was not observed to stain any cells.

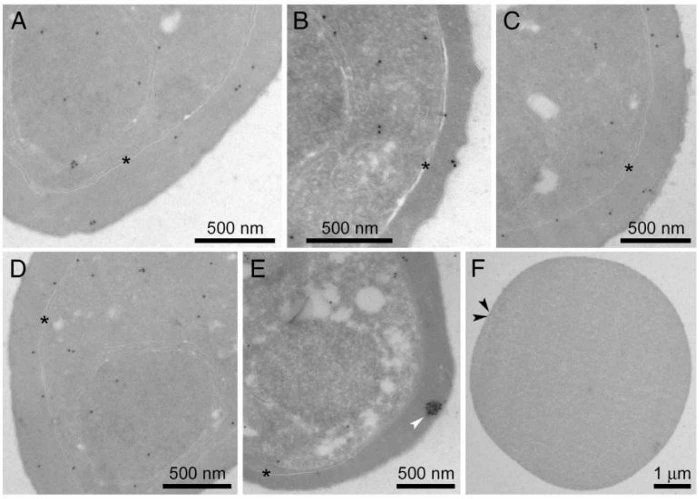

Figure 3. Transmission electron microscope analysis of the subcellular distribution of heparin-FITC added to living *P. falciparum*-infected RBCs. pRBCs **(A-E)** show homogeneus intracellular staining both in the erythrocyte cytosol and inside the parasitophorous vacuole membrane containing the parasites. The white arrowhead in panel **(E)** indicates an electron dense structure intensely stained by secondary gold bead-conjugated antibodies raised against the primary anti-FITC antibodies. A non-parasitized RBC control cell from the same grid **(F)** is completely devoid of staining, except for two gold beads on its periphery (black arrowheads). Asterisks in panels **(A-E)** are placed on the parasitophorous vacuole membrane separating the erythrocyte cytosol from the vacuole inside which the parasite grows.

activity (Figure 1) with an IC_{50} which ranged, depending on the batch used, between 4 and 18 μg/mL, or 0.3 to 1.5 μM considering the nominal molecular mass (M_r 13,000) of the commercial heparin fraction used. In Supplementary Figure 1 is shown a representative example of the flow cytometry dot plots used here for the determination of *P. falciparum* growth inhibition.

Specificity of targeting of heparin toward late form-containing pRBCs *vs.* RBCs had been previously reported,[19] but the results were inconclusive as to whether heparin remains bound at the cell periphery or if it is internalized. Fluorescence microscopy data (Figure 2) reveal that only after 30 min of incubation late-stage living *P. falciparum*-infected RBCs incorporate heparin-FITC in a region adjacent to the DNA of the parasite. In agreement with our previous data, non-infected RBCs were not penetrated by heparin.

Transmission electron microscopy data (Figure 3) confirmed that heparin-FITC added to living *P. falciparum* cultures entered these cells and crossed also the parasitophorous vacuole membrane, being found throughout the cell (Figure 3, *A-D*). However, intracellular heparin locations were not surrounded by a lipid bilayer, suggesting a pRBC entry through a membrane-crossing mechanism not based on endocytic vesicles. Intracellular electron dense structures up to 100 nm across and not enclosed by a lipid bilayer were occasionally found to be stained by gold bead-conjugated secondary antibodies raised against the primary anti-FITC antibody (Figure 3, *E*). Whether they represent entry events of heparin aggregates into pRBCs or artifacts remains to be investigated. Internal controls consisting of non-parasitized erythrocytes eventually found in the same grid where pRBC staining was being observed did seldom show gold beads inside the cell; most beads in these RBCs were in the periphery, likely indicating heparin molecules adhered on the outside the cell.

Fluorescence microscopy examination of mouse blood infected by the rodent malaria parasite *P. yoelii* that had been treated for 90 min with heparin-FITC prior to fixation revealed that heparin exclusively targeted and entered pRBCs (Figure 4, *A*). Free merozoites outside pRBCs were also observed to be targeted by heparin. As a preliminary approximation to elucidate the mechanism responsible for this binding, we were inspired by existing data indicating the binding of GAGs to amyloid structures[30] and the possible existence of an amyloid coat on *Plasmodium* merozoites.[31] Our experimental strategy consisted of incubating for 90 min mouse blood infected with *P. yoelii* mature stages with Congo Red, a dye which upon binding to amyloid fibrils experiences a significant increase in molar extinction coefficient and a shift in maximum absorbance from 484 to 540 nm.[31] We often found colocalization of Congo Red fluorescence and heparin staining on *P. yoelii* free merozoites (Figure 4, *B*), in agreement with the hypothesis that heparin might indeed be interacting with amyloid-prone structures present on the merozoite surface.

Electrostatic conjugation of heparin to liposomes

The specific binding of heparin to pRBCs prompted the exploration of the capacity of heparin as targeting agent of antimalarial drug-loaded nanoparticles directed against *Plasmodium*-infected cells. The electrostatic interaction of heparin with positively charged nanocapsules was explored with the objective of designing the simplest working strategy that could provide a fast and cost-efficient method. As a proof-of-concept model we studied the interaction of heparin with liposomes containing in their formulation the cationic lipid DOTAP (Supplementary Figure 2, *A*). The basic formulation of liposomes consisted of 1,2-dioleoyl-*sn*-glycero-3-phosphatidylcholine (DOPC)/cholesterol in a molar ratio 80:20; in the formulations containing DOTAP, the content of DOPC was decreased proportionally to obtain liposomes containing 1%, 4%, 10%, and 30% DOTAP with the respective formulations DOPC/cholesterol/DOTAP of 79:20:1, 76:20:4, 70:20:10, and 50:20:30. Liposomes containing above 4% DOTAP showed significant antimalarial activity *in vitro* for concentrations higher than 200 μM of total lipid in the culture medium (Supplementary Figure 2, *B*). According to dynamic light scattering analyses, the liposomes measured between 150 and 200 nm, with the highest size and standard deviation for 30% DOTAP-containing liposomes (232 ± 8 nm), which also exhibited the highest polydispersity index (0.16 ± 0.01).

In order to have a first approximation to the optimal DOTAP/heparin ratio we proceeded to test the antimalarial efficacy *in vitro* of two different heparin concentrations as targeting agent of drug-containing liposomes. The heparin concentrations selected were 20 μg/mL (close to the IC_{90} of the corresponding batch), and 125 μg/mL. The liposomes contained different amounts of DOTAP and encapsulated the antimalarial drug primaquine adjusted to be delivered to living pRBC cultures at a concentration of 3 μM, close to its *in vitro* IC_{50}. Primaquine was selected because its high *in vitro* IC_{50} allowed for an immediate and easy sample concentration determination, but also for reasons regarding current needs in antimalarial chemotherapy. In patients with glucose-6-phosphate dehydrogenase (G6PD) deficiency primaquine generally produces a hemolysis which may be severe.[32,33] Such toxicological concerns have led to restrictions in the use of primaquine since the incidence of G6PD genetic anomaly is particularly high in areas where malaria is endemic,[34] a situation that calls for new methods addressed to the targeted delivery of primaquine to pRBCs.

Figure 5 presents an example of such preliminary assays using liposomes containing either 1% or 10% DOTAP, where free 3 μM primaquine had its expected antimalarial activity reducing the viability of pRBCs by *ca.* 50%. The same amount of primaquine delivered as a liposomal formulation without heparin showed a significant decrease in drug efficacy that was not complete likely due to a basal targeting of liposomes toward pRBCs.[8] Electrostatic conjugation of the same liposomes to heparin had different outcomes depending on the respective DOTAP and heparin concentrations. Regardless of DOTAP content, at a high heparin concentration of 125 μg/mL the antimalarial activity of the samples was high and independent of the presence of primaquine; this result suggested that the potential targeting activity of heparin was being masked by its *Plasmodium* growth inhibition capacity. The presence of 20 μg/mL heparin improved the antimalarial activity of primaquine-containing liposomes, although this effect was found to be more pronounced at the lower 1% DOTAP concentration. Taking into account the

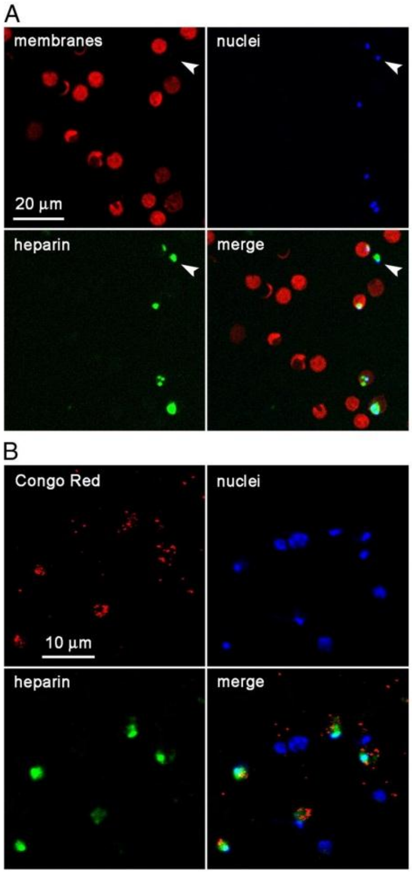

Figure 4. Specific targeting of heparin to the murine malaria species *P. yoelii*. **(A)** Specific binding of heparin to *P. yoelii*-infected pRBCs *vs.* non-infected RBCs in mouse blood. The arrowhead indicates a free merozoite being stained by heparin-FITC. **(B)** Colocalization of Congo Red fluorescence and heparin binding on free merozoites.

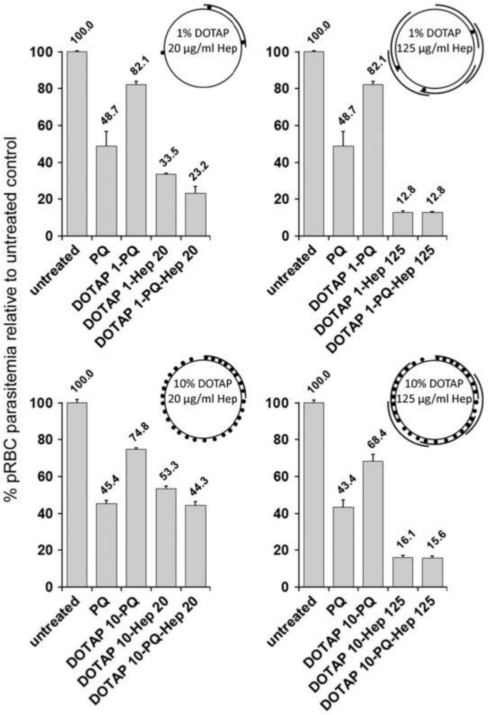

Figure 5. Preliminary study of the antimalarial activity and targeting capacity of heparin electrostatically bound to 1% or 10% DOTAP-containing liposomes. For each liposome–heparin design, the data represent the percentage of *P. falciparum* growth inhibition *in vitro* relative to an untreated pRBC culture. Heparin was preincubated with liposomes for 90 min before adding them to *Plasmodium* cultures, to obtain final heparin concentrations of 20 and 125 µg/mL. The cartoons illustrate the relative amounts of DOTAP (*dots*) and heparin (*lines*) in liposomes.

preliminary data obtained in this type of assays we decided to select heparin concentrations below 20 µg/mL and liposomes containing 4% DOTAP (with a *Z* potential of *ca.* 0.5). This amount of DOTAP in the liposomes was observed to have no cytotoxic effects on human umbilical vein endothelial cell cultures up to 250 µM total lipid (data not shown).

ITC assays were performed to establish an upper limit for the heparin concentration in order to minimize its dissociation from liposomes and thus reduce its anticoagulant activity in free form. The corresponding ITC data (Supplementary Figure 3) indicate a complete sigmoidal endothermic binding isotherm for the interaction of heparin with liposomes containing 4% DOTAP, with 50% saturation at a molar ratio lipid/heparin of about 0.3, which corresponds to about 2 mg/mL heparin for a concentration of 50 µM total lipid.

Study of the antimalarial and targeting activities of heparin conjugated to primaquine-loaded liposomes

We have explored two different protocols for the preparation of 4% DOTAP liposome + heparin conjugates, either without or with an ultracentrifugation step for the removal of heparin not bound to liposomes. In preparation for future preclinical assays, both types of samples containing different liposome/heparin ratios were tested for their anticoagulation activity *in vivo* by determination of the activated partial thromboplastin time (aPTT) in mice. The results presented in Table 1 show that heparin, either free or added to liposomes, had anticoagulant activity *in vivo* above 4 µg/mL for a range of total lipid concentration in blood from 50 to 250 µM. On the other hand, 4% DOTAP liposome + heparin conjugates ultracentrifuged to remove unbound heparin did not show anticoagulant activity. Heparin determination assays indicated that in these samples the concentration of heparin was significantly reduced, suggesting

Table 1
In vivo anticoagulation activity in mouse blood of different heparin concentrations, free or electrostatically conjugated to liposomes.

	aPTT (seconds)		
	Free heparin	50 μM liposomes-heparin (unbound heparin not removed)	250 μM liposomes-heparin (unbound heparin removed) *[determined heparin content]*
PBS control	36.5 ± 2.9	31.3 ± 2.3	36.5 ± 2.9
20 μg/mL heparin	>120	>120	35.8 ± 2.4 *[2.6 μg/mL]*
4 μg/mL heparin	55.6 ± 19.5	>120	36.3 ± 2.9 *[1.0 μg/mL]*
1 μg/mL heparin	37.8 ± 3.0	32.6 ± 1.2	35.1 ± 1.5 *[0.6 μg/mL]*

The concentrations correspond to the amounts of total lipid and heparin in the blood of mice. Where unbound heparin was not removed, the data presented are for the samples expected to contain the highest free heparin amount, corresponding to 50 μM total lipid in blood. Where unbound heparin was removed by ultracentrifugation, the data presented are for the samples expected to contain the highest heparin amount, corresponding to 250 μM total lipid in blood; for these samples the determined heparin content is provided. Gray shadow indicates those samples with anticoagulant activity.

that the amounts detected correspond to heparin bound to liposome surfaces. The maximum blood concentration of heparin present in centrifuged samples was 2.6 μg/mL, in agreement with their lack of anticoagulant activity. These results have been confirmed by *in vitro* coagulation tests (Supplementary Table 1).

When preincubated with liposomes containing 4% DOTAP, heparin manifested a dual antimalarial and drug-loaded liposome targeting activity (Figure 6, *A*). At the final concentrations of 1, 4, and 20 μg/mL the *Plasmodium* growth inhibition activity of free heparin was not significantly different from that of the same heparin amounts conjugated to drug-free liposomes. However, when the same amounts of heparin were bound to primaquine-containing liposomes the percentage of parasitemia dropped from 77.8% in the absence of heparin to, respectively, 19.0%, 15.7%, and 13.8%. A significant fraction of this antimalarial activity was that of heparin itself, as indicated by the reduced parasitemia found in heparin–liposomes devoid of drug. However, the remaining activity must be due to the pRBC targeting of drug-containing heparin–liposomes, which represents the main fraction at the non-anticoagulant heparin concentration of 1 μg/mL. Considering that flow cytometry detects also the labeled DNA of dead parasites, these values might be underestimating the antimalarial activity of the nanovectors because pRBCs containing non-viable *Plasmodium* cells contribute to parasitemia counts. The highest antimalarial activities obtained with different heparin batches resulted in parasitemias around 1%, slightly below the initial 1.5%, suggesting that most pathogens were killed inside pRBCs, whereas free merozoites released from pRBCs through egression or upon cell burst went undetected by our flow cytometry assay. In either case, failure of non-viable parasites to invade and proliferate inside new RBCs results in lower parasitemias compared to control untreated samples, being 9% of the control (corresponding to ca. 1% vs. 11.1% parasitemia in the untreated sample) the maximum inhibition obtained in this work with an extremely high heparin concentration (160 μg/mL; Figure 1).

When heparin not bound to liposomes was removed by ultracentrifugation, the resulting sample presumably containing only liposome-bound heparin was still capable of exhibiting antimalarial activity in itself and of acting as targeting element of primaquine-containing liposomes (Figure 6, *B*). Remarkably, samples containing as little as 0.6 μg/mL heparin, well below its IC_{50}, improved by >30% the antimalarial activity of liposome-encapsulated primaquine.

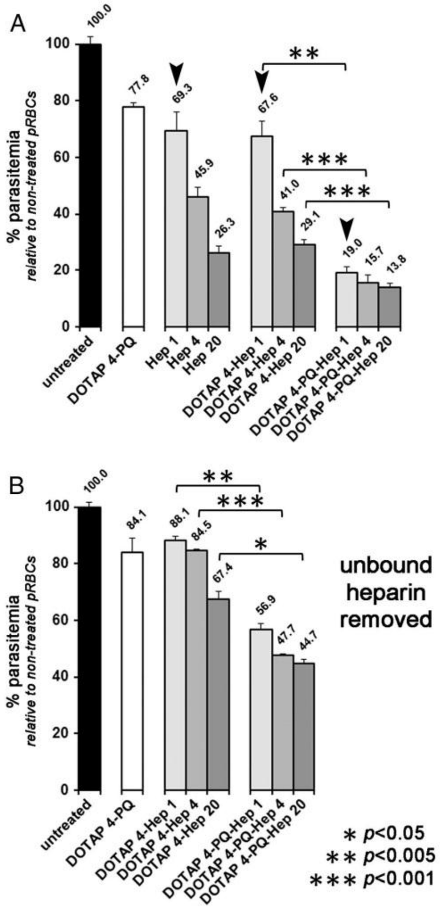

Figure 6. Antimalarial activity and targeting capacity of different initial amounts of heparin (1, 4, and 20 μg/mL) electrostatically bound to liposomes containing 4% DOTAP and encapsulating primaquine. The amount of heparin-free encapsulated primaquine in each experiment was selected to have around 20% of antimalarial activity to be able to detect possible improvements in heparin-containing samples. **(A)** Unbound heparin not removed (50 μM total lipid). Arrowheads indicate those samples corresponding to the non-anticoagulant heparin concentration of 1 μg/mL. **(B)** Unbound heparin removed (250 μM total lipid), where the indicated initial heparin concentrations (1, 4, and 20 μg/mL) correspond to the respective determined amounts of 0.6, 1.0, and 2.6 μg/mL.

Discussion

GAGs have low immunogenicity due mainly to their endogenous nature. Because heparin is eventually found in the blood, *Plasmodium* must have been exposed to it during its long coevolutionary history with humans and yet parasite resistance has not been described so far.[18] The antimalarial mechanism of heparin might be related to its described activity in blocking erythrocyte invasion,[35,36] in agreement with recent proteomic analyses revealing heparin-binding proteins in the *P. falciparum* merozoite[37] and in pRBC membranes.[38] The observed Congo Red fluorescence colocalization with heparin in free parasites is consistent with the described capacity of glycosaminoglycans to bind amyloid.[39,40]

During its intraerythrocytic growth *Plasmodium* modifies the membrane permeability of the host cell in order to uptake nutrients from the plasma, dispose of metabolic waste, and create and maintain electrochemical ion gradients. These changes are of interest from the point of view of antimalarial chemotherapy as possible routes for targeting cytotoxic agents into the intracellular parasite.[41] *Plasmodium* induces new permeation pathways (NPPs) that confer to the pRBC an increased permeability to a wide range of particles up to diameters of 70 nm.[42] NPPs have been found to be nonsaturable within physiologically relevant concentration ranges for all solutes for which kinetic measurements have been made and the activation energy for the transport through them is typical of a diffusive process.[43] In *P. falciparum*, NPPs are induced in the parasitized cell between 10 and 20 h post-invasion, in agreement with the observed intra-pRBC localization of heparin after trophozoite stage. Previous work has suggested that pRBCs become leaky prior to rupture,[44] and that the site of parasite invasion on the membrane never completely closes, leaving a pore and a small duct extending into the parasitophorous vacuole.[42] Such an anomalous membrane has been proposed as an explanation for the observed permeability of pRBCs to certain macromolecules.[45] The efficacy of carriers and/or drugs whose entry would be based on this type of processes could be expected to be less affected by the high antigenic variability of *Plasmodium*.[46] A vehiculation not based on specific interactions of the type ligand-receptor as those found between proteins is consistent with the recognition of pRBCs across widely diverging malaria parasites infecting humans and rodents which has been observed *in vitro* for heparin. In addition to suggesting the possibility of recognizing several *Plasmodium* species, as opposed to the restrictive specificity of antibodies, the good heparin binding to mouse pRBCs will facilitate future *in vivo* assays prior to preclinical studies.

At the non-anticoagulating concentration of 1 μg/mL heparin, the improvement in the activity of liposome-encapsulated primaquine is *ca.* three-fold, of which the majority corresponds to the targeting activity of heparin. Specific pRBC-targeting antibodies used at very high concentrations were capable of improving two-fold the activity of the liposome-encapsulated antimalarial drug chloroquine.[47] These data indicate that relatively low amounts of heparin as a targeting molecule electrostatically attached to nanocarriers can substitute for antibodies in future antimalarial nanotherapies having a reduced anticoagulation activity. Foreseeably, even higher antimalarial and targeting activities might be achieved using higher heparin concentrations, albeit at the cost of an increased hemorrhagic risk. However, several strategies seem to offer reasonable solutions to this problem. First, depolymerized heparin lacking anticoagulant activity has been found to disrupt rosette formation and pRBC cytoadherence *in vitro* and *in vivo* in animal models and in fresh parasite isolates.[36,48] These findings suggest that heparin fragments are worthy of exploration as substitutes for full-length heparin in the design of future nanovectors. Second, the DOTAP content of liposomes in this work has been 4% because higher amounts had significant toxicity for *Plasmodium*, which would mask our study of heparin activity. However, nothing precludes the use of higher DOTAP amounts that could confer a synergistic effect by adding to an increased heparin content the antimalarial activity of the lipid. Third, there is also evidence of non-anticoagulant activity of heparin when covalently immobilized on a substrate.[49] Although electrostatic conjugation is more likely to preserve the antimalarial and pRBC targeting activities of heparin, covalent binding can represent a valid alternative approach. Surface plasmon resonance biosensor studies showed that covalent binding of heparin through its carboxyl groups dramatically reduced the interaction of heparin with antithrombin III,[50] whereas attachment through the reducing amino terminus did not significantly affect it and heparin immobilized via intrachain naturally occurring unsubstituted amine residues had intermediate binding capacity. It is likely then that future nanovector designs based on covalently bound heparin fragments will offer good perspectives of maintaining acceptable nanovector antimalarial activity with reduced hemorrhagic side effects.

The data presented here show that an economically affordable molecule like heparin can be easily and rapidly conjugated to drug-containing nanovessels, maintaining significant antimalarial activity and also pRBC targeting which contributes to lower the drug IC_{50}. The property of heparin to penetrate pRBCs can be of use in the design of new cost-effective methods for the vehiculation of drugs to intracellular components of the pathogen. These results represent a promising starting point in the context of the current malaria socioeconomic and pharmacotherapy scenario outlined above. Heparin might be the spearhead of a new generation of GAG-related molecules exhibiting a synergistic activity as antimalarials and as targeting molecules for the localized delivery of drugs to *Plasmodium*-infected cells.

Acknowledgments

We acknowledge the support of the Scientific and Technological Centres at the University of Barcelona (CCiT-UB). We are indebted to the Cytomics unit of the Institut d'Investigacions Biomèdiques August Pi i Sunyer (IDIBAPS) for technical help.

Appendix A. Supplemenatry data

Supplementary data to this article can be found online at http://dx.doi.org/10.1016/j.nano.2014.06.002.

References

1. World Health Organization. *World Malaria Report*; 2013.
2. Tuteja R. Malaria - an overview. *FEBS J* 2007;**274**(18):4670-9.
3. Griffith KS, Lewis LS, Mali S, Parise ME. Treatment of malaria in the United States: a systematic review. *JAMA* 2007;**297**(20):2264-77.
4. Daily JP. Antimalarial drug therapy: the role of parasite biology and drug resistance. *J Clin Pharmacol* 2006;**46**(12):1487-97.
5. Fidock DA, Rosenthal PJ, Croft SL, Brun R, Nwaka S. Antimalarial drug discovery: efficacy models for compound screening. *Nat Rev Drug Discov* 2004;**3**(6):509-20.
6. Kappe SH, Vaughan AM, Boddey JA, Cowman AF. That was then but this is now: malaria research in the time of an eradication agenda. *Science* 2010;**328**(5980):862-6.
7. Murambiwa P, Masola B, Govender T, Mukaratirwa S, Musabayane CT. Anti-malarial drug formulations and novel delivery systems: a review. *Acta Trop* 2011;**118**(2):71-9.
8. Urbán P, Estelrich J, Cortés A, Fernàndez-Busquets X. A nanovector with complete discrimination for targeted delivery to *Plasmodium falciparum*-infected versus non-infected red blood cells *in vitro*. *J Control Release* 2011;**151**(2):202-11.
9. Beeson JG, Andrews KT, Boyle M, Duffy MF, Choong EK, Byrne TJ, et al. Structural basis for binding of *Plasmodium falciparum* erythrocyte membrane protein 1 to chondroitin sulfate and placental tissue and the influence of protein polymorphisms on binding specificity. *J Biol Chem* 2007;**282**(31):22426-36.
10. Juillerat A, Igonet S, Vigan-Womas I, Guillotte M, Gangnard S, Faure G, et al. Biochemical and biophysical characterisation of DBL1α_1-varO, the rosetting domain of PfEMP1 from the VarO line of *Plasmodium falciparum*. *Mol Biochem Parasitol* 2010;**170**(2):84-92.
11. Boyle MJ, Richards JS, Gilson PR, Chai W, Beeson JG. Interactions with heparin-like molecules during erythrocyte invasion by *Plasmodium falciparum* merozoites. *Blood* 2010;**115**(22):4559-68.
12. Sheehy TW, Reba RC. Complications of falciparum malaria and their treatment. *Ann Intern Med* 1967;**66**(4):807-9.
13. Smitskamp H, Wolthuis FH. New concepts in treatment of malignant tertian malaria with cerebral involvement. *BMJ* 1971;**1**:714-6.
14. Jaroonvesama N. Intravascular coagulation in falciparum malaria. *Lancet* 1972;**1**:221-3.
15. Munir M, Tjandra H, Rampengan TH, Mustadjab I, Wulur FH. Heparin in the treatment of cerebral malaria. *Paediatr Indones* 1980;**20**:47-50.
16. Rampengan TH. Cerebral malaria in children. Comparative study between heparin, dexamethasone and placebo. *Paediatr Indones* 1991;**31**:59-66.
17. World Health Organization Malaria Action Programme. Severe and complicated malaria. *Trans R Soc Trop Med Hyg* 1986;**80**(Suppl):3-50.
18. Marchisio MA, Tongo T, Ferruti P. A selective de-heparinizer filter made of new cross-linked polymers of a poly-amido-amine structure. *Experientia* 1973;**1**(29):93-5.
19. Valle-Delgado JJ, Urbán P, Fernàndez-Busquets X. Demonstration of specific binding of heparin to *Plasmodium falciparum*-infected vs. non-infected red blood cells by single-molecule force spectroscopy. *Nanoscale* 2013;**5**(9):3673-80.
20. Hinterdorfer P, Baumgartner W, Gruber HJ, Schilcher K, Schindler H. Detection and localization of individual antibody–antigen recognition events by atomic force microscopy. *Proc Natl Acad Sci U S A* 1996;**93**(8):3477-81.
21. Kienberger F, Kada G, Mueller H, Hinterdorfer P. Single molecule studies of antibody–antigen interaction strength *versus* intra-molecular antigen stability. *J Mol Biol* 2005;**347**(3):597-606.
22. Morfill J, Blank K, Zahnd C, Luginbühl B, Kühner F, Gottschalk K-E, et al. Affinity-matured recombinant antibody fragments analyzed by single-molecule force spectroscopy. *Biophys J* 2007;**93**(10):3583-90.
23. Fernàndez-Busquets X. Heparin-functionalized nanocapsules: enabling targeted delivery of antimalarial drugs. *Future Med Chem* 2013;**5**(7):737-9.
24. MacDonald RC, MacDonald RI, Menco BP, Takeshita K, Subbarao NK, Hu LR. Small-volume extrusion apparatus for preparation of large, unilamellar vesicles. *Biochim Biophys Acta* 1991;**1061**(2):297-303.
25. Frazier SB, Roodhouse KA, Hourcade DE, Zhang L. The quantification of glycosaminoglycans: a comparison of HPLC, carbazole, and Alcian Blue methods. *Open Glycosci* 2008;**1**:31-9.
26. Cranmer SL, Magowan C, Liang J, Coppel RL, Cooke BM. An alternative to serum for cultivation of *Plasmodium falciparum in vitro*. *Trans R Soc Trop Med Hyg* 1997;**91**(3):363-5.
27. Lambros C, Vanderberg JP. Synchronization of *Plasmodium falciparum* erythrocytic stages in culture. *J Parasitol* 1979;**65**(3):418-20.
28. Dluzewski AR, Ling IT, Rangachari K, Bates PA, Wilson RJ. A simple method for isolating viable mature parasites of *Plasmodium falciparum* from cultures. *Trans R Soc Trop Med Hyg* 1984;**78**(5):622-4.
29. Urbán P, Valle-Delgado JJ, Mauro N, Marques J, Manfredi A, Rottmann M, et al. Use of poly(amidoamine) drug conjugates for the delivery of antimalarials to Plasmodium. *J Control Release* 2014;**177**:84-95.
30. Valle-Delgado JJ, Alfonso-Prieto M, de Groot NS, Ventura S, Samitier J, Rovira C, et al. Modulation of Aβ_{42} fibrillogenesis by glycosaminoglycan structure. *FASEB J* 2010;**24**(11):4250-61.
31. Adda CG, Murphy VJ, Sunde M, Waddington LJ, Schloegel J, Talbo GH, et al. *Plasmodium falciparum* merozoite surface protein 2 is unstructured and forms amyloid-like fibrils. *Mol Biochem Parasitol* 2009;**166**(2):159-71.
32. Beutler E, Duparc S. Glucose-6-phosphate dehydrogenase deficiency and antimalarial drug development. *Am J Trop Med Hyg* 2007;**77**(4):779-89.
33. Burgoine KL, Bancone G, Nosten F. The reality of using primaquine. *Malar J* 2010;**9**(1):376.
34. Chan TK, Todd D, Tso SC. Drug-induced haemolysis in glucose-6-phosphate dehydrogenase deficiency. *BMJ* 1976;**2**:1227-9.
35. Xiao L, Yang C, Patterson PS, Udhayakumar V, Lal AA. Sulfated polyanions inhibit invasion of erythrocytes by plasmodial merozoites and cytoadherence of endothelial cells to parasitized erythrocytes. *Infect Immun* 1996;**64**(4):1373-8.
36. Vogt AM, Pettersson F, Moll K, Jonsson C, Normark J, Ribacke U, et al. Release of sequestered malaria parasites upon injection of a glycosaminoglycan. *PLoS Pathog* 2006;**2**(9):853-63.
37. Kobayashi K, Takano R, Takemae H, Sugi T, Ishiwa A, Gong H, et al. Analyses of interactions between heparin and the apical surface proteins of *Plasmodium falciparum*. *Sci Rep* 2013;**3**:3178.
38. Zhang Y, Jiang N, Lu H, Hou N, Piao X, Cai P, et al. Proteomic analysis of *Plasmodium falciparum* schizonts reveals heparin-binding merozoite proteins. *J Proteome Res* 2013;**12**(5):2185-93.
39. Díaz-Nido J, Wandosell F, Avila J. Glycosaminoglycans and β-amyloid, prion and tau peptides in neurodegenerative diseases. *Peptides* 2002;**23**(7):1323-32.
40. McLaurin J, Fraser PE. Effect of amino-acid substitutions on Alzheimer's amyloid-β peptide-glycosaminoglycan interactions. *Eur J Biochem* 2000;**267**(21):6353-61.
41. Kirk K. Membrane transport in the malaria-infected erythrocyte. *Physiol Rev* 2001;**81**(2):495-537.
42. Goodyer ID, Pouvelle B, Schneider TG, Trelka DP, Taraschi TF. Characterization of macromolecular transport pathways in malaria-infected erythrocytes. *Mol Biochem Parasitol* 1997;**87**(1):13-28.
43. Staines HM, Ellory JC, Kirk K. Perturbation of the pump-leak balance for Na(+) and K(+) in malaria-infected erythrocytes. *Am J Physiol Cell Physiol* 2001;**280**(6):C1576-87.
44. Lyon JA, Carter JM, Thomas AW, Chulay JD. Merozoite surface protein-1 epitopes recognized by antibodies that inhibit *Plasmodium falciparum* merozoite dispersal. *Mol Biochem Parasitol* 1997;**90**(1):223-34.
45. Bergmann-Leitner ES, Duncan EH, Angov E. MSP-1p42-specific antibodies affect growth and development of intra-erythrocytic parasites of *Plasmodium falciparum*. *Malar J* 2009;**8**:183-94.
46. Rovira-Graells N, Gupta AP, Planet E, Crowley VM, Mok S, Ribas de Pouplana L, et al. Transcriptional variation in the malaria parasite *Plasmodium falciparum*. *Genome Res* 2012;**22**(5):925-38.

47. Urbán P, Estelrich J, Adeva A, Cortés A, Fernàndez-Busquets X. Study of the efficacy of antimalarial drugs delivered inside targeted immunoliposomal nanovectors. *Nanoscale Res Lett* 2011;**6**:620.
48. Leitgeb AM, Blomqvist K, Cho-Ngwa F, Samje M, Nde P, Titanji V, et al. Low anticoagulant heparin disrupts *Plasmodium falciparum* rosettes in fresh clinical isolates. *Am J Trop Med Hyg* 2011;**84**(3):390-6.
49. Miura Y, Aoyagi S, Kusada Y, Miyamoto K. The characteristics of anticoagulation by covalently immobilized heparin. *J Biomed Mater Res* 1980;**14**(5):619-30.
50. Osmond RIW, Kett WC, Skett SE, Coombe DR. Protein–heparin interactions measured by BIAcore 2000 are affected by the method of heparin immobilization. *Anal Biochem* 2002;**310**(2):199-207.

Supplementary Data

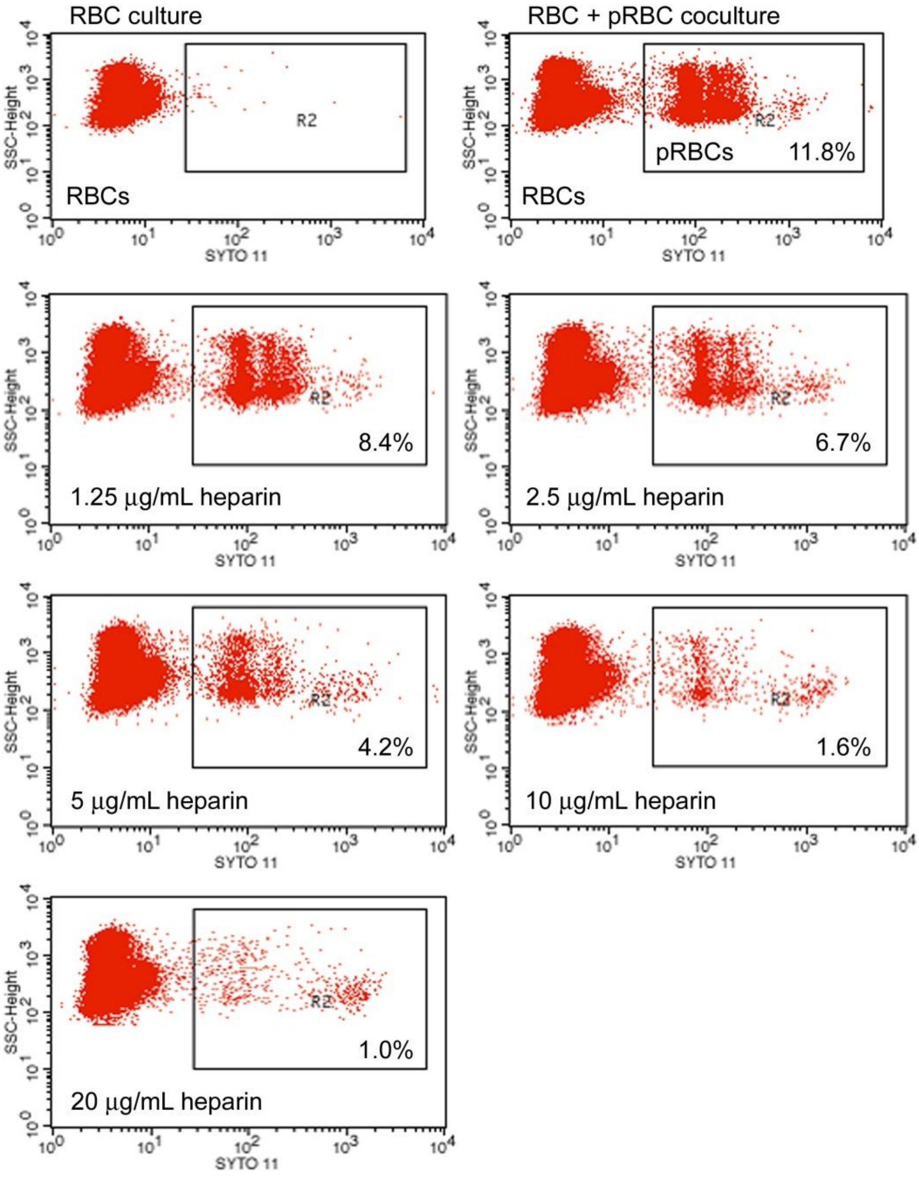

Supplementary Figure 1. Representative flow cytometry dot plots used for the determination of *P. falciparum* growth inhibition. The two upper panels show plots corresponding to RBCs alone (left) and RBC+pRBC cocultures. The other five panels correspond to RBC+pRBC cocultures treated for 48 h with the indicated heparin concentrations before proceeding to parasitemia determination. The percentages indicate the respective fractions of pRBCs relative to [RBCs+pRBCs]. The IC_{50} of this particular heparin batch was around 4 µg/mL.

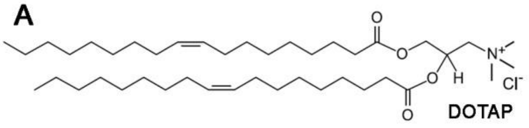

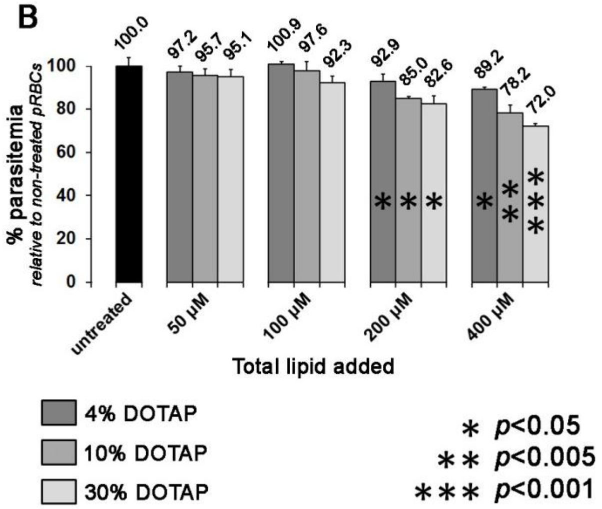

Supplementary Figure 2. Effect of DOTAP on *P. falciparum* viability. (A) DOTAP structure (from Avanti Lipids catalog). (B) *P. falciparum* growth inhibition assay in the presence of different concentrations of liposomes (50, 100, 200, and 400 μM total lipid) containing increasing DOTAP amounts (4, 10, and 30% of total lipid).

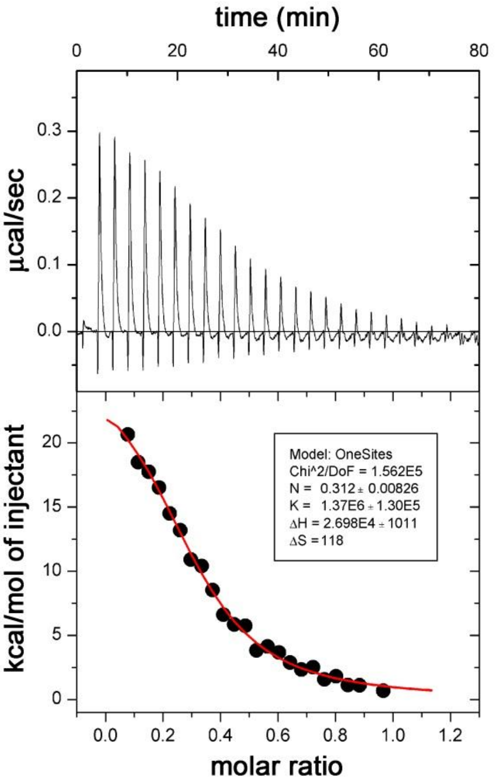

Supplementary Figure 3. ITC study in PBS of the interaction heparin-liposomes containing 4% DOTAP. Aliquots of a 0.05 mM heparin solution were added to a 0.01 mM total lipid solution in the reaction cell.

Supplementary Table 1. PT1/Quick *in vitro* coagulation test of different heparin concentrations, free or electrostatically conjugated to liposomes. The concentrations correspond to the amounts of total lipid and heparin in the test tube. Where unbound heparin was not removed, the data presented are for the samples expected to contain the highest free heparin amount, corresponding to 50 µM total lipid. Where unbound heparin was removed by ultracentrifugation, the data presented are for the samples expected to contain the highest heparin amount, corresponding to 250 µM total lipid; for these samples the determined heparin content is provided. Shadowed in grey are indicated those samples with anticoagulant activity.

	PT1/Quick (%)		
	Free heparin	50 µM liposomes-heparin (unbound heparin not removed)	250 µM liposomes-heparin (unbound heparin removed) *[determined heparin content]*
PBS control	**101.0**	**101.0**	**101.0**
20 µg/mL heparin	**<25**	**<25**	**95.2** *[2.6 µg/mL]*
4 µg/mL heparin	**64.1**	**66.2**	**109.4** *[1.0 µg/mL]*
1 µg/mL heparin	**102.9**	**102.9**	**111.8** *[0.6 µg/mL]*

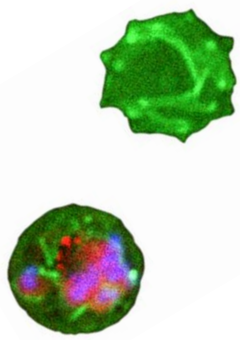

Article 2

ARTICLE 2

Article 2: Marine organism sulfated polysaccharides exhibiting significant antimalarial activity and inhibition of red blood cell invasion by *Plasmodium*.

Taking into account the ceaseless need for new antimalarials and the high anticoagulation activity of heparin which hinders its use on antimalarial therapies, we explored the possibility of using sulfated polysaccharides derived from marine organisms that present a chemical structure similar to that of heparin. In this work we have focused on the antimalarial and anticoagulating activities of FucCSs and fucans from the sea cucumbers *Ludwigothurea grisea* and *Isostichopus badionotus*, of a galactan from the red alga *Botryocladia occidentalis*, and of a branched glycan from the marine sponge *Desmapsamma anchorata*.

We have concluded that most of the sulfated polysaccharides mentioned above present an antimalarial activity comparable to that of heparin but with significantly lower anticoagulant capacity which represents an interesting potential in future malaria therapies. We have not found any correlation between the size of the molecules and the respective antimalarial capacity, but we did find a correlation between anticoagulant action and antimalarial capacity.

Here, we have shown by direct microscopic visualization that the sulfated polysaccharides used in this work inhibit the invasion of RBCs by *P. falciparum* merozoites. These promising results support the belief that this class of marine derived products could be applied as adjunct therapies in the treatment of severe malaria.

ARTICLE 2

Marine Organism Sulfated Polysaccharides Exhibiting Significant Antimalarial Activity and Inhibition of Red Blood Cell Invasion by *Plasmodium*

Joana Marques[1-3], Eduardo Vilanova[4], Paulo A. S. Mourão[4] and Xavier Fernàndez-Busquets[1-3]*

[1]Nanomalaria Group, Institute for Bioengineering of Catalonia (IBEC), Barcelona, Spain; [2]Barcelona Institute for Global Health (ISGlobal, Hospital Clínic-Universitat de Barcelona), Barcelona, Spain; [3]Nanoscience and Nanotechnology Institute (IN2UB), University of Barcelona, Spain; [4]Hospital Universitário Clementino Fraga Filho and Instituto de Bioquímica Médica, Universidade Federal do Rio de Janeiro, Brazil

*Corresponding author. Tel: +34-93-2275400 (ext. 4581); Fax: +34-93-3129410; E-mail: xfernandez_busquets@ub.edu

Running title: Antimalarial sulfated polysaccharides

Keywords: heparin; malaria; *Plasmodium falciparum*; *Plasmodium yoelii*

Abstract

The significant antimalarial activity of heparin, against which there are no resistances known, has not been therapeutically exploited due to its potent anticoagulating activity. Marine organisms are a rich source of heparin-like sulfated polysaccharides whose potential medical use has been largely neglected. We have explored the antimalarial capacity of fucosylated chondroitin sulfates and fucans from the sea cucumbers *Ludwigothurea grisea* and *Isostichopus badionotus*, of a galactan from the red alga *Botryocladia occidentalis*, and of a glycan from the marine sponge *Desmapsamma anchorata*. *In vitro* growth inhibition assays of *Plasmodium falciparum* cultures and clotting assays revealed a correlation between sulfated polysaccharide antimalarial and anticoagulant activities. Confocal fluorescence microscopy analysis indicated that heparin enters *Plasmodium*-infected red blood cells, inside which it binds intraerythrocytic parasite merozoites. *In vitro* assays demonstrated significant inhibition of *P. falciparum* growth for most polysaccharides at low-cytotoxic, low-anticoagulant concentrations. This antimalarial activity was found to operate through inhibition of erythrocyte invasion by *Plasmodium*, likely mediated by a coating of the parasite similar to that observed for heparin. *In vivo* four-day suppressive tests showed that the *I. badionotus* fucan was capable of curing *Plasmodium yoelii*-infected mice, and Western blot analysis revealed that the plasma of surviving animals contained antibodies against *P. yoelii* antigens. The retarded invasion mediated by sulfated polysaccharides, and the ensuing prolonged exposure of *Plasmodium* to the immune system, can be applied to the design of new therapeutic/vaccination approaches against malaria where heparin-related polysaccharides of low anticoagulating activity could play a dual synergistic role as antimalarial drugs and as vaccine adjuvants.

Author Summary

Malaria is a potentially lethal parasitic disease against which most drugs in use have already induced the evolution of resistance in the pathogen, the protist *Plasmodium spp*. Perhaps the only exception to this is the polysaccharide heparin, whose antimalarial activity has so far no resistant strains reported, although the anticoagulant activity of heparin has hampered its clinical application to malaria due to haemorrhagic side-effects. From several marine organisms can be extracted in abundance heparin-related sulfated polysaccharides having low clotting activity. We have investigated *in vitro* and *in vivo* the antimalarial activity of several of these compounds, and found that most of them inhibit significantly the growth of *Plasmodium* at concentrations where no toxic or anticoagulant effects are manifested. The antiplasmodial activity of marine sulfated polysaccharides has been found to operate by inhibiting the entry of *Plasmodium* into its host cell, the erythrocyte. The resulting prolonged exposure of the parasite to the blood circulating cells allows more time for the building of an immune response in the infected person. This dual activity of sulfated polysaccharides as antimalarial drugs and as boosters of immune responses offers interesting perspectives for the development of new antimalarial strategies based on these compounds.

Introduction

Among the infectious diseases, malaria ranks probably first in the perversity of its causal agent, the protist *Plasmodium spp*. This parasite distributes its life cycle [1] between two hosts, humans and the females of certain species of mosquitoes from the genus *Anopheles*. Following a mosquito bite, in a matter of minutes sporozoites enter hepatocytes, where they will develop and replicate into thousands of merozoites that are released into the blood circulation to invade red blood cells (RBCs). Because RBCs are unable to process and present antigens, early intraerythrocytic ring stages remain invisible to the immune system until the late stages trophozoites and schizonts develop and significantly modify the parasitized RBC (pRBC) plasma membrane to meet their needs for membrane transport processes [2]. Even then, the proteins exported to the pRBC plasma membrane have a very high antigenic variation [3] which leads to waves of parasitemia and persistent infections despite antibody-mediated immune pressure. Erythrocytes infected with mature stages of the malaria parasite bind to endothelial cells in the capillaries of tissues in a phenomenon known as sequestration, which allows *Plasmodium* to replicate while evading splenic clearance [1]. pRBCs can also adhere to non-infected RBCs giving rise to rosettes [4], and they can form clumps through platelet-mediated binding to other pRBCs. These events, which may lead to occlusion of the microvasculature, are thought to play a major role in the fatal outcome of severe malaria. Because the blood-stage infection is responsible for all symptoms and pathologies of malaria, pRBCs have traditionally been a main chemotherapeutic target [5].

Negatively charged polysaccharides, such as heparin, chondroitin and dextran sulfates, fucoidan, and the nonsulfated glycosaminoglycan (GAG) hyaluronan, block cytoadhesion of pRBCs to various host receptors [6-9] and disrupt *P. falciparum* rosettes [10,11]. Heparin and related sulfated polysaccharides possess antimalarial activity that has been described to operate through inhibition of RBC invasion by merozoites [8,12-15]. Proteomic analysis has revealed that heparin interacts with multiple apical surface proteins in *P. falciparum* merozoites [16,17], likely blocking their association with the erythrocyte membrane after initial attachment. Naturally acquired immunity to malaria is largely directed against extracellular merozoites [18], but currently there are no drugs targeting erythrocyte invasion by *Plasmodium*

[19], although some candidates have been proposed [20]. The potential use of heparin as drug in malaria therapy [21-25] has been hindered by its high anticoagulation and bleeding properties [26] and by the potential risk of infection since some GAGs are obtained from mammals. As an interesting alternative, non-mammalian marine organisms are a rich source of unique sulfated polysaccharides, some of them with structures resembling pRBC-binding GAGs [27-29]. The fucosylated chondroitin sulfate (FucCS) from the echinoderm *Ludwigothurea grisea* had been shown to have serpin-unrelated anticoagulant properties [30,31], which differ from the serpin-dependent anticoagulant mechanism of mammalian heparins. Former data showing dissociation of the anticoagulant, bleeding, and antithrombin effects of *L. grisea* FucCS [32], together with recent results revealing its inhibition of *P. falciparum* cytoadhesion and growth [13], suggest that marine sulfated glycans might offer interesting alternatives to heparin for future antimalarial therapies. To trace correlations between the structure of these new sulfated polysaccharides and their inhibition of *Plasmodium* growth, we have examined several compounds with well-defined structures, determining the antimalarial and anticoagulating activities of FucCSs and sulfated fucans from the sea cucumbers *L. grisea* [28,33] and *Isostichopus badionotus*, of a sulfated galactan from the red alga Botryocladia occidentalis, and of a sulfated glycan from the marine sponge *Desmapsamma anchorata*. Most of these polysaccharides contain sulfated fucose units in a well-defined repetitive sequence.

Results

Characterization of sulfated polysaccharide size and integrity

I. badionotus FucCS has simple branches of sulfated α-fucose (Fig. 1a), composed of a single monosaccharide unit, either disulfated at positions 2 and 4 (~90%) or exclusively 4-sulfated (~10%) [34]. *L. grisea* FucCS has more complex branching structures, mostly composed of disaccharide units of α-fucose, non-sulfated and 3-sulfated at the nonreducing and reducing ends, respectively. This FucCS also has small amounts of branches composed of single α-fucose units, either 2,4-disulfated (~27%) or 2,3-disulfated (~20%) [34]. The linear sulfated fucans from these echinoderms (Fig. 1b) contain repetitive tetrasaccharide sequences, defined by the patterns of sulfation at positions 2 and 4 [35,36], which differ exclusively in the sulfation of the second residue of the tetrasaccharide: 2-sulfated in *I. badionotus* and non-sulfated in *L. grisea*. Unlike the majority of sulfated galactans from red algae, that from *B. occidentalis* (Fig. 1c) has a relatively simple structure, varying only in the sulfation pattern of its units [37]. The sponge glycan used here (Mr ~200 kDa) has its structure only partially elucidated; preliminary gas chromatography/mass spectroscopy analysis indicated that it is a heteropolysaccharide composed of glucose (75%), fucose (17%) and galactose (8%), with a molar ratio sulfate:total sugar of ~1.5 (data not shown). Integrity of these molecules was analyzed by polyacrylamide gel electrophoresis (Fig. 2), and the result obtained was found to be consistent with the respective approximate molecular masses calculated by size exclusion chromatography after polysaccharide purification from their natural sources, indicating the absence of significant degradation. The bands observed in 6% polyacrylamide gels exhibited a certain degree of size polydispersity, as it is typical of this group of compounds.

Antimalarial and anticoagulating activities *in vitro* of sulfated polysaccharides

The antimalarial activity of the polysaccharides was analyzed in *in vitro* cultures of *P. falciparum* (Fig. 3a), revealing for most of them a significant capacity for the inhibition of the parasite's growth, with IC50s between 2.3 and 20.3 μg/mL. These activities were similar to those found for different heparin batches (between 4 and 18 µg/mL according to our own data) [38]. The sole exception was the *D. anchorata* glycan, whose antimalarial activity was found to be relatively low, with an IC50 of ~270 µg/mL. No correlation was found between *Plasmodium* growth inhibition and polysaccharide size, since the two best activities were for the largest and smallest structures corresponding, respectively, to the *B. occidentalis* galactan (~700 kDa) and the *L. grisea* FucCS (~30 kDa).

When determining the activated partial thromboplastin time *in vitro* for the sulfated polysaccharides used in this work (Fig. 3b), a remarkable correlation was found between antimalarial and anticoagulant activities, with the three best antimalarial polysaccharides (both FucCSs and the galactan) being the most anticoagulant and the three polymers more innocuous for *Plasmodium* (both fucans and the sponge glycan) exhibiting the worst anticoagulant activities. Nevertheless, the anticlotting properties of the marine sulfated polysaccharides used in this work were relatively modest, never reaching values above 18% that of heparin.

Sulfated polysaccharides inhibit *Plasmodium* invasion of red blood cells

Since the antimalarial mechanism of heparin and related polysaccharides had been described to operate through inhibition of the invasion of RBCs by *Plasmodium*, we proceeded to investigate the invasion inhibition activity of the marine sulfated polysaccharides. Late-stage pRBC cultures that had been treated with the different structures revealed upon microscopic examination at 20 and 40 h post-treatment a clear decrease in, respectively, ring and late stages relative to untreated samples (Fig. 4). Polysaccharide-treated samples showed a delayed intraerythrocytic *P. falciparum* cycle as evidenced by the presence of a significant fraction of ring stages relative to untreated controls, which at 40 h within the intraerythrocytic cycle contained, as expected, trophozoites and schizonts only. Quantitative flow cytometry analysis confirmed microscopic observations (Fig. 5), with both FucCSs and the galactan having the highest invasion inhibition potency and both fucans and the sponge glycan being less active, in close correlation with the respective parasite growth inhibition activities reported in Fig. 3.

Heparin binds to merozoites inside pRBCs

The accumulated experimental evidence indicates that invasion inhibition is the antimalarial mechanism through which sulfated polysaccharides operate. However, the short time that free merozoites are present in the blood circulation suggests that the process of parasite binding might occur, at least in part, inside pRBCs. To explore this possibility, as a proof of concept assay, we added fluorescein-labeled heparin to live pRBC cultures and after 30 min of incubation the samples were processed for confocal fluorescence microscopy analysis. The resulting data show that heparin added to living pRBC cultures not only specifically targeted pRBCs vs. RBCs *in vitro*, but it entered live pRBCs and bound intraerythrocytic developing merozoites (Fig. 6).

In vivo antimalarial activity analysis of sulfated polysaccharides

P. yoelii-infected mice were treated iv with polysaccharide doses according to their *in vitro* antimalarial activity, anticoagulation capacity, and unspecific cytotoxicity (Fig. 7a). Except for *D. anchorata* glycan and *L. grisea* fucan, all compounds reduced parasitemia when compared to untreated controls (Fig. 7b), although only *I. badionotus* fucan provided a clear improvement in mice survival, being able to cure one of the treated animals. The parasitemia at day 4 of this particular mouse was 10.4%, indicating a successful infection and therefore a curative effect of the sulfated polysaccharide. Western blot analysis revealed clearly increased IgG levels against *P. yoelii* antigens in the plasma of the *I. badionotus* fucan-treated surviving mouse (Fig. 7c). Such IgG increase was also observed in the surviving CQ-treated animals.

Discussion

Previous work had demonstrated that the presence of sulfate groups was paramount for the binding of *L. grisea* FucCS to human lung endothelial cells and placenta cryosections under static and flow conditions [13], and that sulfated FucCS was capable of inhibiting pRBC cytoadherence in these cell models. Because pRBC sequestration in the microvasculature of vital organs plays a key role in the pathogenesis of cerebral and pregnancy malaria, *L. grisea* FucCS has been proposed for the treatment of severe disease. The crucial role of sulfate groups in the context of malaria was further evidenced by the ability of *L. grisea* FucCS to disrupt *P. falciparum* rosettes, which was significantly lost upon desulfation [13]. Other evidences illustrating the physiological importance of sulfate groups came from reports showing that their removal abolished the antithrombotic and anticoagulant effects of FucCS [32], and that their presence was essential for preserving the inhibitory effects of the polysaccharide in interactions mediated by P- and L-selectin [39].

The *in vitro* data reported here show that polysaccharides containing α-fucose as internal units are less active as antimalarials than polymers having α-fucose as branches, mirroring a similar effect of these structures on anticoagulation activity [40]. The sulfated fucan from *I. badionotus* was found to have a slightly higher *in vitro* antimalarial activity than that of *L. grisea*, probably because of the additional 2-sulfation. The observation that both FucCSs have similar *in vitro* antimalarial effect despite the marked differences in their α-fucose-containing branches suggests that, beyond a minimal threshold, the presence of additional 2,4-disulfated fucose units does not result in higher antiplasmodial potency, as it was similarly reported for the anticoagulant activity of FucCS [34]. *In vivo* data, where the administered doses were chosen considering anticlotting capacity, placed *I. badionotus* fucan as the structure with the best balance between antimalarial and anticoagulating properties.

We have observed that formation of ring-stage parasites was clearly reduced in the presence of sulfated polysaccharides, in agreement with preexisting data indicating that their antimalarial activity unfolds by inhibition of merozoite invasion [7,8,12-15,41-44]. The mechanism through which this invasion blocking proceeds has not been elucidated yet, although the finding that sulfation patterns are crucial for the inhibitory effect of heparin and similar compounds [15], suggests that it is the result not only of nonspecific ionic interactions but also of particular conformations of anions present in the polysaccharides [7]. The consequence of a retarded invasion is the ensuing prolonged exposure of the pathogens to the immune system, which might be applied to the design of new malaria vaccination approaches where heparin-related polysaccharides could play a dual synergistic role as antimalarial drugs and as vaccine adjuvants.

The data presented here indicate that ~13-kDa heparin is capable of penetrating schizont-stage pRBCs and of adsorbing on intracellular parasites before they have completed their intraerythrocytic cycle. Whereas binding of heparin to merozoites has been described to be mediated by multiple protein receptors [16, 17], GAG-pRBC associations are mainly based on interactions with the parasite-derived adhesion, *P. falciparum* erythrocyte membrane protein 1, PfEMP1 [45]. The subsequent internalization of heparin into pRBCs might be an unspecific uptake through the tubulovesicular network induced by *Plasmodium* during its intraerythrocytic growth [46]. Such entry into pRBCs and coating of developing merozoites before they egress, permits the invasion inhibition activity of heparin to be manifested since the first moment when *Plasmodium* cells are free in the blood circulation. This is important regarding possible future therapeutic applications of sulfated polysaccharides; if the observed activity were only exerted upon binding to free merozoites, their rapid invasion of RBCs [47] would severely compromise clinical applications. Because heparin is capable of penetrating live pRBCs and of binding intracellular merozoites, heparin-based antimalarial therapies can be administered during the wide time frame when late stages are present in clinical malaria. Smaller fragments of marine polysaccharides might also have this behavior, although the finding that ~700 kDa *B. occidentalis* galactan has antimalarial activity similar to that of the ~30-40 kDa FucCSs from *L. grisea* and *I. badionotus* suggests that pRBC internalization of the polymers might not be essential for their capacity to inhibit *Plasmodium* growth.

Although remarkable antimalarial activity is obtained *in vitro* at sulfated polysaccharide concentrations below those being highly anticoagulating, this risk can be further minimized using alternative strategies based on the evidence of a significantly reduced anticlotting activity of heparin when covalently immobilized on a substrate [48]. Surface plasmon resonance biosensor studies showed that covalent binding through its carboxyl groups dramatically reduced the interaction of heparin with antithrombin III [49], whereas attachment through the reducing amino terminus did not significantly affect it and heparin immobilized via intrachain naturally occurring unsubstituted amine residues had intermediate binding capacity. Covalent conjugation to nanoparticles can be explored as an interesting approach to reduce potential haemorrhagic side-effects. As it has been shown with heparin [38], antimalarial drugs can be encapsulated in such nanocarriers where sulfated polysaccharides exhibit a dual activity as pRBC targeting molecules and as antimalarial drugs themselves thus potentiating therapeutic activity.

The polysaccharides used in this work do not require fractionation and/or chemical modification after purification [30] and, unlike heparin, are not derived from mammals, thus reducing the risk of contamination by human-affecting pathogens. These compounds are present at high concentrations in marine organisms and can be isolated with relatively high yields of ~1% dry weight. In addition to being less anticoagulant than heparin, they exert their antimalarial activity *in vitro* (and *in vivo* for *I. badionotus* fucan) at concentrations lower than those required to trigger anticlotting effects. FucCS can be satisfactorily administered orally [50], without toxic or cumulative effects in tissue observed after daily doses to animals of 50 mg/kg for 30 days (Mourão, unpublished data), raising hopes that this family of sulfated polysaccharides can enter in the short term the preclinical pipeline of future antimalarial treatments.

Materials and Methods

Materials

Except where otherwise indicated, reactions were performed at room temperature (20°C), and reagents were purchased from Sigma-Aldrich Corporation (St. Louis, MO, USA).

Ethics statement

The studies reported here were performed under protocols reviewed and approved by the Ethical Committee on Clinical Research from the Hospital Clínic de Barcelona (Reg. HCB/2014/0910) and the Ethical Committee on Animal Experimentation from the Barcelona Science Park (Reg. 20140917). All the human blood samples used for *P. falciparum in vitro* cultures were purchased from the Banc de Sang i Teixits (http://www.bancsang.net/) and irreversibly anonymized prior to their arrival.

Extraction and purification of sulfated polysaccharides

Samples of the marine organisms were cut into 1 mm^3 pieces, immersed three times in acetone and dried at 60°C. Sulfated polysaccharides were extracted from 10 g of the dried tissues by extensive papain digestion, and the extracts were partially purified by cetylpyridinium and ethanol precipitations as described [51]. Approximately 100 mg dry weight of crude polysaccharide extract was obtained from each species. Extracts were applied to a high-performance liquid chromatography system-linked Mono Q column (GE Healthcare, UK), equilibrated with 5 mM ethylenediaminetetraacetic acid, 20 mM Tris-HCl, pH 7.0. The polysaccharides were eluted from the column using a 0-3 M NaCl linear gradient at a flow rate of 1 mL/min. 0.5 mL fractions were collected and checked by metachromatic assay using 1,9-dimethylmethylene blue [52], and by measuring conductivity to estimate NaCl concentration. The fractions containing sulfated polysaccharides were pooled, dialyzed against distilled water and lyophilized, and the corresponding structures confirmed by nuclear magnetic resonance analysis as described [34,36,37].

P. falciparum cell culture and growth inhibition assays

The *P. falciparum* 3D7 strain was grown *in vitro* in group B human RBCs using previously described conditions [53]. Briefly, parasites (thawed from glycerol stocks) were cultured at 37°C in Petri dishes containing RBCs in Roswell Park Memorial Institute (RPMI) complete medium under a gas mixture of 92% N_2, 5% CO_2, and 3% O_2. Synchronized cultures were obtained by 5% sorbitol lysis, and the medium was changed every 2 days keeping 3% hematocrit. For culture maintenance, parasitemias were kept below 5% late forms by dilution with washed RBCs prepared as described elsewhere [53]. For growth inhibition assays, parasitemia was adjusted to 1.5% with more than 90% of parasites at ring stage after sorbitol synchronization. 150 µL of this *Plasmodium* culture was plated in 96-well plates and incubated in the presence of polysaccharides for 48 h in the conditions described above. Parasitemia was determined by flow cytometry, after staining pRBC DNA with the nucleic acid dye Syto 11, added 10 min before analysis. Samples were analyzed using a BD FACSCalibur™ flow cytometer and parasitemia was expressed as the number of parasitized cells per 100 erythrocytes.

Merozoite invasion inhibition assay

Synchronized cultures of *P. falciparum* 3D7 were enriched using Percoll (GE Healthcare) purification to obtain late trophozoites and early schizonts, and diluted to ~1% initial parasitemia and 3% hematocrit. Assays were performed in 24-well, flat-bottomed microculture plates where 1 mL of culture was incubated in RPMI supplemented with different amounts of each polysaccharide in study, for 20 h as described above. After incubation, smears were prepared by fixing cells in methanol for a few seconds and then staining them for 10 min with Giemsa (Merck Chemicals, Germany) diluted 1:10 in Sorenson’s Buffer, pH 7.2. Plates were incubated for another 20 h before preparing a new set of smears. Slides were observed with an optical microscope Nikon Eclipse 50i (Japan) and pictures were taken with a Nikon Digital Sight DS-U2 camera. For quantitative determinations, the cultures were analyzed by flow cytometry by staining pRBC DNA with the nucleic acid dye Syto 11, added 10 min before analysis. Samples were analyzed using a BD FACSCalibur™ flow cytometer and parasitemia was expressed as the number of parasitized cells per 100 erythrocytes. To assess invasion and maturation rates, respectively, the following formulae were applied:

$$\text{Invasion} = \frac{\text{rings}_{\text{day } n}}{(\text{trophozoites} + \text{schizonts})_{\text{day } n\text{-}1}}$$

$$\text{Maturation} = \frac{(\text{trophozoites} + \text{schizonts})_{\text{day } n}}{\text{rings}_{\text{day } n\text{-}1}}$$

Activated partial thromboplastin time (APTT) assay

Various concentrations of sulfated polysaccharides in 100 µL of human plasma were mixed with 100 µL of undiluted APTT reagent (kaolin bovine phospholipid reagent from Biolab-Merieux AS, Rio de Janeiro, Brazil). After incubating for 2 min at 37°C, 100 µL of 25 mM $CaCl_2$ was added to the mixture, and the clotting time was recorded in an Amelung KC4A coagulometer (Heinrich Amelung GmbH, Lemgo, Germany). The results were expressed as the clotting time ratio in the presence vs. absence of different polysaccharide concentrations. Anticoagulant activity was indicated as IU/mg using a parallel standard curve based on the 6th International Heparin Standard (2,145 units per vial, 200.04 IU/mg), obtained from the National Institute for Biological Standards and Control (Potters Bar, UK).

Fluorescence microscopy

Living *P. falciparum* cultures with mature stages of the parasite were incubated in the presence of 10 µg/mL fluorescein-labeled heparin (Life Technologies) in phosphate buffered saline, pH 7.4 (PBS) supplemented with 0.75% bovine serum albumin for 90 min at 37°C with gentle stirring. After PBS washing, blood smears were prepared and cells were fixed for 20 min with 1% (v/v) paraformaldehyde in PBS. Parasite nuclei were stained with 4′6-diamino-2-phenylindole (DAPI) and the RBC membrane was labeled with wheat germ agglutinin-tetramethylrhodamine conjugate. Slides were finally mounted with ProLong® Gold antifade reagent, and analyzed with a Leica TCS SP5 laser scanning confocal microscope.

Polyacrylamide gel electrophoresis

Electrophoresis was performed in 6% polyacrylamide gels using a Mini-Protean Tetra Cell System (Bio-Rad Laboratories Inc.). Samples containing 20 µg polysaccharide (at 1 mg/mL) were boiled in the presence of nonreducing sample buffer for 5 min, and electrophoresed at 100 V for 40 min. The gel was stained with 0.5% Alcian Blue solution in 3% acetic acid/25% isopropanol for 30 min with gentle stirring. Finally, the gel was de-stained in 10% acetic acid/40% ethanol overnight and digitalized.

Unspecific cytotoxicity assay

Human umbilical vein endothelial cells (primary culture provided by Dr. Francisco J. Muñoz, Pompeu Fabra University, Barcelona, Spain) were seeded in 96-well plates at a density of 5000 cells/100 µL/well, and incubated for 24 h at 37°C in Medium 199 with Earle's salts, supplemented with L-glutamine and fetal calf serum (FCS; LabClinics). After that time the medium was carefully removed with a pipette, and 100 µL of new medium (without FCS in this case) containing different sample concentrations was added. After incubating for 48 h at 37°C, 10 µL of the cell proliferation assay reagent WST-1 (Roche Life Science) were added, and 1 h later absorbance was measured at 440 nm.

Antimalarial activity assay *in vivo*

The *in vivo* antimalarial activity of sulfated polysaccharides was studied in a 4-day-blood suppressive test as previously described [54]. Briefly, Balb/C female mice (n = 5/sample; Janvier Laboratories) were inoculated intraperitoneally with 2 x 10^6 RBCs infected by the *Plasmodium yoelii yoelii* 17 XL lethal strain. Treatment with the antimalarial drug chloroquine (5 mg kg^{-1} day^{-1}) [55] or polysaccharides dissolved in PBS started 2 h later (day 0) with a 200 µL single dose administered intravenously, followed by identical dose administration for the next 3 days. A control untreated group received PBS. Activity was determined by microscopic counting at day 4 of blood smears stained with Wright's solution (Merck Chemicals). Mice were fed a commercial diet *ad libitum* and treated with humane care, being euthanized if reaching a 20% weight loss for two consecutive days. The sacrifice method was exposure to 95% CO_2 following anesthesia with 5% isoflurane vaporized in O_2.

P. yoelii protein extraction from infected whole blood

Protein lysates were extracted from the whole blood of infected Balb/C female mice having >50% parasitemia. Blood was collected in Microvette® CB 300 tubes (Sarstedt, Germany) and kept at -80°C until protein extraction. RBC lysis was performed by adding 10 x vol of saponin 0.1% (w/v) in PBS. After washing twice with cold PBS, the pellet was treated with 2 vol of extraction buffer consisting of 50 mM NaCl, 0.5% Mega 10, 3% CHAPS, and 50 mM Tris-HCl, pH 8.0, supplemented with a protease inhibitor cocktail (Roche). The samples were subjected to four freeze-thaw cycles, and the lysates were finally centrifuged at 20,000 g for 30 min (4°C). Protein concentration was determined by the DC protein assay (Bio-Rad), and *P. yoelii* total protein samples were stored at -20°C until use.

Western blot

10 µg of *P. yoelii* total protein extract were fractionated in a reducing 10% SDS-PAGE (Bio-Rad), transferred to polyvinylidene difluoride membranes and blocked

with Z buffer (100 mM $MgCl_2$, 0.5% Tween 20, 1% Triton X-100, 1% BSA,100 mM Tris-HCl, pH 7.4, supplemented with 5% FCS). Membranes were then incubated at 4°C overnight with 1:10,000 dilutions of sera from the mice that survived the infection, followed by a 1 h incubation with the secondary horseradish peroxidase-labeled anti-mouse IgG (Amersham Biosciences) at a 1:10,000 dilution.

Acknowledgments

We are grateful to Miriam Ramírez and Ernest Moles for their experimental support.

Funding

This work was supported by the Ministerio de Economía y Competitividad, Spain (grant BIO2014-52872-R, which included FEDER funds); the Generalitat de Catalunya, Spain (grant 2014-SGR-938); the Conselho Nacional de Desenvolvimento Científico e Tecnológico (CNPq, Brazil); and the Fundação de Amparo à Pesquisa do Estado do Rio de Janeiro (FAPERJ, Brazil).

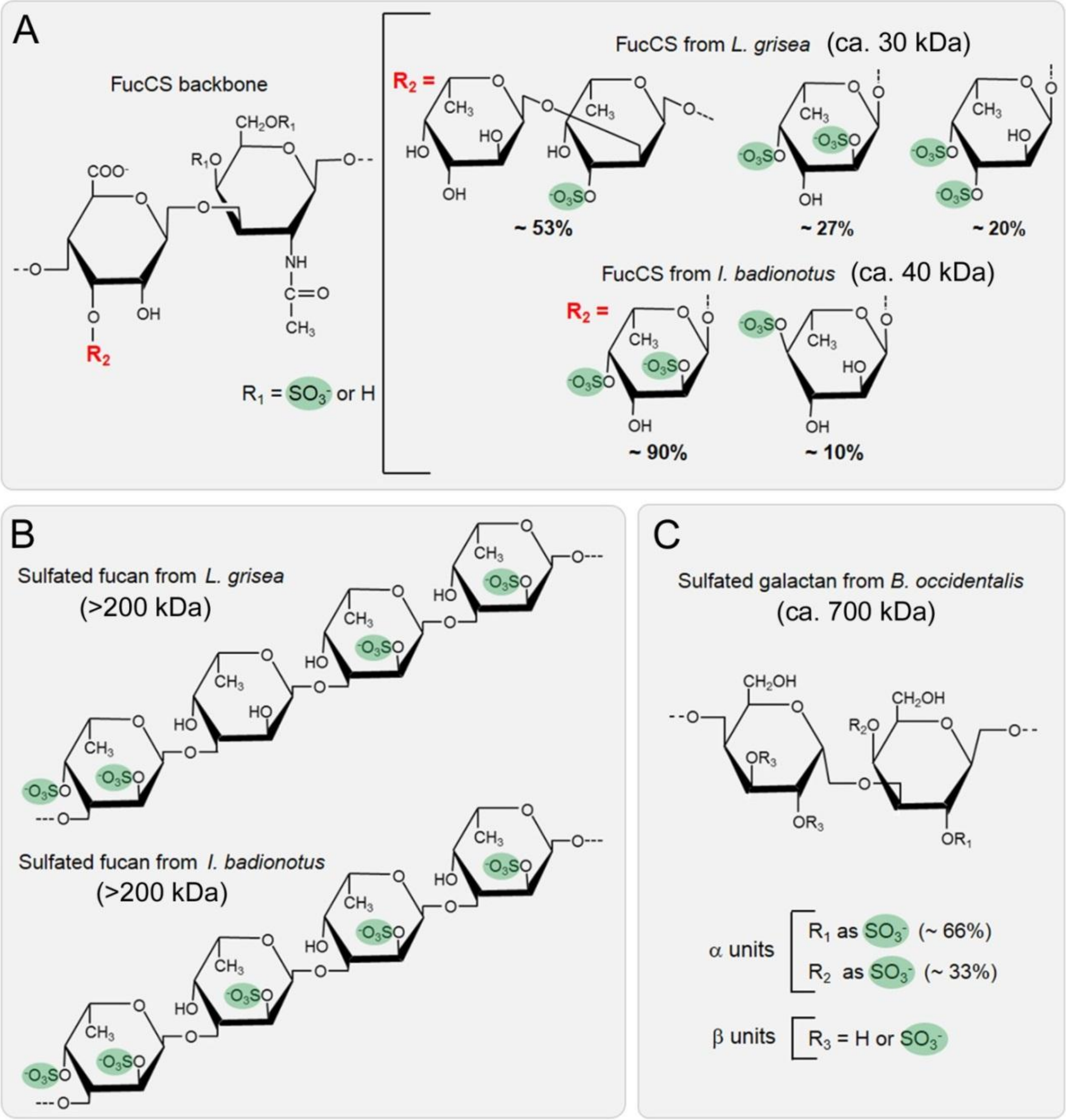
A
FucCS backbone
COO-
CH2OR1
R1O
NH
C=O
CH3
OH
R2
R1 = SO3- or H
FucCS from L. grisea (ca. 30 kDa)
R2 =
~ 53%
~ 27%
~ 20%
FucCS from I. badionotus (ca. 40 kDa)
R2 =
~ 90%
~ 10%
B
Sulfated fucan from L. grisea
(>200 kDa)
Sulfated fucan from I. badionotus
(>200 kDa)
C
Sulfated galactan from B. occidentalis
(ca. 700 kDa)
CH2OH
OR3
R2O
OR1
α units
R1 as SO3- (~ 66%)
R2 as SO3- (~ 33%)
β units
R3 = H or SO3-

Figure 1. Chemical structures of the sulfated polysaccharides used in this work. (A) The *L. grisea* and *I. badionotus* fucosylated chondroitin sulfates share a similar backbone (left) but differ on their sulfated fucose branches (right). (B) *L. grisea* and *I. badionotus* sulfated fucans have similar tetrasaccharide repeating structures but differ exclusively on the sulfation of the second unit. (C) The sulfated galactan from the red alga *B. occidentalis* contains alternating α- and β-galactose units with distinct sulfation patterns. Sulfation sites are highlighted in green.

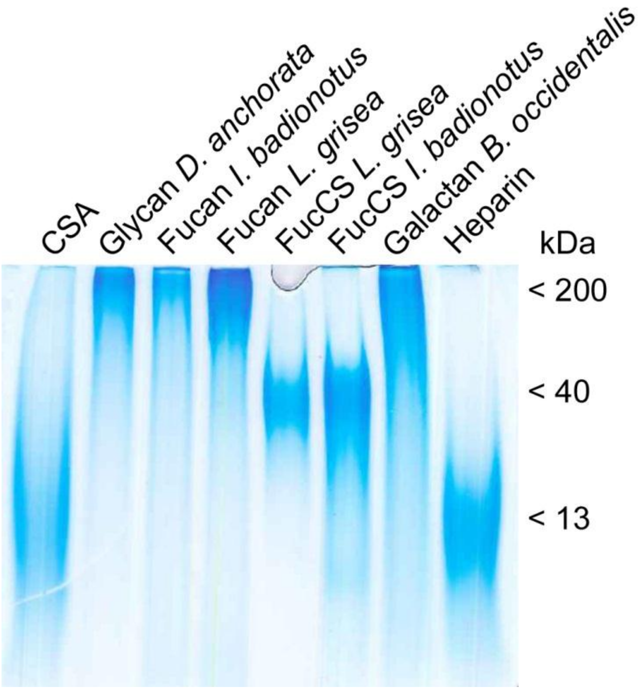
CSA
Glycan D. anchorata
Fucan I. badionotus
Fucan L. grisea
FucCS L. grisea
FucCS I. badionotus
Galactan B. occidentalis
Heparin
kDa
< 200
< 40
< 13

Figure 2. Alcian Blue-stained polyacrylamide gel electrophoresis analysis of sulfated polysaccharides. Approximate molecular masses were confirmed by size exclusion chromatography.

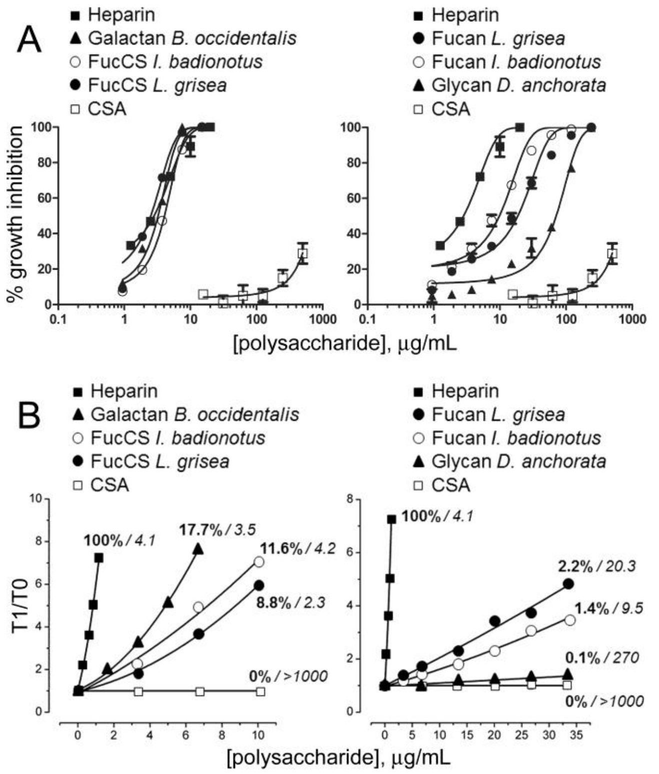

Figure 3. ***In vitro*** **analysis of antimalarial and anticoagulating activities of sulfated polysaccharides.** (A) Growth inhibition assays of *P. falciparum* cultures. (B) APTT assay of anticoagulant activities, expressed as the ratio between clotting times in the presence (T1) and absence (T0) of polysaccharides. Percentages represent the respective anticoagulant activities relative to that of heparin. For each polysaccharide is indicated in *italics* the corresponding *in vitro* antimalarial IC50 (in µg/mL) derived from the data presented in panel (a).

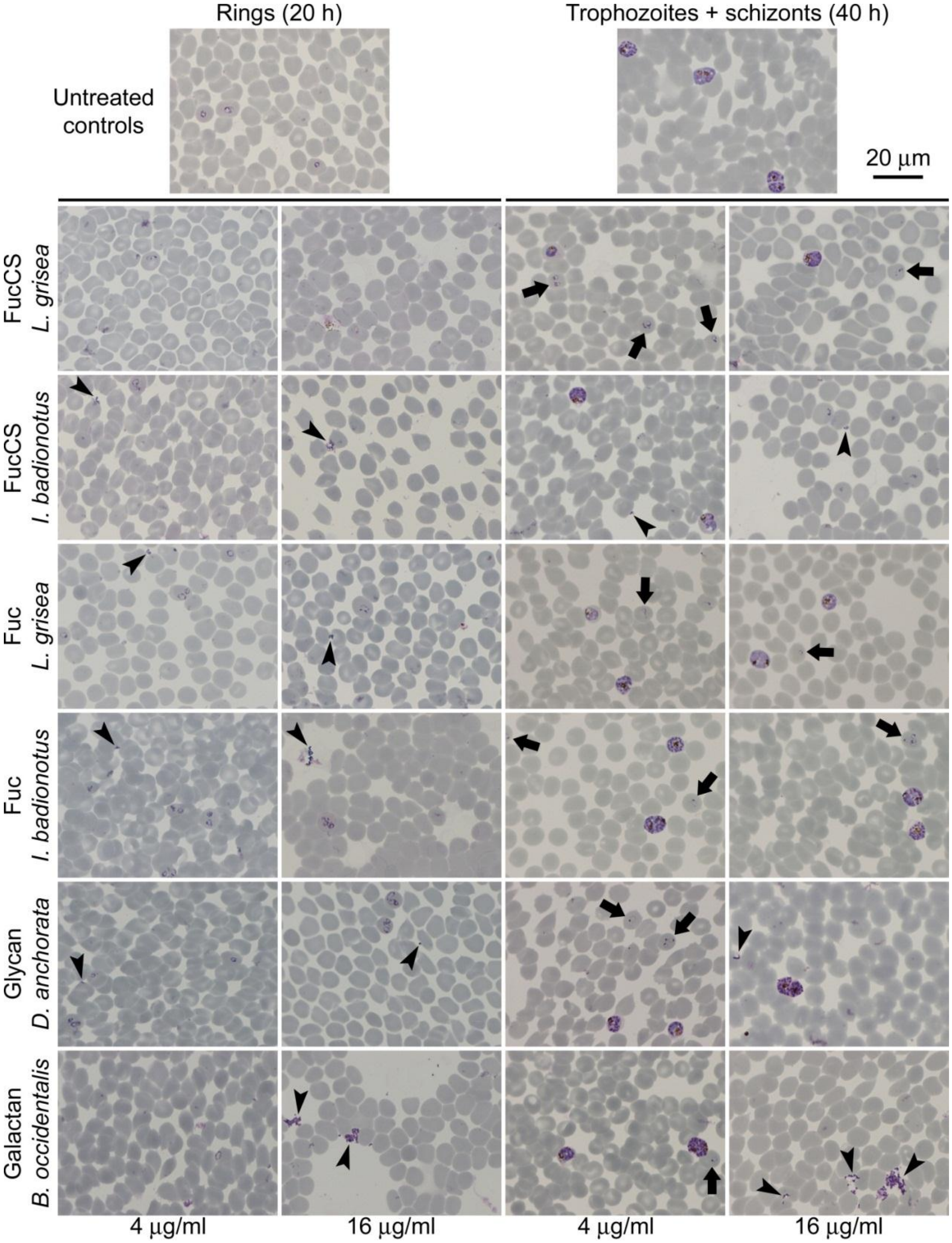
Rings (20 h)
Trophozoites + schizonts (40 h)
Untreated controls
20 µm
FucCS L. grisea
FucCS I. badionotus
Fuc L. grisea
Fuc I. badionotus
Glycan D. anchorata
Galactan B. occidentalis
4 µg/ml
16 µg/ml
4 µg/ml
16 µg/ml

Figure 4. Microscopic images of Giemsa-stained *in vitro* pRBC cultures of *P. falciparum* treated with sulfated polysaccharides. Pictures corresponding to the cycle

phases when rings and trophozoites+schizonts are the dominant forms expected were taken, respectively, 20 and 40 h after treatment. Arrows indicate ring stages and arrowheads indicate merozoites that have failed to invade pRBCs.

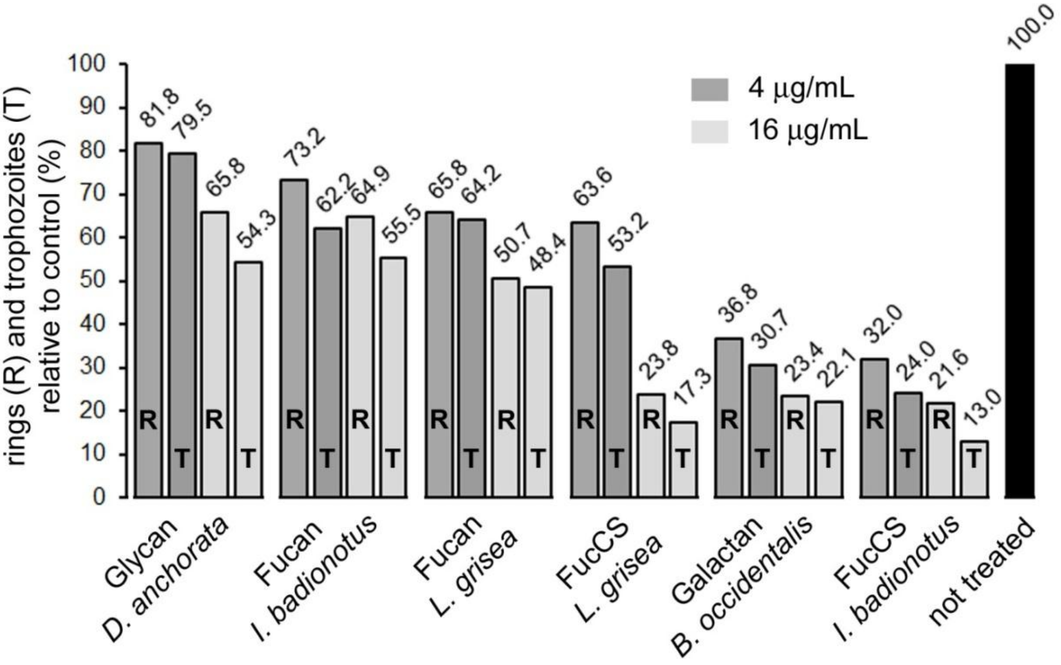

Figure 5. Quantitative flow cytometry analysis of the inhibition of red blood cell invasion by *P. falciparum* in the presence of sulfated polysaccharides. Percentages indicate the proportion of rings (R, 20 h after treatment) and trophozoites (T, 40 h after treatment) relative to untreated controls.

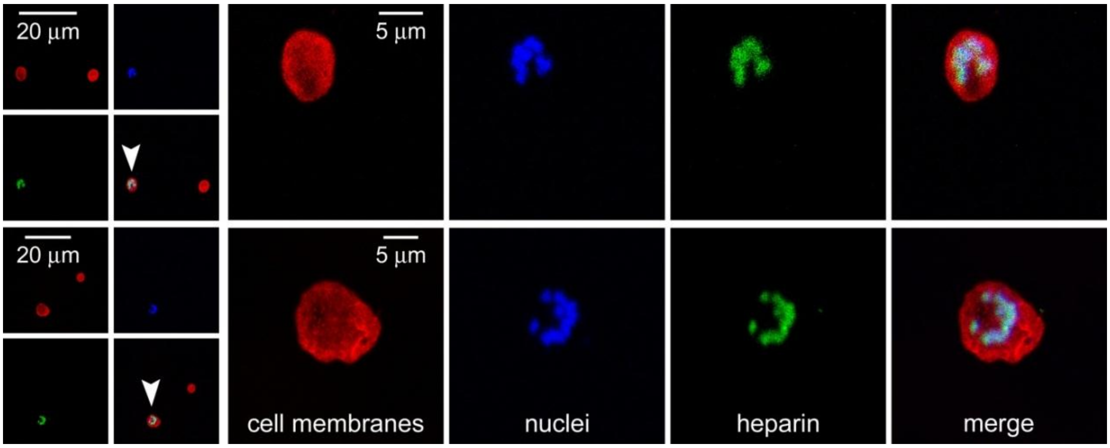
20 µm
5 µm
20 µm
5 µm
cell membranes
nuclei
heparin
merge

Figure 6. Binding of heparin to *P. falciparum* merozoites inside pRBCs. Fluorescein-labeled heparin was added to pRBC cultures that were processed for fluorescence microscopy after 30 min of incubation. The four small panels to the left of each series are included to show pRBC vs. RBC specificity. Arrowheads indicate pRBCs (revealed by DAPI stain of *Plasmodium* DNA within the otherwise anucleated RBC) imaged at higher resolution in the right-hand panels.

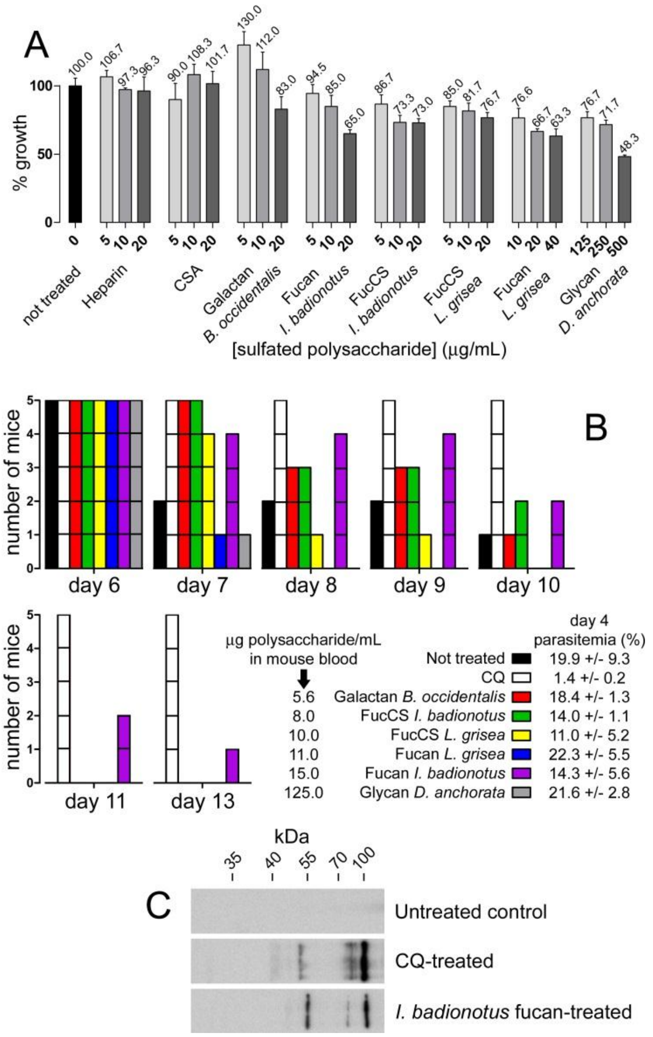

Figure 7. Cytotoxicity and *in vivo* antimalarial activity analyses of sulfated polysaccharides. (A) Unspecific *in vitro* toxicity on human umbilical vein endothelial cells of sulfated polysaccharides assayed at concentrations around their respective IC50 for *P. falciparum* growth. (B) *In vivo* assay of the effect on *P. yoelii*–infected mice (n = 5 animals/sample) of polysaccharides administered iv at the indicated μg mL^{-1} day^{-1}. Chloroquine (CQ) was administered iv as a positive control at a dose of 5 mg kg^{-1} day^{-1}. Shown are the histograms of those days after infection when changes in the number of surviving animals were recorded. All surviving animals at day 13 were alive and without symptoms of disease at day 40. (C) Western blot for the detection of IgGs against *P. yoelii* antigens in the serum of surviving infected mice that had been treated 35 days before with CQ or with the *I. badionotus* fucan. The untreated control corresponds to a noninfected mouse of the same age.

References

1. Miller LH, Baruch DI, Marsh K, Doumbo OK (2002) The pathogenic basis of malaria. Nature 415: 673-679. 10.1038/415673a.
2. Maier AG, Cooke BM, Cowman AF, Tilley L (2009) Malaria parasite proteins that remodel the host erythrocyte. Nat Rev Microbiol 7: 341-354.
3. Kyes S, Horrocks P, Newbold C (2001) Antigenic variation at the infected red cell surface in malaria. Annu Rev Microbiol 55: 673-707.
4. Juillerat A, Igonet S, Vigan-Womas I, Guillotte M, Gangnard S, Faure G, Baron B, Raynal B, Mercereau-Puijalon O, Bentley GA (2010) Biochemical and biophysical characterisation of DBL1α_1-varO, the rosetting domain of PfEMP1 from the VarO line of *Plasmodium falciparum*. Mol Biochem Parasitol 170: 84-92. doi: 10.1016/j.molbiopara.2009.12.008.
5. Griffith KS, Lewis LS, Mali S, Parise ME (2007) Treatment of malaria in the United States: a systematic review. JAMA 297: 2264-2277.
6. Andrews KT, Klatt N, Adams Y, Mischnick P, Schwartz-Albiez R (2005) Inhibition of chondroitin-4-sulfate-specific adhesion of *Plasmodium falciparum*-infected erythrocytes by sulfated polysaccharides. Infect Immun 73: 4288-4294.
7. Clark DL, Su S, Davidson EA (1997) Saccharide anions as inhibitors of the malaria parasite. Glycoconj J 14: 473-479.
8. Xiao L, Yang C, Patterson PS, Udhayakumar V, Lal AA (1996) Sulfated polyanions inhibit invasion of erythrocytes by plasmodial merozoites and cytoadherence of endothelial cells to parasitized erythrocytes. Infect Immun 64: 1373-1378.
9. Adams Y, Freeman C, Schwartz-albiez R, Ferro V, Parish CR, Andrews KT (2006) Inhibition of *Plasmodium falciparum* growth *in vitro* and adhesion to chondroitin-4-sulfate by the heparan sulfate mimetic PI-88 and other sulfated oligosaccharides. Antimicrob Agents Chemother 50: 2850-2852.
10. Carlson J, Ekre H-P, Helmby H, Gysin J, Greenwood BM, Wahlgren M (1992) Disruption of *Plasmodium falciparum* erythrocyte rosettes by standard heparin and heparin devoid of anticoagulant activity. Am J Trop Med Hyg 46: 595-602.

11. Rowe A, Berendt AR, Marsh K, Newbold CI (1994) *Plasmodium falciparum*: a family of sulfated glycoconjugates disrupts erythrocyte rosettes. Exp Parasitol 79: 506-516.
12. Najer A, Wu D, Bieri A, Brand F, Palivan CG, Beck HP, Meier W (2014) Nanomimics of host cell membranes block invasion and expose invasive malaria parasites. ACS Nano 8: 12560-12571.
13. Bastos MF, Albrecht L, Kozlowski EO, Lopes SCP, Blanco YC, Carlos BC, Castilheiras C, Vicente CP, Werneck CC, Wunderlich G, Ferreira MU, Marinho CRF, Mourão PAS, Pavão MSG, Costa FTM (2014) Fucosylated chondroitin sulfate inhibits *Plasmodium falciparum* cytoadhesion and merozoite invasion. Antimicrob Agents Chemother 58: 1862-1871.
14. Kulane A, Ekre HP, Perlmann P, Rombo L, Wahlgren M, Wahlin B (1992) Effect of different fractions of heparin on *Plasmodium falciparum* merozoite invasion of red blood cells *in vitro*. Am J Trop Med Hyg 46: 589-594.
15. Boyle MJ, Richards JS, Gilson PR, Chai W, Beeson JG (2010) Interactions with heparin-like molecules during erythrocyte invasion by *Plasmodium falciparum* merozoites. Blood 115: 4559-4568.
16. Zhang Y, Jiang N, Lu H, Hou N, Piao X, Cai P, Yin J, Wahlgren M, Chen Q (2013) Proteomic analysis of *Plasmodium falciparum* schizonts reveals heparin-binding merozoite proteins. J Proteome Res 12: 2185-2193.
17. Kobayashi K, Takano R, Takemae H, Sugi T, Ishiwa A, Gong H, Recuenco FC, Iwanaga T, Horimoto T, Akashi H, Kato K (2013) Analyses of interactions between heparin and the apical surface proteins of *Plasmodium falciparum*. Sci Rep 3.
18. Doolan DL, Dobaño C, Baird JK (2009) Acquired immunity to malaria. Clin Microbiol Rev 22: 13-36.
19. Kappe SH, Vaughan AM, Boddey JA, Cowman AF (2010) That was then but this is now: malaria research in the time of an eradication agenda. Science 328: 862-866.
20. Srinivasan P, Yasgar A, Luci DK, Beatty WL, Hu X, Andersen J, Narum DL, Moch JK, Sun H, Haynes JD, Maloney DJ, Jadhav A, Simeonov A, Miller LH (2013) Disrupting malaria parasite AMA1-RON2 interaction with a small molecule prevents erythrocyte invasion. Nat Commun 4.

21. Sheehy TW, Reba RC (1967) Complications of *falciparum* malaria and their treatment. Ann Intern Med 66: 807-809.

22. Smitskamp H, Wolthuis FH (1971) New concepts in treatment of malignant tertian malaria with cerebral involvement. Br Med J 1: 714-716.

23. Jaroonvesama N (1972) Intravascular coagulation in *falciparum* malaria. Lancet 1: 221-223.

24. Munir M, Tjandra H, Rampengan TH, Mustadjab I, Wulur FH (1980) Heparin in the treatment of cerebral malaria. Paediatr Indones 20: 47-50.

25. Rampengan TH (1991) Cerebral malaria in children. Comparative study between heparin, dexamethasone and placebo. Paediatr Indones 31: 59-66.

26. World Health Organization Malaria Action Programme. (1986) Severe and complicated malaria. Trans R Soc Trop Med Hyg 80 (Suppl): 3-50.

27. Chen S, Hu Y, Ye X, Li G, Yu G, Xue C, Chai W (2012) Sequence determination and anticoagulant and antithrombotic activities of a novel sulfated fucan isolated from the sea cucumber *Isostichopus badionotus*. Biochim Biophys Acta - General Subjects 1820: 989-1000.

28. Mourão PAS, Pereira MS, Pavão MSG, Mulloy B, Tollefsen DM, Mowinckel MC, Abildgaard U (1996) Structure and anticoagulant activity of a fucosylated chondroitin sulfate from echinoderm: sulfated fucose branches on the polysaccharide account for its high anticoagulant action. J Biol Chem 271: 23973-23984.

29. Tapon-Bretaudière J, Drouet B, Matou S, Mourão PAS, Bros A, Letourneur D, Fischer AM (2000) Modulation of vascular human endothelial and rat smooth muscle cell growth by a fucosylated chondroitin sulfate from echinoderm. Thromb Haemost 84: 332-337.

30. Glauser BF, Pereira MS, Monteiro RQ, Mourão PAS (2008) Serpin-independent anticoagulant activity of a fucosylated chondroitin sulfate. Thromb Haemost 100: 420-428.

31. Glauser BF, Mourão PA, Pomin VH (2013) Marine sulfated glycans with serpin-unrelated anticoagulant properties. Adv Clin Chem 62: 269-303.

32. Zancan P, Mourão PA (2004) Venous and arterial thrombosis in rat models: dissociation of the antithrombotic effects of glycosaminoglycans. Blood Coagul Fibrinolysis 15.

33. Mourão PAS, Bastos IG (1987) Highly acidic glycans from sea cucumbers. Eur J Biochem 166: 639-645.
34. Santos GRC, Glauser BF, Parreiras LA, Vilanova E, Mourão PAS (2015) Distinct structures of the a-fucose branches in fucosylated chondroitin sulfates do not affect their anticoagulant activity. Glycobiology .
35. Pomin VH, Mourão PAS (2008) Structure, biology, evolution, and medical importance of sulfated fucans and galactans. Glycobiology 18: 1016-1027.
36. Ribeiro AC, Vieira RP, Mourão PAS, Mulloy B (1994) A sulfated a-L-fucan from sea cucumber. Carbohydr Res 255: 225-240.
37. Farias WRL, Valente AP, Pereira MS, Mourão PAS (2000) Structure and anticoagulant activity of sulfated galactans: isolation of a unique sulfated galactan from the red algae *Botryocladia occidentalis* and comparison of its anticoagulant action with that of sulfated galactans from invertebrates. J Biol Chem 275: 29299-29307.
38. Marques J, Moles E, Urbán P, Prohens R, Busquets MA, Sevrin C, Grandfils C, Fernàndez-Busquets X (2014) Application of heparin as a dual agent with antimalarial and liposome targeting activities towards *Plasmodium*-infected red blood cells. Nanomedicine: NBM 10: 1719-1728.
39. Borsig L, Wang L, Cavalcante MCM, Cardilo-Reis L, Ferreira PL, Mourão PAS, Esko JD, Pavão MSG (2007) Selectin blocking activity of a fucosylated chondroitin sulfate glycosaminoglycan from sea cucumber: effect on tumor metastasis and neutrophil recruitment. J Biol Chem 282: 14984-14991.
40. Fonseca RJC, Santos GRC, Mourão PAS (2009) Effects of polysaccharides enriched in 2,4-disulfated fucose units on coagulation, thrombosis and bleeding. Thromb Haemost 102: 829-836.
41. Cagayat Recuenco F, Kobayashi K, Ishiwa A, Enomoto-Rogers Y, Fundador NG, Sugi T, Takemae H, Iwanaga T, Murakoshi F, Gong H, Inomata A, Horimoto T, Iwata T, Kato K (2014) Gellan sulfate inhibits *Plasmodium falciparum* growth and invasion of red blood cells *in vitro*. Sci Rep 4.
42. Chen JH, Lim JD, Sohn EH, Choi YS, Han ET (2009) Growth-inhibitory effect of a fucoidan from brown seaweed Undaria pinnatifida on *Plasmodium* parasites. Parasitol Res 104: 245-250.

43. Vogt AM, Pettersson F, Moll K, Jonsson C, Normark J, Ribacke U, Egwang TG, Ekre HP, Spillmann D, Chen Q, Wahlgren M (2006) Release of sequestered malaria parasites upon injection of a glycosaminoglycan. PLoS Pathog 2: e100.

44. Evans SG, Morrison D, Kaneko Y, Havlik I (1998) The effect of curdlan sulphate on development *in vitro* of *Plasmodium falciparum*. Trans R Soc Trop Med Hyg 92: 87-89.

45. Rasti N, Wahlgren M, Chen Q (2004) Molecular aspects of malaria pathogenesis. FEMS Immunol Med Microbiol 41: 9-26.

46. Kirk K (2001) Membrane transport in the malaria-infected erythrocyte. Physiol Rev 81: 495-537.

47. Cowman AF, Berry D, Baum J (2012) The cellular and molecular basis for malaria parasite invasion of the human red blood cell. J Cell Biol 198: 961-971.

48. Miura Y, Aoyagi S, Kusada Y, Miyamoto K (1980) The characteristics of anticoagulation by covalently immobilized heparin. J Biomed Mater Res 14: 619-630. 10.1002/jbm.820140508.

49. Osmond RIW, Kett WC, Skett SE, Coombe DR (2002) Protein-heparin interactions measured by BIAcore 2000 are affected by the method of heparin immobilization. Anal Biochem 310: 199-207.

50. Fonseca RJC, Mourão PAS (2006) Fucosylated chondroitin sulfate as a new oral antithrombotic agent. Thromb Haemost 96: 822-829.

51. Vieira RP, Mulloy B, Mourão PA (1991) Structure of a fucose-branched chondroitin sulfate from sea cucumber. Evidence for the presence of 3-O-sulfo-beta-D-glucuronosyl residues. J Biol Chem 266: 13530-13536.

52. Farndale RW, Buttle DJ, Barrett AJ (1986) Improved quantitation and discrimination of sulphated glycosaminoglycans by use of dimethylmethylene blue. Biochim Biophys Acta - General Subjects 883: 173-177.

53. Urbán P, Estelrich J, Cortés A, Fernàndez-Busquets X (2011) A nanovector with complete discrimination for targeted delivery to *Plasmodium falciparum*-infected versus non-infected red blood cells *in vitro*. J Control Release 151: 202-211.

54. Fidock DA, Rosenthal PJ, Croft SL, Brun R, Nwaka S (2004) Antimalarial drug discovery: efficacy models for compound screening. Nat Rev Drug Discov 3: 509-520.

55. Rivera N, Ponce YM, Arán VJ, Martínez C, Malagón F (2013) Biological assay of a novel quinoxalinone with antimalarial efficacy on *Plasmodium yoelii yoelii*. Parasitol Res 112: 1523–1527.

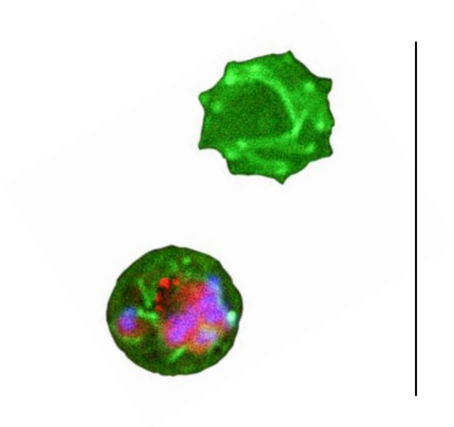

Article 3

ARTICLE 3

Article 3: Adaptation of nanocarriers to changing requirements in antimalarial drug delivery.

Malaria pathophysiology is too complex and the disease is too widespread to be fought with a single weapon, and it is generally accepted that to walk the path towards eradication a well-designed attack will be necessary using a combination of strategies. These include the improvement of existing approaches and the development of new ones[172], whereas drug therapy remains the mainstay of treatment and prevention[173]. Current chemotherapeutic approaches against malaria infections are targeted at the asexual blood-stage parasites that are responsible for all symptoms and pathologies of the disease[13]. However, as there can be several hundred billion pRBCs in the bloodstream of a patient, multiple-dose administrations are required, with ACTs resistance now emerging there is an urgent need for the development of new drugs or new strategies for the delivery of already known broad-spectrum antimalarials or highly toxic drugs. For these reasons and with the objective of designing the best nanocarrier (**Figure 15**) we tested different approaches such as better drugs (consisting of toxic lipids for the parasite contained in the LPs formulation), different carriers (chitosan nanoparticles), and news targets (more specifically the transmission stages from the mosquito vector).

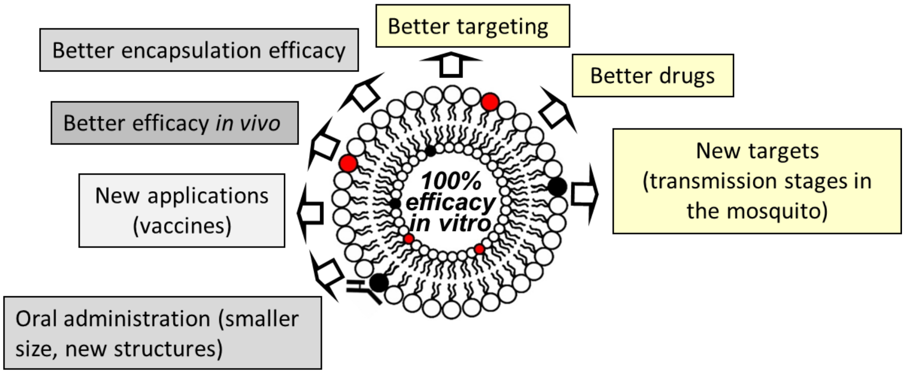
Better targeting
Better encapsulation efficacy
Better drugs
Better efficacy *in vivo*
New targets (transmission stages in the mosquito)
New applications (vaccines)
100% efficacy in vitro
Oral administration (smaller size, new structures)

Figure 15. Schematic demonstration of the best prototype we aim to design. In this particular paper we have explored the three approaches represented in yellow.

ARTICLE 3

Adaptation of targeted nanocarriers to changing requirements in antimalarial drug delivery

Joana Marques [a,b,c], Juan José Valle-Delgado [a,b,c], Patricia Urbán [d], Elisabet Baró [a,b,c], Rafael Prohens [e], Alfredo Mayor [b], Pau Cisteró [b], Michael Delves [f], Robert Sinden [f], Christian Grandfils [g], Chantal Sevrin [g], José Luis de Paz [h], José Antonio García-Salcedo [i], and Xavier Fernàndez-Busquets [a,b,c,*]

[a] Nanomalaria Group, Institute for Bioengineering of Catalonia (IBEC), Baldiri Reixac 10-12, ES-08028 Barcelona, Spain
[b] Barcelona Institute for Global Health (ISGlobal, Hospital Clínic-Universitat de Barcelona), Rosselló 149-153, ES-08036 Barcelona, Spain
[c] Nanoscience and Nanotechnology Institute (IN2UB), University of Barcelona, Martí i Franquès 1, ES-08028 Barcelona, Spain
[d] European Commission, Joint Research Centre, Institute for Health and Consumer Protection, IT-21027 Ispra (VA), Italy
[e] Unitat de Polimorfisme i Calorimetria, Centres Científics i Tecnològics, Universitat de Barcelona, Baldiri Reixac 10, ES-08028 Barcelona, Spain
[f] Imperial College, 6th Floor SAF Building, South Kensington, London, SW7 2AZ, UK
[g] Interfacultary Research Center of Biomaterials (CEIB), University of Liège, Chemistry Institute, Liège (Sart-Tilman), Belgium
[h] Instituto de Investigaciones Químicas (IIQ) CSIC-US, Centro de Investigaciones Científicas Isla de La Cartuja, Americo Vespucio, 49, ES-41092 Sevilla, Spain
[i] Instituto de Parasitología y Biomedicina "López-Neyra", Consejo Superior de Investigaciones Científicas, Avda. del Conocimiento s/n, Parque Tecnológico de Ciencias de la Salud, ES-18100 Armilla, Spain
*e-mail: xfernandez_busquets@ub.edu

Current address for J.J.V.-D.: Department of Forest Products Technology, School of Chemical Technology, Aalto University, P.O. Box 16300, FI-00076 Aalto, Finland

Abstract

A number of liposome- and polymer-based nanocarriers engineered for the targeted delivery of antimalarial drugs are being developed despite the lack of economic incentives for research in nanomedicine applications to malaria. Although successful efforts have been made to obtain new nanostructures having affordable synthesis costs while exhibiting good performance in lowering the IC50 of drugs, new approaches are required to further optimize a scarcity of resources. In this regard, the adaptation of existing nanovector designs to new *Plasmodium* stages, antimalarial drugs, targeting molecules, or encapsulating structures is a strategy that can provide new cost-efficient therapies. We have explored here the adaptation of different liposome prototypes that had been developed in our group for the delivery to *Plasmodium*-infected red blood cells (pRBCs) of the antimalarial drugs chloroquine and primaquine. These new models include: (i) immunoliposome delivery of new lipid-based antimalarials; (ii) liposomes targeted to pRBCs with covalently linked heparin to reduce anticoagulation risks; (iii) adaptation of heparin to pRBC targeting of chitosan nanoparticles; (iv) use of heparin for the targeting of *Plasmodium* stages in the mosquito vector; and (v) use of the non-anticoagulant glycosaminoglycan chondroitin sulfate A as an heparin surrogate for pRBC targeting. The results presented indicate that the tuning of existing nanovessels to new malaria-related targets is a valid low-cost alternative to the development from scratch of new targeted nanosystems.

Keywords: immunoliposomes; malaria; nanomedicine; *Plasmodium*; targeted drug delivery

Introduction

With malaria elimination now firmly on the global research agenda, but resistance to the currently available drugs on the rise, there is an urgent need to invest in the research and development of new therapeutic strategies [1]. Encapsulation of drugs in targeted nanovectors is a rapidly growing area with a clear applicability to infectious disease treatment [2], and pharmaceutical nanotechnology has been identified as a potentially essential tool in the future fight against malaria [3,4]. Nanoparticle-based targeted delivery strategies can play an important role for the treatment of malaria because they might allow (i) low overall doses that limit the toxicity of the drug for the patient, (ii) administration of sufficiently high local amounts to minimize the evolution of resistant parasite strains [5], (iii) improvement of the efficacy of currently used hydrophylic (low membrane trespassing capacity) and lipophylic antimalarials (poor aqueous solubility), and (iv) use of orphan drugs never assayed as malaria therapy, e.g. because of their elevated and wide-spectrum toxicity. In the very nature of nanovectors resides their versatility that enables assembling several elements to obtain chimeric nanovessels tailored to fit the requirements for different administration routes, particular intracellular targets, or combinations of drugs.

Antimalarial drugs can potentially target a suite of pathogen life stages inside two different hosts: humans and the insect vector. Infection starts when a parasitized female *Anopheles* mosquito inoculates sporozoites of the malaria parasite, the protist *Plasmodium spp.*, into a person while taking a blood meal. Within a few minutes, sporozoites have migrated through the skin and bloodstream to the liver, where they invade hepatocytes. Sporozoites develop into merozoites [6], which enter the circulation, invade red blood cells (RBCs) [7], and replicate asexually to produce daughter cells that invade new RBCs to perpetuate the blood-stage cycle that unfolds through ring, trophozoite, and schizont stages. Some parasites eventually differentiate into sexual stages, female or male gametocytes that are ingested by a mosquito from peripheral blood. When an infected bloodmeal reaches the insect's midgut, micro- and macrogametocytes develop into male and female gametes. Following fertilization, the zygote differentiates into an ookinete that moves through the midgut epithelium and forms an oocyst, which releases sporozoites. The malaria transmission cycle is restarted when sporozoites migrate to the salivary glands and are injected into a human with the mosquito's next bite.

The so-called combination therapies, where several drugs are simultaneously administered [8], significantly improve the antimalarial effect of the individual compounds. Liposomes are particularly adept structures in this regard because they allow the encapsulation of hydrophobic drugs in their lipid bilayer and of water-soluble compounds in their lumen, thus being a potentially interesting platform for combination therapies where lipophilic and hydrophilic drugs are delivered together. One of the limitations of liposomes as carriers for drug delivery to *Plasmodium*-infected RBCs (pRBCs) is that because of the lack of endocytic processes in these cells, a relatively fluid liposome lipid bilayer is required to favor fusion events with the pRBC plasma membrane. As a result, these liposomes are leaky for drugs encapsulated in their lumen, and when membrane fusion occurs, a relatively small fraction of the originally contained drug is injected into the cell. On the other hand, liposomes made of saturated lipids have less fluid bilayers that contain drugs with high efficacy, although fusion events with pRBC membranes are greatly diminished, which also reduces the amount of luminal drug delivered to the target cell.

One of the main pRBC-binding molecules are glycosaminoglycans (GAGs), some of whose members include heparin, heparan sulfate (HS), and chondroitin sulfate (CS). Chondroitin 4-sulfate (CSA) has been found to act as a receptor for pRBC binding in the microvasculature [9] and the placenta [10], and adhesion of pRBCs to placental CSA has been linked to the severe disease outcome of pregnancy-associated malaria [11]. The high pathogenicity of *P. falciparum* in placental malaria is partly due to the ability of mature trophozoite- and schizont-stage-infected pRBCs to adhere to the placental syncytiotrophoblast. pRBC adhesion to the endothelium of postcapillary venules is mediated by the parasite-derived antigen *P. falciparum* erythrocyte membrane protein 1 (PfEMP1) [12], whereas CSA has been identified as the main receptor for PfEMP1 attachment to placental cells [10,13]. Single-molecule force spectroscopy data have revealed a complete specificity of adhesion of heparin to pRBCs vs. RBCs, with a binding strength matching that of antibody-antigen interactions [14]. Heparin had actually been used in the treatment of severe malaria [15], but it was abandoned because of its strong anticoagulant action, with side effects such as intracranial bleeding. It has been shown that heparin electrostatically bound to liposomes acts as an antibody surrogate, having a dual activity as a pRBC-targeting molecule but also as an antimalarial drug in itself acting mainly on trophozoite and schizont stages [16]. Because heparin is significantly cheaper to obtain than specific (monoclonal) antibodies the resulting heparin-liposomes have a cost about ten times lower than that of an equally performing immunoliposome. Since resistances of *Plasmodium* to heparin are not known so far [17], heparin-based targeting will foreseeably be more long-lasting than pRBC recognition relying on antibodies, which typically are raised against highly variable exposed antigens whose expression is constantly varied by different generations of the parasite. A question that remained open is whether the heparin-mediated targeting of liposomes to pRBCs could be extended to other glycosaminoglycans, to different *Plasmodium* stages, and to new nanoparticle types.

The three elements that constitute a targeted therapeutic nanovector (nanocapsule, targeting molecule and the drug itself) can be exchanged, as if they were LEGO parts, to obtain new structures better suited to each particular situation. Through modification of its constituting elements, nanovector design is susceptible of improvement and of adaptation to new targets such as different *Plasmodium* species or infected cells other than the erythrocyte. Of particular interest here is the targeting of the transmission stages that allow transfer of the parasite between human and mosquito and vice-versa, which represent the weakest spots in the life cycle of the pathogen [18]. Heparin and HS are targets for the circumsporozoite protein in the sporozoite attachment to hepatocytes during the primary stage of malaria infection in the liver [19]. CS proteoglycans in the mosquito midgut and synthetic CS mimetics have been described to bind *Plasmodium* ookinetes as an essential step of host epithelial cell invasion [20,21], whereas ookinete-secreted proteins have been found to have significant binding to heparin [22]. This body of accumulated evidence suggests that GAGs might be adequate to target antimalarial-loaded nanovectors to *Plasmodium* mosquito stages, either through a direct entry into gametocytes, ookinetes, and sporozoites, or indirectly through delivery to pRBCs for those pRBCs that differentiate into gametocytes. Engineering antimalarial nanomedicines designed to be delivered directly to *Anopheles* and targeted to *Plasmodium* stages exclusive of the insect might spectacularly reduce costs because the clinical trials required for therapies to be administered to people could be significantly simplified.

Here we have explored whether the heparin- and antibody-mediated targeting of drug-containing liposomes to pRBCs could be adapted in a straightforward way to other GAGs as targeting molecules, to different *Plasmodium* stages as target cells, and to new nanoparticle and drug types.

Materials and Methods

Materials

Except where otherwise indicated, reactions were performed at room temperature (20°C), and reagents were purchased from Sigma-Aldrich Corporation (St. Louis, MO, USA).

Liposome preparation

Liposomes were prepared by the lipid film hydration method (Bioh, Uni-, & Biology, 1991). All lipids were purchased from Avanti Polar Lipids Inc., Alabaster, AL, USA. Liposomes used for conjugation with half antibodies consisted of cholesterol, 1,2-dioleoyl-*sn*-glycero-3-phosphoethanolamine-N(lissamine rhodamine B sulfonyl) (DOPE-Rho), 1,2-dipalmitoyl-*sn*-glycero-3-phosphoethanolamine-N-(4-(p-maleimidophenyl)butyramide (MPB-PE), and 1,2-dioleoyl-sn-glycero-3-phosphatidylcholine (DOPC) in a proportion DOPC:cholesterol:MPB-PE:DOPE-Rho 72:20:1:7. Liposomes used for the covalent binding of heparin consisted of DOPC, cholesterol, L-α-phosphatidylethanolamine (PE), and 1,2-dioleoyl-3-trimethylammonium-propane (DOTAP) in a proportion 46:20:30:4. Lipids were dissolved in chloroform:methanol (2:1 v/v) in a round-bottomed flask where organic solvents were removed by rotary evaporation under reduced pressure at a temperature higher than the lipid melting point to yield a thin lipid film on the walls of the flask, and remaining solvent traces were eliminated by drying under N2 flow for 30 min. The dry lipids were hydrated in phosphate-buffered saline (PBS) (with or without the antimalarial drug primaquine) at 37 °C to obtain a concentration of 10mM and multilamellar liposomes were formed by 3 cycles of constant vortexing followed by bath sonication for 4 min each. Multilamellar liposomes were down-sized to form uni- or oligolamellar vesicles by extrusion through 200- nm polycarbonate membranes (Poretics, Livermore, CA, USA) in an extruder device (LiposoFast, Avestin, Ottawa, Canada). Liposome size was determined by dynamic light scattering using a Zetasizer NanoZS90 (Malvern Ltd, Malvern, UK).

Immunoliposome preparation

The mild reducing agent 2-mercaptoethylamine-HCl (MEA, Pierce Biotechnology) was used to generate half-antibodies (Karyakin, Presnova, Rubtsova, & Egorov, 2000; Raab et al., 1999). 90 µl of a 0.1 mg/ml antibody solution in PBS was added to 10 µl of 10 × reaction buffer (PBS containing 5mM EDTA and 50mM MEA), and incubated for 90 min at 37 °C in a water bath. Unreacted MEA was separated from reduced half-antibodies by molecular exclusion chromatography. For the coupling of targeting antibodies to liposomes we followed established protocols (Martin & Papahadjopoulos, 1982) that use MPB-PE to incorporate proteins into liposomes through the reaction of the maleimide group in the lipid with a thiol group from the ligand. In the case of antibodies the free thiol was obtained by generating half-antibodies as described above. MPB-PE-containing liposomes were incubated with half-antibodies (0.01 µg/µl, 133 nM half-antibody assuming complete reduction by MEA) overnight at 4 °C. Immunoliposomes were pelleted by ultracentrifugation (100,000 g for 90 min at 4 °C), and finally resuspended in 10 volumes of PBS and kept at 4 °C for up to 2 weeks before adding them to RBC-containing samples.

Primaquine encapsulation and quantification

The antimalarial drug primaquine was encapsulated in DOTAP-containing liposomes by dissolving it in PBS at a primaquine concentration of 1.2 mM, removing non-encapsulated drug by molecular exclusion chromatography (encapsulated PQ concentration of 0.12 mM). Heparin (sodium salt from porcine intestinal mucosa; 13,000 kDa mean molecular mass) was covalently bound by addition of 1 vol of heparin solution in PBS to the liposomes. Unbound heparin was removed by ultracentrifugation and the resulting liposome pellet was taken up in 10 pellet volumes of PBS immediately before addition to pRBC cultures with a further 20-fold dilution (ca. 3 µM final primaquine concentration in the culture). For the quantification of encapsulated primaquine, a lipid extraction of the liposomes was performed. Briefly, following ultracentrifugation the liposome pellet was treated with methanol:chloroform:0.1 M HCl (1.8:2:1) and after phase separation primaquine content in the upper water-methanol phase was determined by measuring A320.

Heparin and CSA determination

For the determination of heparin and CSA concentration the Alcian Blue method was used (Frazier, Roodhouse, Hourcade, & Zhang, 2008). Shortly, 10 µl of heparin-containing solution was mixed with 10 µl of a solution containing 27 mM H_2SO_4, 0.375% Triton X-100, and 4 M guanidine-HCl. To the resulting 20 µl were added 100 µl of 1 mg/ml Alcian Blue 8GX solution in 0.25% Triton X-100, 18 mM H_2SO_4. Samples were centrifuged and the pellet was resuspended in 500 µl of 8 M guanidine-HCl. Finally, after spinning down debris, A600 of the supernatant was recorded and heparin content was determined from a standard linear regression of known concentrations. Unspecific cytotoxicity and hemolysis assays were performed as described previously (Urbán et al., 2011).

Covalent binding of heparin to liposomes

Liposomes containing 30% PE were prepared as described previously. The amine groups present in the liposomes were crosslinked with the carboxyl groups of heparin by dissolving the heparin sodium salt in an activation buffer consisting of 0.1M 2-[N-morpholino]ethane sulfonic acid and 0.5M NaCl (MES buffer), pH 5.0. A final concentration of 2mM of N-(3-dimethylaminopropyl)-N'-ethylcarbodiimide hydrochloride (EDAC, Fluka) and 5 mM N-hydroxysuccinimide (NHS, Fluka) were added to the activated heparin solution. After 15 min reaction the binding of heparin to liposomes was performed by incubation for 2 h with gentle stirring to obtain the desired PE:heparin ratios. To remove unbound heparin, liposomes were pelleted by ultracentrifugation (150.000 g, 1.5 hours at 4°C), and finally resuspended in PBS and stored at 4°C.

Chitosan nanoparticle synthesis

Chitosan NPs were prepared by a coacervation method described elsewhere (Arias, López-Viota, Gallardo, & Adolfina Ruiz, 2010). Briefly, chitosan (1%, w/v) was dissolved in 50 ml of an aqueous solution of acetic acid (2%, v/v) containing 1% (w/v) pluronic® F-68. About 12.5 ml of a solution of sodium sulfate (20%, w/v) was added dropwise (2.5 ml/min) to the chitosan solution under mechanical stirring (1200 rpm). After the addition of sodium sulfate, stirring was continued for 1 hour to obtain the aqueous suspension of chitosan NPs. The colloidal suspension was then subjected to a cleaning procedure that included repeated cycles of centrifugation (40 min at 73,920 × g, Centrikon T-124 high-speed centrifuge; Kontron, Paris, France) and re-dispersion in water, until the conductivity of the supernatant was $\leq$ 10 µS/cm.

Isothermal titration calorimetry (ITC)

ITC measurements were performed with a VP-ITC microcalorimeter. The working cell was filled with the chitosan nanoparticles suspension at a concentration of 0.1 mg/ml in PBS and the reference cell with the corresponding nanoparticles-free PBS solution. 10-µl aliquots of 1 mg/ml heparin solution in PBS were injected stepwise into the working cell at 200 s intervals. The corresponding reference blank experiments were also performed, namely, titration of PBS in the nanoparticles suspension and titration of heparin solution in PBS. The sample cell was constantly stirred at 300 rpm, and the measurements were performed at 25 °C. The data analyses were carried out with Origin software provided by MicroCal.

Fluorescence confocal microscopy

Living *P. falciparum* cultures with mature stages of the parasite were incubated in the presence of 100 µM immunoliposomes in PBS supplemented with 0.75% bovine serum albumin for 90 min at 37 °C with gentle stirring. After washing with PBS, blood smears were prepared and cells were fixed for 20 min with 1% (v/v) paraformaldehyde in PBS. Parasite nuclei were stained with 4′6-diamino-2-phenylindole (DAPI) and the RBC membrane was labeled with wheat germ agglutinin-Alexa Fluor 488 conjugate (Life Technologies). Slides were finally mounted with ProLong® Gold antifade reagent, and analyzed with a Leica TCS SP5 laser scanning confocal microscope. For fluorescein-labeled CSA-stained samples, mature stages of the *P. falciparum* CS2 parasite were incubated in the presence of 3.2 mg/mL CSA-FITC for 90 minutes at 37 ºC with gentle stirring. After washing 3 x with PBS, parasite nuclei were stained with Hoechst solution for 30 minutes at room temperature and gentle stirring. Finally, after performing 2 washing steps, the culture was diluted 10 x in PBS and analyzed with a Leica TCS SP5 laser scanning confocal microscope.

Plasmodium falciparum cell culture

The *P. falciparum* 3D7 and CS2 strains were grown *in vitro* in group B human RBCs using previously described conditions (Cranmer, Magowan, Liang, Coppel, & Cooke). Briefly, parasites (thawed from glycerol stocks) were cultured at 37 °C in Petri dishes containing RBCs in Roswell Park Memorial Institute (RPMI) complete medium under a gas mixture of 92% N_2, 5% CO_2, and 3% O_2. Synchronized cultures were obtained by 5% sorbitol lysis, and the medium was changed every 2 days maintaining 3% hematocrit. For culture maintenance, parasitemias were kept below 5% late forms by dilution with washed RBCs prepared as described elsewhere (Urbán, Estelrich, Cortés, & Fernàndez-Busquets, 2011). For growth inhibition assays, parasitemia was adjusted to 1.5% with more than 90% of parasites at ring stage after sorbitol synchronization. One hundred fifty microliters of this *Plasmodium* culture was plated in 96-well plates and incubated in the presence of test compounds for 48 h in the conditions described above. Parasitemia was determined by flow cytometry, after staining pRBC DNA with the nucleic acid dye Syto 11, added 10 min before analysis without any further washing step. Samples were analyzed using a BD FACSCalibur™ flow cytometer and parasitemia was expressed as the number of parasitized cells per 100 erythrocytes.

Plasmodium berghei ookinete culturing and targeting assay

Ookinete culture media consisted of 16.4 g RPMI with HEPES and L-glutamine in 1 litre, 2% w/v $NaHCO_3$, 0.05% w/v hypoxanthine, 100 µM xanthurenic acid, 50 units/ml penicillin, 50 µg/ml streptomycin (100x penicillin and streptomycin, Invitrogen), pH 7.4. Complete medium was prepared just before use by supplementing with heat inactivated FBS (Invitrogen) to a final concentration of 20%. Six days prior to performing the targeting assay, a mouse was treated intraperitoneally with phenylhydrazine (PHZ) 10 ug/ml. Three days after PHZ treatment the mouse was infected by intraperitoneal injection with *P. berghei mCherry* pBRCs and, 3 days later, 1 ml infected blood was collected by cardiac puncture onto 30 ml ookinete media, and incubated for 24 hours at 19-21ºC with 70-80% relative humidity. For ookinete targeting assays, 100 µl of heparin 0.25 mg/ml were added to 100 µl of culture and incubated in the dark for 90 min under orbital stirring at 300 rpm. After the incubation period, samples were centrifuged for 1.5 min at 2000 rpm and washed with PBS 3 times. Fixed cells slides were prepared by adding 0.5 µl of FBS to 0.5 µl of pellet and by fixing the smear with 4% PFA for 15 min. After performing 3 washing steps with PBS, slides were mounted with Vectashield® DAPI-containing media (Vector Laboratories, UK).

Cryo-transmission electron microscopy

Chitosan NPs binding to heparin-FITC (Life Technologies) was also assessed by cryo transmission electron microscopy (cryo-TEM) analysis. 1mg/ml heparin-FITC was added to 2 mg/ml NPs for 90 min with gentle stirring. When the incubation was finished, the sample was centrifuged for 60 min at 4 °C and 100.000 x g to discard the non-bounded heparin. The pellet was treated with 5 µg/ml PBS of a primary antibody anti-FITC (Rockland Immunochemicals Inc., Limerick, PA, USA) for one hour with gentle orbital stirring; after PBS washing, the secondary anti-goat antibody conjugated to 6-nm colloidal gold (Jackson ImmunoResearch Laboratories Inc.) was added at a concentration of 50 µg/ml PBS and incubated for 90 min as above. To remove the antibody portion that did not react, we performed a Micro Bio-Spin Chromatography Column™ (Bio Rad) packed with sepharose CL-4B. Finally, a thin aqueous film was formed by placing a 5 µl sample drop on a glow-discharged holey carbon grid and then blotting the grid against filter paper. The resulting thin films spanning the grid holes were vitrified by plunging the grid (kept at 100% humidity) into ethane, which was maintained at its melting point with liquid nitrogen, using a Vitrobot (FEI Company, Eindhoven, The Netherlands). The vitreous films were transferred to a Tecnai F20 TEM (FEI Company) using a Gatan cryotransfer (Gatan, Pleasanton, CA), and the samples were observed in a low dose mode. Images were acquired at 200 kV at a temperature between 170 and 175 °C, using low-dose imaging conditions not exceeding 20 $e^-/\text{Å}^2$, with a CCD Eagle camera (FEI Company).

In vitro coagulation test

In vitro coagulation tests were performed adopting human blood from healthy volunteer donors. Blood, collected in Terumo Venosafe citrated tubes (Terumo Europe N. V., Belgium) were assessed within 2 h after blood collection. All tests were performed with the agreement of the local ethical committee from the Medicine Faculty at the University of Liège. Whole blood and GAG-containing samples were mixed and incubated for 15 min at 37 °C. Samples were centrifuged at 2,000 g for 5 min, and the supernatants were collected, recalcified to reverse the effect of citrate anticoagulant, and supplied with the specific activators of coagulation (thromboplastin). Prothrombin time (PT), to evaluate the extrinsic pathway, was measured directly with a Dade Behring Coagulation Timer analyzer (Siemens Healthcare Diagnostics NV/SA, Belgium) using commercial reagents (Thromborel® S, Dade Behring/Siemens). Kaolin reagent was used as a positive control and PBS as a negative control. Clotting time was measured for each sample, and coagulation capacity was expressed as a percentage, taking the value of standard human plasma (Dade Behring/Siemens) as 100%. Measurements were done in duplicate with differences between both replicas <1% (coagulation equipment is programmed to realize at least 2 different measurements on the same samples, and if the difference between them is below 5 % the analysis is not repeated; otherwise, it is repeated once more).

Fluorescent labeling of CSA

In an adaptation of existing protocols [23], an appropriate amount of CSA (Mr ca. 20 kDa) was dissolved in 0.1 M MES buffer (pH 5.0), different amounts of EDC and NHS were added, and incubated at 37 °C for 3 h. The mixture was precipitated by the addition of cooled ethanol. CSA activated in its carboxyl groups was separated from the ethanol solution containing excess EDC and its by-products by centrifugation at 8000 rpm for 2 min. CSA-NHS was dissolved in PBS and mixed with aminofluorescein, and the reaction was allowed to proceed for 12 h, obtaining a final fluorescein:carboxyl ratio of 0.7%. Unreacted aminofluorescein was removed by size exclusion chromatography with a Sephadex G-25 gel column, and labeled CSA was finally collected and freeze-dried.

Analysis of purity and total sugar in CSA-FITC

Pure polysaccharide was prepared as 1 g/L solutions. Thin-layer chromatography (TLC) was applied for the analysis of the purity of fluorescent CSA. For TLC analysis, aliquots (0.5 nL) of samples were applied to a TLC plate and developed in propanol/water (3:1, V/V) for 10 min. Plates can directly be analyzed without any stain. For fluorescently labeled CSA, the total sugar was analyzed by the carbazole-sulfuric acid method. Fluorescence intensity of the polysaccharide was determined using a standard curve of fluorescence.

Force spectroscopy

Binding forces between CSA and pRBCs infected with the *P. falciparum* CS2 strain were measured with an MFP-3D atomic force microscope (Asylum Research, Santa Barbara, CA, USA). CSA molecules were immobilized on the tip of NP-S cantilevers (Veeco Instruments Inc.; spring constants in the range 0.05-0.08 N m^{-1} obtained by thermal method) that were previously silanized in vapour phase with 3-aminopropyl triethoxysilane (APTES, Fluka, Buchs, Switzerland). The immobilization via covalent bonds between carboxyl groups of the CSA molecules and amine groups of the silanized cantilevers took place by immersing the cantilevers in a solution of 100 μg ml^{-1} CSA containing 2.5 mM N-(3-dimethylaminopropyl)-N'-ethylcarbodiimide hydrochloride (EDAC, Fluka) and 10 mM N-hydroxysuccinimide (NHS, Fluka) for about one hour, followed by rinsing with PBS. In parallel to CSA immobilization, 50 μl of a Percoll-purified pRBC solution in RPMI medium were deposited on poly-L-lysine-coated glass slides, which were prepared in advance by covering the glass slides (StarFrost, Waldemar Knittel Glasbearbeitungs GmbH, Braunschweig, Germany) with 0.01% poly-L-lysine solution for 30 min followed by rinsing with double deionised water (Milli-Q) and drying by evaporation. After about one hour of adsorption, weakly and non-attached pRBCs were discarded by rinsing the glass slides several times with 100 μl PBS using an automatic pipette. Force curves were acquired in PBS by approaching the cantilever tip with immobilized CSA to the pRBCs adsorbed on the glass slide and retracting it after contact. The approaching velocity was kept constant at 3 μm s^{-1}, whereas the retraction speed was varied between 3 and 14.5 μm s^{-1} (dynamic force spectroscopy). The corresponding loading rates were calculated by multiplying the retraction velocities by the effective spring constant of the system [24], which was ca. 10% of the spring constants of the cantilevers. Maximum applied forces were below 0.5 nN to prevent cell lysis [25]. In a typical experiment, between 500 and 2000 force curves were collected in 25-100 different spots on the same or different cells. Adhesion between CSA and pRBC was evaluated from the unbinding events in the retraction force curves. When several unbinding events were observed, only the last one was considered for analysis. Force histograms were fitted to Gaussian or 2-peak Gaussian functions to obtain the average binding forces. Control experiments with non-infected RBCs were also performed.

Results and Discussion

Use of targeted liposomes for the delivery of antimalarial lipids to *Plasmodium*

Preliminary data suggesting antimalarial activity of certain lipids [26] led us to explore this observation in more detail. The lipid MPB-PE, used for the covalent crosslinking to liposomes of antibodies through thioether bonds, exhibits significant concentration-dependent inhibition of the *in vitro* growth of *P. falciparum* when incorporated in the formulation of liposomes (Fig. 1).

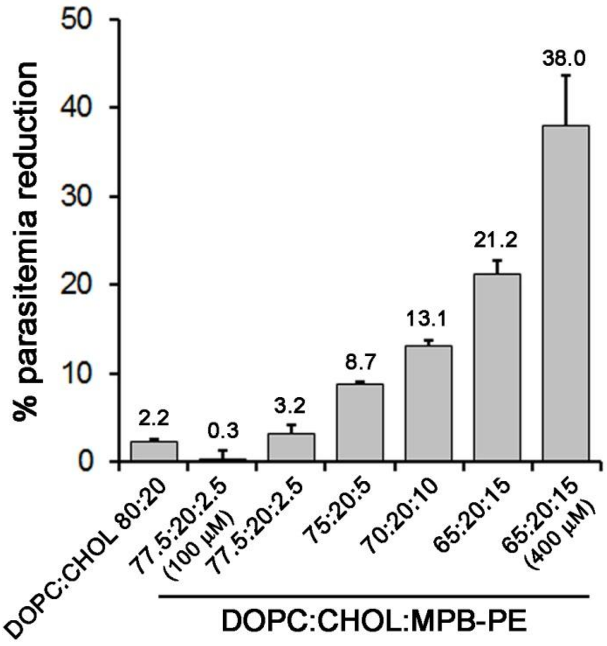

Fig. 1. Flow cytometry determination of the concentration-dependent effect of the lipid MPB-PE on the *in vitro* growth of *P. falciparum*. Concentrations in the cultures of the liposome formulations were 200 µM lipid except where otherwise indicated.

The inhibitory effect of MPB-PE incorporated in liposomes on *P. falciparum* growth suggested that, upon random interactions of liposomes with pRBCs, lipids entered the cell and reached the parasite. To explore whether such process occurred through whole liposome entry (e.g. via the tubulovesicular network) or was mediated by transfer phenomena between the apposed lipid bilayers of liposomes and pRBCs, we performed confocal fluorescence microscopy analysis of pRBC-targeted immunoliposomes [26] containing in their formulation 7% of the rhodamine-tagged lipid DOPE-Rho. The results obtained (Fig. 2) showed that liposome-delivered lipids penetrated pRBCs and after 90 min of incubation colocalized with intracellular parasites. The observation of diffuse fluorescence and the lack of punctate patterns characteristic of whole intact liposomes [27] suggests that upon contact with the pRBC plasma membrane, liposomes fused with the cell and their constituent lipids were incorporated by the growing parasites. Higher resolution images of cells prepared at earlier stages in the drug delivery process reveal phenomena consistent with the interaction of liposomes with pRBCs immediately before or just after their constituent lipids are incorporated into the cell plasma membrane (Fig. 3).

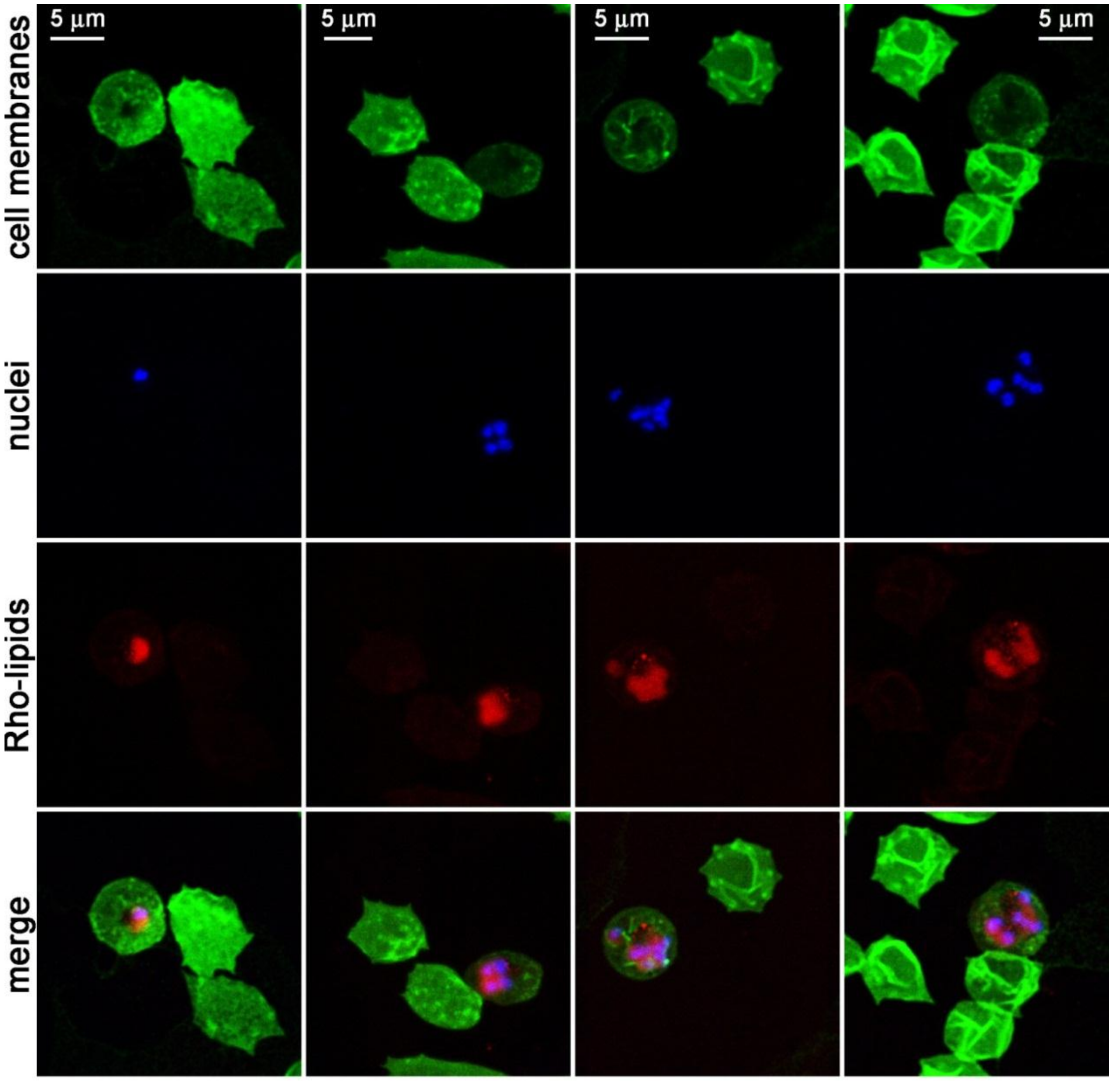
cell membranes
nuclei
Rho-lipids
merge
5 µm
5 µm
5 µm
5 µm

Fig. 2. Fluorescence confocal microscopy analysis of the fate of Rho-labeled lipids incorporated in the formulation of pRBC-targeted immunoliposomes added to living *P. falciparum* cultures and incubated for 90 min before proceeding to sample processing.

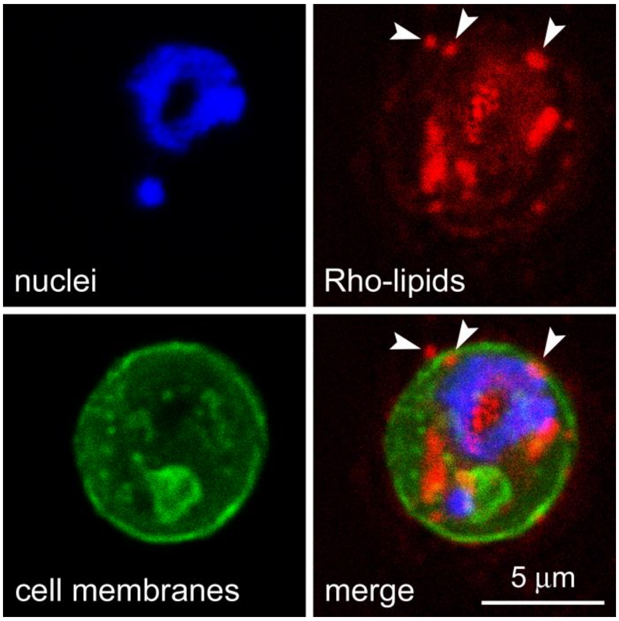

Fig. 3. Fluorescence confocal microscopy analysis of the subcellular distribution of Rho-labeled lipids incorporated in the formulation of pRBC-targeted immunoliposomes added to living *P. falciparum* cultures. Arrowheads indicate structures compatible with plasma membrane-liposome merging events.

Antimalarial activity of drug-loaded liposomes targeted with covalently bound heparin

The dual activity of heparin as antimalarial drug and as pRBC targeting element has been proposed as a promising new avenue for future malaria therapies [16]. However, existing models contain electrostatically bound heparin that is prone to peel off from liposome surfaces while in the blood circulation, incurring the risk of anticoagulation and of internal bleeding. To explore strategies that could minimize these adverse effects, we have modified our previous design to incorporate covalently bound heparin. This new liposome prototype exhibits the additive effect previously observed for non-covalently bound heparin, whereby primaquine-loaded liposomes have a significantly improved antimalarial activity when targeted with covalently bound heparin (Fig. 4), suggesting its double role both as drug and targeting molecule. The anticoagulant activity of heparin covalently bound to liposomes was found to be significantly smaller than similar amounts electrostatically bound (Grandfils data, Table 1), in agreement with previous evidence of non-anticoagulant activity of heparin when covalently immobilized on a substrate [28].

Depolymerized heparin lacking anticoagulant activity had been found to disrupt rosette formation and pRBC cytoadherence *in vitro* and *in vivo* in animal models and in fresh parasite isolates [29]. Shorter heparin fragments consisting of hexa- (dp6) and octasaccharides (dp8) had a much smaller antimalarial activity *in vitro* than the native polymer (Fig. 5), but are also expected to present an insignificant anticoagulant activity (ongoing experiment).

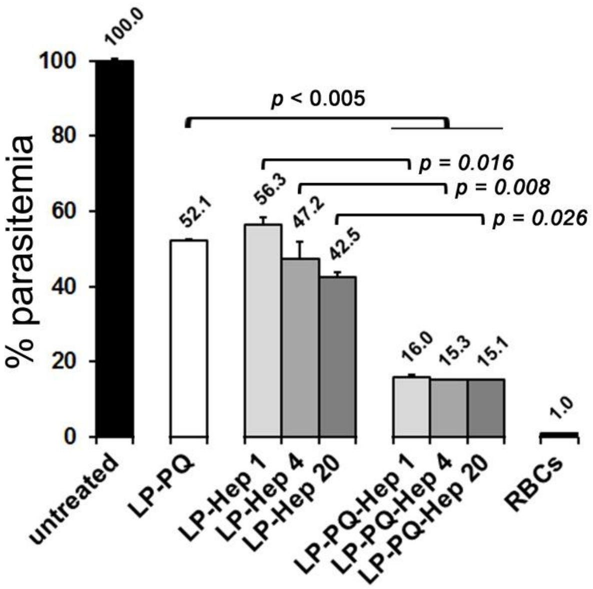

Fig. 4. Antimalarial activity and targeting capacity of different initial amounts of heparin (1, 4, and 20 µg/ml) covalently bound to primaquine-containing liposomes (LP-PQ-Hep). Controls include heparin-free, primaquine-containing liposomes (LP-PQ) and primaquine-free liposomes targeted with covalently-bound heparin (LP-Hep). PQ concentration in the pRBC culture was 3 µM for all samples.

Table 1. PT1/Quick *in vitro* coagulation test of different heparin concentrations, free or covalently conjugated to liposomes. Coagulation capacity is expressed as a percentage relative to the value obtained with standard human plasma. The concentrations indicated correspond to the amounts of total lipid and heparin in the test tube. Where unbound heparin was removed by ultracentrifugation, the determined heparin content is provided. Shadowed in grey are indicated those samples with anticoagulant activity.

	Free heparin	250 μM liposomes-heparin *[determined heparin content]*
PBS (no heparin)	**101.0**	**101.0**
20 μg/ml heparin	**<25**	**114.2** *[6.0* μg/ml*]*
4 μg/ml heparin	**64.1**	**109.4** *[1.2* μg/ml*]*
1 μg/ml heparin	**102.9**	**109.4** *[0.3* μg/ml*]*

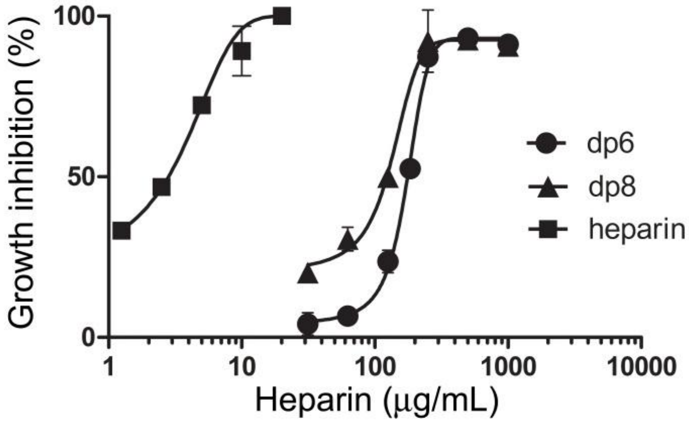

Fig. 5. Short heparin fragments. IC50 dp6=174 μg/ml, dp8=134 μg/ml.

Functionalization of chitosan nanoparticles with heparin

The highly specific targeting of heparin towards pRBCs prompted the exploration of its capacity as targeting agent of nanoparticles other than liposomes. The electrostatic interaction of heparin with positively charged nanocapsules has been explored as a proof of concept with the objective of designing the simplest working strategy. ITC was used to analyze the interaction of heparin with the cationic polymer chitosan (Fig. 6). A complete sigmoidal binding exothermic isotherm for the interaction heparin-chitosan was obtained, with a 50% saturation obtained at a molar ratio chitosan:heparin of 0.25 (Fig. 6A). When chitosan was added in the form of nanoparticles with a mean diameter of ca. 200 nm (Fig. 6C), a strong cooperative effect was observed (Fig. 6B); likely, the association of multiple chitosan molecules in a nanoparticle favored the cooperative binding of heparin to adjacent chitosan chains following an initial interaction. According to *in vitro P. falciparum* growth inhibition assays the interaction of heparin with chitosan did not affect its antimalarial activity (Fig. 6D).

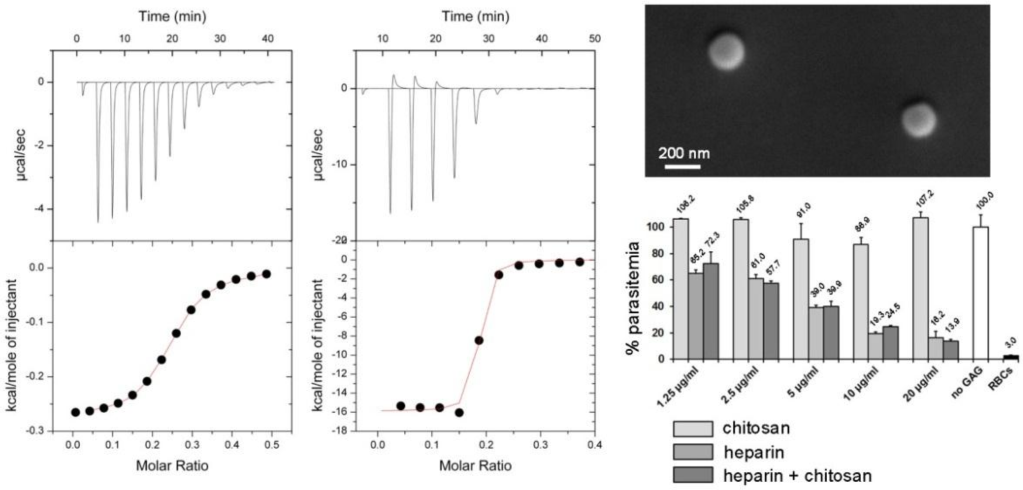

Fig. 6. Study of the interaction heparin-chitosan. (A) Representative data from an ITC experiment in which heparin was titrated into the reaction cell containing chitosan. Injections of a 0.05 mM heparin solution were added to a 0.01 mM chitosan solution in the ITC cell. The area underneath each injection peak (top panel) is equal to the total heat released for that injection. When this integrated heat is plotted against the

molar ratio of ligand added to macromolecule in the cell, a complete binding isotherm for the interaction is obtained (bottom panel). (B) Representative data from an ITC experiment in which 1 mg/ml heparin was titrated into the reaction cell containing 0.1 mg/ml chitosan nanoparticles. The first addition was half the volume of the other additions and was not used in the fit. The experiment was performed at 25 °C. (C) Scanning electron microscopy image of the chitosan nanoparticles used. (D) Effect of the interaction with chitosan on the antimalarial activity of heparin.

Targeting of heparin to *Plasmodium* stages in the mosquito vector

The straightforward binding of heparin to chitosan nanoparticles, expected to be innocuous for insects given the endogenous nature of this polymer in these animals, stimulated us to study the targeting capacity of heparin towards the *Plasmodium* stages in *Anopheles*. Fluorescently labeled heparin-FITC added to preparations containing *Plasmodium* gametocytes, ookinetes, oocysts and sporozoites was observed to bind only ookinetes (Fig. 7) derived from the murine malaria parasite *P. berghei*, in agreement with previous data reporting on heparin binding to ookinete-secreted proteins [22].

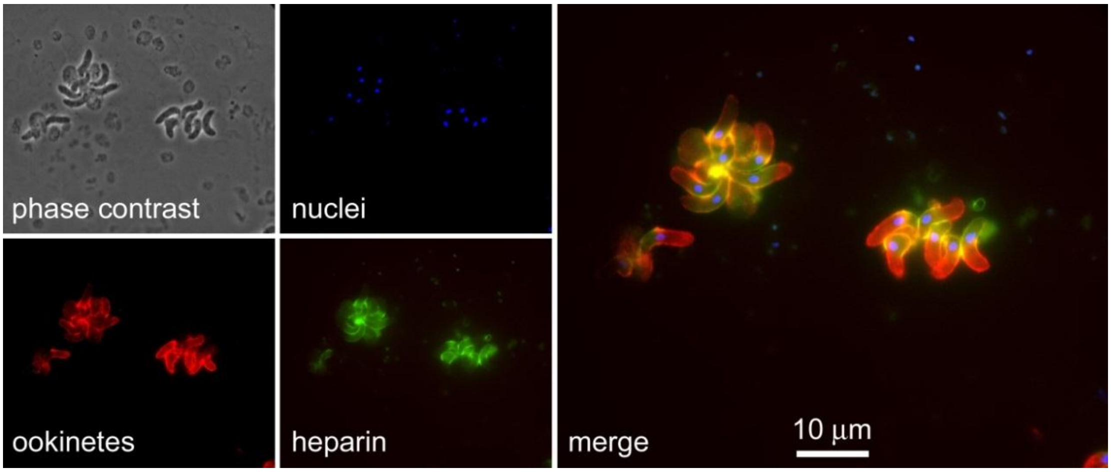

Fig. 7. Heparin-FITC was added to living cultures of *P. berghei* ookinetes and incubated for 90 minutes before sample preparation for microscopic analysis. Here we show in the same sample ookinetes and pRBCs as control of the specificity of the targeting.

Use of CSA for the targeting of pRBCs

The potential use of heparin as drug in malaria therapy [15,30-33] has been hindered by its anticoagulation properties [34], but heparin-related polysaccharides exist which are known to have little anticoagulating activity (Marques et al., 2015, submitted). One such polysaccharides is CSA, which lacks antimalarial activity (Marques et al., 2015, submitted) but whose pRBC targeting capacity has never been explored. The binding forces between CSA and Percoll-purified pRBCs or non-infected RBCs deposited on poly-L-lysine-coated glass slides were measured by AFM force spectroscopy. CSA molecules were immobilized on the tip of cantilevers used as force sensors, which were approached to the adsorbed erythrocytes and retracted from them after contact in order to obtain a force curve. Single-molecule CSA-pRBC adhesion forces in PBS were evaluated from the unbinding events found in ca. 50 to 71% of total retraction force curves (Fig. 8A). As the CSA-coated tip withdrew, a decompression and stretching of the pRBC was observed in the retraction force curves for distances up to 4 μm, which was followed by a vertical jump (arrows in Fig. 8A) corresponding to the detachment of the tip from the cell membrane. A flat baseline was finally reached, indicating no interaction between cell and tip after their complete separation. Fig. 8B shows a representative histogram for CSA-pRBC adhesion at a loading rate of 24 nN s^{-1}. A 2-peak Gaussian fit of the histogram yielded an average binding force of 41 ± 1 pN for the main peak. A second, smaller peak at 70 ± 17 pN, and even a third peak at about 120 pN (not included in the fit for being very small), could correspond to the simultaneous unbinding of 2 and 3 interacting groups on the same or different CSA molecules, respectively. Binding forces between 32 pN and 51 pN were calculated for the main peaks of the histograms obtained in experiments at different loading rates (dynamic force spectroscopy, Fig. 8C). A linear relation between binding force and logarithm of loading rate was observed, in agreement with the predictions from Bell-Evans model for binary interactions [35,36]. Control experiments with non-infected RBCs showed adhesion to CSA in only a small proportion (12%) of the retraction force curves, with an average binding force of 32 ± 1 pN (Fig. 8B). The adhesion between pRBCs infected by the CSA-binding P. *falciparum* FCR3-CSA strain and Chinese hamster ovary (CHO) cells expressing CSA on their surface had been explored by AFM force spectroscopy [37], yielding a mean rupture force of 43 pN, similar to that obtained here using purified CSA. Because CSA interaction with pRBCs has been described to occur through the binding to PfEMP1 on erythrocyte surfaces, the adhesive force between both cell types had been assigned entirely to the CSA-PfEMP1 association [37]. However, the binding of CSA on the AFM cantilever to pRBCs could not be inhibited by the presence of 500 µg CSA/ml in solution, whereas pRBC-CHO adhesion had been shown to be blocked by 100 µg CSA/ml [38]. This result suggests that CSA-saturable cell membrane receptors exist on CHO cells that are necessary for pRBC binding.

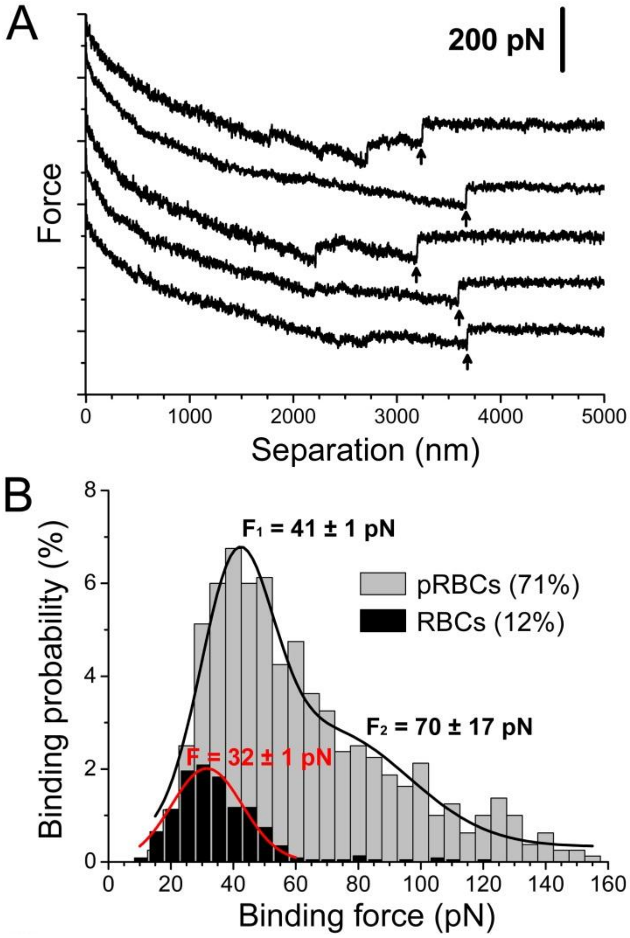

Fig. 8. Binding of CSA to erythrocytes. (A) Typical force curves obtained when retracting CSA-functionalized cantilever tips from pRBCs. Arrows indicate individual CSA-pRBC unbinding events. For the sake of clarity, the force curves were shifted vertically to avoid overlapping. (B) Representative force histograms for the binding of

CSA to pRBCs (grey) and RBCs (black) at a loading rate of 24 nN s−1. Force histograms were fitted to a Gaussian (RBC) or a 2-peak Gaussian function (pRBC).

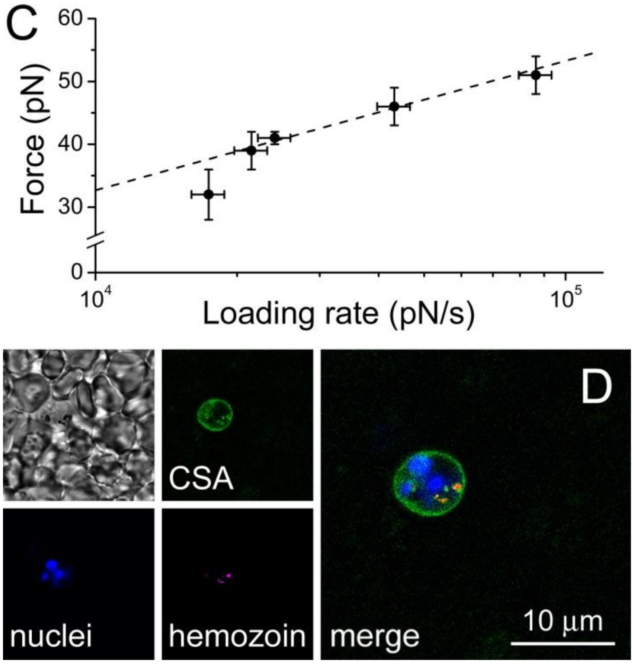

Fig. 8. Binding of CSA to erythrocytes. (C) Average binding forces between CSA and pRBCs at different loading rates. (D) Fluorescence confocal microscopy analysis of live late-stage *P.falciparum* CS2 parasites incubated with CSA-FITC.

Acknowledgements

This work was supported by grants BIO2014-52872-R from the Ministerio de Economía y Competitividad, Spain, which included FEDER funds, and 2014-SGR-938 from the Generalitat de Catalunya, Spain.

Reference List

[1] P.L. Alonso and M. Tanner, Public health challenges and prospects for malaria control and elimination, Nat. Med., 19 (2013) 150-155.

[2] P. Urbán, J.J. Valle-Delgado, E. Moles, J. Marques, C. Díez, and X. Fernàndez-Busquets, Nanotools for the delivery of antimicrobial peptides, Curr. Drug Targets, 13 (2012) 1158-1172.

[3] P. Urbán and X. Fernàndez-Busquets, Nanomedicine against malaria, Curr. Med. Chem., 21 (2014) 605-629.

[4] N. Kuntworbe, N. Martini, J. Shaw, and R. Al-Kassas, Malaria intervention policies and pharmaceutical nanotechnology as a potential tool for malaria management, Drug Dev. Res., 73 (2012) 167-184.

[5] J.K. Baird, Effectiveness of antimalarial drugs, N. Engl. J. Med., 352 (2005) 1565-1577.

[6] M. Prudêncio, A. Rodriguez, and M.M. Mota, The silent path to thousands of merozoites: the *Plasmodium* liver stage, Nat. Rev. Microbiol., 4 (2006) 849-856.

[7] A.F. Cowman and B.S. Crabb, Invasion of red blood cells by malaria parasites, Cell, 124 (2006) 755-766.

[8] J. Burrows, R. Hooft van Huijsduijnen, J. Möhrle, C. Oeuvray, and T. Wells, Designing the next generation of medicines for malaria control and eradication, Malar. J., 12 (2013) 187.

[9] J. Gysin, B. Pouvelle, M. Le Tonquèze, L. Edelman, and M.C. Boffa, Chondroitin sulfate of thrombomodulin is an adhesion receptor for *Plasmodium falciparum*-infected erythrocytes, Mol. Biochem. Parasitol., 88 (1997) 267-271.

[10] M. Fried and P.E. Duffy, Adherence of *Plasmodium falciparum* to chondroitin sulfate A in the human placenta, Science, 272 (1996) 1502-1504.

[11] K.T. Andrews, N. Klatt, Y. Adams, P. Mischnick, and R. Schwartz-Albiez, Inhibition of chondroitin-4-sulfate-specific adhesion of *Plasmodium falciparum*-infected erythrocytes by sulfated polysaccharides, Infect. Immun., 73 (2005) 4288-4294.

[12] D.I. Baruch, J.A. Gormley, C. Ma, R.J. Howard, and B.L. Pasloske, *Plasmodium falciparum* erythrocyte membrane protein 1 is a parasitized erythrocyte receptor for adherence to CD36, thrombospondin, and intercellular adhesion molecule 1, Proc. Natl. Acad. Sci. U. S. A., 93 (1996) 3497-3502.

[13] J.C. Reeder, A.F. Cowman, K.M. Davern, J.G. Beeson, J.K. Thompson, S.J. Rogerson, and G.V. Brown, The adhesion of *Plasmodium falciparum*-infected erythrocytes to chondroitin sulfate A is mediated by *P. falciparum* erythrocyte membrane protein 1, Proc. Natl. Acad. Sci. U. S. A., 96 (1999) 5198-5202.

[14] J.J. Valle-Delgado, P. Urbán, and X. Fernàndez-Busquets, Demonstration of specific binding of heparin to *Plasmodium falciparum*-infected vs non-infected red blood cells by single-molecule force spectroscopy, Nanoscale, 5 (2013) 3673-3680.

[15] T.W. Sheehy and R.C. Reba, Complications of *falciparum* malaria and their treatment, Ann. Intern. Med., 66 (1967) 807-809.

[16] J. Marques, E. Moles, P. Urbán, R. Prohens, M.A. Busquets, C. Sevrin, C. Grandfils, and X. Fernàndez-Busquets, Application of heparin as a dual agent with antimalarial and liposome targeting activities towards *Plasmodium*-infected red blood cells, Nanomedicine: NBM, 10 (2014) 1719-1728.

[17] M.J. Boyle, J.S. Richards, P.R. Gilson, W. Chai, and J.G. Beeson, Interactions with heparin-like molecules during erythrocyte invasion by *Plasmodium falciparum* merozoites, Blood, 115 (2010) 4559-4568.

[18] K. Paaijmans and X. Fernàndez-Busquets, Antimalarial drug delivery to the mosquito: an option worth exploring?, Future Microbiol., 9 (2014) 579-582.

[19] J.B. Ancsin and R. Kisilevsky, A binding site for highly sulfated heparan sulfate is identified in the N terminus of the circumsporozoite protein: significance for malarial sporozoite attachment to hepatocytes, J. Biol. Chem., 279 (2004) 21824-21832.

[20] R.R. Dinglasan, A. Alaganan, A.K. Ghosh, A. Saito, T.H. van Kuppevelt, and M. Jacobs-Lorena, *Plasmodium falciparum* ookinetes require mosquito midgut chondroitin sulfate proteoglycans for cell invasion, Proc. Natl. Acad. Sci. U. S. A., 104 (2007) 15882-15887.

[21] D.K. Mathias, R. Pastrana-Mena, E. Ranucci, D. Tao, P. Ferruti, C. Ortega, G.O. Staples, J. Zaia, E. Takashima, T. Tsuboi, N.A. Borg, L. Verotta, and R.R. Dinglasan, A small molecule glycosaminoglycan mimetic blocks *Plasmodium* invasion of the mosquito midgut, PLoS Pathog., 9 (2013) e1003757.

[22] F. Li, T.J. Templeton, V. Popov, J.E. Comer, T. Tsuboi, M. Torii, and J.M. Vinetz, *Plasmodium* ookinete-secreted proteins secreted through a common micronemal pathway are targets of blocking malaria transmission, J. Biol. Chem., 279 (2004) 26635-26644.

[23] Z.R. HAN, Y.F. WANG, X. LIU, J.D. WU, H. CAO, X. ZHAO, W.G. CHAI, and G.L. YU, Fluorescent labeling of several glycosaminoglycans and their interaction with anti-chondroitin sulfate antibody, Chin. J. Anal. Chem., 39 (2011) 1352-1357.

[24] A. Fuhrmann, D. Anselmetti, R. Ros, S. Getfert, and P. Reimann, Refined procedure of evaluating experimental single-molecule force spectroscopy data, Physical Review E, 77 (2008) 031912.

[25] A. Hategan, R. Law, S. Kahn, and D.E. Discher, Adhesively-tensed cell membranes: lysis kinetics and atomic force microscopy probing, Biophysical Journal, 85 (2003) 2746-2759.

[26] P. Urbán, J. Estelrich, A. Cortés, and X. Fernàndez-Busquets, A nanovector with complete discrimination for targeted delivery to *Plasmodium falciparum*-infected versus non-infected red blood cells *in vitro*, J. Control. Release, 151 (2011) 202-211.

[27] E. Moles, P. Urbán, M.B. Jiménez-Díaz, S. Viera-Morilla, I. Angulo-Barturen, M.A. Busquets, and X. Fernàndez-Busquets, Immunoliposome-mediated drug delivery to *Plasmodium*-infected and non-infected red blood cells as a dual therapeutic/prophylactic antimalarial strategy, J. Control. Release, 210 (2015) 217-229.

[28] Y. Miura, S. Aoyagi, Y. Kusada, and K. Miyamoto, The characteristics of anticoagulation by covalently immobilized heparin, J. Biomed. Mater. Res., 14 (1980) 619-630.

[29] A.M. Leitgeb, K. Blomqvist, F. Cho-Ngwa, M. Samje, P. Nde, V. Titanji, and M. Wahlgren, Low anticoagulant heparin disrupts *Plasmodium falciparum* rosettes in fresh clinical isolates., Am. J. Trop. Med. Hyg., 84 (2011) 390-396.

[30] H. Smitskamp and F.H. Wolthuis, New concepts in treatment of malignant tertian malaria with cerebral involvement., Br. Med. J., 1 (1971) 714-716.

[31] N. Jaroonvesama, Intravascular coagulation in *falciparum* malaria, Lancet, 1 (1972) 221-223.

[32] M. Munir, H. Tjandra, T.H. Rampengan, I. Mustadjab, and F.H. Wulur, Heparin in the treatment of cerebral malaria, Paediatr. Indones., 20 (1980) 47-50.

[33] T.H. Rampengan, Cerebral malaria in children. Comparative study between heparin, dexamethasone and placebo, Paediatr. Indones., 31 (1991) 59-66.

[34] World Health Organization Malaria Action Programme., Severe and complicated malaria., Trans. R. Soc. Trop. Med. Hyg., 80 (Suppl) (1986) 3-50.

[35] G.I. Bell, Models for the specific adhesion of cells to cells, Science, 200 (1978) 618-627.

[36] E. Evans and K. Ritchie, Dynamic strength of molecular adhesion bonds, Biophys. J., 72 (1997) 1541-1555.

[37] P.A. Carvalho, M. Diez-Silva, H. Chen, M. Dao, and S. Suresh, Cytoadherence of erythrocytes invaded by *Plasmodium falciparum*: Quantitative contact-probing of a human malaria receptor, Acta Biomater., 9 (2013) 6349-6359.

[38] Y. Adams, C. Freeman, R. Schwartz-albiez, V. Ferro, C.R. Parish, and K.T. Andrews, Inhibition of *Plasmodium falciparum* growth *in vitro* and adhesion to chondroitin-4-sulfate by the heparan sulfate mimetic PI-88 and other sulfated oligosaccharides, Antimicrob. Agents Chemother., 50 (2006) 2850-2852.

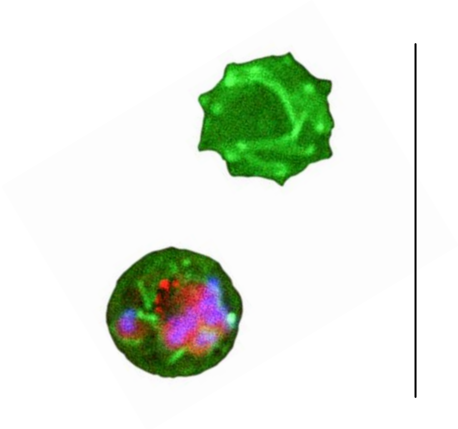

Internship project

With malaria elimination now firmly on the global research agenda, but resistance to the currently available drugs on the rise, there is an urgent need to invest in the research and development of new antimalarial strategies[174]. Drugs can potentially target a suite of parasite life stages inside two different hosts: the human and the mosquito vector. Malaria infection starts when a parasitized female *Anopheles* mosquito inoculates during a blood meal sporozoites of the malaria parasite, the protist *Plasmodium spp.*, which migrate through the skin into the circulation and then to the liver. In a few minutes sporozoites invade hepatocytes, where they will develop into merozoites[9] that enter the circulation to invade RBCs[76], where they replicate asexually to produce daughter cells that invade new erythrocytes to perpetuate the blood-stage cycle. Some parasites eventually differentiate into sexual stages, female or male gametocytes that are ingested by a mosquito from peripheral blood, and reach the insect's midgut where micro- and macrogametocytes develop into male and female gametes. Following fertilization the zygote differentiates into an ookinete that moves through the midgut epithelium of the mosquito host and forms an oocyst from which sporozoites are released and migrate to the salivary glands to restart the cycle at the next bite.

Asexual blood-stages are still the main target for current chemotherapeutic approaches[13]. Nevertheless, there might be several hundred billion pRBCs in the bloodstream of an infected patient which makes it roughly impossible to clear infections with single-dose administrations. Consequently, multiple doses are required instead, increasing the likelihood for resistance development and decreasing treatment efficacy. This fact is inciting research oriented to target bottlenecks in the parasite life cycle[17].

Previous results obtained by our group indicated that certain polymers like heparin can have a dual role as antimalarial drugs and as targeting elements towards pRBCs. For this reason, we explored if it could also be used as targeting agent against gametocytes, sporozoites, ookinetes, and oocysts.

1. *P. falciparum* gametocytes culturing and targeting assay

Gametocytes of *P. falciparum* NF54 were established from continuously maintained cultures of asexual blood-stage parasites, setting up flasks at 1% parasitaemia and 3% haematocrit. Gametocytes began to form in significant numbers in blood culture only following daily medium change. For the targeting assays, a 10 mL *P. falciparum* gametocytes stage V culture was centrifuged at 37°C for 5 minutes, 500 xg. The culture pellet was then resuspended in 3 mL incomplete RPMI and added to heparin on a 1vol : 1vol proportion. Samples were incubated for 90 minutes at 37°C. Following the incubation period, cultures were spun down and washed 3 times with incomplete RPMI. Smears were fixed with 4% paraformaldehyde (PFA) and stained with 4’6-diamino-2-phenylindole (DAPI).

Fluorescence microscopy examination of a *P. falciparum* 14 days-old coculture of pRBCs and gametocytes that had been treated for 90 min with 0.25 mg/mL heparin labeled with fluorescein (FITC) prior to fixation revealed that the polymer exclusively targeted and entered pRBCs and was not capable of targeting stage V gametocytes (**Figure 15**). Earlier stages of *P. falciparum* gametocytes were also included in the study and heparin showed no targeting activity towards these cells (data not shown).

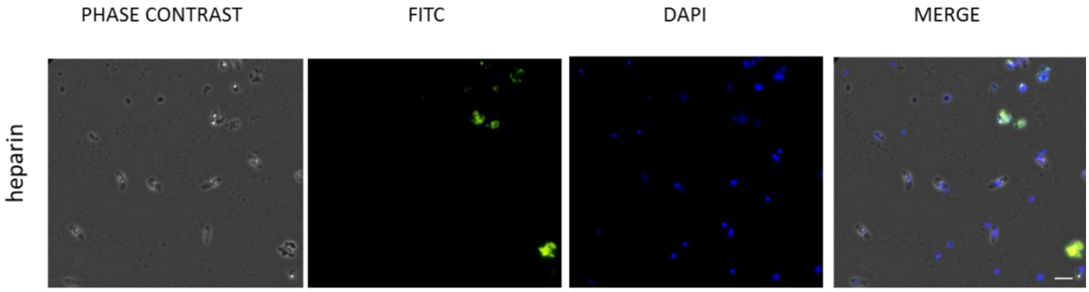

Figure 15. Targeting assay of heparin to stage V *P. falciparum* gametocytes. Heparin-FITC was added to living cultures of *P. falciparum* and incubated for 90 minutes before sample preparation for microscopic analysis. Here we show in the same sample stage V gametocytes and pRBCs as control of the specificity of the targeting. Scale bars correspond to 10 µm.

2. *P. berghei* ookinetes culturing and targeting assay

Ookinete culture media consisted of 16.4 g RPMI with HEPES and L-glutamine (Sigma-Aldrich) in 1 litre, 2% w/v $NaHCO_3$, 0.05% w/v hypoxanthine (Sigma-Aldrich), 100 µM xanthurenic acid (Sigma-Aldrich), 50 units/mL penicillin, 50 µg/ml streptomycin (100x penicillin and streptomycin, Invitrogen), pH 7.4. Complete medium was prepared just before use by supplementing with heat inactivated fetal bovine serum (Invitrogen) to a final concentration of 20%.

Six days prior to performing the targeting assay, a mouse was treated intraperitoneally with phenylhydrazine (PHZ). Three days after PHZ treatment the mouse was infected by intraperitoneal injection with *P. berghei* pBRCs. After 3 days, 1 mL infected blood was collected by cardiac puncture onto 30 mL ookinete media, and incubated for 24 hours at 19-21°C with 70-80% relative humidity.

For the ookinetes targeting assays, 100 µL of heparin were added to 100 µL of culture and incubated in the dark for 90 minutes at room temperature (RT), 300 rpm. After the incubation period, the sample was centrifuged for 1,5 minutes at 2000 rpm and washed with PBS. Fixed cells slides were done by adding 0,5uL FBS to 0,5 µL pellet and by fixing the smear with 4% PFA (15 minutes incubation at RT). After performing 3 washing steps with PBS, the slides were mounted. Fluorescence microscopy examination of a *P. berghei* coculture of pRBCs and ookinetes that had been treated for 90 min with 0.25 mg/mL heparin-FITC prior to fixation revealed that the polymer not only was capable of targeting pRBCs but also ookinetes (**Figure 16**). Parasite nuclei were stained with DAPI and cell membranes were labeled with cy3 * 13.1 mAb[175].

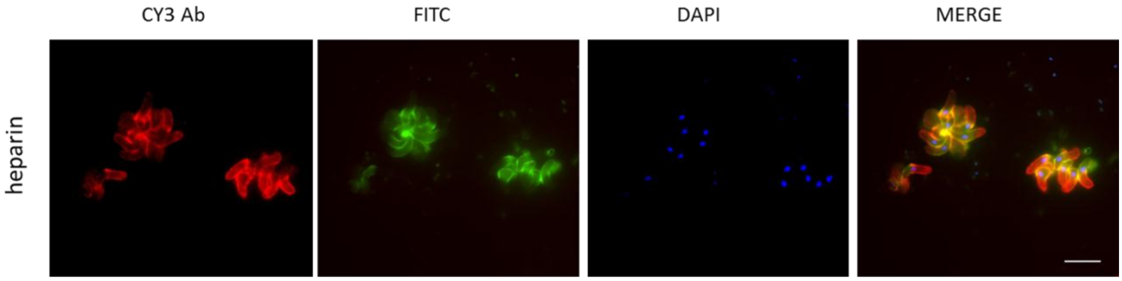

Figure 16. Heparin- FITC was added to living cultures of *P. berghei* ookinetes and incubated for 90 minutes before sample preparation for microscopic analysis. Here we show in the same sample ookinetes and pRBCs as control of the specificity of the targeting. It is important to highlight that heparin seems to compete with the specific antibody binding site on the ookinetes apical surface. Scale bars correspond to 10 µm.

3. *P. berghei* sporozoites culturing and targeting assay

To assess a direct feeding on malaria-infected mice, 6 days prior to feeding female *Anopheles stephensi* mosquitoes, a mouse was treated intraperitoneally with PHZ. Three days after PHZ treatment the mouse was infected by intraperitoneal injection with *P. berghei mCherry* pBRCs. One day prior to feeding, a warm container was placed on one side of a cage containing mosquitoes (4 to 7 days post-emergence) so that female mosquitoes were attracted to the heat source and could be collected in a pot selectively. Mosquitoes were not fed with sugar in the 24 hours preceding the blood feed but were hydrated with water.

On the day of the feed, the parasitemia and gametocytemia of the mouse were recorded, and an exflagellation test was also performed. Subsequently, the mouse was anesthetized and placed on the netting of the mosquito cage. The feed was maintained for 30 minutes at 19-21°C in the dark. On the day 1 post-feeding, the mosquitoes were anesthetized with CO_2 and kept on ice while the unfed ones were removed. Mosquitoes were then fed with Fructose/4-aminobenzoic acid every 2 days and maintained for 21 days at 19-21°C and 70-80% humidity.

For the sporozoites targeting assay (**Figure 17**), mosquitoes were dissected for salivary glands on day 21 post-feeding. Firstly, we anesthetized the mosquitoes with CO_2 and kept them on ice. For the dissection, 1 mL syringes with 26G needles were filled with incomplete RPMI. The mosquito was oriented in a drop of incomplete medium on a slide so it lied on its side. The neck was pressured gently with one needle so that it bulged out at the bottom. With the other needle the bulge was sliced and the contents escaped by maintaining pressure with the first needle. The head with the intact salivary glands was carefully detached and the carcass was removed. Finally, glands were sliced from the head and transferred to an eppendorf tube containing 50 µL of incomplete medium. After centrifugation for 10 minutes at 5000 rpm, the pellet was resuspended in 100 µL 0.20 mg/mL heparin-FITC and incubated for 90 minutes at 37°C, with gentle stirring. Samples were then centrifuged and washed with incomplete RPMI. When the last wash was completed, the pellet was resuspended in Hoescht solution (0.05 µg/mL). The pellet was lastly resuspended in incomplete RPMI and the slides containing live cells were prepared for confocal microscopy analyses.

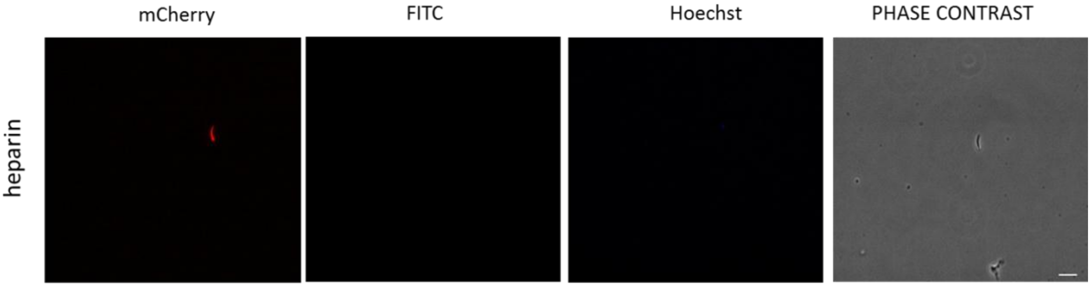

Figure 17. Fluorescence microscopy examination of a *P. berghei* culture of sporozoites that had been treated for 90 min with 0.20 mg/mL heparin-FITC prior to fixation revealed that the polymer do not show targeting capability for sporozoites. Scale bars correspond to 10 µm.

4. *P. berghei* oocysts culturing and targeting assay

To assess a direct feeding on malaria-infected mice, 6 days prior to feeding female *A. stephensi* mosquitoes a mouse was treated intraperitoneally with PHZ. Three days after PHZ treatment the mouse was infected by intraperitoneal injection with *P. berghei mCherry* pBRCs. One day prior to feeding, a warm container was placed on one side of a cage containing mosquitoes (4 to 7 days post-emergence) so that female mosquitoes were attracted to the heat source and could be collected in a pot selectively. Mosquitoes were not fed with sugar in the 24 hours preceding the blood feed but were hydrated with water.

On the day of the feed, the parasitemia and gametocytemia of the mouse were recorded, and an exflagellation test was also performed. Subsequently, the mouse was anesthetized and placed on the netting of the mosquito cage. The feed was maintained for 30 minutes at 19-21°C in the dark. On the day 1 post-feeding, the mosquitoes were anesthetized with CO_2 and kept on ice while the unfed ones were removed. Mosquitoes were then fed with Fructose/4-aminobenzoic acid every 2 days and maintained for 10 days at 19-21°C and 70-80% humidity.

For the oocysts targeting assay (**Figure 18**), mosquitoes were dissected for midguts on day 10 post-feeding. Firstly, we anesthetized the mosquitoes with CO_2 and kept them on ice. Under a dissecting microscope we added the mosquito to ~300 µl incomplete medium and removed the midguts. For the dissection, we held the mosquito with microtweezers and grasped the second to last segment of the mosquito abdomen. After pulling away gently, the blood-filled midgut comes away and the midguts were carefully collected onto a 24 wells plate containing 500 µl incomplete RPMI (5 midguts/well). The guts were transferred to a well containing heparin-FITC dissolved in incomplete RPMI at 0.25 mg/mL, and incubated for 90 minutes at RT with gentle stirring. Midguts were then washed 2 times with PBS, and fixed with 4% PFA for 15 minutes at RT. After fixation, 2 washing steps with PBS were performed, and the slides were finally prepared by transferring the midguts to a slide containing a few µL of mounting media (DAPI staining included).

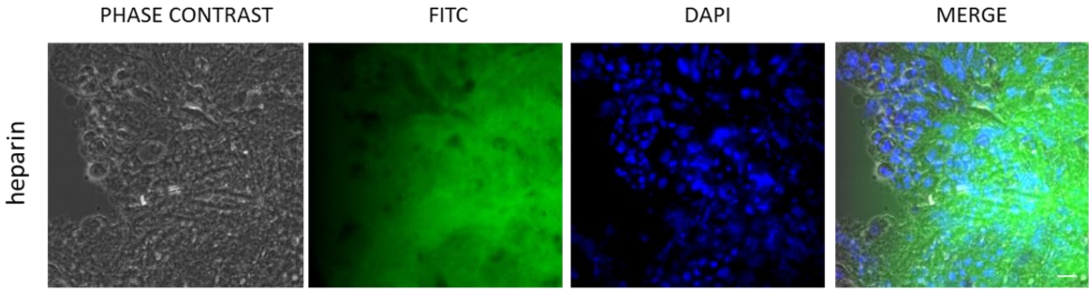
PHASE CONTRAST
FITC
DAPI
MERGE
heparin

Figure 18. Heparin-FITC was added to living cultures of *P. berghei* oocysts and incubated for 90 minutes before sample preparation for microscopic analysis. It is important to point out that midguts are highly autofluorescent as observed in the control experiment where cells were only treated with PBS (data not shown). Scale bars correspond to 20 μm.

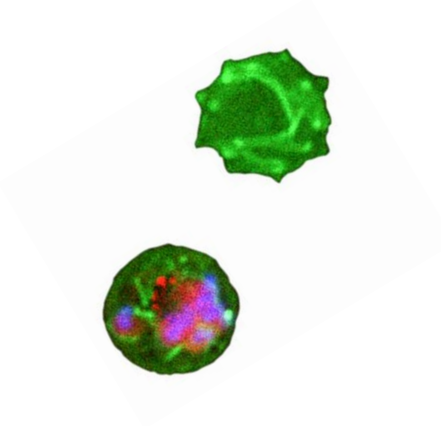

Article 4

ARTICLE 4

Article 4: Use of poly(amidoamine) drug conjugates for the delivery of antimalarials to *Plasmodium*.

The emergence of drug resistance severely limits the arsenal of available drugs against pathogens, a situation which is favored when parasites are exposed to low levels of antimalarial drugs, for instance where a full course of treatment is not completed, or where long-acting drugs are administered, which are eliminated slowly from the body. Novel delivery formulations are likely to optimize the therapeutic efficacy of antimalarials. In particular, targeted nanovectors, such as liposomes, solid-lipid nanoparticles, nano-/microemulsions and polymer-based nanocarriers have been receiving special attention in order to minimize the side effects of drug therapy and achieve the intake of doses sufficiently low to be innocuous for the patient but locally high enough to be lethal for the malaria parasite. In this work we have studied the ability of 3 PAA polymers (ISA1, ISA23, and AGMA1) to inhibit the growth of *P. falciparum* both *in vitro* and *in vivo*.

ISA23 is an amphoteric PAA prevailingly anionic at pH 7.4, non-cytotoxic (IC_{50}=5 mg mL^{-1}) and non-hemolytic. Moreover, ISA23 demonstrated in *in vivo* experiments with mice to be stealth and capable of circulating for several hours in the bloodstream. This characteristic is of paramount relevance in view of the target application, since it increases the chances to interact with pRBCs. Interestingly, not only analysis by FACS indicated that FITC-labeled ISA23 specifically targets, but also confocal microscopy demonstrated that it enters pRBCs, virtually neglecting RBCs. The *in vitro* experiments demonstrated that ionic complexes of ISA23 with primaquine (PQ) and chloroquine significantly increased the activity of the drug. Comparable results were obtained with AGMA1, amphoteric but prevailingly cationic at pH 7.4, non-cytotoxic (IC_{50}=5 mg mL^{-1}) and non-hemolytic, which, moreover, proved endowed with remarkable antimalarial activity *per se*. ISA1 has been left aside since it presented significant toxicity in mice.

ARTICLE 4

Journal of Controlled Release 177 (2014) 84–95

Contents lists available at ScienceDirect

Journal of Controlled Release

journal homepage: www.elsevier.com/locate/jconrel

Use of poly(amidoamine) drug conjugates for the delivery of antimalarials to *Plasmodium*

Patricia Urbán [a,b,c], Juan José Valle-Delgado [a,b,c], Nicolò Mauro [d], Joana Marques [a,b,c], Amedea Manfredi [d], Matthias Rottmann [e], Elisabetta Ranucci [d], Paolo Ferruti [d], Xavier Fernàndez-Busquets [a,b,c,*]

[a] *Nanomalaria Group, Institute for Bioengineering of Catalonia (IBEC), Baldiri Reixac 10-12, ES-08028 Barcelona, Spain*
[b] *Barcelona Centre for International Health Research (CRESIB, Hospital Clínic-Universitat de Barcelona), Rosselló 149-153, ES-08036 Barcelona, Spain*
[c] *Biomolecular Interactions Team, Nanoscience and Nanotechnology Institute (IN2UB), University of Barcelona, Martí i Franquès 1, ES-08028 Barcelona, Spain*
[d] *Department of Chemistry, Università degli Studi di Milano, Via Golgi 19, IT-20133 Milano, Italy*
[e] *Swiss Tropical and Public Health Institute, Socinstrasse 57, PO Box, CH-4002 Basel, Switzerland*

A R T I C L E I N F O

Article history:
Received 6 November 2013
Accepted 21 December 2013
Available online 7 January 2014

Keywords:
malaria
nanomedicine
Plasmodium
polyamidoamines
polymer–drug carriers
targeted drug delivery

A B S T R A C T

Current malaria therapeutics demands strategies able to selectively deliver drugs to *Plasmodium*-infected red blood cells (pRBCs) in order to limit the appearance of parasite resistance. Here, the poly(amidoamines) AGMA1 and ISA23 have been explored for the delivery of antimalarial drugs to pRBCs. AGMA1 has antimalarial activity per se as shown by its inhibition of the *in vitro* growth of *Plasmodium falciparum*, with an IC_{50} of 13.7 μM. Fluorescence-assisted cell sorting data and confocal fluorescence microscopy and transmission electron microscopy images indicate that both polymers exhibit preferential binding to and internalization into pRBCs versus RBCs, and subcellular targeting to the parasite itself in widely diverging species such as *P. falciparum* and *Plasmodium yoelii*, infecting humans and mice, respectively. AGMA1 and ISA23 polymers with hydrodynamic radii around 7 nm show a high loading capacity for the antimalarial drugs primaquine and chloroquine, with the final conjugate containing from 14.2% to 32.9% (w/w) active principle. Intraperitoneal administration of 0.8 mg/kg chloroquine as either AGMA1 or ISA23 salts cured *P. yoelii*–infected mice, whereas control animals treated with twice as much free drug did not survive. These polymers combining into a single chemical structure drug carrying capacity, low unspecific toxicity, high biodegradability and selective internalization into pRBCs, but not in healthy erythrocytes for human and rodent malarias, may be regarded as promising candidates deserving to enter the antimalarial therapeutic arena.

© 2014 Elsevier B.V. All rights reserved.

1. Introduction

More than 40% of the world's population lives at risk of contracting malaria. The most recent estimates indicate several hundred million clinical cases and 660,000 deaths in 2010 [1,2], of which the large majority are children below 5 years old [3,4]. The recent call for elimination and eradication of the disease requires research from multiple fronts, including developing strategies for the efficient delivery of new medicines [5]. Five *Plasmodium* species cause disease in humans, namely, *P. vivax*, *P. ovale*, *P. malariae*, *P. knowlesi* [6] and *P. falciparum*, with the latter being responsible for the most deadly and severe cases. When taking a blood meal, the female *Anopheles* mosquito inoculates *Plasmodium* sporozoites that in the liver infect hepatocytes and proliferate into thousands of merozoites [7]. Merozoites invade red blood cells (RBCs), where they build a parasitophorous vacuole inside which the parasite develops first into rings, and then into the late forms trophozoites and schizonts. Schizont-infected RBCs burst and release more merozoites, which start the blood cycle again. Because the blood-stage infection is responsible for all symptoms and pathologies of malaria, *Plasmodium*-infected RBCs (pRBCs) are a main chemotherapeutic target [8].

Since antimalarial drug delivery currently relies on compounds with little or no specificity for pRBCs, the administration of most drugs requires high doses. However, the unspecificity of toxic drugs demands low concentrations to minimize undesirable side effects, thus incurring the risk of sublethal doses favoring the appearance of resistant pathogen strains [9]. Nanomedicine, which uses nanosized tools for the treatment of disease [10], can fulfill the objective of achieving the intake of total amounts sufficiently low to be innocuous for the patient, but locally still lethal for the parasite. The development of novel delivery approaches is less expensive than finding new antimalarial drugs and may optimize their rate of release [11]. Current immunoliposomal prototypes engineered for the delivery of antimalarial drugs specifically to pRBCs [12,13] rely on antibody targeting and contain special lipids, making their synthesis too expensive for their practical widespread use in the routine treatment of most malaria cases, which are in developing areas with low per capita incomes. An essential aspect for the successful development of antimalarial nanomedicines resides on the choice of targeting elements, of which it has to be considered their

---

[*] Corresponding author at: Nanomalaria Unit, Centre Esther Koplowitz, 1st floor, CRESIB, Rosselló 149-153, ES-08036 Barcelona, Spain.
E-mail address: xfernandez_busquets@ub.edu (X. Fernàndez-Busquets).

0168-3659/$ – see front matter © 2014 Elsevier B.V. All rights reserved.
http://dx.doi.org/10.1016/j.jconrel.2013.12.032

biocompatibility, cell specificity, binding affinity, ease of modification and conjugation to the drugs, production cost, scalability and stability in mass production. Polymers offer virtually unlimited diversity in chemistry, dimensions and topology, rendering them a class of materials that is particularly suitable for applications in nanoscale drug delivery strategies [14].

Poly(amidoamine)s [15,16] (PAAs) are a family of synthetic polymers exhibiting a combination of properties imparting them a potential in the biomedical field. They can be designed to be biocompatible and bioeliminable, and degrade to oligomeric products in aqueous media within days or weeks, depending on their structures [17–19]. Three PAAs were selected for the present study, namely, AGMA1, ISA23 and ISA1 (Fig. 1 and Supplementary data, Table S1). AGMA1 is obtained by polyaddition of 4-aminobutylguanidine (agmatine) with 2,2-bis(acrylamido)acetic acid and contains *tert*-amine, carboxyl and guanidine groups. It is amphoteric with isoelectric point of 10.0 and therefore at pH 7.4 is prevailingly cationic with, on average, 0.55 excess positive charges per unit. ISA23 is obtained by polyaddition of 2-methylpiperazine with 2,2-bis(acrylamido)acetic acid. Notwithstanding carrying two *tert*-amine groups and one carboxyl group per unit, it has isoelectric point of 5.5, being prevailingly anionic at pH 7.4 with, on average, 0.38 excess negative charges per unit. ISA1 is obtained by polyaddition of bis(acryloyl)piperazine with 2-methylpiperazine and bis(hydroxyethylethylenediamine). It is a rather weak polymeric base with, on average, 0.55 positive charges per unit at pH 7.4. All these polymers have been reported as vectors for the intracellular delivery of nucleic acids [20–22]. ISA1 and ISA23 have been also studied for protein delivery [22–24] and as anticancer drug carriers [25,26]. ISA23 had proven endowed with stealth-like properties and did not selectively concentrate in the liver [27], whereas a significant portion of AGMA1 showed hepatic localization after intravenous injection in mice [28]. pRBCs are known to be permeable to high molecular mass solutes [29] including peptides and proteins, with which PAAs share some features, such as the polyelectrolyte behavior and the presence of amide groups in the main chain. This led us to explore the potential of ISA1, ISA23 and AGMA1 as antimalarial drug carriers.

2. Materials and methods

Unless otherwise indicated, all reagents were purchased from Sigma-Aldrich (St. Louis, MO, USA).

2.1. Synthesis of ISA1, ISA23 and AGMA1 with different molecular weight

Linear ISA23, [26] ISA1 [26] and AGMA1 [29] were synthesized as previously described, but prolonging the reaction time to 7 days. They were subsequently fractionated by sequential ultrafiltration through membranes (Amicon, Millipore) with decreasing nominal molecular weight cutoffs, namely, 100,000, 30,000, 10,000, 5,000 and 1,000 Da, in order to obtain for each polymer four fractions identified with a letter in alphabetical order for increasing molecular weight (e.g., for the AGMA1 series, the molecular weight follows the trend AGMA1-a < AGMA1-b < AGMA1-c < AGMA1-d).

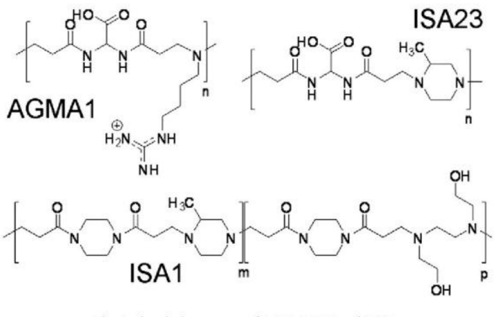

Fig. 1. Chemical structures of AGMA1, ISA1 and ISA23.

2.2. Synthesis of FITC-labeled AGMA1 and ISA23

FITC-labeled AGMA1 ($\overline{M}_n = 15{,}200$, $\overline{M}_w/\overline{M}_n = 1.05$) was prepared as previously reported [28]. Briefly, an AGMA1 sample carrying amine groups (AGMA1-NH_2) was prepared by substituting 7% on a molar basis of mono(*tert*-butoxycarbonyl)ethylenediamine for agmatine and subsequently deprotecting with 5% hydrochloric acid. A pH 7.4 AGMA1-NH_2 solution (10 mg/ml) was then treated with excess of an FITC solution in methanol (0.2 mg/ml). The mixture was stirred overnight at room temperature and centrifuged to eliminate insoluble impurities. The resultant clear solution was then dialyzed against water (membrane with 2,000 Da nominal molecular weight cutoff) and the fluorescein-labeled polymer isolated by freeze-drying the retained portion, with a quantitative recovery. The conjugation of AGMA1-NH_2 with FITC was confirmed by NMR and fluorescence microscopy, and the efficiency of the labelling procedure determined by measuring the fluorescence intensity at $\lambda_{ex} = 480$ nm and $\lambda_{em} = 520$ nm of a solution of AGMA1-FITC versus a standard FITC solution of known concentration. FITC-labeled ISA23 ($\overline{M}_n = 10{,}900$, $\overline{M}_w/\overline{M}_n = 1.17$) was prepared by substituting 7% on a molar basis of N-Boc ethylenediamine for 2-methylpiperazine in the preparation recipe and then deblocking and treating the resultant product as reported above for AGMA1-FITC. On a molar basis relative to the polymer repeating units, FITC content was 7.2% and 6.5% for AGMA1-FITC and ISA23-FITC, respectively.

2.3. Preparation of ISA23- and AGMA1-drug salts

Primaquine (PQ) free base was prepared as reported elsewhere [30]; briefly, a 10-mg/ml primaquine diphosphate aqueous solution was brought to pH 12 by the addition of 0.1 M NaOH, whereby PQ free base separated as an oil that was extracted (4 × 50 ml) with ether. The combined ether extracts were dried over Na_2SO_4 and evaporated in vacuo, leaving PQ as a dark brown oil with a yield of 50.9% w/w. Chloroquine (CQ) free base was prepared following the same procedure described for PQ, except for the initial dissolution of CQ diphosphate in an emulsion of 1:1 H_2O/ether. Then, CQ free base was recovered, after separation and evaporation of ethereal phase, as a white solid with a yield of 59.1% w/w. An ISA23 sample with $\overline{M}_n = 29{,}800$ and $\overline{M}_w/\overline{M}_n = 1.28$ was prepared as previously reported [27], but with a reaction time of 10 days, and brought to its isoelectric point (pH 5.4). A methanol solution of PQ or CQ free base (0.1 mg/ml) was added drop-wise to a solution of the polymer (10 mg/ml) until pH 7.4 was reached. The resultant clear solution was freeze-dried and the polymer salt retrieved as a white powder. The lyophilized product was perfectly soluble in water whereas the drug, as free-base, was not. The drug payload, calculated from the amount of drug needed to reach pH 7.4, corresponded to 15.1% and 32.9% (w/w) of the product for PQ and CQ, respectively. An AGMA1 sample with $\overline{M}_n = 20{,}800$ and $\overline{M}_w/\overline{M}_n = 1.38$, prepared as reported above [31], was treated using the same procedure followed for the ISA23–drug conjugate, apart from the fact that the drug addition was performed until pH 7.4 was reached, even though the isoelectric point of AGMA1 was 10.4. The drug payload (w/w), calculated as mentioned above in the case of ISA23 salts, was 29.4% for PQ and 14.2% for CQ.

2.4. Size exclusion chromatography (SEC) and dynamic light scattering (DLS) analysis

SEC analysis was performed using a Knauer Pump 1000 equipped with a Knauer Autosampler 3800, TKSgel G4000 PX and G3000 PX TosoHaas columns connected in series, light scattering/viscometer Viscotek 270 Dual Detector and a refractive index detector Waters model 2410. The mobile phase was 0.2 M NaCl, 0.1 M Tris buffer (pH 8.1 ± 0.05). The sample concentration was about 2% (w/v) and the flow rate 1 ml/min. The absence of nanoaggregates in the polymer–drug conjugates was assessed by DLS analysis using a Malvern Nano-ZS instrument with fixed angle of 173° with respect to the incident beam laser. The experiments were performed at 25 °C at a concentration of 0.1 mg/ml in phosphate-buffered saline (PBS) buffer (137 mM NaCl, 2.7 mM KCl, 10 mM phosphate buffer; pH 7.4).

2.5. Analysis of drug and FITC released from polymer conjugates, hemolysis and unspecific cytotoxicity assays

A 500-μl volume of the PAA–drug salts containing either CQ (50 mg/ml) or PQ (25 mg/ml) was dialyzed at 25 °C against 25 ml of PBS, using a membrane with 2,000 Da nominal molecular weight cutoff. At prefixed times, 150 μl of the external solution, containing only the free drug after diffusion at equilibrium, were withdrawn. The concentration of PQ or CQ outside the dialysis bag was determined spectrophotometrically ($\lambda_{PQ} = 352$ nm, $\varepsilon_{PQ} = 3{,}254\ M^{-1}\ cm^{-1}$; $\lambda_{CQ} = 340$ nm, $\varepsilon_{CQ} = 18{,}570\ M^{-1}\ cm^{-1}$). The absence of FITC release from PAA–FITC conjugates was assessed similarly by dialyzing in PBS buffer a polymer solution containing 1.44 mg/ml FITC. FITC concentration outside the dialysis bag was determined fluorimetrically by withdrawing at different times 150-μl samples ($\lambda_{ex} = 480$ nm, $\lambda_{em} = 520$ nm). Hemolysis and unspecific cytotoxicity assays were done as described elsewhere [12].

2.6. P. falciparum cell culture and growth inhibition assays (GIAs)

P. falciparum 3D7 was grown *in vitro* in rinsed human RBCs of blood group type B prepared as described elsewhere [12] using previously established conditions [32]. Briefly, parasites (thawed from glycerol stocks) were cultured at 37 °C in Petri dishes containing RBCs in Roswell Park Memorial Institute (RPMI) complete medium under a gas mixture of 92% N_2, 5% CO_2 and 3% O_2. Synchronized cultures were obtained by 5% sorbitol lysis [33], and the medium was changed every 2 days maintaining 3% hematocrit. For culture maintenance, parasitemias were kept below 5% late forms by dilution with washed RBCs. For standard growth inhibition assays, parasitemia was adjusted to 1.5% with more than 90% of parasites at ring stage after sorbitol synchronization. For modified growth inhibition assays, synchronized cultures with a starting parasitemia of 0.9% were incubated for 24 h before the addition of drug to allow for the appearance of late forms. Two hundred microliters of these living *Plasmodium* cultures were plated in 96-well plates and incubated for 48 h at 37 °C in the presence of free drugs and PAA–drug conjugates. Parasitemia was determined by microscopic counting of blood smears or by fluorescence-assisted cell sorting (FACS), as previously described [12].

2.7. Confocal fluorescence microscopy

Living *P. falciparum* 3D7 cultures or blood freshly extracted from *P. yoelii*–infected mice were incubated in the presence of 0.2 to 0.5 mg/ml ISA23-FITC or AGMA1-FITC for 90 minutes at 37 °C with gentle stirring. After washing, blood smears were prepared and cells were fixed in acetone/methanol (90:10). Parasite nuclei were stained with 4',6-diamino-2-phenylindole (DAPI, Invitrogen) and the RBC membrane was labeled with wheat germ agglutinin–tetramethylrhodamine conjugate (Molecular Probes, Eugene, OR, USA). Slides were finally mounted with Mowiol (Calbiochem, Merck Chemicals, Darmstadt, Germany), and analyzed with a Leica TCS SP5 laser scanning confocal microscope.

2.8. Fluorescence-assisted cell sorting analysis

For targeting analysis, *P. falciparum* cultures synchronized at mature stages at an approximate parasitemia of 4% were incubated with PAA–FITC at a final concentration of 0.5 mg/ml for 90 minutes at 37 °C. Cells were then washed with PBS and parasite nuclei were stained with Hoechst 33342. pRBCs were diluted to a final concentration of 1 to 10 × 10^6 cells/ml, and samples were analyzed using a Gallios multi-color flow cytometer instrument (Beckman Coulter, Inc, Fullerton, CA) set up with the three lasers, 10 colors standard configuration. The single-cell population was selected on a forward-side scatter scattergram. FITC was excited using a blue laser (488 nm), and its fluorescence collected through a 525/40-nm filter. Hoechst was excited with a violet laser (405 nm), and its fluorescence collected using a 450/40-nm filter.

2.9. Transmission electron microscopy (TEM) of cell sections

Gelatin-purified living pRBCs were incubated with 0.5 mg/ml FITC-labeled polymers for 90 minutes at 37 °C. After washing, cells were chemically fixed at 4 °C with a mixture of 4% paraformaldehyde and 0.1% glutaraldehyde (both from Electron Microscopy Sciences, Hatfield, PA, USA) in 10 mM phosphate buffer (PB), pH 7.0. Prior to embedding in 12% gelatin (Calbiochem, Merck, Germany) and infusion in 2.3 M sucrose, cells were washed with PB containing 50 mM glycine. Mounted gelatin blocks were frozen in liquid nitrogen, and ultrathin sections were prepared in an ultracryomicrotome (Leica EM Ultracut UC6/FC6, Vienna, Austria). Cryosections were collected with 2% methylcellulose in 2.3 M sucrose and incubated at room temperature on drops of 2% gelatin in PBS for 20 min at 37 °C, followed by 50 mM glycine in PBS during 15 min, 10% foetal bovine serum (FBS) in PBS during 10 min, and 5% FBS in PBS for 5 min. Then, they were incubated for 30 min in the presence of anti-FITC antibody (Rockland Antibodies, PA, USA) at a final concentration of 3 μg of antibody per microliter in PBS supplemented with 5% FBS. After three washes with drops of PBS for 10 min, sections were incubated for 20 min using IgG anti-goat coupled to 6-nm colloidal gold particles (Jackson ImmunoResearch) using a 1:30 dilution in PBS supplemented with 5% FBS. This was followed by three washes with drops of PBS for 10 min and two washes with distilled water. The observations were done in a Tecnai Spirit electron microscope (FEI Company, Eindhoven, The Netherlands) with a CCD SIS Megaview III camera. Controls included omission of polymer-FITC, omission of anti-FITC antibody, incubation with free FITC plus detection with anti-FITC antibody, and staining of non-infected RBCs.

2.10. Cryogenic transmission electron microscopy (cryo-TEM) of polymers

A bare glow-discharged holey carbon grid was dipped in a 1 mg/ml polymer solution in water, which after withdrawal was blotted against filter paper. The resulting thin sample aqueous films spanning the grid holes were vitrified by immersion into ethane maintained at its melting point by liquid nitrogen, using a Vitrobot (FEI Company), keeping the sample at 100% humidity before freezing. The temperature at which the thin films were and from which vitrification was initiated was at room temperature. The vitreous sample films were transferred to a Tecnai F20 electron microscope (FEI Company, Eindhoven, Netherlands) using a Gatan Cryo Transfer. The images were taken at 200 kV with a 4,096 × 4,096 pixel CCD Eagle camera (FEI Company) at a temperature between −170 °C and −175 °C and using low-dose imaging conditions.

2.11. Determination of polymer blood residence time and toxicity assay in mice

Inbred BALB/cAnNHsd female, 6- to 8-week-old mice (Harlan Laboratories) were injected intraperitoneally with a 100-μl solution in PBS of AGMA1-FITC, ISA23-FITC or FITC (all 100 mg FITC/kg). The pH of all samples was checked prior to administration and, when needed, adjusted to between 6 and 7 by the addition of NaOH. Blood samples (15 μl) were collected in Microvette tubes (Sarstedt) using the cross-sectional cut method, before injection (t_0) and up to 72 h post-injection. Blood samples were centrifuged for 5 minutes (4,000×*g*), and 10 μl of the supernatant was used to measure FITC fluorescence. For *in vivo* toxicity assays, polymer solutions were prepared in PBS at pH 7.4 and each sample was injected intraperitoneally in three mice; PBS was administered to control animals. Mice weight and behavior was followed daily for 1 week.

2.12. Antimalarial activity assay in vivo

The *in vivo* antimalarial activity of free chloroquine and primaquine and of PAA–CQ and PAA–PQ conjugates was analyzed by using a 4-day blood suppressive test as previously described [34]. Briefly, BALB/c mice were inoculated 2 × 10^6 RBCs from *P. yoelii yoelii* 17XL (PyL) MRA-267–infected mice by intraperitoneal injection. Treatment started 2 hours later (day 0) with a single dose of 1.9 ± 0.3 or 0.8 ± 0.2 mg kg^{-1} day^{-1} chloroquine or 1.0 ± 0.2 mg kg^{-1} day^{-1} primaquine administered as diphosphate–drug, ISA23–drug or AGMA1–drug by a 100-μl intraperitoneal injection followed by identical dose administration for the next 3 days. Tested compounds were prepared at appropriate doses in PBS, and the control groups received PBS. Parasitemia was monitored daily by microscopic examination of Wright's-stained thin blood smears, and antimalarial activity was calculated by microscopic counting of smears from day 4. Efficacy is expressed as the percentage of parasitemia reduction compared with untreated control mice and survival was monitored until day 30, when all surviving animals had completely cleared *Plasmodium* infection.

2.13. Statistical analysis

Data are presented as the mean ± standard error of at least three independent experiments, and the corresponding standard errors in histograms are represented by error bars. Statistical analyses were performed using Stata Software version 12. Percentages of viability were obtained using non-treated cells as control of survival and IC_{50} values were calculated by nonlinear regression with an inhibitory dose–response model using GraphPad Prism5 software. Concentrations were transformed using natural log for linear regression. Regression models were adjusted for replicates and assay data.

3. Results

3.1. PAAs selected as antimalarial drug carriers

As a proof of concept for PAA encapsulation and delivery, we selected the widely used antimalarial drugs chloroquine (CQ) and primaquine (PQ). AGMA1 and ISA23, but not ISA1, were able to solubilize substantial amounts of PQ and CQ in water, which (as free bases) are only slightly soluble in aqueous media (see Methods). Since carboxyl groups were required for drug solubilization, there is little doubt that polymeric PQ and CQ salts were formed. However, the fact that AGMA1 also reacted notwithstanding its basic properties and the presence of strongly basic guanidine pendants, suggests that the salts were stabilized by secondary interactions, such as for instance hydrogen bonds and hydrophobic interactions. The polymeric salts recovered by lyophilization from their solutions were dry powders soluble in water and cell culture media. The PBS solutions of the PAA salts at 25 °C and 0.1 mg/ml concentration were examined by DLS (Supplementary data, Table S2). All of them showed hydrodynamic radii slightly larger than, but comparable to, those of the parent polymers at the same concentration, pointing to the conclusion that the establishment of polymer–drug interactions did not induce supramolecular effects, such as mediating intermolecular entanglements or forming ionic aggregates.

CQ and PQ release from PAA-salts in PBS solution was determined in comparison with the drug diphosphate salts, from here on termed, free forms (Fig. 2). CQ release rate from its AGMA1- and ISA23-salts was significantly slowed down in comparison to the dialysis of an equal amount of the free drug, whereas no significant difference existed between the retention power of the two polymers. By contrast, the release rate of PQ was much less affected by the interactions with polymers. The superior retention of CQ compared with PQ with both PAA salts correlates with its higher basicity (CQ: $pK_{a1} = 8.4$; $pK_{a2} = 10.8$ [35]; PQ: $pK_{a1} = 3.2$; $pK_{a2} = 10.4$ [36]), and higher hydrophobicity ($\log P_{oct/water}$ CQ = 3.73 [35], $\log P_{oct/water}$ PQ = 2.20 [37]).

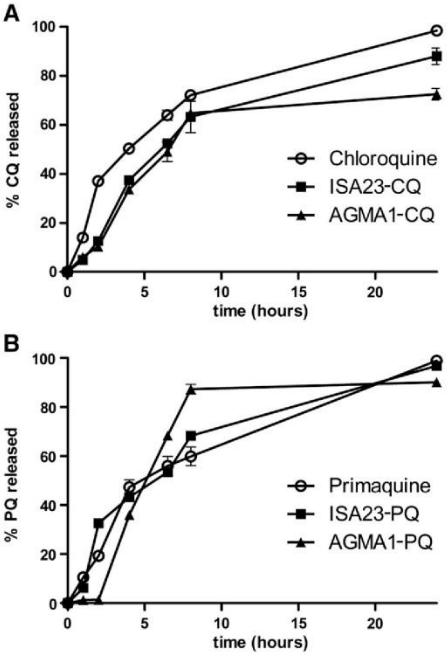

Fig. 2. Release profiles of CQ (A) and PQ (B), from AGMA1- (▲) and ISA23- (■) drug salts in PBS solution. For comparison purposes, dialysis of the drug diphosphate salts (○) is also reported.

3.2. Characterization and toxicity studies of drug-free PAAs

The capacity of AGMA1 and ISA23 to incorporate and release PQ and CQ indicated that the polymers might have a therapeutic potential against malarial infections, but *in vitro* studies were deemed opportune before proceeding to *in vivo* activity tests. Drug-free AGMA1 and ISA23 were first investigated for their possible interactions with RBCs and pRBCs. ISA1, even if useless as a PQ and CQ carrier, was included in this preliminary investigation for comparison purposes because its positive charges at pH 7.4 are nearly equivalent to the excess positive charges of AGMA1 at the same pH (~0.55).

As it is well known that the biological properties of bioactive polymers may depend on their molecular weight, four different fractions for AGMA1, ISA1 and ISA23 (Table 1) were obtained by ultrafiltration through membranes with different molecular weight cutoffs. Triple detector size exclusion chromatography (SEC) allowed determining their absolute number average molecular weight and polydispersity (refractive index and light scattering detectors) and hydrodynamic radii (viscometric detector).

Table 1
Number average molecular weight ($\overline{M}_n$), polydispersity (PD) and hydrodynamic radius (Rh) of PAAs, determined by SEC analysis.

Sample	$\overline{M}_n$	PD	Rh (nm)
AGMA1-a	2,900	1.81	3.4
AGMA1-b	7,400	1.47	4.9
AGMA1-c	10,700	1.31	5.6
AGMA1-d	21,200	1.43	6.8
ISA1-a	8,900	1.48	5.3
ISA1-b	14,000	1.15	5.8
ISA1-c	19,700	1.23	6.3
ISA1-d	24,800	1.19	7.1
ISA23-a	7,700	1.88	2.7
ISA23-b	13,700	1.35	4.0
ISA23-c	21,000	1.41	5.1
ISA23-d	22,200	1.17	6.4

The polymer fractions were characterized by variable polydispersities, resulting from the fractionation procedure adopted, the broad distribution of the parent stepwise polymers, and the amphoteric, that is, zwitterionic nature of ISA23 and AGMA1. The hydrodynamic radius of PAAs determined by SEC analysis is consistent with the presence of linear soluble macromolecules with limited mutual interactions, whose size increases with the molecular mass.

The polymers and polymer–drug salts were directly observed by atomic force microscopy (AFM) and cryo-TEM. Cryo-TEM images (Fig. 3) revealed a globular-spherical conformation in solution, which swelled up to diameters ranging from ~20 to 40 nm in the absence of salt screening the repulsion between the polymer charges. The globular conformation of the polymers was confirmed in AFM images of AGMA1, ISA23 and ISA1 adsorbed on mica substrates, showing a homogenous polymer size distribution (Supplementary data, Fig. S1). The size overestimation introduced by the radius of curvature of the AFM tip and the fact that polymers may spread onto mica after adsorption prevented a precise determination of polymer size from AFM data. Despite this limitation, AFM images showed that the polymer size did not change significantly after conjugation to antimalarial drugs, in agreement with DLS data.

At a polymer concentration of 1 mg/ml, and under the experimental conditions adopted, neither AGMA1 nor ISA23 showed hemolytic activity above 0.5%, whereas ISA1 induced a modest hemolysis (3%). These data agree with previous literature reporting that AGMA1 was not hemolytic *in vitro* up to a concentration of 7.5 mg/ml in the pH range of 4 to 6.5 and up to 10 mg/ml at pH 7.4 [31]. ISA23 at >1 mg/ml was reported to be weakly hemolytic at pH 7.4 and highly hemolytic at pH 5 to 5.5 [27], whereas ISA1 at >1 mg/ml was found to be hemolytic at pH 7.4 [27].

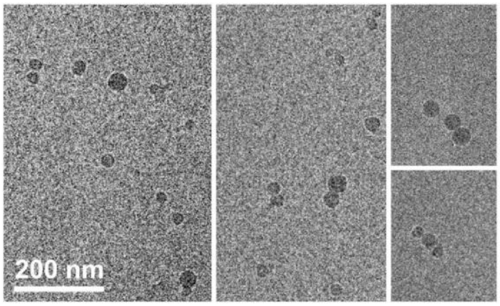

Fig. 3. Cryo-TEM analysis of AGMA1-d.

In vitro cytotoxicity of the polymers was observed to depend on their molecular mass (Supplementary data, Fig. S2). In particular, AGMA1 and ISA1 toxicity on human umbilical vein endothelial cells was significant for the -d fractions above 0.5 mg/ml, and for the AGMA1-c fraction at >1 mg/ml. On the other hand, only minor cytotoxicity was observed for the ISA23-a fraction at concentrations higher than 5 mg/ml. *In vivo* toxicity assays in mice indicated that ISA23 and AGMA1, free or loaded with PQ and CQ, did not have observable pernicious effects on the animals up to an intraperitoneal dose of 200 mg/kg, but ISA1 was toxic at 50 mg/kg, where all the animals died in less than 1 h after polymer administration.

3.3. *In vitro study of AGMA1 and ISA23 cell targeting and subcellular localization*

FACS analysis after 90 min incubation with living RBC/pRBC cocultures (Fig. 4) revealed that fluorescein-labeled AGMA1 preferentially targeted pRBCs, but also interacted with a significant amount of RBCs (Fig. 4C and D). RBC binding of AGMA1 was not observed to increase significantly with polymer size (Fig. 4E and F). On the other hand, ISA1 and ISA23 exhibited a highly specific selectivity towards pRBCs (Fig. 4G–J), but lacked significant binding to RBCs.

ISA1, notwithstanding its preferential interaction with pRBCs, was not considered for further targeting studies since, besides being relatively toxic, it was unable to solubilize PQ and CQ. The targeting of AGMA1 and ISA23 to *Plasmodium*-infected erythrocytes was also examined by confocal fluorescence microscopy analysis in living *P. falciparum* pRBC/RBC cocultures (Fig. 5) and in blood freshly extracted from *P. yoelii*–infected mice (Fig. 6) treated with FITC-labeled polymers. The fluorescence due to AGMA1-FITC (Fig. 5A) and ISA23-FITC (Fig. 5B) was observed inside pRBCs infected by *P. falciparum* trophozoites (appearing about 20 h post-RBC invasion) and schizonts, but not in ring-infected pRBCs or in non-infected erythrocytes. After 90 min incubation with the labeled polymers, both PAAs internalized in pRBCs mostly localized in close proximity to *Plasmodium* DNA. Routine dialysis equilibrium controls did not detect any significant FITC release from the polymers up to 10 h incubation in the same buffer used for the fluorescence microscopy assays (data not shown), thus confirming that the observed signal could only be ascribed to pRBC-internalized PAA–FITC.

In vitro transportation of AGMA1 and ISA23 into pRBCs could also be observed for the rodent malaria parasite *P. yoelii* (Fig. 6), where, in addition to trophozoites and schizonts, AGMA1 was also found to penetrate ring stages and ISA23 ring/early trophozoite forms (Fig. 6A). The ISA23 binding to merozoites was particularly striking (Fig. 6B), a result offering attractive possibilities for PAAs as selective drug carriers not only toward pRBCs but also toward free merozoites.

TEM images of pRBCs after 90 min of incubation in the presence of AGMA1 or ISA23 prior to fixation revealed that both polymers localized in the pRBC cytosol and inside the area enclosed by the parasitophorous vacuole membrane (PVM; Fig. 7). Whereas ISA23 was more abundant in the pRBC cytosol than beyond the PVM, the opposite was observed for AGMA1. The subcellular penetration of AGMA1 inside the PV was consistent with its known ability to be internalized in cells, reaching the perinuclear region [28]. The preferential targeting of AGMA1 and ISA23 to pRBCs versus RBCs is similar to that obtained with pRBC-specific monoclonal antibodies [12]. However, unlike antibodies, the polymers penetrate living pRBCs *in vitro* and colocalize with the intracellular pathogens, a property opening interesting perspectives regarding the use of PAAs for the delivery of drugs directly to the parasite and, possibly, as transfection vectors for *Plasmodium* genetic engineering.

TEM analysis also showed that inside pRBCs the polymers were not surrounded by a lipid bilayer, thus suggesting a membrane crossing mechanism not based on the formation of endocytic vesicles, although the differences observed in their intracellular distribution suggest

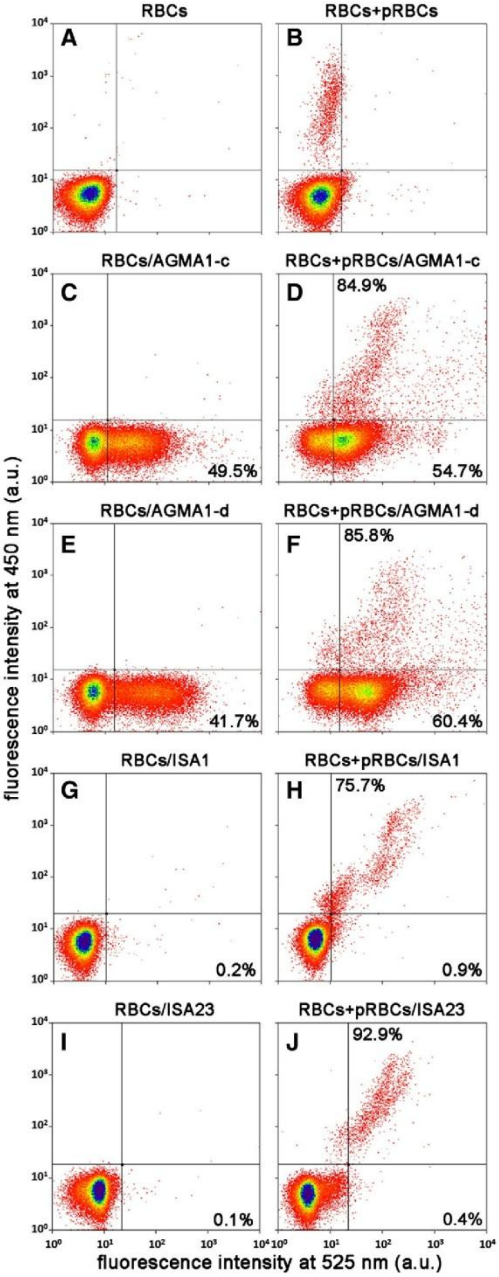

Fig. 4. FACS analysis of the interaction with RBCs and pRBCs of AGMA1-c and -d, and of non-fractionated ISA1 and ISA23. The upper areas contain pRBCs (Hoechst fluorescence) and the right-hand areas contain PAA-bound cells (FITC fluorescence). Percentage values indicate the fraction of PAA-bound pRBCs (upper right areas) and RBCs (lower right areas).

different entry modes for AGMA1 and ISA23. AGMA1 was often found associated with Maurer's clefts, Golgi-like organelles that are part of the exomembrane system that the parasite establishes in the host cell cytoplasm [38]. The cytosolic areas around small bumps on the pRBC membrane (termed knobs) were also enriched in AGMA1, suggesting that these structures, assembled by the parasite molecular machinery and involved in cytoadhesion events, might constitute entry gates for AGMA1. Compared with RBCs, pRBCs have different morphological, physicochemical and rheological characteristics [39–41], resulting in profoundly altered functional properties that confer higher membrane fluidity (hence permeability), adhesiveness and protein trafficking activity. In particular, the malaria parasite increases the permeability of the host RBC membrane to low molecular mass solutes [42] as well as proteins [43], whereas particles up to 70 nm in diameter have been found to have direct access to intraerythrocytic *Plasmodium* through areas of apparent membrane continuity between the pRBC membrane and the PVM [29]. In the case of PAAs, although the inactivity toward healthy RBCs can be explained by the absence of the endocytic uptake route in these cells, the intracellular localization of amphoteric PAA molecules in pRBCs is likely primarily due to their polyelectrolyte zwitterionic nature. AGMA1 and ISA23 have large repeating units and assume extended conformations in aqueous media [44]. The positive and negative charges of amphoteric PAAs are located in discrete positions along the polymer chain and, consequently, favor intermolecular ionic interactions and induce a strong tendency to associate in solution [45]. The same polymers may be expected to interact with pRBC membranes, characterized by altered charge and plasticity [40] and by a significant increase of electrical conductivity [39]. These interactions might well trigger complex internalization mechanisms.

3.4. Intrinsic in vitro antimalarial activity of PAAs

In *in vitro P. falciparum* growth inhibition assays (GIAs), only AGMA1 showed significant antimalarial activity (Fig. 8A), which augmented with polymer size (Supplementary data, Tables S3A and S3B). From the data in Fig. 8A, we calculated that the AGMA1-d IC_{50} in *P. falciparum* GIAs was about 0.29 mg/ml, or 13.7 μM, considering its average molecular mass of 21,200 Da (Table 1). Compared with AGMA1, ISA23 showed a remarkably inferior, albeit still molecular weight–dependent *P. falciparum* growth inhibitory activity (Fig. 8C), whereas ISA1 did not significantly inhibit the parasite's growth (Fig. 8B). The superior antimalarial activity of AGMA1 was most probably related to its combination of functions among which the guanidine pendants played a prominent role in establishing membrane interactions. In a modified GIA where AGMA1 was added to trophozoites, i.e. 24 h after pRBC culture synchronization, and incubated for a further 24 h before parasitemia determination, the observed antimalarial activity of the smaller fractions increased significantly (Fig. 8D). This result suggests a toxicity mechanism possibly based on a facilitated polymer entry in late stage parasite-containing pRBCs due to their more deeply altered plasma membrane [46].

Microscopic observation of AGMA1-d–treated samples at longer times after the addition of polymer (48 h or more) showed a remarkable proportion of free merozoites outside RBCs (Fig. 9A), whereas control untreated samples regularly completed the invasion step following merozoite egression from mature schizonts and mostly consisted of intracellular ring stages (Fig. 9B). Since invasion proceeded normally with RBCs treated with AGMA1 prior to their addition to pRBC cultures (data not shown), the observed perturbation of the invasion capacity was likely due to a direct effect of AGMA1 on the merozoites.

The binding of AGMA1 to merozoites observed in *P. yoelii* fluorescence microscopy studies might be the triggering event responsible for the invasion inhibition reported above. Many merozoites fail to invade RBCs likely because of initial weak adhesions [47].

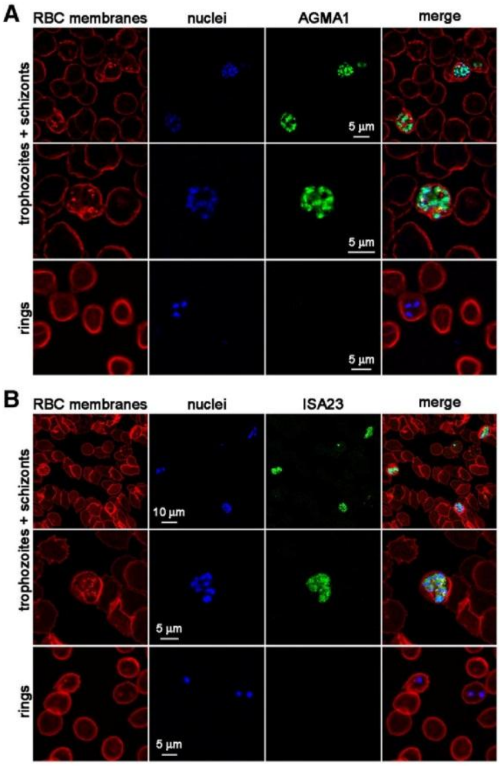

Fig. 5. Confocal fluorescence microscopy targeting study of AGMA1 and ISA23 to *P. falciparum*-containing pRBCs. FITC-labeled AGMA1-d (A) or ISA23-d (B) was added to living *P. falciparum* cultures of the 3D7 strain and, after 90 min of incubation, the samples were processed for confocal fluorescence microscopy analysis. PAA localization (green) was explored on cells parasitized by trophozoites, schizonts, or rings. DAPI (blue) staining of *Plasmodium* nuclei was used to indicate pRBCs. The RBC plasma membrane is shown in red.

An AGMA1 merozoite coating could possibly either block the necessary molecular recognition events or hamper dynamic processes required for orienting the parasites in an invasion-competent position. The corresponding mechanism could be related to AGMA1 interfering with the binding of adhesins and invasins to their receptors on the RBC membrane [48] or to the blocking of external signals leading to the activation of cAMP and Ca^{2+}-dependent signaling pathways unleashing the release of internally located parasite ligands that regulate the assembly of its acto-myosin motor complex required for invasion [49].

3.5. Antimalarial activity of the PAA PQ and CQ salts

From the above reported studies it was hypothesized that AGMA1 and ISA23 could selectively transport PQ and CQ as polymeric salts into pRBCs and thereby enhance their antimalarial activity. This possibility was explored both *in vitro* and *in vivo*.

3.5.1. In vitro studies

The results of standard *in vitro* GIAs performed with AGMA1 and ISA23 PQ and CQ salts are reported in Table 2. It may be observed that the *in vitro* antimalarial capacity of the drugs relative to their free forms was not significantly increased, except for AGMA1-PQ, where PQ IC_{50} was reduced by ca. 35% (Table 2 and Supplementary data, Fig. S3).

Addition of free drugs and PAA–drug salts at trophozoite stage in a modified GIA or incubation with either ring or trophozoite stage for 1 h before removing the drugs and incubating for another 48 h before parasitemia determination improved polymer–drug performance *in vitro* for some AGMA1 salts up to 25%. The highest reductions in IC_{50} were obtained for salts incorporated into the cultures at trophozoite stage, in agreement with the preferential binding of PAAs to pRBCs infected by *P. falciparum* late forms. The concentrations of AGMA1 and ISA23 used in GIAs were never above 0.05 and 0.1 mg/ml, respectively, that is, well below their *in vitro* antimalarial activity threshold determined for *P. falciparum* (Fig. 8). The preferential pRBC localization determined by FACS and fluorescence microscopy was completed in 90 min, whereas after that time under the same conditions only a minor drug portion was released from the PAA-salts (Fig. 2). These observations are consistent with an increased efficacy of PAA–drug salts in comparison to free drugs due to the specific PAA ability of binding to and penetrating into pRBCs.

3.5.2. In vivo studies

Drug-free AGMA1-FITC and ISA23-FITC and a free FITC control were intraperitoneally injected in mice and their blood permanence monitored fluorimetrically. Both polymers showed a concentration peak at ~1.5 h after injection, but AGMA1 was quantitatively removed within 3 h whereas ISA23 was still detectable in circulation after 72 h (Supplementary data, Fig. S4). The maximum fluorescence detected in blood for

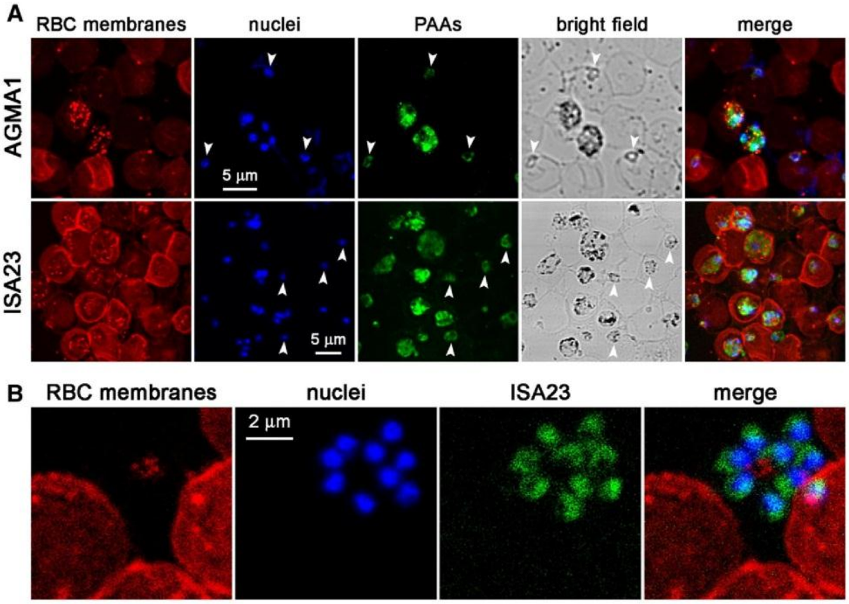

Fig. 6. *In vitro* confocal fluorescence microscopy internalization and binding study of AGMA1 and ISA23 in *P. yoelii*. (A) FITC-labeled AGMA1-d or ISA23-d was added to *P. yoelii*–infected mouse blood and, after 90 min of incubation, the samples were processed for confocal fluorescence microscopy analysis. Arrowheads indicate rings in the AGMA1 sample and rings/early trophozoites in the ISA23 sample. (B) Details of the ISA23 sample showing binding to merozoites. PAA–FITC localization is shown in green, DAPI (blue) staining of *Plasmodium* nuclei was used to indicate pRBCs, and the RBC plasma membrane is shown in red.

both free FITC and AGMA1-FITC corresponded to ~1/3 of the signal expected assuming a homogeneous distribution throughout the body of a 20-g mouse having 2 ml of blood (i.e. about 10% of initial dose). By contrast, in the case of ISA23-FITC, the amount found in blood was about twice as much as expected, suggesting a higher concentration in the circulation relative to other body districts, in agreement with previous literature data on the stealth-like properties of this polymer [26]. AGMA1 shows a strong structural resemblance to the tripeptide arginine-glycine-aspartic acid (RGD sequence) [31], which is known to play a role in the binding of extracellular proteins to cell surface integrins. An increased adhesion of AGMA1 to integrin-expressing cells might explain its scarce localization in and fast disappearance from blood compared with ISA23.

AGMA1-CQ and ISA23-CQ salts and a free CQ control were intraperitoneally administered to *P. yoelii*–infected mice in a 4-day suppressive test (Fig. 10). Malaria-infected animals treated with 4 × 0.8 mg/kg doses of CQ loaded into AGMA1 or ISA23 were nearly freed of parasites by day 4 after administration, whereas the same dose of free CQ only reduced parasitemia by 16% (Fig. 10A and B). The administration of a higher dose of PAA-conjugated CQ (1.9 mg kg^{-1} day^{-1}) led to parasite removal at day 4 that was very close to 100% for both AGMA1-CQ and ISA23-CQ, whereas the same dose of free CQ cleared only about 50% parasitemia. All PAA–drug-treated mice survived and were monitored until day 30 (Fig. 10C), when they exhibited normal behavior, did not experience weight loss, and did not carry any detectable *Plasmodium* parasites in their blood. By contrast, all animals treated with the same doses of free CQ were dead by days 9 (0.8 mg kg^{-1} day^{-1}) and 12 (1.9 mg kg^{-1} day^{-1}). The administration to *P. yoelii*–infected mice of drug-free AGMA1 or ISA23 at concentrations higher than those used in the above experiments with their CQ salts did not show any detectable antimalarial activity compared with controls (data not shown).

The favorable results obtained with the PAA–CQ salts were not doubled with PQ. At day 4, the administration under the above conditions of 4 × 1 mg/kg doses of PQ as AGMA1 or ISA23 salts failed to show any efficacy improvement in parasitemia reduction compared with the free drug. This result can be explained because at the low concentration used *in vivo* PQ efficacy as antimalarial is thought to be dependent on its hepatic metabolization [50,51], whereas the pRBC-targeted drug will likely escape passage through the liver.

4. Discussion

Several polymeric nanocarriers have been proposed for the delivery of antimalarials *in vivo* [11], including quinine [52], halofantrine [53], curcumin [54], artemisinin derivatives [55], chloroquine [56,57] and primaquine [58–60]. However, only four literature reports described the efficacy of polymer–drug formulations compared with the free drugs in malaria-infected animals. Orally administered lipid nanoemulsions of primaquine at a dose of 1.5 mg kg^{-1} day^{-1} improved the mean survival time of *P. berghei*–infected mice from 13 to 39 days, and reduced parasitemia fourfold relative to the free drug [60]; oral delivery of curcumin bound to chitosan nanoparticles cured all *P. yoelii*–infected mice when administered at 100 mg/kg, whereas the same amount of free drug cured only one-third of the animals [54]; intravenous administration to *P. berghei*–infected rats of several doses of 75 mg kg^{-1} day^{-1} quinine enclosed in nanocapsules prepared with poly(ε-caprolactone) and Polysorbate 80 improved by 30% the efficacy of free quinine; finally, a single intravenous dose of 1 mg/kg halofantrine encapsulated in poly(D,L-lactide)-based polymer cured 80% of *P. berghei*–infected mice, when the same dose of the free drug was unable to arrest the infection or prolong the survival of the animals [53].

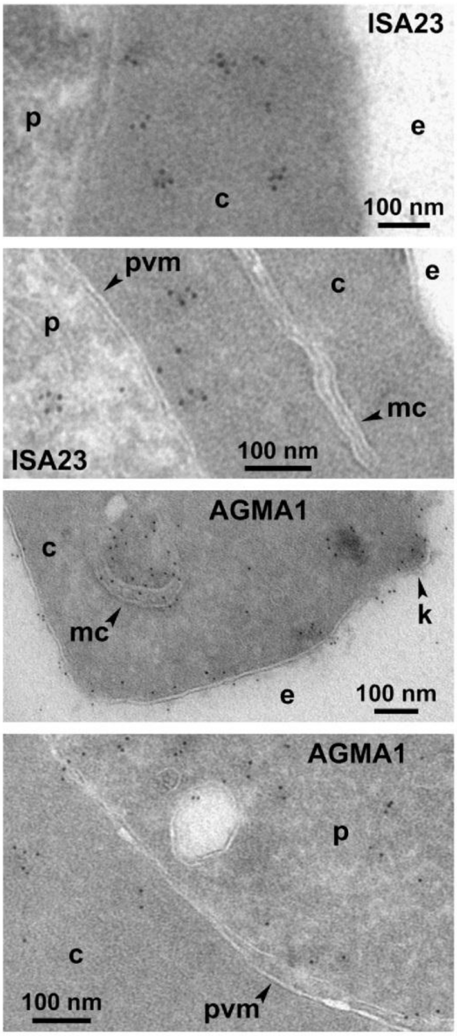

Fig. 7. TEM analysis of the subcellular localization in *P. falciparum* of AGMA1 and ISA23. Living pRBCs were treated with FITC-labeled AGMA1-d or ISA23-d for 90 min before TEM processing. e, extracellular area; c, pRBC cytosol; p, *Plasmodium*; pvm, parasitophorous vacuole membrane; mc, Maurer's cleft; k, knob. Non-infected RBC controls showed no intracellular staining.

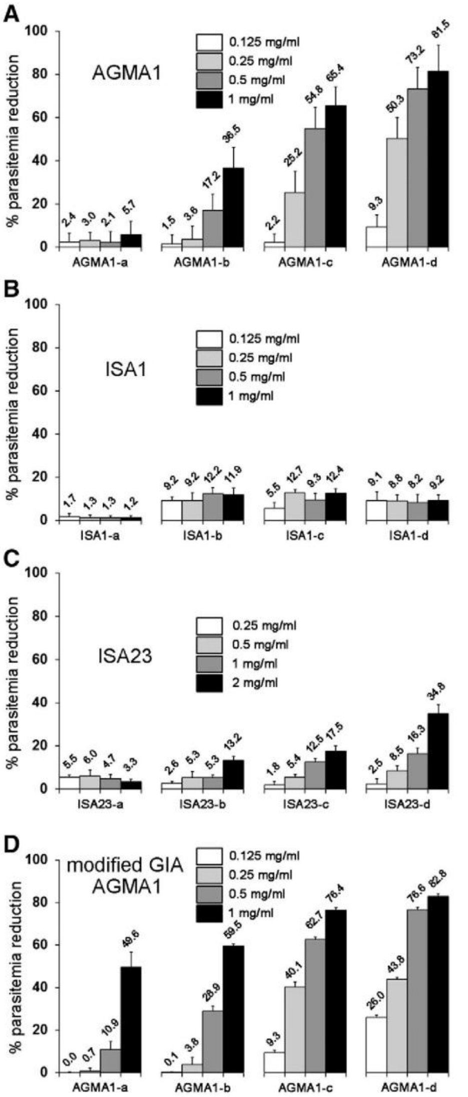

Fig. 8. Effect of AGMA1, ISA1 and ISA23 on the growth of *P. falciparum*. (A–C) Conventional GIAs, where the polymers were added to *P. falciparum* cultures synchronized at the ring stage, and incubated for 48 h before determining parasitemia. (D) Modified GIA, where AGMA1 was added 24 h after pRBC culture synchronization, and incubated for a further 24 h before parasitemia determination.

In the present study, it has been demonstrated that intraperitoneal administration of 0.8 mg kg^{-1} day^{-1} of AGMA1- and ISA23-chloroquine salts cured all *P. yoelii*–infected mice treated and eliminated parasitemia, whereas the same or even a higher amount of free drug (1.9 mg kg^{-1} day^{-1}) failed to cure the animals. The good performance of PAA-conjugated CQ is highlighted by the challenge of improving CQ therapy, given the fast action of the drug in blood stage parasites, its low toxicity, good bioavailability in oral administration, water solubility of its diphosphate salt, high volume of distribution in the body and low cost. The improved *in vivo* activity of PAA-transported CQ could be explained because the random encounters between pRBCs and polymers required for targeting specificity to be manifested are favored by the turbulent mixing in the blood circulation, although this would also apply for free CQ, which has an endogenous carrier across human erythrocyte membranes that accumulates the drug selectively in these cells

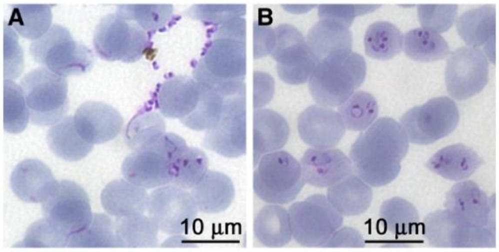

Fig. 9. Microscopy study of the effect of AGMA1 on the invasion of RBCs. (A) Image from a Giemsa-stained *P. falciparum* culture at ring stage after a complete cycle following treatment with 1 mg/ml AGMA1-d. (B) Control sample without AGMA1.

[61]. More likely, the *ex vivo* targeting observed for AGMA1 and ISA23 to earlier forms, such as rings, in the erythrocytic cycle of the rodent malaria parasite *P. yoelii*, might give the drugs a head start resulting in an improved efficacy in comparison to *P. falciparum in vitro* assays, where PAAs enter pRBCs at the trophozoite stage.

During its intraerythrocytic growth, *Plasmodium* modifies the membrane permeability of the host cell in order to uptake nutrients from the plasma, dispose of metabolic waste, and create and maintain electrochemical ion gradients. These changes are of interest from the point of view of antimalarial chemotherapy as possible routes for targeting cytotoxic agents into the intracellular parasite [62]. *Plasmodium* induces new permeation pathways (NPPs) that confer to the pRBC an increased permeability to a wide range of particles up to diameters of 70 nm [29], well above the size of the PAAs presented here. NPPs have been found to be nonsaturable within physiologically relevant concentration ranges for all solutes for which kinetic measurements have been made and the activation energy for the transport through them is typical of a diffusive process [63]. In *P. falciparum*, NPPs are induced in the parasitized cell between 10 and 20 h post-invasion, in agreement with the observed intra-pRBC localization of PAAs not before trophozoite stage. Previous work has suggested that pRBCs become leaky prior to rupture [64], and that the site of parasite invasion on the membrane never completely closes, leaving a pore and a small duct extending into the parasitophorous vacuole [29]. This anomalous membrane has been proposed as an explanation for the observed permeability of pRBCs to certain macromolecules [65]. The efficacy of nanovectors whose targeting would be based on this type of processes could be expected to be less affected by the high antigenic variability of *Plasmodium* [66], which complicates vaccination and targeted drug delivery strategies. Such a targeting not based on specific interactions of the type ligand–receptor as those found between proteins is consistent with the recognition of pRBCs across widely diverging malaria parasites infecting humans and rodents, which has been observed *in vitro* for ISA23 and AGMA1. In addition to suggesting the possibility of recognizing several *Plasmodium* species, as opposed to the restrictive specificity of antibodies, the good PAA binding to mouse pRBCs will facilitate future *in vivo* assays prior to preclinical studies. In the case of AGMA1, its suspected interference with invasion in *P. falciparum* might confer additional antimalarial properties related with potentiation of the immunitary system if AGMA1-bound merozoites are kept for a longer time accessible to antigen-presenting cells.

5. Conclusion

The experimental results reported in this article demonstrate that AGMA1- and ISA23-chloroquine polymeric salts are remarkably more effective *in vivo* than the free drug and definitely warrant potential as antimalarials. *In vitro* and *ex vivo* tests on infected mice strongly suggest that the superior activity of PAA–chloroquine salts is due to the selective targeting of the polymers to and entering into pRBCs with little or no internalization into healthy RBCs. The indication that AGMA1 and ISA23 are able to recognize several *Plasmodium* species, as opposed to the restrictive specificity of antibodies, widens their scope as therapeutic adjuvants for antimalarial therapy.

Supplementary data to this article can be found online at http://dx.doi.org/10.1016/j.jconrel.2013.12.032.

Disclosure

Patent application: Amphoteric polyamidoamines in the treatment of malaria, PCT/EP2013/073762.

Acknowledgment

This work was supported by grants BIO2008-01184 and BIO2011-25039 from the Ministerio de Ciencia e Innovación, Spain, which included FEDER funds, and by grant 2009SGR-760 from the Generalitat de Catalunya, Spain. J.J.V-D. acknowledges the financial support from Juan de la Cierva Programme of the Ministerio de Ciencia e Innovación, Spain. A fellowship of the Instituto de Salud Carlos III (Spain) is acknowledged by P.U. We thank Fabio Fenili for setting up synthesis methods and for technical support. We are indebted to the Scientific and Technological Centres from the University of Barcelona (CCiT-UB) for their technical support.

Table 2

IC_{50} values derived from *in vitro* antimalarial activity of PAA–drug conjugates. *P. falciparum* pRBC cultures were treated for either 1 h or 48 h with ISA23 or AGMA1 loaded with chloroquine (CQ) or primaquine (PQ) added at the ring or trophozoite stage. After drug administration, the cultures were incubated for 48 h before proceeding to parasitemia determination. Control samples consisted of the free drugs. Bold numbers indicate IC_{50} improvement relative to the free drug, and underlined values correspond to IC_{50} improvements >25%.

	Free CQ (nM)	ISA23-CQ (nM)	AGMA1-CQ (nM)	Free PQ (μM)	ISA23-PQ (μM)	AGMA1-PQ (μM)
Rings/48 h	*15.6*	19.8	**14.6**	*3.8*	4.0	**2.5**
Trophozoites/48 h	*83.1*	93.0	**61.4**	*6.5*	11.9	**4.5**
Rings/1 h	*57.4*	62.1	**56.3**	*14.8*	17.6	**12.9**
Trophozoites/1 h	*98.6*	109.5	**73.4**	*12.0*	17.7	**11.7**

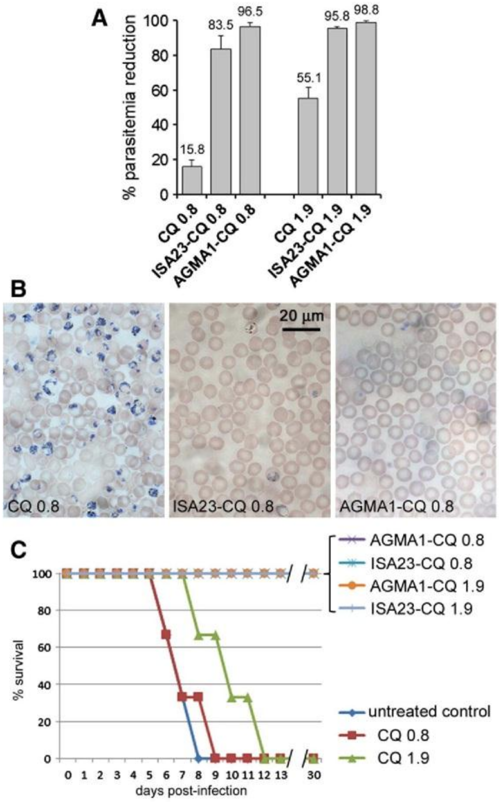

Fig. 10. *In vivo* antimalarial activity of PAA–chloroquine conjugates. (A) Percentage of parasitemia reduction relative to untreated control at day 4 in *P. yoelii*–infected mice treated intraperitoneally with 0.8 or 1.9 mg kg^{-1} day^{-1} CQ, either free or loaded into ISA23 or AGMA1. (B) Microscopy images of Giemsa-stained smears of the blood from mice treated with 0.8 mg kg^{-1} day^{-1} CQ, either free or loaded into ISA23 or AGMA1. The presence of parasites is clearly evident in the left panel. (C) Mice survival graph of *P. yoelii*–infected mice treated with 0.8 or 1.9 mg kg^{-1} day^{-1} CQ, either free or loaded into ISA23 or AGMA1.

References

[1] World Health Organization: World Malaria Report 2012, http://www.who.int/malaria/publications/world_malaria_report_2012/report/en/.

[2] S.H. Kappe, A.M. Vaughan, J.A. Boddey, A.F. Cowman, That was then but this is now: malaria research in the time of an eradication agenda, Science 328 (2010) 862–866.

[3] S. Vangapandu, M. Jain, K. Kaur, P. Patil, S.R. Patel, R. Jain, Recent advances in antimalarial drug development, Med. Res. Rev. 27 (2007) 65–107.

[4] E.A. Okiro, A. Al Taiar, H. Reyburn, R. Idro, J.A. Berkley, R.W. Snow, Age patterns of severe paediatric malaria and their relationship to *Plasmodium falciparum* transmission intensity, Malar. J. 8 (2009) 4.

[5] T.N. Wells, P.L. Alonso, W.E. Gutteridge, New medicines to improve control and contribute to the eradication of malaria, Nat. Rev. Drug Discov. 8 (2009) 879–891.

[6] N.J. White, *Plasmodium knowlesi*: the fifth human malaria parasite, Clin. Infect. Dis. 46 (2008) 172–173.

[7] R. Tuteja, Malaria - an overview, FEBS J. 274 (2007) 4670–4679.

[8] K.S. Griffith, L.S. Lewis, S. Mali, M.E. Parise, Treatment of malaria in the United States: a systematic review, JAMA 297 (2007) 2264–2277.

[9] J.K. Baird, Effectiveness of antimalarial drugs, N. Engl. J. Med. 352 (2005) 1565–1577.

[10] R. Duncan, R. Gaspar, Nanomedicine(s) under the microscope, Mol. Pharm. 8 (2011) 2101–2141.

[11] P. Murambiwa, B. Masola, T. Govender, S. Mukaratirwa, C.T. Musabayane, Anti-malarial drug formulations and novel delivery systems: a review, Acta Trop. 118 (2011) 71–79.

[12] P. Urbán, J. Estelrich, A. Cortés, X. Fernàndez-Busquets, A nanovector with complete discrimination for targeted delivery to *Plasmodium falciparum*-infected versus non-infected red blood cells *in vitro*, J. Control. Release 151 (2011) 202–211.

[13] P. Urbán, J. Estelrich, A. Adeva, A. Cortés, X. Fernàndez-Busquets, Study of the efficacy of antimalarial drugs delivered inside targeted immunoliposomal nanovectors, Nanoscale Res. Lett. 6 (2011) 620.

[14] C.M. Paleos, D. Tsiourvas, Z. Sideratou, L.A. Tziveleka, Drug delivery using multifunctional dendrimers and hyperbranched polymers, Expert Opin. Drug Deliv. 7 (2010) 1387–1398.

[15] P. Ferruti, M.A. Marchisio, R. Duncan, Polyamidoamines: biomedical applications, Macromol. Rapid Commun. 23 (2002) 332–355.

[16] P. Ferruti, Poly(amidoamine)s: past, present, and perspectives, J. Polym. Sci. Part A: Polym. Phys. 51 (2013) 2319–2353.

[17] P. Ferruti, E. Ranucci, F. Bignotti, L. Sartore, P. Bianciardi, M.A. Marchisio, Degradation behaviour of ionic stepwise polyaddition polymers of medical interest, J. Biomater. Sci. Polym. Ed. 6 (1995) 833–844.

[18] E. Ranucci, G. Spagnoli, P. Ferruti, D. Sgouras, R. Duncan, Poly(amidoamine)s with potential as drug carriers: degradation and cellular toxicity, J. Biomater. Sci. Polym. Ed. 2 (1991) 303–315.

[19] F. Bignotti, P. Sozzani, E. Ranucci, P. Ferruti, NMR studies, molecular characterization, and degradation behavior of poly(amido amine)s. 1. Poly(amido amine) deriving from the polyaddition of 2-methylpiperazine to 1,4-bis(acryloyl)piperazine, Macromolecules 27 (1994) 7171–7178.

[20] S.C. Richardson, N.G. Pattrick, Y.K. Man, P. Ferruti, R. Duncan, Poly(amidoamine)s as potential nonviral vectors: ability to form interpolyelectrolyte complexes and to mediate transfection *in vitro*, Biomacromolecules 2 (2001) 1023–1028.

[21] R. Cavalli, A. Bisazza, R. Sessa, L. Primo, F. Fenili, A. Manfredi, E. Ranucci, P. Ferruti, Amphoteric agmatine containing polyamidoamines as carriers for plasmid DNA *in vitro* and *in vivo* delivery, Biomacromolecules 11 (2010) 2667–2674.

[22] M.W. Pettit, P. Griffiths, P. Ferruti, S.C. Richardson, Poly(amidoamine) polymers: soluble linear amphiphilic drug-delivery systems for genes, proteins and oligonucleotides, Ther. Deliv. 2 (2011) 907–917.

[23] S.C.W. Richardson, N.G. Pattrick, N. Lavignac, P. Ferruti, R. Duncan, Intracellular fate of bioresponsive poly(amidoamine)s *in vitro* and *in vivo*, J. Control. Release 142 (2010) 78–88.

[24] N.G. Pattrick, S.C. Richardson, M. Casolaro, P. Ferruti, R. Duncan, Poly(amidoamine)-mediated intracytoplasmic delivery of ricin A-chain and gelonin, J. Control. Release 77 (2001) 225–232.

[25] P. Ferruti, E. Ranucci, F. Trotta, E. Gianasi, E.G. Evagorou, M. Wasil, G. Wilson, R. Duncan, Synthesis, characterisation and antitumour activity of platinum(II) complexes of novel functionalised poly(amido amine)s, Macromol. Chem. Phys. 200 (1999) 1644–1654.

[26] N. Lavignac, J.L. Nicholls, P. Ferruti, R. Duncan, Poly(amidoamine) conjugates containing doxorubicin bound via an acid-sensitive linker, Macromol. Biosci. 9 (2009) 480–487.

[27] S. Richardson, P. Ferruti, R. Duncan, Poly(amidoamine)s as potential endosomolytic polymers: evaluation *in vitro* and body distribution in normal and tumour-bearing animals, J. Drug Target. 6 (1999) 391–404.

[28] P. Ferruti, J. Franchini, M. Bencini, E. Ranucci, G.P. Zara, L. Serpe, L. Primo, R. Cavalli, Prevailingly cationic agmatine-based amphoteric polyamidoamine as a nontoxic, nonhemolytic, and "stealthlike" DNA complexing agent and transfection promoter, Biomacromolecules 8 (2007) 1498–1504.

[29] I.D. Goodyer, B. Pouvelle, T.G. Schneider, D.P. Trelka, T.F. Taraschi, Characterization of macromolecular transport pathways in malaria-infected erythrocytes, Mol. Biochem. Parasitol. 87 (1997) 13–28.

[30] R. Allahyari, A. Strother, I.M. Fraser, A.J. Verbiscar, Synthesis of certain hydroxy analogues of the antimalarial drug primaquine and their *in vitro* methemoglobin-producing and glutathione-depleting activity in human erythrocytes, J. Med. Chem. 27 (1984) 407–410.

[31] J. Franchini, E. Ranucci, P. Ferruti, M. Rossi, R. Cavalli, Synthesis, physicochemical properties, and preliminary biological characterizations of a novel amphoteric agmatine-based poly(amidoamine) with RGD-like repeating units, Biomacromolecules 7 (2006) 1215–1222.

[32] S.L. Cranmer, C. Magowan, J. Liang, R.L. Coppel, B.M. Cooke, An alternative to serum for cultivation of *Plasmodium falciparum in vitro*, Trans. R. Soc. Trop. Med. Hyg. 91 (1997) 363–365.

[33] C. Lambros, J.P. Vanderberg, Synchronization of *Plasmodium falciparum* erythrocytic stages in culture, J. Parasitol. 65 (1979) 418–420.

[34] D.A. Fidock, P.J. Rosenthal, S.L. Croft, R. Brun, S. Nwaka, Antimalarial drug discovery: efficacy models for compound screening, Nat. Rev. Drug Discov. 3 (2004) 509–520.

[35] R.K. Verbeeck, H.E. Junginger, K.K. Midha, V.P. Shah, D.M. Barends, Biowaiver monographs for immediate release solid oral dosage forms based on biopharmaceutics classification system (BCS) literature data: chloroquine phosphate, chloroquine sulfate, and chloroquine hydrochloride, J. Pharm. Sci. 94 (2005) 1389–1395.

[36] P.S. Bonato, R. Bortocana, C.M. Gaitani, F.O. Paias, M.H. Iha, R.P. Lima, Enantiomeric resolution of drugs and metabolites in polysaccharide- and protein-based chiral stationary phases, J. Braz. Chem. Soc. 13 (2002) 190–199.

[37] T.K. Chatterjee, Chemotherapy of Tropical Parasitic Infections, PHI Learning Pvt. Ltd., New Delhi, India, 2000.

[38] E. Hanssen, P. Carlton, S. Deed, N. Klonis, J. Sedat, J. DeRisi, L. Tilley, Whole cell imaging reveals novel modular features of the exomembrane system of the malaria parasite, *Plasmodium falciparum*, Int. J. Parasitol. 40 (2010) 123–134.

[39] P. Gascoyne, J. Satayavivad, M. Ruchirawat, Microfluidic approaches to malaria detection, Acta Trop. 89 (2004) 357–369.

[40] H.-G. Heidrich, L. Rüssmann, B. Bayer, A. Jung, Free-flow electrophoresis for the separation of malaria infected and uninfected mouse erythrocytes and for the isolation of free parasites (*Plasmodium vinckei*): a new rapid technique for the liberation of malaria parasites from their host cells, Z. Parasitenkd. 58 (1979) 151–159.

[41] J.P. Shelby, J. White, K. Ganesan, P.K. Rathod, D.T. Chiu, A microfluidic model for single-cell capillary obstruction by *Plasmodium falciparum*-infected erythrocytes, Proc. Natl. Acad. Sci. U. S. A. 100 (2003) 14618–14622.

[42] K. Kirk, K.J. Saliba, Targeting nutrient uptake mechanisms in *Plasmodium*, Curr. Drug Targets 8 (2007) 75–88.

[43] A. El Tahir, P. Malhotra, V. Chauhan, Uptake of proteins and degradation of human serum albumin by *Plasmodium falciparum*–infected human erythrocytes, Malar. J. 2 (2003) 11.

[44] P. Ferruti, S. Manzoni, S.C.W. Richardson, R. Duncan, N.G. Pattrick, R. Mendichi, M. Casolaro, Amphoteric linear poly(amido-amine)s as endosomolytic polymers: a correlation between physicochemical and biological properties, Macromolecules 33 (2000) 7793–7800.

[45] R. Mendichi, P. Ferruti, B. Malgesini, Evidence of aggregation in dilute solution of amphoteric poly(amido-amine)s by size exclusion chromatography, Biomed. Chromatogr. 19 (2005) 196–201.

[46] E.S. Zuccala, J. Baum, Cytoskeletal and membrane remodelling during malaria parasite invasion of the human erythrocyte, Br. J. Haematol. 154 (2011) 680–689.

[47] P.R. Gilson, B.S. Crabb, Morphology and kinetics of the three distinct phases of red blood cell invasion by *Plasmodium falciparum* merozoites, Int. J. Parasitol. 39 (2009) 91–96.

[48] A.F. Cowman, D. Berry, J. Baum, The cellular and molecular basis for malaria parasite invasion of the human red blood cell, J. Cell Biol. 198 (2012) 961–971.

[49] P. Sharma, C.E. Chitnis, Key molecular events during host cell invasion by Apicomplexan pathogens, Curr. Opin. Microbiol. 16 (2013) 1–6.

[50] S. Ganesan, B.L. Tekwani, R. Sahu, L.M. Tripathi, L.A. Walker, Cytochrome P450-dependent toxic effects of primaquine on human erythrocytes, Toxicol. Appl. Pharmacol. 241 (2009) 14–22.

[51] B. Pybus, S. Marcsisin, X. Jin, G. Deye, J. Sousa, Q. Li, D. Caridha, Q. Zeng, G. Reichard, C. Ockenhouse, J. Bennett, L. Walker, C. Ohrt, V. Melendez, The metabolism of primaquine to its active metabolite is dependent on CYP 2D6, Malar. J. 12 (2013) 212.

[52] S.E. Haas, C.C. Bettoni, L.K. de Oliveira, S.I.S. Guterres, T. Dalla Costa, Nanoencapsulation increases quinine antimalarial efficacy against *Plasmodium berghei in vivo*, Int. J. Antimicrob. Agents 34 (2009) 156–161.

[53] V.C.F. Mosqueira, P.M. Loiseau, C. Bories, P. Legrand, J.P. Devissaguet, G. Barratt, Efficacy and pharmacokinetics of intravenous nanocapsule formulations of halofantrine in *Plasmodium berghei*-infected mice, Antimicrob. Agents Chemother. 48 (2004) 1222–1228.

[54] F. Akhtar, M.M.A. Rizvi, S.K. Kar, Oral delivery of curcumin bound to chitosan nanoparticles cured *Plasmodium yoelii* infected mice, Biotechnol. Adv. 30 (2012) 310–320.

[55] D. Bhadra, S. Bhadra, N.K. Jain, Pegylated lysine based copolymeric dendritic micelles for solubilization and delivery of artemether, J. Pharm. Pharm. Sci. 8 (2005) 467–482.

[56] D. Bhadra, S. Bhadra, N.K. Jain, PEGylated peptide dendrimeric carriers for the delivery of antimalarial drug chloroquine phosphate, Pharm. Res. 23 (2006) 623–633.

[57] P. Agrawal, U. Gupta, N.K. Jain, Glycoconjugated peptide dendrimers-based nanoparticulate system for the delivery of chloroquine phosphate, Biomaterials 28 (2007) 3349–3359.

[58] M.D. Green, M.J. D'Souza, J.M. Holbrook, R.A. Wirtz, *In vitro* and *in vivo* evaluation of albumin-encapsulated primaquine diphosphate prepared by nebulization into heated oil, J. Microencapsul. 21 (2004) 433–444.

[59] D. Bhadra, A.K. Yadav, S. Bhadra, N.K. Jain, Glycodendrimeric nanoparticulate carriers of primaquine phosphate for liver targeting, Int. J. Pharm. 295 (2005) 221–233.

[60] K.K. Singh, S.K. Vingkar, Formulation, antimalarial activity and biodistribution of oral lipid nanoemulsion of primaquine, Int. J. Pharm. 347 (2008) 136–143.

[61] A. Yayon, H. Ginsburg, The transport of chloroquine across human erythrocyte membranes is mediated by a simple symmetric carrier, Biochim. Biophys. Acta 686 (1982) 197–203.

[62] K. Kirk, Membrane transport in the malaria-infected erythrocyte, Physiol. Rev. 81 (2001) 495–537.

[63] H.M. Staines, J.C. Ellory, K. Kirk, Perturbation of the pump-leak balance for Na^+ and K^+ in malaria-infected erythrocytes, Am. J. Physiol. Cell Physiol. 280 (2001) C1576–C1587.

[64] J.A. Lyon, J.M. Carter, A.W. Thomas, J.D. Chulay, Merozoite surface protein-1 epitopes recognized by antibodies that inhibit *Plasmodium falciparum* merozoite dispersal, Mol. Biochem. Parasitol. 90 (1997) 223–234.

[65] E.S. Bergmann-Leitner, E.H. Duncan, E. Angov, MSP-1p42-specific antibodies affect growth and development of intra-erythrocytic parasites of *Plasmodium falciparum*, Malar. J. 8 (2009) 183–194.

[66] N. Rovira-Graells, A.P. Gupta, E. Planet, V.M. Crowley, S. Mok, L. Ribas de Pouplana, P.R. Preiser, Z. Bozdech, A. Cortés, Transcriptional variation in the malaria parasite *Plasmodium falciparum*, Genome Res. 22 (2012) 925–938.

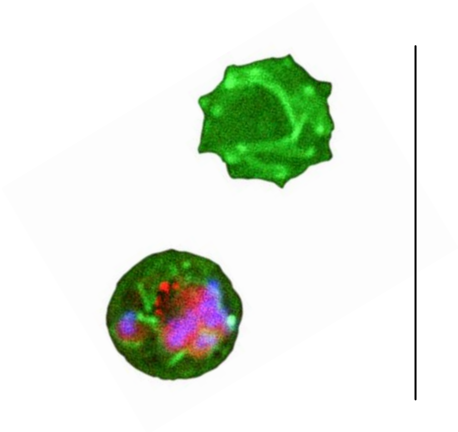

DISCUSSION

DISCUSSION

Malaria is the most devastating parasitic disease of humans in developing countries and one of the main medical concerns worldwide. There is an urgent need for new therapeutic strategies against malaria including the constant search of new antimalarial drugs and of improved methods for their efficient administration. The ability of *Plasmodium* to escape the immune system of the host resides in several incredibly refined mechanisms that hamper vaccine approaches and trigger the rapid appearance of strains resistant to newly developed drugs. Early intraerythrocytic stages are invisible to the immune system because RBCs are not capable of processing and presenting antigens[76]. Even when the parasite begins to modify the pRBC membrane to obtain nutrients required for its development and survival, and to eliminate waste products, the proteins exported to the pRBC plasma membrane present a fairly high antigenic variation[176] which also contributes to evasion from the immune surveillance by the parasite. Additionally, mature intraerythrocytic stages (trophozoites and schizonts) have the ability to adhere to endothelial cells from different tissues and organs leading to parasite replication while escaping splenic clearance[177]. Multiple receptors, which include both proteins and carbohydrates, are known to be involved in this process which is thought to play a major role in the fatal outcome of severe malaria[41]. The major part of virulence for *P. falciparum* malaria infection results from increased rigidity and adhesiveness of infected host RBCs. These changes are caused by parasite proteins exported to the erythrocyte using novel trafficking machinery assembled in the host cell. As GAGs are one of the main pRBC-binding molecules, GAG-based therapies have been suggested for future antimalarial approaches. Previous studies showed that soluble CSA, heparin, HS, heparin-HS-derivatives and other sulfated glycoconjugates can either inhibit pRBC sequestration[178-181], disrupt rosettes[57,137,159,182], or block sporozoites adhesion to hepatocytes[183,184]. GAGs are economically affordable in large quantities and have low immunogenicity due especially to their endogenous nature. Concerning heparin, as it is probably present in the blood, the parasite must have been exposed to it during its long coevolutionary history with humans and no parasite resistance has been described so far[31]. Heparin and low molecular weight heparin are the principal anticoagulant and antithrombotic drugs currently used in medicine. Besides their well-described anticoagulant/antithrombotic actions, heparin and heparin-like molecules are known to interact with multiple proteins modulating several biological processes[185]. However, their further clinical use is challenged by their strong anticoagulant activity and hemorrhagic complications[186]. DBL1α domain (close to the N-terminal segment of PfEMP1 that appears on the pRBC membrane at the early trophozoite phase) has been suggested as the ligand receptor for heparin binding on pRBCs[57,187-189]. The antimalarial mechanism of heparin has not been yet fully established but it might be related to its capacity in blocking erythrocyte invasion[137,149], in agreement with proteomic analyses that revealed the presence of heparin-binding proteins in the *P. falciparum* merozoite[35] and in pRBC membranes[147]. Furthermore, the high specificity of heparin binding to pRBCs infected with late forms of *P. falciparum* has been demonstrated by fluorescence microscopy, FACS, and single-molecule force spectroscopy[40] opening up the possibility of using this natural polymer as a targeting agent towards *Plasmodium*-infected cells. We then tested the targeting capacity of heparin-FITC towards *P. yoelii*-infected RBCs *versus* non-infected RBCs demonstrating that this system can be applied to different parasite strains exhibiting similar target specificity. Heparin has actually been employed in the treatment of severe malaria[190-192] but its use was discontinued due to adverse side effects such as intracranial bleeding[158]. However, it has been demonstrated that the pentamer responsible for anticoagulant activity is not essential for binding to the DBL1α domain, and that oxidation does not affect the rosette disruptive capacity or the inhibition of endothelial binding mediated by this domain[159]. Moreover, there is also evidence showing that depolymerized heparin (devoid of anticoagulant activity) was able to disrupt rosette formation and pRBC cytoadherence both *in vitro* and *in vivo*, and that when heparin is covalently immobilized onto a substrate it significantly loses its anticoagulating action[160]. Taking all these findings into account we decided to investigate if heparin electrostatically bound to antimalarial drug-containing liposomes could be used as a reasonable strategy to overcome its main limitation without losing its antimalarial capacity and specific targeting activity. In addition, heparin has been used at the surface of solid nanoparticles to achieve long circulation times in the bloodstream for drug delivery in cancer therapy[193,194]. PQ was the chosen antimalarial drug due to (i) an easy quantification, (ii) a high *in vitro* IC50, and (iii) because its use was hampered in patients with glucose-6-phosphate dehydrogenase deficiency for toxicological reasons. Our starting point was to explore the electrostatic binding instead of the covalent one because the target sites of electrostatic interactions are likely to be relatively large areas that therefore are not so prone to quick *Plasmodium* evolutionary modification as the small antigens recognized by antibodies for instance, contributing to minimize resistance induction. After confirming that soluble heparin has a dose-dependent antimalarial activity in a *P. falciparum* culture and that it presents a specific targeting ability towards pRBCs, we investigated if it could be used as a dual agent. For this, we tested different conditions and compared the activity of same amounts of heparin bound to PQ-free LPs with PQ-containing LPs, observing that the last ones dropped the parasitemia significantly. It is also important to underline that at the non-anticoagulating concentration of 1 μg mL^{-1}, heparin improved the activity of LPs-encapsulated PQ ca. four-fold. Activity of free heparin was not significantly different from that of the same heparin amounts conjugated to drug-free LPs demonstrating that the polymer antimalarial activity is not affected by the electrostatic binding. At this point and after performing several assays with different DOTAP contents, we settled at 4% so the heparin and PQ activities were not masked by the antimalarial capacity of the lipid observed above 4% for concentrations higher than 200 μM of total lipid in the culture *in vitro*. When heparin not bound to LPs was removed by ultracentrifugation, the resulting sample was still capable of exhibiting antimalarial activity in itself and of acting as targeting element of PQ-containing LPs even though these samples contained heparin concentrations well below its IC50, improving by more than 30% the antimalarial activity of LPs-encapsulated PQ. In previous studies it has been shown that macromolecules can access *P. falciparum*-infected RBCs through the cytostome, via NPPs induced by the parasite[129]. There is also evidence of another macromolecular transport pathway consisting of internalization of macromolecules and other membrane-impermeable compounds from the external medium to the erythrocyte cytosol through a duct left as a remnant of merozoite entry, whereby the RBC and the parasitophorous vacuole membrane would fuse prior to parasite invasion by a process resembling fluid-phase endocytosis[195]. Using a variety of latex beads, it was determined that molecules up to 50-80 nm in diameter are able to access intracellular parasites. This size exclusion is consistent with the dimensions of the parasitophorous duct pathway revealed by electron microscopy[129]. The existence of such an anomalous membrane, which becomes leaky prior to rupture, has been proposed as an explanation for the observed permeability of pRBCs to several macromolecules[130]. Our LPs presented an average size of 150 nm, so we hypothesize that it might as well enter through the NPPs or by membrane fusion processes. In addition to specific targeting to pRBCs, the planned antimalarial targeted drug delivery system allowed the release of LPs cargo inside target cells as required. Since our final product was expected to be used in malaria endemic regions, which in most cases are located in developing areas with low *per capita* income[121], we designed nanoparticles economically affordable whose cost was at least 50 times less than that of our first immunoliposomal prototype[115] for a similar efficacy. The use of markedly low amounts of heparin as a targeting agent opens up new opportunities in future antimalarial nanotherapies and in other GAG-related molecules exhibiting a synergistic activity as antimalarials and as targeting agents for the specific delivery of drugs to *Plasmodium*-infected cells. The administration route is an important aspect to be considered when designing malaria therapies, being the oral route the first choice for uncomplicated malaria. Our liposomal prototype is adequate for parenteral delivery, indicated in all patients with severe or complicated malaria, those at high risk of developing severe disease, or in case the patient is vomiting and unable to take oral antimalarials. Additionally, heparin blocking erythrocyte invasion (antimalarial action) contributes to an increase in the exposure of *P. falciparum* infective forms to the immune system which reveals a vaccine-like action. Recent results by others reported the use of a nanostructure based on polymersomes bound to parasite-derived ligands involved in the initial attachment to host cells that efficiently blocked reinvasion of malaria parasites after their egress from host cells *in vitro*[196]. This dual role as drug and as vaccination adjuvant represents a completely new and innovative approach to the treatment of the disease that offers interesting options for severe malaria and enables a promising method to modulate the host immune response.

Considering the molecular mechanism of the anti-inflammatory effect of heparin, its side effects, and the possibility of pathogen contamination, it becomes extremely relevant the search for alternative heparin-like compounds, obtained from non-mammalian sources, possessing similar biological activities, but devoid of the undesired side effects[170]. Polysaccharides are ubiquitous in animals and plant cells where they play a significant role in a number of physiological situations such as, hydration, mechanical properties of cell walls and ionic regulation[197]. GAGs analogs showing unique structures and pharmacological activities have been described among different marine invertebrates[170]. Anticoagulant activities of polysaccharides have been described to depend mainly on the sulfate groups present within the molecule[198]. Nevertheless, there are other structural characteristics such as polyanionic features or the molecular weight[199,200] influencing their biological activity. It has been demonstrated that sulfation, and thus electronegative-charge density in marine carbohydrates is not the only structural feature determining the resultant anticoagulant effect of these molecules and that, indeed, the anticoagulant capacity of certain marine glycans is attributed to specific combinations of sulfation patterns and glycosylation types[168]. There is evidence of a FucCS isolated from the sea cucumber *Ludwigothurea grisea* showing significant therapeutic effect after oral administration, attenuating metastasis and inflammation due to the high anti-selectin capacity of the sulfated fucose branches[170]. Thus, previous studies performed with the same compound showed that presence of sulfated fucose branches on the native FucCS were essential for inhibiting *P. falciparum* growth and that removal of these branches from the molecule abolished its anticoagulant and antithrombotic activities[150]. Although the exact mechanism of inhibition by sulfated polysaccharides has yet to be defined, it appears to involve the interactions of *Plasmodium* invasion proteins with sulfated proteoglycans, like HS and CSA, that are present on the surface of most cell types, including RBCs[201]. In addition to the effects and characteristics described above, FucCS does not require fractionation nor chemical modification after its purification, it can be isolated with relatively high yield[169], and it is suitable for oral administration, which is an advantage in comparison to other sulfated polysaccharides[150]. For instance, heparin is not suitable for oral administration because (i) due to the acidic environment present on the stomach, its sulfate groups would be destroyed and (ii) it is insufficiently absorbed on the intestine. As an alternative strategy to the use of heparin we explored the antimalarial and anticoagulant activities of FucCSs and fucans from two different sea cucumbers (*L. grisea* and *Isostichopus badionotus*), of a galactan from a red alga (*Botryocladia occidentalis*), and of a branched glycan from a marine sponge (*Desmapsamma anchorata*). By performing growth inhibition assays *in vitro* using *P. falciparum* cultures, we observed that all the sulfated polysaccharides included in the study were able to inhibit the parasite growth. We found no correlation between the size of the compounds in study and their antimalarial capacity since the ones that showed better growth inhibition activity were the smallest and the largest sulfated polysaccharides. However, as the nature of the GIA means that inhibitory effects measured may be due to activity distinct from direct merozoite invasion inhibition, such as inhibition of intraerythrocytic growth, schizont rupture and/or merozoite dispersal[38], we decided to perform merozoite invasion inhibition assays as well. In accordance to previous published data from another group working with a similar compound[150], we concluded that all the sulfated polysaccharides were capable of inhibiting the invasion of RBCs by *P. falciparum* merozoites but not the maturation of the ones that could invade the host erythrocytes. Currently, the majority licensed malaria therapeutic agents target the intraerythrocytic development of the parasite, yet there may be a great potential for the use of merozoite invasion inhibitory drugs in combination with drugs targeting the intraerythrocytic development[38] as merozoite invasion is a key point in parasite development. Moreover, our data showed an interesting correlation between anticoagulant capacity and antimalarial activity in which higher antimalarial activity corresponded to polysaccharides exhibiting higher anticoagulant capacity. Interestingly the molecules having higher antimalarial and anticoagulant activities present their α-fucose units as branches in contrary to the ones displaying less activity that contain their α-fucose groups as internal units. The fact that all the studied marine-derived compounds act by inhibiting merozoites invasion of RBCs, suggests that these polysaccharides may act as vaccine adjuvants because the parasite becomes more exposed to the immune system helping the host modulating an immune response.

Furthermore, to study their antimalarial capacity *in vivo* we treated *P.yoelii*-infected mice intravenously with polysaccharides doses according to their antimalarial activity *in vitro*, anticoagulation capacity and unspecific toxicity. Mice were treated with low doses of the sulfated polysaccharides for 4 days and parasitemia counts on the first day without treatment revealed that except for the glycan and the *L. grisea* fucan, the treatment reduced the parasitemia when compared to untreated controls that received PBS. Nevertheless, only the fucan from *I. badionotus* was able to provide an improvement in mice survival since one mouse was capable of beating infection. It has been observed that a FucCS administered orally for 30 days at a 50 mg kg^{-1} dose presented no toxic or cumulative effects in mice tissue *in vivo* (unpublished data from Mourão) indicating that the oral administration route might offer an interesting alternative approach for the use of marine polysaccharides as antimalarials. Favorably all primary sources of these potential therapeutic compounds exist in abundance among different parts of the world, especially in western seas, where they can be cultivated in large scale and easily isolated through procedures already well-established on the preparation of pharmaceutical heparin[170].

With the aim of improving our nanocarrier prototype and taking into account that the three elements that constitute a targeted therapeutic nanovector (nanocapsule, targeting molecule and the drug) can be exchanged, as if they were LEGO parts, to obtain new structures better suited to each particular situation[202], we explored different conditions and scenarios. Firstly, we observed that certain lipids present on the liposomes bilayer showed a significant degree of toxicity to the parasite *per se*. For this reason, we hypothesize that if we add them to our LPs formulation we might sum up to our heparin-functionalized prototype activity the additional antimalarial capacity from the toxic lipids itself. Furthermore, the DOTAP content was initially settled to 4% because higher amounts showed toxicity for *Plasmodium* which would mask our study of heparin activity. Nevertheless, increasing its content on our liposomes bilayer would allow us to augment the heparin amounts binding to the nanovectors and confer a synergistic effect by adding to an increased heparin content the antimalarial activity of the lipid. In addition, through fluorescence microscopy assays, we noted that by incubating a coculture of living late stage parasites with immuno-LPs labeled with rhodamine, the lipids seemed to be internalized in the pRBCs by a membrane fusion mechanism.

Another strategy that we tested trying to overcome the main limitation of using heparin in antimalarial therapies, besides using heparin-like molecules lacking a strong anticoagulant action, was to perform a covalent binding between the polymer and the nanocarriers instead of an electrostatic one. It is certain that through the electrostatic binding we were more likely to maintain the dual activity of heparin but on the other hand, previous studies demonstrated that covalent binding of heparin through its carboxyl groups dramatically reduced the interaction of heparin with antithrombin III[203] thus decreasing its anticoagulant capacity. However, after examining the dual role of heparin when covalently bounded to LPs we concluded that it was still capable of performing its antimalarial and specific targeting activities toward infected RBCs, and of significantly improving the PQ-containing LPs antimalarial effect. In addition, heparin covalently bound to PQ-encapsulating LPs presented much lower anticoagulant action than the same amounts of heparin binding electrostatically to the same nanovectors.

As referred to above, depolymerized heparin has previously been shown to disrupt rosette formation and pRBCs cytoadherence both *in vivo* and *in vitro*[159]. Sevuparin, which is a heparin analogue with low anticoagulant activity but presenting the same anti-adhesive properties, is currently being tested in a phase II clinical trial. Results from phase I have not been published yet but were reported as promising[204] and, at this moment, sevuparin has proven to be safe when given intravenously every 6 hours for 3 days, but the primary efficacy end point of a higher number of mature infected erythrocytes in peripheral blood was not met[205]. Nevertheless, results showed a decrease of ring stage parasites and a very slight increase of late stage parasites during the first hours after the first dose of treatment compared with the control[205]. Inspired by these data we also tested the antimalarial activity of shorter heparin fragments *in vitro*, hexa- and octasaccharides, and observed that they presented much lower growth inhibition capacity than the larger polymer in free form.

Moreover, we explored the use of other nanocapsules with the objective of surpassing LPs main limitations, such as, poor stability and structural integrity *in vivo*[206]. For this, we analyzed the interaction of soluble low molecular weight chitosan and chitosan nanoparticles (ca. 200 nm) with heparin trough isothermal titration calorimetry assays. Chitosan is a polysaccharide obtained by the deacetylation of chitin, which is one of the most widespread polymers in nature. Chitosan is chemically defined as a cationic copolymer of two residues: 2-amino-2-deoxy-D-glucopyranose (D-glucosamine) and 2-acetamido-2-deoxy-D-glucopyranose (N-acetyl-D-glucosamine)[207]. The specific properties of chitosan, such as its bioactivity, biocompatibility, biodegradability, solubility in an aqueous solution, and ability to form complexes and non-toxicity for humans, have resulted in increased interest in its potential biomedical applications, such as, in bone substitutes, drug delivery systems, delivery of proteins/peptides and genes, artificial skins, and wound dressings, as well as carriers for contrast agents[208-214]. For these reasons, and because heparin showed a highly specific targeting capacity of LPs, we considered chitosan nanoparticles would be a valuable strategy as antimalarial drug delivery systems targeted to pRBCs by heparin. After confirming that the electrostatic binding between heparin and chitosan did not affect heparin activity, we analyzed their association concluding they interact through an exothermic reaction and that if chitosan is added in the form of nanoparticles instead of the free soluble form, a strong cooperative effect is observed due to the binding of heparin to adjacent chitosan chains following an initial interaction. Finally, we hypothesize that chitosan nanoparticles might offer an interesting tool in antimalarial drug therapies when conjugated to heparin or heparin-like molecules.

Plasmodium early stages are ideal therapeutic targets because drugs delivered to them would have a longer period of time to kill the parasite before it completes its development, although the permeability of the infected erythrocyte to ions and small nonelectrolytes, including some drugs, does not increase until ca. six hours after invasion[215]. Nevertheless, to eliminate malaria completely, broadly acting medicines must be developed that cure the symptomatic asexual blood-stage, clear the preceding liver stage infection and block parasite transmission to mosquitoes[216]. There is a crucial need for therapeutics that go beyond treating acute infections and have the potential to eradicate the disease[217]. For this, blocking disease transmission by targeting parasite sexual stages has been pointed out as one of the most important approaches to eliminate the disease. Of particular interest is the targeting of the transmission stages that allow transfer of the parasite between human and mosquito and vice-versa, which represent the weakest spots in the life cycle of the pathogen[218]. With the idea of targeting the mosquito stages to block transmission and prevent new infections, we tested the targeting capacity of FITC-labeled heparin towards gametocytes, ookinetes, oocysts, and sporozoites. It has been observed, in accordance to previous published data[161], that heparin was able to specifically target ookinetes derived from the murine malaria parasite *P. berghei*. For parasite development to continue, ookinetes must find and adhere to membrane-associated ligands on the midgut epithelial surface, a pre-requisite for cell invasion. Clearly, negotiating the midgut tissue barrier in the vector is crucial for successful establishment of the parasite in the mosquito and hence, subsequent transmission to human hosts[163]. This fact suggests that glycosaminoglycans (such as heparin) might be adequate to target antimalarial-loaded PAA-based nanovectors to

Plasmodium mosquito stages, either through a direct entry into ookinetes or indirectly through delivery to pRBCs for those pRBCs that will later differentiate into gametocytes. For these reasons, we aim to target these mosquito stages in the future and explore the antimalarial activity of heparin-functionalized nanovectors.

As referred to previously, there are many heparin-related polysaccharides which present much lower anticoagulant action, namely CSA that lacks antimalarial activity but whose pRBC targeting capacity has not been described so far. In addition, one of the most malaria vulnerable groups are pregnant women, more specifically the ones expecting their first child, and this susceptibility has been attributed to the lack of antibodies capable of blocking the binding of *P. falciparum* to CSA in the placenta[219]. Through single molecule force spectroscopy assays we studied the binding forces between CSA and *P. falciparum* CSA binding line (CS2)-infected pRBCs or non-infected erythrocytes concluding that the polysaccharide interacts with pRBCs with binding forces around 32 and 51 pN, whereas it interacts with RBCs in a much smaller proportion (10 % comparing to 70% when using infected-RBCs) and with an average force of 33 pN. In a similar study, heparin proved to bind late stage *P. falciparum* parasites with a specific binding force in a range between 28 and 46 pN[40], very approximate to the values we obtained for CSA and CS2 parasites. After analyzing these data we suggest CSA can be used as a substitute of heparin regarding its targeting capacity and taking into account it lacks the anticoagulating adverse effect contrary to what happens with heparin.

Further investigation is needed in order to design a strategy balanced in terms of complexity, efficacy, and cost, necessary to obtain the simplest and cheapest system capable of significantly reducing or eliminating detectable parasitemia in people living in malaria-endemic regions.

In addition, we have observed that encapsulation of drugs in the PAA synthetic polymer AGMA1 resulted in nanoparticles entering the target cells and having a synergistic antimalarial effect by adding the activity of the polymer to that of the antimalarial, comparable to what happens by using heparin as a dual agent. PAAs were first tested for their ability to form polyelectrolyte stable complexes with heparin, in order to neutralize its anticoagulant activity[110,111], results later extended to PAA-crosslinked resins. Depending on their polymer content and formulation, these resins were able to incorporate from 30 to 100% w/w of heparin, without affecting other blood parameters[220]. We hypothesize that it would be a valuable approach to use heparin as a targeting molecule of such polymers in future nanotherapies, which on the one hand would result in a higher antimalarial activity and on the other hand would work as an alternative strategy to get rid of heparin's potent anticoagulant effect. Also, the binding between both molecules might be easily achieved through electrostatic bonds since they present opposite charges.

Currently available chemotherapeutic strategies against malaria rely on the use of antimalarial drug combination therapies. The concept of combination therapy is based on the synergistic or additive potential of two or more drugs, to improve therapeutic efficacy and also delay the development of resistance to the individual components of the combination[221]. In correlation to this concept, we investigated the application of two different antimalarial mechanisms simultaneously (**Figure 19**). One of our approaches was the use of heparin as a dual agent, on the one hand as an antimalarial drug itself and, on the other hand, as a targeting agent of PQ-containing liposomes. A second approach was to use sulfated polysaccharides derived from marine organisms that act as antimalarial drugs and also as vaccine adjuvants. These polysaccharides inhibit RBCs invasion by malaria parasites and, as a consequence, the pathogens encounter a prolonged exposure to the host immune system which might be applied to the design of new malaria vaccination strategies. Finally, we explored the use of liposomes (as drug nanocarriers) that contained in their formulation toxic lipids affecting the parasite growth and development (antimalarial action).

These promising synergistic effects, combining two different mechanisms of action, represent a radically new approach to the treatment and/or prophylaxis of malaria.

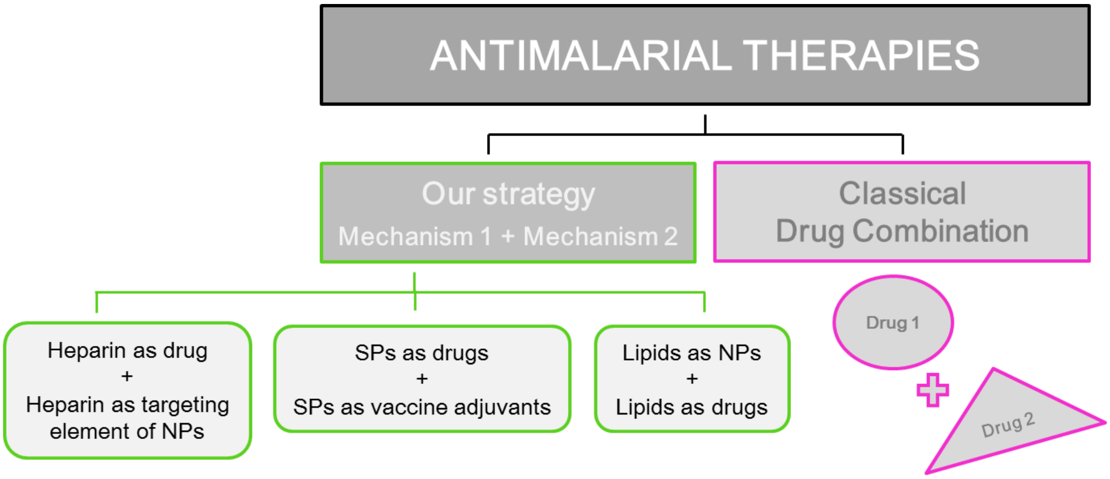
ANTIMALARIAL THERAPIES
Our strategy
Mechanism 1 + Mechanism 2
Classical
Drug Combination
Heparin as drug
+
Heparin as targeting element of NPs
SPs as drugs
+
SPs as vaccine adjuvants
Lipids as NPs
+
Lipids as drugs
Drug 1
Drug 2

Figure 19. Representative diagram of the different approaches addressed in this project (in green). SPs, sulfated polysaccharides; NPs, nanoparticles.

Future goals and prospects

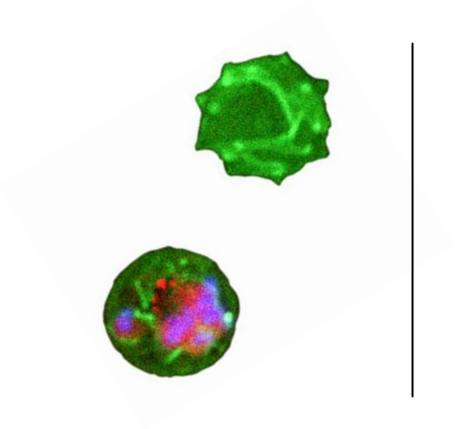

CONCLUSIONS

CONCLUSIONS

1. *In vitro P. falciparum* growth inhibition assays showed that free heparin from porcine intestinal mucosa (nominal molecular mass of 13 000 kDa) has antimalarial activity in a dose dependent manner with an IC50 ranging from 4 to 18 µg/mL, depending on the batch used. Most of the sulfated polysaccharides derived from marine organisms presented antimalarial activities similar to that of heparin with IC50 values between 2.3 and 20.3 µg/mL. The only exception was a glycan from *D. anchorata* whose IC50 was found to be relatively high (270 µg/mL).

2. All the sulfated polysaccharides included in this work showed relatively low hemolysis and low unspecific cytotoxicity for the studied concentration ranges. Sulfated polysaccharides from marine origin presented an antimalarial activity comparable to that of heparin but with a much smaller anticoagulant capacity, representing an interesting potential in future malaria therapies.

3. Our data revealed specific targeting ability of heparin to pRBCs whereas non-infected RBCs are not targeted by this polymer. The property of heparin to penetrate pRBCs and localize in a region adjacent to the parasite's DNA can be of use in the design of new cost-effective methods for the vehiculation of drugs to intracellular components of the pathogen.

4. An economically affordable molecule like heparin can be easily and rapidly conjugated to drug-containing liposomes, maintaining significant antimalarial activity and also pRBC targeting which contributes to lower the drug IC50. Heparin might be the spearhead of a new generation of GAG-related molecules exhibiting a synergistic activity as drug and nanocapsules targeting element.

5. The antimalarial activity of sulfated polysaccharides unfolds by inhibiting the pRBC invasion of *Plasmodium* merozoites. The consequence of a delayed invasion is a prolonged exposure of merozoites to the host immune system which might contribute to potentiate immune responses against the parasite. These sulfated polysaccharides act by performing a therapeutics role (as antimalarials) and a prophylactic one (as vaccine adjuvants).

6. Fluorescence microscopy assays showed that heparin possesses binding capacity to the apical surface of *P. berghei* ookinetes, which suggests that this natural polymer can be used as a specific targeting agent towards these *Plasmodium* transmission stages found in *Anopheles* mosquitoes.

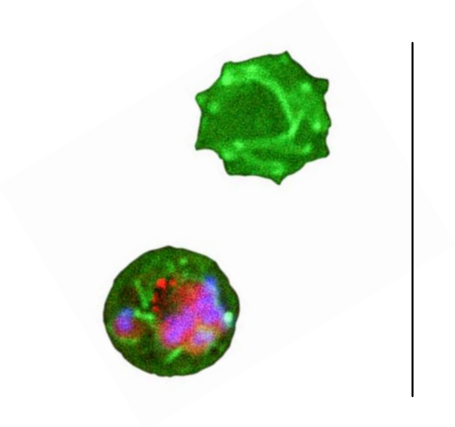

ANNEXES

ANNEXES

1. Review

Current Drug Targets 13 (2012) 1158-1172

“Nanotools for the delivery of antimicrobial peptides.”

Patricia Urbán, Juan José Valle-Delgado, Ernest Moles, Joana Marques, Cinta Díez, and Xavier Fernàndez-Busquets

2. Patent

“**Heparin-lipidic nanoparticle conjugates.**”

Inventors: Joana Marques, Ernest Moles, and Xavier Fernàndez-Busquets
Application number: 13152187.4-1453
Date of filing: 22/January/2013

3. Report by the Director

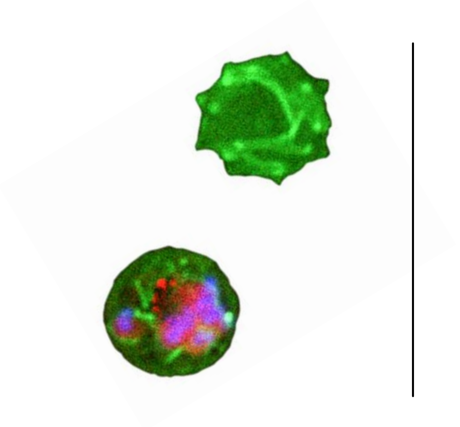

Annex 1

Current Drug Targets, 2012, *13*, 000-000 FINAL 1

Nanotools for the Delivery of Antimicrobial Peptides

Patricia Urbán[#], Juan José Valle-Delgado[#], Ernest Moles, Joana Marques, Cinta Díez and
Xavier Fernàndez-Busquets*

[1]*Nanobioengineering Group, Institute for Bioengineering of Catalonia, Baldiri Reixac 10-12, Barcelona E08028, Spain;* [2]*Barcelona Centre for International Health Research (CRESIB, Hospital Clínic-Universitat de Barcelona), Rosselló 149-153, Barcelona E08036, Spain;* [3]*Biomolecular Interactions Team, Nanoscience and Nanotechnology Institute (IN^{2}UB), University of Barcelona, Martí i Franquès 1, Barcelona E08028, Spain*

Abstract: Antimicrobial peptide drugs are increasingly attractive therapeutic agents as their roles in physiopathological processes are being unraveled and because the development of recombinant DNA technology has made them economically affordable in large amounts and high purity. However, due to lack of specificity regarding the target cells, difficulty in attaining them, or reduced half-lives, most current administration methods require high doses. On the other hand, reduced specificity of toxic drugs demands low concentrations to minimize undesirable side-effects, thus incurring the risk of having sublethal amounts which favour the appearance of resistant microbial strains. In this scenario, targeted delivery can fulfill the objective of achieving the intake of total quantities sufficiently low to be innocuous for the patient but that locally are high enough to be lethal for the infectious agent. One of the major advances in recent years has been the size reduction of drug carriers that have dimensions in the nanometer scale and thus are much smaller than —and capable of being internalized by— many types of cells. Among the different types of potential antimicrobial peptide-encapsulating structures reviewed here are liposomes, dendritic polymers, solid core nanoparticles, carbon nanotubes, and DNA cages. These nanoparticulate systems can be functionalized with a plethora of biomolecules providing specificity of binding to particular cell types or locations; as examples of these targeting elements we will present antibodies, DNA aptamers, cell-penetrating peptides, and carbohydrates. Multifunctional Trojan horse-like nanovessels can be engineered by choosing the adequate peptide content, encapsulating structure, and targeting moiety for each particular application.

Keywords: Antibodies, aptamers, dendrimers, liposomes, nanomedicine, nanoparticles, nanovectors, targeting.

ANTIMICROBIAL PEPTIDES

Some peptides are extremely potent *in vivo* antimicrobials that disrupt biological membranes or enter cells to interfere with pathogen metabolism [1]. Members of the cationic host defence peptide family are widely distributed in nature and vary substantially in their amino acid sequences, secondary structures, inducibility, potency, and activity spectra. In general, they have between 12 and 50 amino acids of which two to nine are positively charged lysine or arginine residues and as many as 50% are hydrophobic. Usually the peptides are expressed by innate immune cells as inactive propeptides that require cleavage by a protease. Although microbial and host structures share many components, antimicrobial polypeptides achieve specificity by exploiting differences between corresponding host and microbial structures, thus selectively concentrating themselves on microbial surfaces.

The mechanism of the direct antimicrobial activity of peptides is based on the folding of their processed, biologically active forms, into different secondary structures: amphipathic α-helices, β-hairpins, extended conformations, and cyclic species. Some of these structures fold after insertion into pathogen membranes such that the charged/polar and hydrophobic residues form patches on the surface of the cell, which in turn can lead to a rearrangement of the peptides to form one of four accepted models: barrel, carpet, toroidal pore, and aggregate. If this induces a substantial local perturbation of the lipid bilayer, cell membrane permeability is altered leading to cell death. An interesting example is that of the eosinophil cationic protein (ECP or RNase 3), a ribonuclease that is part of the human innate immune system [2], which has anti-pathogenic capabilities against viruses, bacteria [3], and protozoa [4, 5] and is involved in inflammatory processes mediated by eosinophils [6]. The antimicrobial activity of ECP has been associated primarily with its ability to disrupt membranes and it is dependent on both hydrophobic and cationic residues exposed on the surface of the protein [7]. ECP has been shown to partially insert into liposomes, promoting their aggregation and lysis according to a carpet-like mechanism [8].

Medicinal use of peptides has been often hampered by their rapid degradation by proteolytic enzymes in the gastrointestinal tract, which limits their administration to a parenteral route, although proteases in the bloodstream are also abundant. As a result, the biological half-life of peptides is short and demands frequent intake, whereas their transport across biological barriers is poor because of limited diffusivity and low partition coefficients. In the case of antimicrobial drugs it is essential to deliver sufficiently high local amounts

---

*Address correspondence to this author at the Nanomalaria Group, Centre Esther Koplowitz, 1st floor, CRESIB, Rosselló 149-153, Barcelona E08036, Spain; Tel: +34 93 227 5400 (ext 4276); Fax: + 34 93 403 7181;
E-mail: xfernandez_busquets@ub.edu

[#] *Both authors contributed equally*

1389-4501/12 $58.00+.00 © 2012 Bentham Science Publishers

to avoid creating resistant parasite strains [9], a common risk when using sustained low doses in order to limit the toxicity of the drug for the patient. In this context, nanoparticulate biodegradable systems have been proposed as an efficient means of peptide administration [10]. Rapidly increasing in the literature are reports on nanosized structures for the delivery of a number of therapeutic peptides, among which insulin, interferon, or the glycopeptide antibiotic vancomycin [11-15]. Here we will present an overview of nanoparticulate systems that can be applied to the targeted administration of antimicrobial peptides.

CONTROLLED DRUG DELIVERY

As stated in Paracelsus' Law of dose response, *There are no safe molecules nor toxic ones. It is the dose that makes the poison*. The challenge of antimicrobial drug delivery is the liberation of drug agents at the right time in a safe and reproducible manner, usually to a specific target site [16, 17]. Conventional dosage forms, such as orally administered pills and subcutaneous or intravenous injection, are the predominant administration routes, but they typically provide an immediate release. Consequently, to achieve therapeutic activity extending over time, the initial concentration of the drug in the body must be high, causing peaks (often adjusted to stay just below known levels of toxicity) that gradually diminish over time to an ineffective level. While the last three decades have seen considerable advances in drug delivery technology, major unmet needs remain. Among these are the broad categories of (i) continuous release of therapeutic agents over extended time periods and in accordance with a predetermined temporal profile [18, 19], (ii) targeted delivery at local sites to overcome systemic drug toxicity and ameliorate activity [20], and (iii) improved ease of administration, which would increase patient compliance while reducing the need for intervention by health care personnel and decreasing the length of hospital stays [21]. Success in addressing some or all of these challenges would lead to improvements in efficacy and limitation of side effects [22]. The potential therapeutic advantages of continuous-release antimicrobial drug delivery systems are significant and include minimized peak plasma levels, predictable and extended duration of action, and reduced inconvenience of frequent dosing [23, 24]. New drugs with ever increasing potency are being developed, many of them of peptidic nature and with a narrow therapeutic window (the concentration range outside the toxic regime where the drug is effective). Toxicity is observed for concentration spikes, which renders traditional methods of drug delivery ineffective [25]. In addition, conventional oral doses of these agents are frequently useless because the drugs are destroyed during intestinal transit or poorly absorbed. These limitations have fostered research in drug delivery systems providing a controlled release, which include transdermal patches, implants, inhalation systems, bioadhesive systems, and nanoencapsulation.

NANOVECTORS FOR TARGETED DRUG DELIVERY

The potential intersection between nanotechnology and the biological sciences is vast. The ability to assemble and study materials with nanoscale precision leads to opportunities in both basic biology (e.g., testing of biological hypotheses that require nanoscale manipulations) and development of new biomedical technologies such as drug delivery systems, imaging probes, or nanodevices [26-28]. It was Paul Ehrlich who popularized the *magic bullet* concept [29], according to which therapeutic agents would be directed specifically to destroy their diseased targets without harming any of the surrounding healthy cells. However, a century later the clinical implementation of this medical holy grail continues being a challenge in three main fronts [30]: identifying the right molecular or cellular targets for a particular disease, having a drug that is effective against it, and finding a strategy for the efficient delivery of sufficient amounts of the drug in an active state exclusively to the selected targets. This last requirement has to overcome the physiological mechanisms evolved to prevent the entry of alien structures into and clear them from the organism, namely physical barriers and the immune system. Nanovessels are one of the most promising structures being studied for their use in targeted drug delivery. Nanoparticulate systems are a miscellaneous family of submicron structures that can be inorganic, liposomal, polymeric, and even carbon nanotube-based. They are typically self-assembling and unable to self-replicate, and the main feature that makes them attractive drug carriers is their small size up to several hundred nm, which allows them to cross biological barriers. Since biological function depends heavily on units that have nanoscale dimensions, engineered devices at the nanoscale are small enough to interact directly with sub-cellular compartments and to probe intracellular events. Because many cells will internalize drug-loaded nanoscale particles, then nanoparticles can be used to deliver high drug doses into cells, and to release them in an environmentally controlled, temporally expanded profile. At the expense of lower drug loading capacity, the nanometer size range also reduces the risk of undesired clearance from the body through the liver or spleen and minimizes uptake by the reticuloendothelial system [31, 32]. Smaller particles have greater surface area/volume ratios, which increase dissolution rates, enabling them to overcome solubility-limited bioavailability [33]. Even within the nanoscale range, size variation strongly affects bioavailability and blood circulation time [34, 35]. Following systemic administration, particles below 10 nm are rapidly removed through extravasation and renal clearance [36] and those between 10 and 70 nm can penetrate even very small capillaries [37], whereas particles with diameters ranging from 70 to 200 nm show the most prolonged circulation times [34]. Larger particles are usually sequestered by the spleen and eventually removed by phagocytes [38].

A second essential characteristic of most nanoparticles is that their surface can be modified with appropriate molecules to dock them to specific target sites, and with camouflage elements designed to evade immune surveillance and to extend their blood residence time and half-life [39]. The most significant effect of functionalizing nanoparticles with targeting ligands is the increased intracellular uptake by target cells [40-42], which usually translates into a higher efficacy of encapsulated drugs [43]. Nanoparticles can also be modified to achieve efficient intracellular targeting to specific organelles: anionic particles usually remain in lysosomes whereas those positively charged become predominantly localized in the cytoplasm and within mitochondria [44].

Because of this combination of properties —subcellular size, controlled-release capability, and susceptibility to external activation— devices provided by nanotechnology will enable imminent new applications in biological and medical science [16, 45, 46].

TYPES OF NANOTOOLS FOR PEPTIDE TARGETED DELIVERY

As we have outlined above, several attempts have been made at delivering polypeptides as nanoparticulate systems. Proteins precipitated as spherical particles ranging in size from 100 to 500 nm were successfully prepared and used for aerosol delivery [47]. A biodegradable albumin core coated with fatty acids was assayed to encapsulate vancomycin for improved colon-specific release [13]. Administration of peptides inside biodegradable gelatin [12] or lipid nanoparticles has also been tested as a strategy to achieve a more efficient therapy through sustained release, e.g. for the administration of the antibiotic decapeptide polymyxin B [11]. Although these were successful approaches that represented an improvement when compared with the administration of free peptide, they had limited control over particle size and hardly any influence on the site of drug release at cell level. Here we are going to focus on encapsulation nanodevices of controlled dimensions and having the capability of being targeted to specific cell types or subcellular compartments.

Liposomes

Liposomes were first proposed as drug delivery vehicles by Gregoriadis in the 1970's [48]. They are self-assembling artificial lipid bilayer-bounded spheres up to several hundred nm in diameter, generally formed by amphiphilic phospholipids and cholesterol enclosing an aqueous inner cavity, and with a polar surface which can be neutral or charged. For drug delivery applications [49] liposomes are usually unilamellar and range in diameter from 50 to 200 nm, with larger liposomes being rapidly removed from the blood circulation. Encapsulation of hydrophobic or water-soluble drugs into, respectively, the bilayer or the hydrophilic core, can be done with a variety of loading strategies [50], which include the pH gradient [51] and ammonium sulfate [52] methods, and the direct drug entrapping simultaneously with liposome formation, or lipid film hydration [43]. Liposomes improve the delivery of bioactive molecules by functioning as circulating microreservoirs for sustained release because of their unique advantages which include the protection of drugs from degradation and the possibility of targeting them to the site of action and reducing their toxicity or side effects [53, 54]. The stability of the liposomal membrane, i.e., its mechanical strength as well as its function as a permeability barrier, depends on the packing of the hydrocarbon chains of lipid molecules. Neutral liposomes with tightly packed membranes exhibit increased drug retention and circulation half-life *in vivo*. The compact lipid asociation reduces binding of proteins which tend to destabilize the membrane and mark the liposomes for removal by phagocytic cells. The development of novel formulations with, e.g., polyethylene glycol (PEG) lipid derivatives resulted in sterically stabilized liposomes, termed stealth liposomes [55], with reduced mononuclear phagocyte system uptake and prolonged blood residence times [56, 57]. For conventional liposomes, circulation half-lives up to 12 h can be obtained, which are highly dependent on dose, whereas stealth liposomes have blood residence times above 24 h, with dose-independent clearance kinetics. Liposomes are naturally removed from the blood by resident macrophages mainly in the liver and spleen, an advantageous phenomenon when this cell type is the intended target, as is the case for many intracellular parasites localizing in phagocytic cells [50].

A drug carrier of clinical utility must be able to efficiently balance drug retention while in circulation with the ability to make the drug bioavailable at the disease site. Different liposome formulations provide passive control of drug release rates depending on lipid composition [50]. Active release, on the other hand, relies on a triggering mechanism to destabilize the liposomal bilayer once the drug reaches the pathogen. This can be a change in environmental factors encountered at disease sites such as a low pH or particular enzymes, or an external factor such as local heating or photochemical induction. Nanosized carriers have been receiving special attention with the aim of minimizing the side effects of malaria therapy by increasing bioavailability and selectivity of drugs [58]. Red blood cells (RBCs) have very poor endocytic processes, and for this reason liposomes docked by specific antibodies to RBCs can be an efficient system to deliver cargo into the cell by a simple membrane fusion process [43, 59-61], without the need for including fusogenic lipids in the liposome formulation. Many antibiotics are inactive against Gram-negative bacteria because of their inability to cross the outer membrane of these cells. Fusogenic liposomes have been used to localize vancomycin to the periplasmic space, showing an *in vitro* ability to inhibit to a certain extent the growth of Gram-negative bacterial strains when neither the free antibiotic nor vancomycin-loaded non-fusogenic liposomes had a significant antibacterial effect [62]. Liposomes encapsulating polymyxin B [63] have been proposed for the treatment of resistant Gram-negative bacterial infections due to the ability of the liposomal formulation to overcome the permeability and cell surface alterations responsible for the development of microbial resistance. When liposomal tobramycin or polymyxin B were tested against *Pseudomonas aeruginosa* in the cystic fibrosis sputum, the results obtained suggested their potential applications for the treatment of cystic fibrosis lung infections [64].

Liposomes bearing cell-specific recognition ligands on their surfaces have been widely considered as drug carriers in therapy due to their non-toxic and biodegradable character [65]. And yet, despite this versatility, major drawbacks to the use of liposomal nanocarriers in targeted drug delivery exist: limited control over release of the drug and thus potential leakage before reaching the target site, low encapsulation efficacy, relatively poor stability during storage, short *in vivo* circulation times, large size, and difficulty in formulation for oral administration. Most of these flaws can be overcome with the use of other types of nanocapsules.

Polymeric Structures

Polymers offer effectively unlimited diversity in chemistry, dimensions and topology, rendering them a class of materials that is particularly suitable for applications in nanoscale drug delivery systems [66]. Biodegradable polymeric nanoparticles are made of natural or artificial polymers and range in size between 10 and 1000 nm, and if adequately targeted they can be used to deliver highly localized drug doses into specific cell types or tissues [67]. Nanoparticles can carry drugs in adsorbed, dissolved, entrapped, encapsulated, or covalently bound form. Drug loading into nanoparticles is generally done by one of three methods: incorporation of the drug at the time of nanoparticle synthesis, absorption after nanoparticles formation by incubating these in a solution of the drug, or chemical conjugation of drugs into preformed nanoparticles. Drug release from nanoparticles is a process governed by either cleavage or desorption of surface-bound or adsorbed drugs, respectively, diffusion through the nanosphere matrix or nanocapsule polymer wall, or biodegradation resulting in nanoparticle disintegration in a particular physiological environment. Long-circulating polymeric nanoparticles have been obtained mainly by two methods: surface coating with hydrophilic polymers/surfactants and development of biodegradable copolymers with hydrophilic segments [68]. Some widely used coating materials are PEG, polyethylene oxide, poloxamer, polysorbate (e.g. Tween-80), and lauryl ethers (e.g. Brij-35). Methods for the preparation of surface-modified sterically stabilized particles are reviewed in the literature [68, 69]. Properties of the nanoparticles are largely dependent on the polymer employed, and biocompatibility issues are a main concern. Polycations are often cytotoxic, haemolytic, and complement-activating, whereas polyanions are less cytotoxic but can induce anticoagulant activity and cytokine release [70]. An ever increasing number of biocompatible polymer blocks are being used to synthesize polymeric nanoparticles, among them poly(D,L-lactide-co-glycolide) [71], poly(alkylcyanoacrylate) [72], chitosan [73-75], gelatin [12], poly(methylidene malonate) [76], starch [77], alginate [78], or polyethylene carbonate [79]. Hydrogels are an interesting type of polymeric nanoparticles formed by three-dimensional networks composed of ionic or neutral hydrophilic polymers physically and/or chemically crosslinked [80, 81], whose common characteristic is their ability to swell by imbibing large amounts of water. Physiologically responsive hydrogels can exhibit dramatic changes in volume, network structure, permeability, or mechanical strength in response to different stimuli like variations in pH, ionic strength or temperature. This special behavior has inspired the design of biocompatible drug delivery systems [80-83] where the encapsulated drug is usually released during the swelling of the hydrogel [84-87], although drug delivery as a result of a squeezing mechanism has also been reported [88].

In the case of biodegradable polymers, which decompose into products that can be completely eliminated by the body, significant advantages are their history of safe use, proven biocompatibility, a high surface/volume ratio, and ability to control the time and rate of polymer degradation and peptide release, thus increasing the half-life of bioactives [89]. The most promising degradable synthetic polymers used in biomedical applications are poly(hydroxyacid)s, poly(caprolactone)s, poly(ether-ester)s, poly(orthoester)s, poly(anhydride)s, poly(phosphazene)s, and poly(aminoacid)s. Biodegradable polymers containing entrapped drugs can be used for localized delivery and/or controlled release over a controlled release over a period of months. The release rates of drugs from biodegradable polymers can be controlled by a number of factors, such as biodegradation kinetics of the polymers, physicochemical properties of polymers and drugs, or thermodynamic compatibility between them. Hybrid polymer-based constructs have already shown that they can satisfy the requirements of industrial development and regulatory authority approval. Poly(amidoamine)s (PAAs), a family of biodegradable and biocompatible polymers, are promising materials for different pharmaceutical and biotechnological applications. They display membrane disruptive properties in response to a decrease in pH, conferring endosomolytic properties *in vitro* and *in vivo*, and are being studied as a synthetic alternative to fusogenic peptides as they display upon protonation at reduced pH conformational changes leading to membrane perturbation [90].

Some antimicrobial peptides have their targets in pathogens found inside the brain, such as the yeast *Cryptococcus neoformans* responsible for a form of meningitis [91]. Treatment in these cases is complicated by the poor penetration of most drugs across the blood-brain barrier (BBB). The BBB is formed by the tight endothelial cell junctions of the capillaries within the brain, which limits the ability of many molecules to enter the central nervous system (CNS). Surface-modified polymeric nanoparticles able to cross the BBB have been used to deliver chemicals acting on the CNS [92], and promising results have been obtained using such *Trojan horse* nanocapsules [93, 94]. The mechanism of enhancement of drug transport from the coated nanoparticles through the BBB is thought to be due to [68] (i) binding of the nanoparticles to the endothelium of brain capillaries and delivery of drugs to the brain by providing a large concentration gradient which enhances passive diffusion, and/or (ii) brain endothelial uptake by phagocytosis.

Dendritic Polymers

Dendrimers are a type of polymeric nanoparticles having definite molecular mass, shape, and size, formed by synthetic, highly branched, monodisperse macromolecules [95-97]. They possess three distinguishing architectural components, namely an initiator core, an interior layer radially attached to the initiator and composed of repeating units added in successive synthetic generations, and an outer functionalized layer bound to the outermost interior generation. The core is sometimes denoted generation zero (G0); the core for a polypropylene imine (PPI) dendrimer is 1,4-diaminobutane, whereas for a PAA dendrimer is ammonia. This type of architecture induces the formation of nanocavities, the environment of which determines their encapsulating properties, whereas the external groups primarily define solubility and chemical behavior. Hyperbranched polymers (Fig. **1**) are nonsymmetrical, polydisperse, and less expensive than dendrimers, which are prepared under tedious multistep reaction schemes [96]. Dendrimeric and hyperbranched polymers are called collectively dendritic polymers.

Dendritic polymers have a vacant inner core that can encapsulate drug molecules [98-101], often with high drug payloads [102]. Dendrimers are, despite their relatively large molecular size, structurally well defined, with a low polydis-

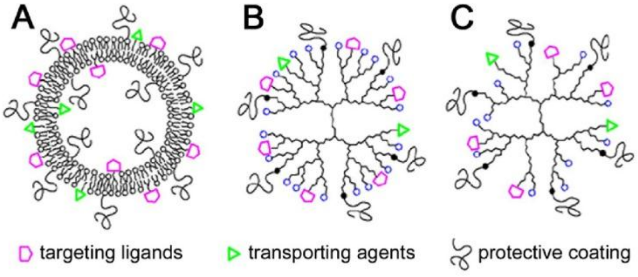

Fig. (1). Schematic representation of multifunctional (**A**) liposomal, (**B**) dendrimeric, and (**C**) hyperbranched polymeric systems. From the National Center of Scientific Research "Demokritos", Greece, web site (http://ipc.chem.demokritos.gr).

branched dendrimers such as PAA have been extensively studied for their biocompatible and non-immunogenic properties and for their ability to cross cell membranes with minimal perturbation [103]. Dendrimers of a sufficiently small size can be internalized by cells [104, 105], an attractive characteristic for drug delivery applications. Investigations using cationic and anionic PAA dendrimers in the size range 3-7 nm revealed that their uptake in everted rat intestinal systems most likely occurs across enterocytes by transcytosis [106]. Dendrimers protect their encapsulated drugs from fast degradation in the physiological environment and offer a continuous and temporally expanded release. In contrast to proteins, which consist of folded, linear polypeptide chains, the branched architecture of the dendrimer interior is to a large extent formed by covalent bonds, resulting in a somewhat less flexible structure. In addition, the dendrimer is on average less compact than a protein, and it contains a substantially higher number of surface functional groups than proteins of comparable molecular mass. However, polypeptide dendrimers have been synthesized [107], and glycoconjugated peptide dendrimers have been successfully assayed to encapsulate the antimalarial drugs chloroquine [108] and primaquine [109].

One of the advantages of dendrimers is the possibility of modulating their properties through modification of their large surface area [110]. This surface modification can be used for the covalent attachment of drugs, or to functionalize the dendrimer with targeting molecules such as cell penetrating peptides, carbohydrates [111], or antimicrobial peptides [112]. The multivalency of their surface provides a tighter binding than the low affinity of single ligands [100]. However, in spite of their broad applicability, associated toxicity due to the terminal amino groups and cationic charge of PAA and PPI dendrimers hampers their clinical applications [109]. One approach to improve dendrimer biocompatibility contemplates surface modifications [113], including capping of the terminal $-NH_2$ groups with neutral or anionic moieties such as PEG. It has been found that amino-terminated PAA dendrimers and their partially PEG-coated derivatives possess attractive antimicrobial properties, particularly against Gram-negative bacteria [114, 115]. Partial modification of amino-terminated PAA with PEG did not reduce toxicity to *P. aeruginosa*, while it greatly reduced toxicity to epithelial cells. Furthermore, G4-PAA-OH dendrimers have shown bactericidal effect and ability to treat *Escherichia coli* infections *in vivo* in pregnant guinea pigs. The G4-PAA-NH_2 dendrimer, known to be a potent antibacterial agent, was found to be highly cytotoxic in the μg/mL range whereas the G4-PAA-OH dendrimer was non-cytotoxic up to 1 mg/mL. This phenomenon could be attributed to the different interaction of G4-PAA-OH and G4-PAA-NH_2 with bacterial membranes [116].

Solid Core Nanoparticles

The term nanoparticle is a collective name for both nanospheres and nanocapsules. Nanospheres are dense polymeric matrices in which the drug may be dispersed within the particle or adsorbed on the sphere surface, whereas nanocapsules present a polymeric shell surrounding a liquid core where the active substances are usually dissolved, although they may also be adsorbed on the capsule surface. A common approach among nanobiosystem development is building around a core nanoparticle whose material offers good properties regarding stability and/or detection [27, 117]. One of the most extensively explored core nanoparticle material is metals, with gold, silver, iron, cobalt, nickel, platinum, and various metal composite nanoparticles being currently studied [118]. A particularly interesting characteristic of solid core nanocapsules is that they can combine different properties in individual particles, based on different compositions of the core and the shell. The core can be built to have a useful physical property (e.g. semiconductors, metals, magnetic oxides) that can make the nanoparticle responsive to mild external signals (such as light, ultrasounds, or magnetic fields) so that the movement of the particles could be directed from outside the body, or the particles could be activated at particular sites [119-121]. Liposomes can be combined with a large variety of nanomaterials, such as mesoporous silica nanoparticles [122] or superparamagnetic iron oxide nanocores. Because the unique features of both the magnetizable colloid and the versatile lipid bilayer can be joined, the resulting so-called magnetoliposomes [123] can be exploited in a great array of biotechnological and biomedical applications, including magnetic resonance imaging, hyperthermia cancer treatment and drug delivery.

The shell of solid core nanoparticles can be used to functionalize the nanoparticle with targeting molecules in order to direct it to the desired location in drug delivery applications. Gold colloids have been postulated as promising candidates in nanomedicine due to their bioinertness, cellular imaging ability, and presumed nontoxicity [124], and they have even been proposed for the delivery of drugs inside the brain [125]. In addition, conjugation to gold surfaces is readily performed for thiol-containing molecules in aqueous buffers. However, recent data have shown that in a human keratinocyte cell line gold nanoparticles induced changes in cellular morphology, mitochondrial function, mitochondrial membrane potential, intracellular calcium levels, DNA damage-related gene expression, and of p53 and caspase-3 expression levels [126]. Although metallic nanoparticles provide stability and enhanced detection capabilities of the nanobiosystem, some metals are toxic in elemental form. Nanotoxicology is an embryonic field and the dynamics and toxicity of these nanomaterials *in vivo* are not well understood at this time [27, 127]. Toxicity of nanomaterials is difficult to evaluate with the masking presence of hydrophilic coatings used to make these nanostructures biocompatible. Toxicity may well vary with nanoparticle size, and it could increase on an expanded timescale if the biocoatings are removed once inside the cell. Because the toxicity of metallic nanoparticles remains a largely unresolved issue, other biodegradable nanobiosystems threaten their development.

Carbon Nanotubes

Carbon nanotubes (CNT) are cylinders of 10-100 nm in diameter and up to several hundred microns in length, whose walls are formed by one (single-walled CNTs) or several (multi-walled CNTs) rolled-up graphene sheets [128]. Although CNT are insoluble in physiological conditions, the development of efficient methodologies for chemical modifications which increase solubility in aqueous environment has stimulated their application as drug delivery vessels. CNTs can be derivatized with bioactive peptides, proteins, nucleic acids and drugs, and used to deliver their cargoes to cells and organs [129, 130]. Because functionalized CNTs display low toxicity and immunogenicity and have a high propensity to cross cell membranes, they hold great potential as nanocarriers in biomedical applications [128, 131], particularly as vehicles for the delivery of small drug molecules [132-134]. Molecular dynamics simulation studies have been used to explore the chemical and physical interactions between model peptides and carbon nanotubes (Fig. **2**), showing that upon encapsulation peptides remain close to their native conformations [135]. Peptides were detected interacting with the outer walls of nanotubes, encapsulated into, and covalently bound to them. The results suggested that the confined space of the nanotube and its interaction with peptides stabilizes their structure, whereas covalent crosslinking to carbon nanotubes may lead to a change in the peptide conformation. No significant conformation changes were detected for peptides interacting non-covalently with nanotube outer walls.

However, as in the case of metallic nanoparticles, an important issue regarding the applicability of CNTs for antimicrobial peptide delivery is their biocompatibility. Actually, CNTs are not biodegradable at all, and the modification of their surface polarity by the introduction of charged groups results in better solubility but not in better biodegradability [136].

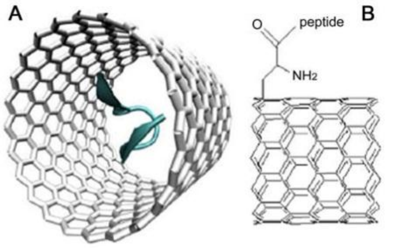

Fig. (2). Schematic representation of a beta-hairpin peptide (A) encapsulated in and (B) covalently linked to the outer wall of a carbon nanotube. From [135], with permission.

DNA Cages

The biological function, nanoscale geometry, low toxicity, biodegradability, and molecular recognition capacity of DNA make it a promising candidate as novel functional nanomaterial [137]. In particular, 3D DNA materials have tremendous potential applications in drug delivery systems. The so-called DNA *origami* technique has been applied to the construction of 3D boxes with controllable lids [138], where six DNA origami faces were designed to assemble into a hollow 3D box. The lid of the box was dynamically opened and closed by introducing *key* oligonucleotide sequences that displaced DNA duplexes holding the lid closed. Opening the box lid could be observed by changes in fluorescence resonance energy transfer between two fluorescent dyes placed on the DNA structure at strategic locations. Cage-like large three-dimensional structures made of DNA molecules have been successfully self-assembled from three different types of single-stranded DNA [139]. The three DNAs spontaneously formed three-point-star motifs, or tiles, that then progressed to polyhedral shapes in a one-pot process. By controlling the flexibility and concentration of the tiles, the molecular assembly yielded tetrahedra, dodecahedra, or buckyballs tens of nanometers across and having pores up to 20 nm (Fig. **3**). These two examples of DNA nanocages could be developed into carriers for controlled drug release.

Pharmacokinetics and Biodistribution of Nanoparticles

As discussed above for liposomes, a number of factors can influence nanoparticle blood residence time and organ-specific accumulation, which include interactions with biological barriers and nanoparticle composition, size, and surface modifications [140]. As a rule of thumb, reduction in the rate of mononuclear phagocyte system uptake and prolongation of the blood circulation half-life will be maximal for neutrally charged nanoparticles with a mean diameter of ca. 100 nm and surface-modified with PEG [141]. Interestingly, worm-shaped nanoparticles composed of a diblock copolymer circulate in the mouse blood with a very long

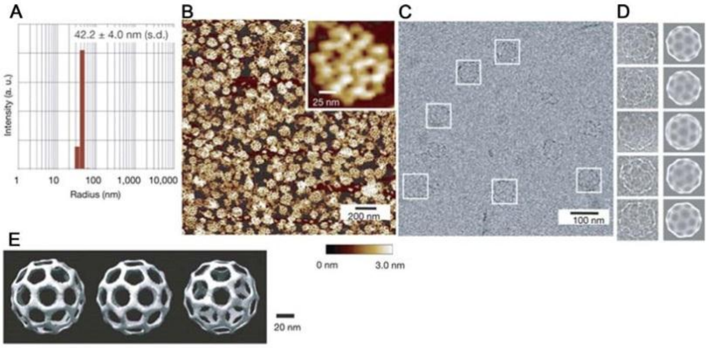

Fig. (3). A DNA cage. (**A**) Size histogram of the DNA buckyball measured by dynamic light scattering. (**B**) An AFM image and (**C**) a cryo-EM image of the DNA assemblies. (**D**) Individual raw cryo-EM images and the corresponding projections of the DNA buckyball 3D structure reconstructed from cryo-EM images. These particles are selected from different image frames to represent views at different orientations. (**E**) Three views of the DNA buckyball structure reconstructed from cryo-EM images. From [139], with permission.

half-life of ca. 5 days [142]. The underlying mechanism seems to be the strong drag force experienced in the fluid flow by the elongated structures such that the macrophages can not engulf them before they are carried away by the flow. Finally, to have pharmacological efficacy, the encapsulated antimicrobial peptide must be released from the nanovectors to the target cells. One strategy can make use of some type of local triggering mechanism to release the drug, such as pH [143]. Different organs, tissues, and subcellular compartments, as well as their pathophysiological states, can be characterized by their pH levels and gradients. Nanovessels can be designed to respond with physicochemical changes in their structure to such pH stimuli. These include swelling, dissociating, or surface charge switching, in a manner that favors drug release at the target sites. A second approach to increase the rate of intracellular delivery contemplates conjugating a targeting ligand on the nanovector surface.

TARGETING MOLECULES

In general, transport across biological barriers is determined by both the nature of carrier molecules such as size, charge, hydrophobicity, flexibility, and geometry, and the characteristics of the barrier itself such as location, function, and permeability. Mechanisms of uptake through the gastrointestinal tract include persorption, endocytosis by enterocytes, paracellular transport, uptake by intestinal macrophages, and passage through the gut-associated lymphoid tissue [144]. Oral delivery of drugs remains the most attractive mode of administration, but bioavailability of oral drugs is low due to the harsh grastrointestinal tract environment. A number of proposed microscale oral delivery devices have been based on the sequestering of the nanoparticles from the external environment [145-149]. Chitosan-containing particles, if smaller than 500 nm, have a greater capacity of being taken up in their original state through intercellular spaces between the enterocytes and M cells lining the Peyer's patches [150], and nanoparticles composed of mucoadhesive polymers have been proposed for oral delivery of peptide drugs [74]. Particles of size ranges up to 1000 nm can penetrate the intestinal mucosa within 30 to 60 min, and have been successfully assayed for the oral delivery of insulin [15, 148, 151]. However, unlike drug molecules, nanoparticles face additional delivery barriers even after systemic absorption, for instance in avoiding clearance by the reticuloendothelial system and overcoming intracellular barriers.

Active targeting of nanoparticles to the specific sites where pathogens are can be achieved by conjugating them to ligands which interact selectively with receptors present on the target cells. Biological molecules can be immobilized on nanoparticles through a variety of strategies that include physical adsorption, electrostatic binding, specific recognition, and covalent coupling [39]. Although any ligand specifically interacting with the intended delivery site can be used as targeting agent, here we will focus on the three types of biomacromolecules which carry specific binding information in their sequences and/or structures, namely proteins, nucleic acids, and polysaccharides.

Antibodies

The capacity of antibodies to recognize with high specificity virtually any new antigen with which they are presented has been long recognized as a useful tool for the targeting of drugs in therapeutic applications, especially in the case of monoclonal antibodies [152]. Monoclonal antibodies are biological products made in the laboratory that share with antisera made in animals the problem of immunogenicity: targeting antibodies are foreign proteins and elicit an immune response when injected into patients. Antibody engineering has provided a number of strategies to produce antibody forms that are sufficiently small or similar to human antibodies to be nonimmunogenic [153]. The simplest approach is to dispense with the protein domains that are not essential to antigen binding. Antibody fragments, such as antigen binding (Fab) and variable (Fv) region fragments retain the antigen-binding site, with much of the immunogenic protein removed. Other antibody subunits are minibodies, diabodies, and nanobodies [117]: minibodies are engineered to contain a fusion of single-chain Fv (scFv) and a C_H3 domain that self assembles into a bivalent dimer [154]; diabodies are covalently or non-covalently linked scFv dimers [155]; nanobodies, which are the smallest of all fully functional antigen-binding fragments, evolved from the variable domain of antibody heavy chains [156]. More recently, small antibody mimetics were formulated by fusing two complementarity-determining regions that retained the antigen recognition of their parent molecules [157]. These 3-kDa entities showed better biodistribution than the original antibodies, suggesting their potential as a new class of targeting ligands. The smaller size of antibody fragments makes them good elements for the targeting of nanovectors expected to diffuse rapidly into tissues and cells, although their single binding site might lead to a weaker interaction with the antigen.

Whatever the type of targeting antibody used, reducing its amount will contribute to minimizing the risk of triggering immune responses leading to nanovector elimination. A fast and efficient strategy for the covalent crosslinking of nanoparticles to antibodies involves the generation of half-antibodies (Fig. **4**), which allows the binding through thiol groups in the hinge regions of immunoglobulin heavy chains [158]. This represents an improvement over the most generally used method for the covalent immobilization of antibody molecules through free amino groups [159], which has the risk of chemically modifying functionally important amino groups in the antigen-binding region of an antibody, causing impairment or loss of function. The resulting significant amount of defective antibody conjugates demands using higher antibody concentrations that will increase the risk of detection by the immune system of the host. An alternative strategy for the oriented immobilization of antibodies is the preparation of immunoconjugates using the oligosaccharide moieties in the antibody Fc region [160].

Immunogenicity is not the only problem encountered when using antibodies for therapy [152]. Some of the biological effects of antibodies are inconvenient in a therapeutic setting, such as the cytokine release reaction triggering a cascade of immunological effects, although such reactions generally depend on crosslinking and are therefore not seen with Fab or Fv fragments.

Antibodies are difficult to formulate for oral administration, which will likely require smaller (but equally 100% specific) targeting agents and drug-containing structures. Orally administered antibodies have been described to be biologically active but only at a local level in the intestinal mucosa [161]. To facilitate intestinal intake, antibodies can be engineered as discussed above to obtain the smallest region preserving an active antigen binding site, still able to carry nanovectors to target cells. Besides their large size,

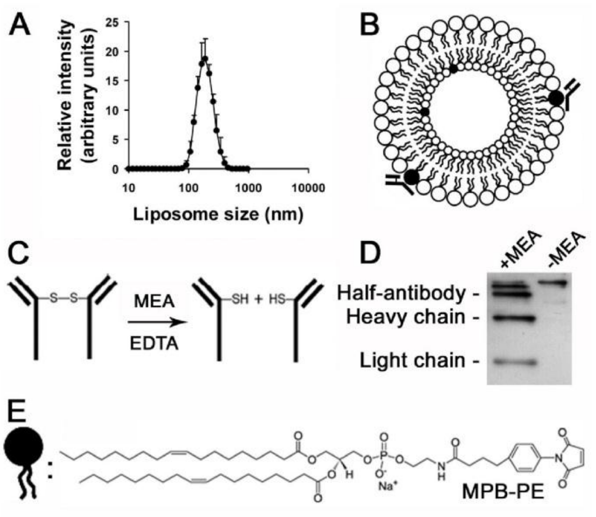

Fig. (4). Preparation of immunoliposomes. (**A**) Dynamic light scattering analysis of liposome size distribution. (**B**) Cartoon showing a liposome functionalized with half-antibodies bound to the thiol-reacting lipid 1,2-dipalmitoyl-sn-glycero-3-phosphoethanolamine-N-[4-(p-maleimidophenyl)butyramide] (MPB-PE), represented as black lipid molecules. (**C**) Scheme of the generation of half-antibodies through reduction with mercaptoethylamine (modified from Pierce Biotechnology catalog). (**D**) Western blot analysis of anti-glycophorin A IgGs (right lane) before and (left lane) after mercaptoethylamine treatment. (**E**) Structure of MPB-PE (extracted from Avanti Lipids catalog), represented as black lipid molecules in panel (**B**). From [43], with permission.

they are relatively expensive to manufacture and their batch-to-batch variability.

Nucleic Acid Structures: DNA Aptamers

Most current methods addressed to the identification of molecular targets that could be used in antimicrobial drug delivery strategies rely on lengthy and costly approaches. These include detailed knowledge of the microbe's physiology and biochemistry or the development of immunological methods such as polyclonal and/or monoclonal antibody generation. However, binding specificities and affinities comparable to those of monoclonal antibodies can be obtained with short nucleic acids or peptides termed aptamers [162], much faster and cheaper to produce. DNA aptamers are small oligonucleotides that fold through intra-molecular interactions into unique conformations with ligand binding characteristics. Aptamers can bind to targets with high sensitivity and specificity, being able to distinguish between protein isoforms and different conformational forms of the same protein. Among their advantages as targeting ligands are a small size of up to ca. 15 kDa and a relatively low immunogenicity which leads to better biodistribution [117]. Aptamers can be identified by *in vitro* selection against almost any target, including toxins and antigens which do not induce immune responses for antibody production in host animals. As a result, this novel class of ligands is highly promising for the development of therapeutics and biotechnological tools. DNA oligomers can be identified that bind to biomarkers expressed only by target cells, e.g. cell surface epitopes that differ between two given cell types or between healthy and diseased cells. The potential utility of aptamers for *in vivo* applications and as therapeutic agents is considerably enhanced by the possibility to introduce chemical modifications that lend resistance to nuclease attack. Moreover, aptamers isolated from combinatorial libraries have low dissociation constants, ranging from nanomolar to femtomolar, similar to the best affinities of interactions between monoclonal antibodies and antigens. Aptamers are not only promising for therapy but also for clinical diagnosis: like antibodies, aptamers can be easily tagged with fluorescent reporters or nanoparticles for localization or pull-down experiments of target proteins. Nucleic acid aptamers can modulate the function of virtually any target of biological interest, making them a preferred method of choice for the identification of new bioactive ligands against essential pathogen targets.

The primary approach to obtain DNA aptamers is using Systematic Evolution of Ligands by EXponential enrichment (SELEX) technique [163, 164]. This procedure starts with a large pool of nucleic acid sequences (typically $\geq 10^{13}$), with fixed regions on either end and a randomized central sequence (commonly approximately 30-60 nucleotides). This DNA library is incubated with the ligand of interest, and oligonucleotides that bind it are isolated. These sequences are then amplified and the enriched nucleic acid pool is subjected to another round of binding and selection, repeating the cycle 6-12 times with increasingly stringent conditions until an aptamer (or set of aptamers) is discovered that binds the ligand with the desired specificity and affinity. The SELEX drawbacks of time requirement, relatively low-throughput nature of the counter-selection process and the necessity of cloning and sequencing have stimulated the appearance of microarray-based systems [165]. In this method, each feature of a microarray contains thousands to millions of a unique aptamer sequence. The microarray is overlaid with a solution of the ligand, whose binding after several stringency washes is detected fluorescently, e.g. with a labeled antibody.

Peptides

Cell adhesive proteins like fibronectin, collagen or laminin have been applied to coat biomaterials in order to ensure an adequate interaction with target cells, but the use of proteins has some important inconveniences for biomedical applications, such as a significant immunogenicity, which could be overcome with the use of small peptides as cell recognition motifs. The RGD sequence (R: arginine; G: glycine; D: aspartic acid) is the most widely employed cell adhesion motif. Different strategies for the immobilization of RGD peptides on polymers have been developed and RGD-functionalized polymers have been evaluated *in vitro* in order to test their effectiveness for cell adhesion, their influence on cell behaviour and their applicability for medical use [166].

Cell-penetrating peptides (CPPs) are interesting targeting agents for nanoparticle functionalization due to their ability to translocate across cellular membranes [167] *via* a mechanism independent of transporters and receptor-mediated endocytosis. CPPs are cationic or amphipathic sequences of, typically, up to 30 amino acids. Some of them are reviewed in [168]: the HIV-1-encoded nuclear trans-activating transcriptor (TAT) peptide YGRKKRRQRRR [169] and the regulator of virion expression Rep peptide TRQARR NRRRRWRERQR, the *Drosophila* Antennapedia protein-derived RQIKIYFQNRRMKWKK, the flock house virus coat-derived RRRRNRTRRNRRRVR, and small oligoarginine and oligolysine. Amphipathic CPPs have mainly lysine residues and a homogeneous content of hydrophobic and hydrophilic amino acids, and present an α-helical structure content as in the model amphipathic peptide MAP, KLALK-LALKALKAALKLA [170]. Proline-rich CPPs such as Sweet Arrow Peptide (SAP), $(VRLPPP)_3$, are water-soluble, non-toxic peptides that also have the property of crossing lipid bilayers with high efficacy [171]. As mentioned above, a common limitation of the therapeutic use of peptides is their metabolic instability. In this regard, the use of all-D-peptide derivatives has been proposed as a strategy to obtain longer half-lives [172].

Functionalization with any of these peptides could represent a strategy to carry small drug-loaded nanoparticles through biological membranes [168, 173]. A potent cytotoxic peptide (R_7-KLA) was synthesized by joining a mitochondrial membrane disrupting peptide, KLA (KLAK-LAKKLAKLAK), with a cell-penetrating domain, R_7 (RRRRRRR) [174]. The IC_{50} of R_7-KLA (3.54 ± 0.11 μM) was more than two orders of magnitude lower than that of KLA. R_7-KLA induced cell death both *in vitro* and *in vivo*, and showed rapid kinetics. Pharmaceutical carriers like liposomes and nanoparticles have also been modified with CPPs to increase their cellular uptake [175]. Although, as we have seen above, these vessels provide protection to their payload and improve drug properties such as solubility, their size might hamper in some cases membrane trespassing. However, nanoparticles and liposomes can be functionalized with a higher amount of CPP per particle, and this surface density has been shown to affect the degree of cell entry and also the internalization pathway [176, 177]: low density of octaarginine on liposomes results in clathrin-mediated endocytosis, whereas a higher density results in macropinocytosis. Some reports suggest the existence of cell uptake *via* endocytic pathways for liposomal [178] and for cationic polymer-based TAT conjugates [179].

Interestingly, cationic CPPs contain clusters of arginine and lysine residues which make them very similar to antimicrobial peptides, suggesting that peptidic nanoparticles could be synthesized having both activities. A novel class of core-shell nanoparticles formed by the self-assembly of an amphiphilic peptide have been shown to have strong antimicrobial properties against a range of bacteria, yeasts and fungi [180]. These nanoparticles showed a high therapeutic index against *Staphylococcus aureus* infection in mice and were more potent than their unassembled peptide counterparts, being able to cross the BBB and suppress bacterial growth in infected brains. In another recent report, cholesterol-conjugated G_3R_6TAT, which contains the TAT sequence, formed self-assembled cationic nanoparticles which demonstrated strong *in vitro* activity against various types of microbes [91]. Biodistribution studies in rabbits revealed that fluorescently labeled peptide nanoparticles were also able to cross the BBB. The combined use of peptides and nanotechnology offers tremendous hope in the treatment of brain disorders [181].

Some peptides, despite not being *bona fide* cell penetrating, can virtually act as such in certain situations. Tuftsin is a natural macrophage activator tetrapeptide (TKPR) which is a part of the Fc portion of the IgG antibody heavy chain. The peptide is known to bind specifically to macrophages, potentiating phagocytosis, pinocytosis, motility, immunogenic response, and bactericidal activity [182]. The inherent tendency of liposomes to concentrate in the mononuclear phagocyte system can be exploited by encapsulating in them antibiotics against intracellular infections that reside in macrophages, e.g. leishmaniasis. This activity can be further enhanced by functionalizing the liposomes with ligands such as tuftsin, which besides binding specifically to phagocytes also enhances their natural killer activity [183].

Carbohydrates

Carbohydrates are emerging as highly versatile adhesion molecules due to the extraordinary plasticity of glycan chains, the low affinity and reversibility of individual binding sites, and the *cluster effect*, i.e. the capacity to form multivalent complexes leading to increased association forces [184]. Individual carbohydrate-mediated interactions are among the weakest biomolecular binding events and, to generate sufficient affinity, glycoconjugates tend to display polyvalent configurations. Glycoproteins and proteoglycans present repetitive epitopes on their carbohydrate chains, whereas glycosphingolipids are associated in clusters or patches. Carbohydrates are ideal for generating compact units with explicit informational properties, since the permutations on linkages are larger than can be achieved by amino acids or nucleotides [185]. The structural diversity of carbohydrates underlies the potential of this class of biomolecules for storing biological information. The resulting high-density coding capacity of oligosaccharides is established by variability in (i) anomeric status, (ii) linkage positions, (iii) ring size, (iv) branching, and (v) introduction of site-specific substitutions [186]. Recognition of carbohydrates by proteins has been shown to be central to a myriad of intra- and extracellular physiological and pathological processes [187], and thus carbohydrate-mediated targeted delivery of drugs is a promising new avenue just being opened. Numerous studies have shown that glycosylated dendrimers are good mimics of natural glycoconjugates and will interact efficiently with natural carbohydrate receptors, in many cases to an extent that allows competition with natural binding substances [100]. PAA dendrimers are easily modified with peptides and carbohydrates [111]. Galactose coating of poly-L-lysine formulations reduced 5 times phagocytosis by macrophages of dendrimers loaded with the antimalarial drug chloroquine [108]. Galactose coating of dendrimers drastically reduced their haemolytic activity and immunogenicity, has been shown to increase drug entrapment efficacy several fold depending upon generations, and extended the release period up to 3 times [109].

RBCs infected with the mature stages of the malaria parasite, *Plasmodium falciparum*, bind to the endothelial cells of capillaries and post-capillary venules of deep tissues such as the brain, heart, lung, and small intestine in a phenomenon called sequestration. Multiple receptors, including both proteins and carbohydrates, are known to be involved in this sequestration process which is thought to play a major role in the fatal outcome of severe malaria [188, 189], and the capacity of wild-type isolates of *Plasmodium*-infected RBCs (pRBCs) to bind glycosaminoglycans (GAGs) has been identified as a marker for severe disease. The sequestration of pRBCs is suggested to be mediated by *P. falciparum* erythrocyte membrane protein 1 (PfEMP1), a parasite-derived polypeptide expressed at the surface of the pRBC. Lectinlike interactions of PfEMP1 have been described with GAGs such as heparin [190] and heparan sulfate (HS) [191]. The GAG chondroitin 4-sulfate (CSA) has been found to act as a receptor for pRBC binding in the microvasculature [192] and the placenta [193, 194], and adhesion of *P. falciparum*-infected erythrocytes to placental CSA has been linked to the severe disease outcome of pregnancy-associated malaria [195]. Heparin and HS have also been implicated in the sporozoite attachment to hepatocytes mediated by the circumsporozoite protein that targets the liver for infection in the first step of developing malaria [196], and interactions with heparin-like molecules have been described during erythrocyte invasion by *P. falciparum* merozoites [197]. Thus, GAGs might be interesting candidates as targeting agents to direct antimicrobial peptide-carrying nanocapsules towards different stages of the malaria parasite.

MULTIFUNCTIONAL NANOVECTORS

Currently used pharmaceutical nanocarriers have a broad variety of useful properties, such as longevity in the blood, specific targeting to certain disease sites due to various targeting ligands attached to their surface, enhanced intracellular penetration with the help of bound cell-penetrating molecules, and ease of tracking by loading the carrier with various available contrast agents that can even permit *in vivo* visualization. The engineering of multifunctional pharmaceutical nanocarriers combining several of these characteristics in one particle can significantly enhance the efficacy of many therapeutic and diagnostic protocols [39, 100, 101, 198]. It is also possible to combine different types of nanocapsules into a composite structure, in a kind of *Russian doll* assembly at the molecular level. Many novel materials are being developed in nanotechnology laboratories that often require methodologies to enhance their compatibility with the biological milieu *in vitro* and *in vivo*. One such system could consist of a liposome encapsulating polymeric nanoparticles: liposomes are structurally suitable to make nanoparticles biocompatible and offer a clinically proven, versatile platform for the further enhancement of pharmacological efficacy. Although liposomes have a decade-long clinical presence as nanoscale delivery systems of encapsulated drugs, their use as delivery systems of nanoparticles is still in the preclinical development stages [199, 200]. However, parenterally administered liposome-nanoparticle hybrid constructs present great opportunities in terms of nanoscale delivery system engineering for combinatory therapeutic-imaging modalities.

A striking example of multicomponent nanovessels are porous nanoparticle-supported lipid bilayers termed protocells, which synergistically combine properties of liposomes and nanoporous particles [122]. Protocells can be loaded with combinations of therapeutic and diagnostic agents and modified to promote endosomal escape and nuclear accumulation of selected cargos. The enormous capacity of the nanoporous core combined with the enhanced targeting efficacy enabled by the fluid supported lipid bilayer allowed a *single* protocell loaded with a drug cocktail to kill a human hepatocellular carcinoma cell, representing a 10^6-fold improvement over classical drug-loaded liposomes of similar size. The foreseeable applications of protocell-like structures to the targeted delivery of antimicrobial peptides are obvious.

Once a nanovector prototype is assembled, its different parts can be exchanged by new elements to adapt to new parasite strains or to be used against entirely different microbes. In such LEGO-like structures better targeting molecules can easily substitute for those made obsolete by the disappearance of formerly exposed antigens, or the same CPP can be attached to either a liposome or a dendrimer, depending on the particular cell type to be targeted. Because each system has its own advantages and drawbacks a universal drug delivery platform may never be realized, but hybrid drug delivery systems that incorporate the benefits of various approaches will be tailored to address the needs of specific applications. However, a balance between complexity, efficacy, and cost will be necessary to obtain for each situation an efficient antimicrobial peptide delivery nanosystem as simple and economically affordable as possible.

CONFLICT OF INTEREST

None declared.

ACKNOWLEDGEMENTS

This work was supported by grants BIO2008-01184, BIO2011-25039, and CSD2006-00012 from the Ministerio de Ciencia e Innovación, Spain, which included FEDER funds, and by grant 2009SGR-760 from the Generalitat de Catalunya, Spain. A fellowship of the Instituto de Salud Carlos III (Spain) is acknowledged by Patricia Urbán.

REFERENCES

[1] Brown KL, Mookherjee N, Hancock REW. Antimicrobial, host defence peptides and proteins. Encyclopedia of Life Sciences. Chichester: John Wiley & Sons, Ltd. 2007. DOI: 10.1002/9780470015902.a0001212.pub2.

[2] Boix E. Eosinophil cationic protein. Methods Enzymol 2001; 341: 287-305.

[3] Torrent M, Navarro S, Moussaoui M, Nogués MV, Boix E. Eosinophil cationic protein high-affinity binding to bacteria-wall lipopolysaccharides and peptidoglycans. Biochemistry 2008; 47(11): 3544-55.

[4] Waters LS, Taverne J, Tai PC, Spry CJ, Targett GA, Playfair JH. Killing of *Plasmodium falciparum* by eosinophil secretory products. Infect Immun 1987; 55(4): 877-81.

[5] Adu B, Dodoo D, Adukpo S, *et al.* Polymorphisms in the *RNASE3* gene are associated with susceptibility to cerebral malaria in Ghanaian children. PLoS One 2011; 6(12): e29465.

[6] Venge P, Byström J, Carlson M, *et al.* Eosinophil cationic protein (ECP): molecular and biological properties and the use of ECP as a marker of eosinophil activation in disease. Clin Exp Allergy 1999; 29(9): 1172-86.

[7] Torrent M, Cuyás E, Carreras E, *et al.* Topography studies on the membrane interaction mechanism of the eosinophil cationic protein. Biochemistry 2007; 46(3): 720-33.

[8] Torrent M, Sánchez D, Buzón V, Nogués MV, Cladera J, Boix E. Comparison of the membrane interaction mechanism of two antimicrobial RNases: RNase 3/ECP and RNase 7. Biochim Biophys Acta 2009; 1788(5): 1116-25.

[9] White NJ. Assessment of the pharmacodynamic properties of antimalarial drugs *in vivo*. Antimicrob Agents Chemother 1997; 41(7): 1413-22.

[10] Couvreur P, Puisieux F. Nano- and microparticles for the delivery of polypeptides and proteins. Adv Drug Deliv Rev 2005; 10(2-3): 141-62.

[11] Pattani AS, Mandawgade SD, Patravale VB. Development and comparative anti-microbial evaluation of lipid nanoparticles and nanoemulsion of Polymyxin B. J Nanosci Nanotechnol 2006; 6(9-10): 2986-990.

[12] Ofokansi K, Winter G, Fricker G, Coester C. Matrix-loaded biodegradable gelatin nanoparticles as new approach to improve drug loading and delivery. Eur J Pharm Biopharm 2010; 76(1): 1-9.

[13] Luppi B, Bigucci F, Cerchiara T, Mandrioli R, Di Pietra AM, Zecchi V. New environmental sensitive system for colon-specific delivery of peptidic drugs. Int J Pharm 2008; 358(1-2): 44-9.

[14] Hamidi M, Zarrin A, Foroozesh M. Novel delivery systems for interferons. Crit Rev Biotechnol 2007; 27(3): 111-27.

[15] Xiong XY, Li YP, Li ZL, *et al.* Vesicles from Pluronic/poly(lactic acid) block copolymers as new carriers for oral insulin delivery. J Control Release 2007; 120(1-2): 11-7.

[16] Saltzman M, Desai T. Drug delivery in the BME curricula. Ann Biomed Eng 2006; 34(2): 270-75.

[17] Orive G, Hernández RM, Rodríguez Gascón A, Domínguez-Gil A, Pedraz JL. Drug delivery in biotechnology: present and future. Curr Opin Biotechnol 2003; 14(6): 659-64.

[18] Sershen S, West J. Implantable, polymeric systems for modulated drug delivery. Adv Drug Deliv Rev 2002; 54(9): 1225-35.

[19] Kikuchi A, Okano T. Pulsatile drug release control using hydrogels. Adv Drug Deliv Rev 2002; 54(1): 53-77.

[20] Fleming AB, Saltzman WM. Pharmacokinetics of the carmustine implant. Clin Pharmacokinet 2002; 41(6): 403-19.

[21] Boudes P. Drug compliance in therapeutic trials: a review. Control Clin Trials 1998; 19(3): 257-68.

[22] Tao SL, Desai TA. Microfabricated drug delivery systems: from particles to pores. Adv Drug Deliv Rev 2003; 55(3): 315-28.

[23] Breimer DD. Future challenges for drug delivery. J Control Release 1999; 62(1-2): 3-6.

[24] Klausner EA, Eyal S, Lavy E, Friedman M, Hoffman A. Novel levodopa gastroretentive dosage form: *in-vivo* evaluation in dogs. J Control Release 2003; 88(1): 117-26.

[25] Davis SS, Illum L. Drug delivery systems for challenging molecules. Int J Pharm 1998; 176(1): 1-8.

[26] Goldberg M, Langer R, Jia X. Nanostructured materials for applications in drug delivery and tissue engineering. J Biomater Sci Polym Ed 2007; 18(3): 241-68.

[27] Seale-Goldsmith MM, Leary JF. Nanobiosystems. Wiley Interdiscip Rev Nanomed Nanobiotechnol 2009; 1(5): 553-67.

[28] Sahoo SK, Labhasetwar V. Nanotech approaches to drug delivery and imaging. Drug Discov Today 2003; 8(24): 1112-20.

[29] Tan SY, Grimes S. Paul Ehrlich (1854-1915): man with the magic bullet. Singapore Med J 2010; 51(11): 842-3.

[30] Fahmy TM, Fong PM, Goyal A, Saltzman WM. Targeted for drug delivery. Nano Today 2005; 8(8): 18-26.

[31] Qiu LY, Bae YH. Polymer architecture and drug delivery. Pharm Res 2006; 23(1): 1-30.

[32] Svenson S, Tomalia DA. Dendrimers in biomedical applications--reflections on the field. Adv Drug Deliv Rev 2005; 57(15): 2106-29.

[33] Rabinow BE. Nanosuspensions in drug delivery. Nat Rev Drug Discov 2004; 3(9): 785-96.

[34] Ishida O, Maruyama K, Sasaki K, Iwatsuru M. Size-dependent extravasation and interstitial localization of polyethyleneglycol liposomes in solid tumor-bearing mice. Int J Pharm 1999; 190(1): 49-56.

[35] Kong G, Braun RD, Dewhirst MW. Hyperthermia enables tumor-specific nanoparticle delivery: effect of particle size. Cancer Res 2000; 60(16): 4440-5.

[36] Vinogradov SV, Bronich TK, Kabanov AV. Nanosized cationic hydrogels for drug delivery: preparation, properties and interactions with cells. Adv Drug Deliv Rev 2002; 54(1): 135-47.

[37] Hawley AE, Davis SS, Illum L. Targeting of colloids to lymph nodes: influence of lymphatic physiology and colloidal characteristics. Adv Drug Deliv Rev 1995; 17(1): 129-48.

[38] Stolnik S, Illum L, Davis SS. Long circulating microparticulate drug carriers. Adv Drug Deliv Rev 1995; 16(2-3): 195-214.

[39] Katz E, Willner I. Integrated nanoparticle-biomolecule hybrid systems: synthesis, properties, and applications. Angew Chem Int Ed Engl 2004; 43(45): 6042-108.

[40] Farokhzad OC, Jon S, Khademhosseini A, Tran TN, Lavan DA, Langer R. Nanoparticle-aptamer bioconjugates: a new approach for targeting prostate cancer cells. Cancer Res 2004; 64(21): 7668-72.

[41] Gu F, Zhang L, Teply BA, *et al.* Precise engineering of targeted nanoparticles by using self-assembled biointegrated block copolymers. Proc Natl Acad Sci USA 2008; 105(7): 2586-91.

[42] Kim SH, Jeong JH, Chun KW, Park TG. Target-specific cellular uptake of PLGA nanoparticles coated with poly(L-lysine)-poly(ethylene glycol)-folate conjugate. Langmuir 2005; 21(19): 8852-7.

[43] Urbán P, Estelrich J, Cortés A, Fernàndez-Busquets X. A nanovector with complete discrimination for targeted delivery to *Plasmodium falciparum*-infected versus non-infected red blood cells *in vitro*. J Control Release 2011; 151(2): 202-11.

[44] Panyam J, Labhasetwar V. Biodegradable nanoparticles for drug and gene delivery to cells and tissue. Adv Drug Deliv Rev 2003; 55(3): 329-47.

[45] Rawat M, Singh D, Saraf S, Saraf S. Nanocarriers: promising vehicle for bioactive drugs. Biol Pharm Bull 2006; 29(9): 1790-8.

[46] Farokhzad OC, Langer R. Impact of nanotechnology on drug delivery. ACS Nano 2009; 3(1): 16-20.

[47] Bustami RT, Chan HK, Dehghani F, Foster NR. Generation of micro-particles of proteins for aerosol delivery using high pressure modified carbon dioxide. Pharm Res 2000; 17(11): 1360-6.

[48] Gregoriadis G. Drug entrapment in liposomes. FEBS Lett 1973; 36(3): 292-6.

[49] Jasmine D, Tushar T. Role of liposomes in nanotechnology and drug delivery. Int J Drug Dev Res 2011; 3(1): 341-50.

[50] Maurer N, Fenske DB, Cullis PR. Developments in liposomal drug delivery systems. Expert Opin Biol Ther 2001; 1(6): 923-47.

[51] Waterhouse DN, Madden TD, Cullis PR, Bally MB, Mayer LD, Webb MS. Preparation, characterization, and biological analysis of liposomal formulations of vincristine. Methods Enzymol 2005; 391: 40-57.

[52] Haran G, Cohen R, Bar LK, Barenholz Y. Transmembrane ammonium sulfate gradients in liposomes produce efficient and stable entrapment of amphipathic weak bases. Biochim Biophys Acta 1993; 1151(2): 201-15.

[53] Storm G, Wilms HP, Crommelin DJ. Liposomes and biotherapeutics. Biotherapy 1991; 3(1): 25-42.

[54] Kadir F, Zuidema J, Crommelin DJA. Liposomes as drug delivery systems for intramuscular and subcutaneous injections. In: Rolland A, Ed. Particulate Drug Carriers in Medical Applications. New York: Marcel Dekker 1993: 165-98.

[55] Čeh B, Winterhalter M, Frederik PM, Vallner JJ, Lasic DD. Stealth® liposomes: from theory to product. Adv Drug Deliv Rev 1997; 24(2-3): 165-77.

[56] Blume G, Cevc G. Liposomes for the sustained drug release *in vivo*. Biochim Biophys Acta 1990; 1029(1): 91-7.

[57] Kajiwara E, Kawano K, Hattori Y, Fukushima M, Hayashi K, Maitani Y. Long-circulating liposome-encapsulated ganciclovir enhances the efficacy of HSV-TK suicide gene therapy. J Control Release 2007; 120(1-2): 104-10.

[58] Santos-Magalhaes NS, Mosqueira VC. Nanotechnology applied to the treatment of malaria. Adv Drug Deliv Rev 2010; 62(4-5): 560-75.

[59] Singhal A, Gupta CM. Antibody-mediated targeting of liposomes to red cells *in vivo*. FEBS Lett 1986; 201(2): 321-26.

[60] Shillcock JC, Lipowsky R. Tension-induced fusion of bilayer membranes and vesicles. Nat Mater 2005; 4(3): 225-8.

[61] Wheeler JJ, Palmer L, Ossanlou M, *et al.* Stabilized plasmid-lipid particles: construction and characterization. Gene Ther 1999; 6(2): 271-81.

[62] Nicolosi D, Scalia M, Nicolosi VM, Pignatello R. Encapsulation in fusogenic liposomes broadens the spectrum of action of vancomycin against Gram-negative bacteria. Int J Antimicrob Agents 2010; 35(6): 553-8.

[63] Alipour M, Halwani M, Omri A, Suntres ZE. Antimicrobial effectiveness of liposomal polymyxin B against resistant Gram-negative bacterial strains. Int J Pharm 2008; 355(1-2): 293-8.

[64] Alipour M, Suntres ZE, Halwani M, Azghani AO, Omri A. Activity and interactions of liposomal antibiotics in presence of polyanions and sputum of patients with cystic fibrosis. PLoS One 2009; 4(5): e5724.

[65] Gregoriadis G. Liposomes as a drug delivery system: optimization studies. Adv Exp Med Biol 1988; 238: 151-159.

[66] Paleos CM, Tsiourvas D, Sideratou Z, Tziveleka LA. Drug delivery using multifunctional dendrimers and hyperbranched polymers. Expert Opin Drug Deliv 2010; 7(12): 1387-98.

[67] Sukhorukov GB, Rogach AL, Garstka M, *et al.* Multifunctionalized polymer microcapsules: novel tools for biological and pharmacological applications. Small 2007; 3(6): 944-55.

[68] Soppimath KS, Aminabhavi TM, Kulkarni AR, Rudzinski WE. Biodegradable polymeric nanoparticles as drug delivery devices. J Control Release 2001; 70(1-2): 1-20.

[69] Agnihotri SA, Mallikarjuna NN, Aminabhavi TM. Recent advances on chitosan-based micro- and nanoparticles in drug delivery. J Control Release 2004; 100(1): 5-28.

[70] Duncan R. The dawning era of polymer therapeutics. Nat Rev Drug Discov 2003; 2(5): 347-60.

[71] Kavanagh OV, Earley B, Murray M, Foster CJ, Adair BM. Antigen-specific IgA and IgG responses in calves inoculated intranasally with ovalbumin encapsulated in poly(DL-lactide-co-glycolide) microspheres. Vaccine 2003; 21(27-30): 4472-80.

[72] Andrieux K, Couvreur P. Polyalkylcyanoacrylate nanoparticles for delivery of drugs across the blood-brain barrier. Wiley Interdiscip Rev Nanomed Nanobiotechnol 2009; 1(5): 463-74.

[73] Fernández-Urrusuno R, Calvo P, Remuñán-López C, Vila-Jato JL, Alonso MJ. Enhancement of nasal absorption of insulin using chitosan nanoparticles. Pharm Res 1999; 16(10): 1576-81.

[74] Yin L, Ding J, He C, Cui L, Tang C, Yin C. Drug permeability and mucoadhesion properties of thiolated trimethyl chitosan nanoparticles in oral insulin delivery. Biomaterials 2009; 30(29): 5691-700.

[75] Prego C, Torres D, Alonso MJ. The potential of chitosan for the oral administration of peptides. Expert Opin Drug Deliv 2005; 2(5): 843-54.

[76] Lescure F, Seguin C, Breton P, Bourrinet P, Roy D, Couvreur P. Preparation and characterization of novel poly(methylidene malonate 2.1.2.)-made nanoparticles. Pharm Res 1994; 11(9): 1270-7.

[77] Wikingsson L, Sjoholm I. Polyacryl starch microparticles as adjuvant in oral immunisation, inducing mucosal and systemic immune responses in mice. Vaccine 2002; 20(27-28): 3355-63.

[78] Aynié I, Vauthier C, Chacun H, Fattal E, Couvreur P. Spongelike alginate nanoparticles as a new potential system for the delivery of antisense oligonucleotides. Antisense Nucleic Acid Drug Dev 1999; 9(3): 301-12.

[79] Bege N, Renette T, Jansch M, *et al.* Biodegradable poly(ethylene carbonate) nanoparticles as a promising drug delivery system with "stealth" potential. Macromol Biosci 2011; 11(7): 897-904.

[80] Peppas NA, Bures P, Leobandung W, Ichikawa H. Hydrogels in pharmaceutical formulations. Eur J Pharm Biopharm 2000; 50(1): 27-46.

[81] Peppas NA, Wood KM, Blanchette JO. Hydrogels for oral delivery of therapeutic proteins. Expert Opin Biol Ther 2004; 4(6): 881-7.

[82] Gupta P, Vermani K, Garg S. Hydrogels: from controlled release to pH-responsive drug delivery. Drug Discov Today 2002; 7(10): 569-79.

[83] Vinogradov SV. Colloidal microgels in drug delivery applications. Curr Pharm Des 2006; 12(36): 4703-12.

[84] Patel VR, Amiji MM. Preparation and characterization of freeze-dried chitosan-poly(ethylene oxide) hydrogels for site-specific antibiotic delivery in the stomach. Pharm Res 1996; 13(4): 588-93.

[85] Li JK, Wang N, Wu XS. Poly(vinyl alcohol) nanoparticles prepared by freezing-thawing process for protein/peptide drug delivery. J Control Release 1998; 56(1-3): 117-26.

[86] Salmaso S, Semenzato A, Bersani S, Matricardi P, Rossi F, Caliceti P. Cyclodextrin/PEG based hydrogels for multi-drug delivery. Int J Pharm 2007; 345(1-2): 42-50.

[87] Gupta NV, Shivakumar HG. Preparation and characterization of superporous hydrogels as pH-sensitive drug delivery system for Pantoprazole sodium. Curr Drug Deliv 2009; 6(5): 505-10.

[88] Gutowska A, Seok Bark J, Chan Kwon I, Han Bae Y, Cha Y, Wan Kim S. Squeezing hydrogels for controlled oral drug delivery. J Control Release 1997; 48(2-3): 141-8.

[89] Tiwari AK, Gajbhiye V, Sharma R, Jain NK. Carrier mediated protein and peptide stabilization. Drug Deliv 2010; 17(8): 605-16.

[90] Pattrick NG, Richardson SC, Casolaro M, Ferruti P, Duncan R. Poly(amidoamine)-mediated intracytoplasmic delivery of ricin A-chain and gelonin. J Control Release 2001; 77(3): 225-32.

[91] Wang H, Xu K, Liu L, *et al.* The efficacy of self-assembled cationic antimicrobial peptide nanoparticles against *Cryptococcus neoformans* for the treatment of meningitis. Biomaterials 2010; 31(10): 2874-81.

[92] Schröder U, Sabel BA. Nanoparticles, a drug carrier system to pass the blood-brain barrier, permit central analgesic effects of i.v. dalargin injections. Brain Res 1996; 710(1-2): 121-4.

[93] Kreuter J. Nanoparticulate systems for brain delivery of drugs. Adv Drug Deliv Rev 2001; 47(1): 65-81.

[94] Roney C, Kulkarni P, Arora V, *et al.* Targeted nanoparticles for drug delivery through the blood-brain barrier for Alzheimer's disease. J Control Release 2005; 108(2-3): 193-214.

[95] Al-Jamal KT, Ramaswamy C, Florence AT. Supramolecular structures from dendrons and dendrimers. Adv Drug Deliv Rev 2005; 57(15): 2238-70.

[96] Marcos M, Martín-Rapún R, Omenat A, Serrano JL. Highly congested liquid crystal structures: dendrimers, dendrons, dendronized and hyperbranched polymers. Chem Soc Rev 2007; 36(12): 1889-901.

[97] Liang C, Fréchet JMJ. Applying key concepts from nature: transition state stabilization, pre-concentration and cooperativity effects in dendritic biomimetics. Prog Polym Sci 2005; 30(3-4): 385-402.

[98] Ihre HR, Padilla De Jesús OL, Szoka FC Jr., Fréchet JM. Polyester dendritic systems for drug delivery applications: design, synthesis, and characterization. Bioconjug Chem 2002; 13(3): 443-52.

[99] Padilla De Jesús OL, Ihre HR, Gagne L, Fréchet JM, Szoka FC Jr. Polyester dendritic systems for drug delivery applications: *in vitro* and *in vivo* evaluation. Bioconjug Chem 2002; 13(3): 453-61.

[100] Boas U, Heegaard PM. Dendrimers in drug research. Chem Soc Rev 2004; 33(1): 43-63.

[101] Paleos CM, Tsiourvas D, Sideratou Z. Molecular engineering of dendritic polymers and their application as drug and gene delivery systems. Mol Pharm 2007; 4(2): 169-88.

[102] Kolhe P, Khandare J, Pillai O, Kannan S, Lieh-Lai M, Kannan RM. Preparation, cellular transport, and activity of polyamidoamine-based dendritic nanodevices with a high drug payload. Biomaterials 2006; 27(4): 660-9.

[103] Kukowska-Latallo JF, Bielinska AU, Johnson J, Spindler R, Tomalia DA, Baker JR Jr. Efficient transfer of genetic material into mammalian cells using Starburst polyamidoamine dendrimers. Proc Natl Acad Sci USA 1996; 93(10): 4897-902.

[104] Crespo L, Sanclimens G, Montaner B, *et al.* Peptide dendrimers based on polyproline helices. J Am Chem Soc 2002; 124(30): 8876-83.

[105] Farrera-Sinfreu J, Giralt E, Castel S, Albericio F, Royo M. Cell-penetrating cis-gamma-amino-l-proline-derived peptides. J Am Chem Soc 2005; 127(26): 9459-68.

[106] Wiwattanapatapee R, Carreño-Gómez B, Malik N, Duncan R. Anionic PAMAM dendrimers rapidly cross adult rat intestine *in vitro:* a potential oral delivery system? Pharm Res 2000; 17(8): 991-8.

[107] Crespo L, Sanclimens G, Pons M, Giralt E, Royo M, Albericio F. Peptide and amide bond-containing dendrimers. Chem Rev 2005; 105(5):1663-81.

[108] Agrawal P, Gupta U, Jain NK. Glycoconjugated peptide dendrimers-based nanoparticulate system for the delivery of chloroquine phosphate. Biomaterials 2007; 28(22): 3349-59.

[109] Bhadra D, Yadav AK, Bhadra S, Jain NK. Glycodendrimeric nanoparticulate carriers of primaquine phosphate for liver targeting. Int J Pharm 2005; 295(1-2): 221-33.

[110] Lee JW, Ko YH, Park SH, Yamaguchi K, Kim K. Novel pseudorotaxane-terminated dendrimers: Supramolecular modification of dendrimer periphery. Angew Chem Int Ed 2001; 40(4): 746-9.

[111] Mitchell JP, Roberts KD, Langley J, Koentgen F, Lambert JN. A direct method for the formation of peptide and carbohydrate dendrimers. Bioorg Med Chem Lett 1999; 9(19): 2785-8.

[112] Chamorro C, Boerman MA, Arnusch CJ, Breukink E, Pieters RJ. Enhancing membrane disruption by targeting and multivalent presentation of antimicrobial peptides. Biochim Biophys Acta 2012 Apr 14. [Epub ahead of print].

[113] Ciolkowski M, Petersen JF, Ficker M, *et al.* Surface modification of PAMAM dendrimer improves its biocompatibility. Nanomedicine. 2012 Apr 26. [Epub ahead of print].

[114] Calabretta MK, Kumar A, McDermott AM, Cai C. Antibacterial activities of poly(amidoamine) dendrimers terminated with amino and poly(ethylene glycol) groups. Biomacromolecules 2007; 8(6): 1807-11.

[115] Lopez AI, Reins RY, McDermott AM, Trautner BW, Cai C. Antibacterial activity and cytotoxicity of PEGylated poly(amidoamine) dendrimers. Mol Biosyst 2009; 5(10): 1148-56.

[116] Wang B, Navath RS, Menjoge AR, *et al.* Inhibition of bacterial growth and intramniotic infection in a guinea pig model of chorioamnionitis using PAMAM dendrimers. Int J Pharm 2010; 395(1-2): 298-308.

[117] Wang AZ, Gu F, Zhang L, *et al.* Biofunctionalized targeted nanoparticles for therapeutic applications. Expert Opin Biol Ther 2008; 8(8): 1063-70.

[118] Veiseh O, Sun C, Gunn J, *et al.* Optical and MRI multifunctional nanoprobe for targeting gliomas. Nano Lett 2005; 5(6): 1003-8.

[119] Durán JD, Arias JL, Gallardo V, Delgado AV. Magnetic colloids as drug vehicles. J Pharm Sci 2008; 97(8): 2948-83.

[120] Xing Y, Smith AM, Agrawal A, Ruan G, Nie S. Molecular profiling of single cancer cells and clinical tissue specimens with semiconductor quantum dots. Int J Nanomedicine 2006; 1(4): 473-81.

[121] Hosseinkhani H, Hosseinkhani M. Biodegradable polymer-metal complexes for gene and drug delivery. Curr Drug Saf 2009; 4(1): 79-83.

[122] Ashley CE, Carnes EC, Phillips GK, *et al.* The targeted delivery of multicomponent cargos to cancer cells by nanoporous particle-supported lipid bilayers. Nat Mater 2011; 10(5): 389-97.

[123] Soenen SJ, Hodenius M, De Cuyper M. Magnetoliposomes: versatile innovative nanocolloids for use in biotechnology and biomedicine. Nanomedicine (Lond) 2009; 4(2): 177-91.

[124] Ghosh P, Yang X, Arvizo R, *et al.* Intracellular delivery of a membrane-impermeable enzyme in active form using functionalized gold nanoparticles. J Am Chem Soc 2010; 132(8): 2642-5.

[125] Guerrero S, Araya E, Fiedler JL, *et al.* Improving the brain delivery of gold nanoparticles by conjugation with an amphipathic peptide. Nanomedicine (Lond) 2010; 5(6): 897-913.

[126] Schaeublin NM, Braydich-Stolle LK, Schrand AM, *et al.* Surface charge of gold nanoparticles mediates mechanism of toxicity. Nanoscale 2011; 3(2): 410-20.

[127] Maynard AD, Warheit DB, Philbert MA. The new toxicology of sophisticated materials: nanotoxicology and beyond. Toxicol Sci 2011; 120(suppl 1): S109-S129.

[128] Bianco A, Kostarelos K, Prato M. Applications of carbon nanotubes in drug delivery. Curr Opin Chem Biol 2005; 9(6): 674-9.

[129] Sanz V, Coley H, Silva S, McFadden J. Modeling the binding of peptides on carbon nanotubes and their use as protein and DNA carriers. J Nanoparticle Res 2012; 14(2): 1-13.

[130] Bandaru NM, Voelcker NH. Glycoconjugate-functionalized carbon nanotubes in biomedicine. J Mater Chem 2012; 22(18): 8748-58.

[131] Beg S, Rizwan M, Sheikh AM, Hasnain MS, Anwer K, Kohli K. Advancement in carbon nanotubes: basics, biomedical applications and toxicity. J Pharm Pharmacol 2011; 63(2): 141-63.

[132] Pantarotto D, Briand JP, Prato M, Bianco A. Translocation of bioactive peptides across cell membranes by carbon nanotubes. Chem Commun 2004; (1): 16-7.

[133] Shi Kam NW, Jessop TC, Wender PA, Dai H. Nanotube molecular transporters: internalization of carbon nanotube-protein conjugates into mammalian cells. J Am Chem Soc 2004; 126(22): 6850-1.

[134] Heister E, Neves V, Lamprecht C, Silva SR, Coley HM, McFadden J. Drug loading, dispersion stability, and therapeutic efficacy in targeted drug delivery with carbon nanotubes. Carbon 2012; 50(2): 622-32.

[135] Trzaskowski B, Jalbout AF, Adamowicz L. Molecular dynamics studies of protein-fragment models encapsulated into carbon nanotubes. Chem Phys Lett 2006; 430(1-3): 97-100.

[136] Kümmerer K, Menz J, Schubert T, Thielemans W. Biodegradability of organic nanoparticles in the aqueous environment. Chemosphere 2011; 82(10): 1387-92.

[137] Yang D, Campolongo MJ, Nhi Tran TN, Ruiz RC, Kahn JS, Luo D. Novel DNA materials and their applications. Wiley Interdiscip Rev Nanomed Nanobiotechnol 2010; 2(6): 648-69.

[138] Andersen ES, Dong M, Nielsen MM, *et al.* Self-assembly of a nanoscale DNA box with a controllable lid. Nature 2009; 459(7243): 73-6.

[139] He Y, Ye T, Su M, *et al.* Hierarchical self-assembly of DNA into symmetric supramolecular polyhedra. Nature 2008; 452(7184): 198-201.

[140] Alexis F, Pridgen E, Molnar LK, Farokhzad OC. Factors affecting the clearance and biodistribution of polymeric nanoparticles. Mol Pharm 2008; 5(4): 505-15.

[141] Li SD, Huang L. Pharmacokinetics and biodistribution of nanoparticles. Mol Pharm 2008; 5(4): 496-504.

[142] Geng Y, Discher DE. Hydrolytic degradation of poly(ethylene oxide)-block-polycaprolactone worm micelles. J Am Chem Soc 2005; 127(37): 12780-1.

[143] Gao W, Chan JM, Farokhzad OC. pH-Responsive nanoparticles for drug delivery. Mol Pharm 2010; 7(6): 1913-20.

[144] Sakthivel T, Toth I, Florence AT. Distribution of a lipidic 2.5 nm diameter dendrimer carrier after oral administration. Int J Pharm 1999; 183(1): 51-5.

[145] Phua K, Leong KW. Microscale oral delivery devices incorporating nanoparticles. Nanomedicine (Lond) 2010; 5(2): 161-3.

[146] Yamanaka YJ, Leong KW. Engineering strategies to enhance nanoparticle-mediated oral delivery. J Biomater Sci Polym Ed 2008; 19(12): 1549-70.

[147] Lin YH, Mi FL, Chen CT, *et al.* Preparation and characterization of nanoparticles shelled with chitosan for oral insulin delivery. Biomacromolecules 2007; 8(1): 146-52.

[148] Wong TW. Design of oral insulin delivery systems. J Drug Target 2010; 18(2): 79-92.

[149] Damgé C, Maincent P, Ubrich N. Oral delivery of insulin associated to polymeric nanoparticles in diabetic rats. J Control Release 2007; 117(2): 163-70.

[150] Pan Y, Li YJ, Zhao HY, *et al.* Bioadhesive polysaccharide in protein delivery system: chitosan nanoparticles improve the intestinal absorption of insulin *in vivo*. Int J Pharm 2002; 249(1-2): 139-47.

[151] Carino GP, Mathiowitz E. Oral insulin delivery. Adv Drug Deliv Rev 1999; 35(2-3): 249-57.

[152] Zola H. Monoclonal antibodies: Therapeutic uses. Encyclopedia of Life Sciences. Chichester: John Wiley & Sons, Ltd. 2011. DOI: 10.1038/npg.els.0004018.

[153] Paul S, Planque S. Antibody engineering. Encyclopedia of Life Sciences. Chichester: John Wiley & Sons, Ltd. 2005. DOI: 10.1038/npg.els.0001278.

[154] Hu S, Shively L, Raubitschek A, *et al.* Minibody: A novel engineered anti-carcinoembryonic antigen antibody fragment (single-chain Fv-C_H3) which exhibits rapid, high-level targeting of xenografts. Cancer Res 1996; 56(13): 3055-61.

[155] Wu AM, Yazaki PJ. Designer genes: recombinant antibody fragments for biological imaging. Q J Nucl Med 2000; 44(3): 268-83.

[156] Cortez-Retamozo V, Backmann N, Senter PD, *et al.* Efficient cancer therapy with a nanobody-based conjugate. Cancer Res 2004; 64(8): 2853-7.

[157] Qiu XQ, Wang H, Cai B, Wang LL, Yue ST. Small antibody mimetics comprising two complementarity-determining regions and a framework region for tumor targeting. Nat Biotechnol 2007; 25(8): 921-9.

[158] Martin FJ, Papahadjopoulos D. Irreversible coupling of immunoglobulin fragments to preformed vesicles. An improved method for liposome targeting. J Biol Chem 1982; 257(1): 286-8.

[159] Owais M, Varshney GC, Choudhury A, Chandra S, Gupta CM. Chloroquine encapsulated in malaria-infected erythrocyte-specific antibody-bearing liposomes effectively controls chloroquine-resistant *Plasmodium berghei* infections in mice. Antimicrob Agents Chemother 1995; 39(1): 180-4.

[160] Vogel C-W. Preparation of immunoconjugates using antibody oligosaccharide moieties. In: Niemeyer CM, Ed. Methods in Molecular Biology. Totowa, NJ: Humana Press Inc., 2004: 87-108.

[161] Ishikawa H, Ochi H, Chen ML, Frenkel D, Maron R, Weiner HL. Inhibition of autoimmune diabetes by oral administration of anti-CD3 monoclonal antibody. Diabetes 2007; 56(8): 2103-9.

[162] Warren CL, Mohandas A, Chaturvedi I, Ansari AZ. Macromolecular interactions: aptamers. Encyclopedia of Life Sciences. Chichester: John Wiley & Sons, Ltd. 2009 DOI: 10.1002/9780470015902.a0003146.

[163] O'Sullivan CK. Aptasensors--the future of biosensing? Anal Bioanal Chem 2002; 372(1): 44-8.

[164] Abelson J. Directed evolution of nucleic acids by independent replication and selection. Science 1990; 249(4968): 488-9.

[165] Collett JR, Cho EJ, Ellington AD. Production and processing of aptamer microarrays. Methods 2005; 37(1): 4-15.

[166] Hersel U, Dahmen C, Kessler H. RGD modified polymers: biomaterials for stimulated cell adhesion and beyond. Biomaterials 2003; 24(24): 4385-415.

[167] Patel LN, Zaro JL, Shen WC. Cell penetrating peptides: intracellular pathways and pharmaceutical perspectives. Pharm Res 2007; 24(11): 1977-92.

[168] Futaki S. Arginine-rich peptides: potential for intracellular delivery of macromolecules and the mystery of the translocation mechanisms. Int J Pharm 2002; 245(1-2): 1-7.

[169] Rao KS, Reddy MK, Horning JL, Labhasetwar V. TAT-conjugated nanoparticles for the CNS delivery of anti-HIV drugs. Biomaterials 2008; 29(33): 4429-38.

[170] Fernández-Carneado J, Kogan MJ, Pujals S, Giralt E. Amphipathic peptides and drug delivery. Biopolymers 2004; 76(2): 196-203.

[171] Pujals S, Fernández-Carneado J, López-Iglesias C, Kogan MJ, Giralt E. Mechanistic aspects of CPP-mediated intracellular drug delivery: relevance of CPP self-assembly. Biochim Biophys Acta 2006; 1758(3): 264-79.

[172] Pujals S, Sabidó E, Tarragó T, Giralt E. all-D proline-rich cell-penetrating peptides: a preliminary *in vivo* internalization study. Biochem Soc Trans 2007; 35(Pt 4): 794-6.

[173] Chen L, Harrison SD. Cell-penetrating peptides in drug development: enabling intracellular targets. Biochem Soc Trans 2007; 35(Pt 4): 821-5.

[174] Law B, Quinti L, Choi Y, Weissleder R, Tung CH. A mitochondrial targeted fusion peptide exhibits remarkable cytotoxicity. Mol Cancer Ther 2006; 5(8): 1944-9.

[175] Dietz GP, Bähr M. Delivery of bioactive molecules into the cell: the Trojan horse approach. Mol Cell Neurosci 2004; 27(2): 85-131.

[176] Zhao M, Kircher MF, Josephson L, Weissleder R. Differential conjugation of tat peptide to superparamagnetic nanoparticles and its effect on cellular uptake. Bioconjug Chem 2002; 13(4): 840-4.

[177] Khalil IA, Kogure K, Futaki S, Harashima H. High density of octaarginine stimulates macropinocytosis leading to efficient intracellular trafficking for gene expression. J Biol Chem 2006; 281(6): 3544-51.

[178] Fretz MM, Koning GA, Mastrobattista E, Jiskoot W, Storm G. OVCAR-3 cells internalize TAT-peptide modified liposomes by endocytosis. Biochim Biophys Acta 2004; 1665(1-2): 48-56.

[179] Hashida H, Miyamoto M, Cho Y, *et al.* Fusion of HIV-1 Tat protein transduction domain to poly-lysine as a new DNA delivery tool. Br J Cancer 2004; 90(6): 1252-8.

[180] Liu L, Xu K, Wang H, *et al.* Self-assembled cationic peptide nanoparticles as an efficient antimicrobial agent. Nat Nanotechnol 2009; 4(7): 457-63.

[181] Teixidó M, Giralt E. The role of peptides in blood-brain barrier nanotechnology. J Pept Sci 2008; 14(2): 163-73.

[182] Fridkin M, Najjar VA. Tuftsin: its chemistry, biology, and clinical potential. Crit Rev Biochem Mol Biol 1989; 24(1): 1-40.

[183] Agrawal AK, Gupta CM. Tuftsin-bearing liposomes in treatment of macrophage-based infections. Adv Drug Deliv Rev 2000; 41(2): 135-46.

[184] Bucior I, Burger MM, Fernàndez-Busquets X. Carbohydrate-carbohydrate interactions. In: Gabius H-J, Ed. The Sugar Code. Weinheim: WILEY-VCH Verlag GmbH & Co. KGaA, 2009: 347-62.

[185] Winterburn PJ, Phelps CF. The significance of glycosylated proteins. Nature 1972; 236(5343): 147-51.

[186] Rüdiger H, Gabius H-J. The biochemical basis and coding capacity of the sugar code. In: Gabius H-J, Ed. The Sugar Code. Weinheim: WILEY-VCH Verlag GmbH & Co. KGaA, 2009: 3-13.

[187] Solis D, Romero A, Menéndez M, Jiménez-Barbero J. Protein-carbohydrate interactions: basic concepts and methods for analysis. In: Gabius H-J, Ed. The Sugar Code. Weinheim: WILEY-VCH Verlag GmbH & Co. KGaA, 2009: 233-45.

[188] Idro R, Jenkins NE, Newton CR. Pathogenesis, clinical features, and neurological outcome of cerebral malaria. Lancet Neurol 2005; 4(12): 827-40.

[189] Craig A, Scherf A. Molecules on the surface of the *Plasmodium falciparum* infected erythrocyte and their role in malaria pathogenesis and immune evasion. Mol Biochem Parasitol 2001; 115(2): 129-43.

[190] Barragan A, Fernandez V, Chen Q, von Euler A, Wahlgren M, Spillmann D. The duffy-binding-like domain 1 of *Plasmodium falciparum* erythrocyte membrane protein 1 (PfEMP1) is a heparan sulfate ligand that requires 12 mers for binding. Blood 2000; 95(11): 3594-9.

[191] Vogt AM, Barragan A, Chen Q, Kironde F, Spillmann D, Wahlgren M. Heparan sulfate on endothelial cells mediates the binding of *Plasmodium falciparum*-infected erythrocytes *via* the DBL1α domain of PfEMP1. Blood 2003; 101(6): 2405-11.

[192] Gysin J, Pouvelle B, Le Tonqueze M, Edelman L, Boffa MC. Chondroitin sulfate of thrombomodulin is an adhesion receptor for *Plasmodium falciparum*-infected erythrocytes. Mol Biochem Parasitol 1997; 88(1-2): 267-71.

[193] Singh K, Gittis AG, Nguyen P, Gowda DC, Miller LH, Garboczi DN. Structure of the DBL3x domain of pregnancy-associated malaria protein VAR2CSA complexed with chondroitin sulfate A. Nat Struct Mol Biol 2008; 15(9): 932-8.

[194] Fried M, Duffy PE. Adherence of *Plasmodium falciparum* to chondroitin sulfate A in the human placenta. Science 1996; 272(5267): 1502-4.

[195] Andrews KT, Klatt N, Adams Y, Mischnick P, Schwartz-Albiez R. Inhibition of chondroitin-4-sulfate-specific adhesion of *Plasmodium falciparum*-infected erythrocytes by sulfated polysaccharides. Infect Immun 2005; 73(7): 4288-94.

[196] Ancsin JB, Kisilevsky R. A binding site for highly sulfated heparan sulfate is identified in the N terminus of the circumsporozoite protein: significance for malarial sporozoite attachment to hepatocytes. J Biol Chem 2004; 279(21): 21824-32.

[197] Boyle MJ, Richards JS, Gilson PR, Chai W, Beeson JG. Interactions with heparin-like molecules during erythrocyte invasion by *Plasmodium falciparum* merozoites. Blood 2010; 115(22): 4559-68.

[198] Torchilin VP. Multifunctional nanocarriers. Adv Drug Deliv Rev 2006; 58(14): 1532-55.

[199] Al-Jamal WT, Kostarelos K. Construction of nanoscale multicompartment liposomes for combinatory drug delivery. Int J Pharm 2007; 331(2): 182-5.

[200] Al-Jamal WT, Kostarelos K. Liposome-nanoparticle hybrids for multimodal diagnostic and therapeutic applications. Nanomedicine (Lond) 2007; 2(1): 85-98.

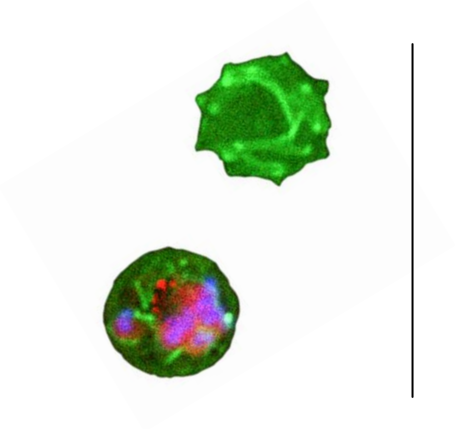

Annex 2

PATENT

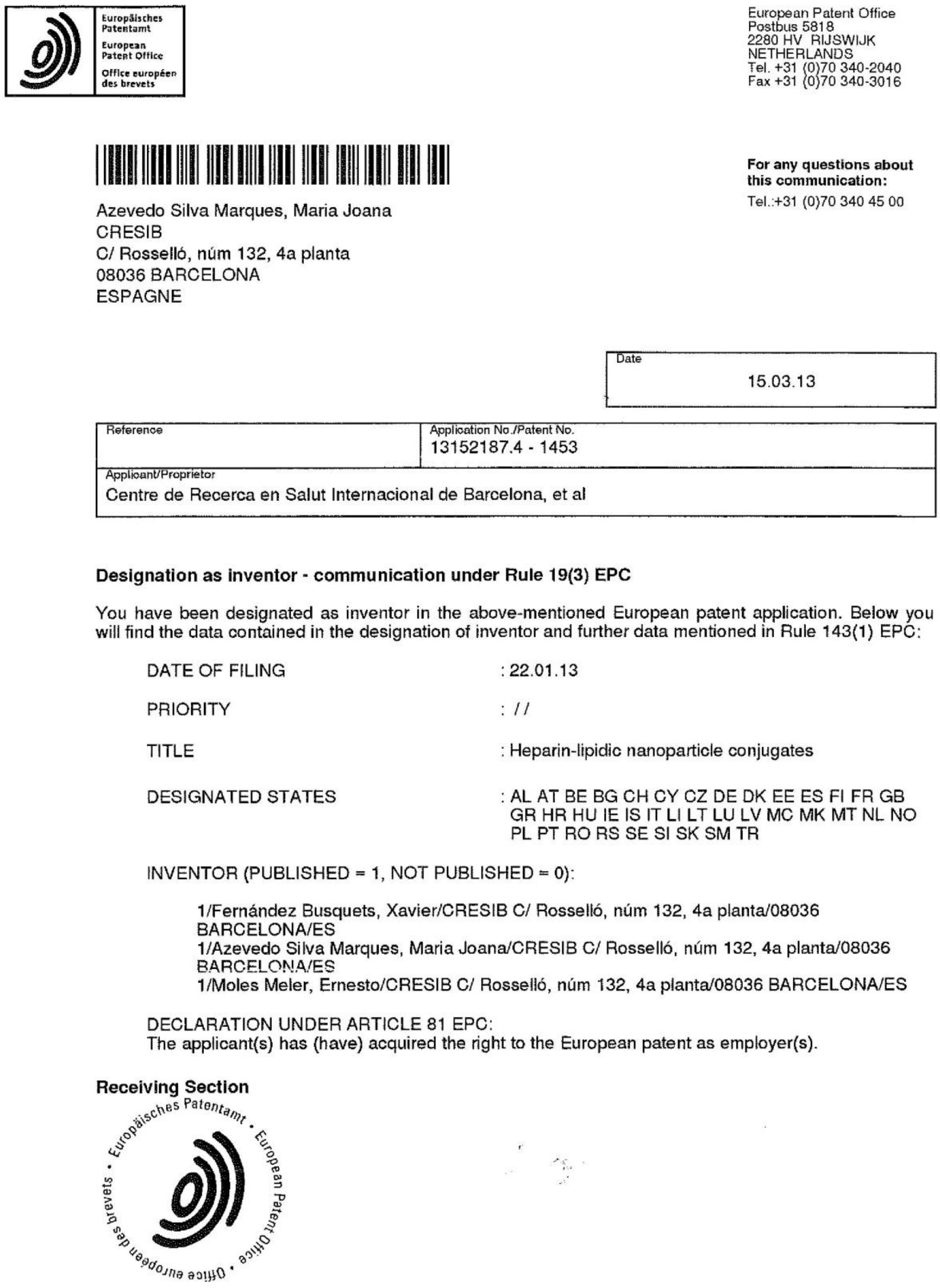

European Patent Office
Postbus 5818
2280 HV RIJSWIJK
NETHERLANDS
Tel. +31 (0)70 340-2040
Fax +31 (0)70 340-3016

For any questions about this communication:
Tel.:+31 (0)70 340 45 00

Azevedo Silva Marques, Maria Joana
CRESIB
C/ Rosselló, núm 132, 4a planta
08036 BARCELONA
ESPAGNE

Date
15.03.13

Reference	Application No./Patent No.
	13152187.4 - 1453

Applicant/Proprietor
Centre de Recerca en Salut Internacional de Barcelona, et al

Designation as inventor - communication under Rule 19(3) EPC

You have been designated as inventor in the above-mentioned European patent application. Below you will find the data contained in the designation of inventor and further data mentioned in Rule 143(1) EPC:

DATE OF FILING	: 22.01.13
PRIORITY	: //
TITLE	: Heparin-lipidic nanoparticle conjugates
DESIGNATED STATES	: AL AT BE BG CH CY CZ DE DK EE ES FI FR GB GR HR HU IE IS IT LI LT LU LV MC MK MT NL NO PL PT RO RS SE SI SK SM TR

INVENTOR (PUBLISHED = 1, NOT PUBLISHED = 0):

1/Fernández Busquets, Xavier/CRESIB C/ Rosselló, núm 132, 4a planta/08036 BARCELONA/ES
1/Azevedo Silva Marques, Maria Joana/CRESIB C/ Rosselló, núm 132, 4a planta/08036 BARCELONA/ES
1/Moles Meler, Ernesto/CRESIB C/ Rosselló, núm 132, 4a planta/08036 BARCELONA/ES

DECLARATION UNDER ARTICLE 81 EPC:
The applicant(s) has (have) acquired the right to the European patent as employer(s).

Receiving Section

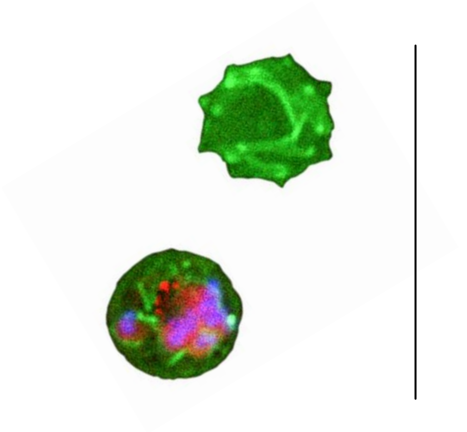

Annex 3

REPORT BY THE DIRECTOR

During her PhD in my group, Ms. Joana Marques has contributed to five papers, three of them published, one submitted, and one in preparation. Her contribution in these works is described below:

1.

Marques, J., Moles, E., Urbán, P., Prohens, R., Busquets, M.A., Sevrin, C., Grandfils, C., and Fernàndez-Busquets, X. (2014) Application of heparin as a dual agent with antimalarial and liposome targeting activities toward *Plasmodium*-infected red blood cells. *Nanomedicine: NBM* **10**, 1719-1728.

IF 2014: 6.2

This work represents a pioneering research on the application of heparin as a targeting element of antimalarial drug-loaded nanoparticles.

Joana performed all the main key experiments, particularly those that ended up as figures in the final published manuscript. She also participated in the experimental design and in the preparation of the manuscript draft.

An important result derived from this work is the registration of a patent:

Patent application: ***Heparin-lipidic nanoparticle conjugates****. Inventors: Fernàndez-Busquets, X.,* ***Marques, J.****, Moles, E. Institutions: IBEC, CRESIB. Application number: EP13152187.4; priority countries: Europe; priority date: January 22, 2013.*

2.

Urbán, P., Valle-Delgado, J.J., Mauro, N., **Marques, J.**, Manfredi, A., Rottmann, M., Ranucci, E., Ferruti, P., and Fernàndez-Busquets, X. (2014) Use of poly(amidoamine) drug conjugates for the delivery of antimalarials to *Plasmodium*. *J. Control. Release* **177**, 84-95.

IF 2014: 7.7

In this work, Joana worked with poly(amidoamine) nanoparticles to examine their capacity for being functionalized with heparin. The application of heparin to the targeting of nanocarriers other than heparin is an important aspect that is dealt with in the Discussion of Joana's PhD Thesis.

Joana performed the drug release assays and the blood residence time experiments that were essential for the completion of the manuscript, and which are condensed in Figure 2 and in the Supplementary Material.

3.

Urbán, P., Valle-Delgado, J.J., Moles, E., **Marques, J.**, Díez, C., and Fernàndez-Busquets, X. (2012) Nanotools for the delivery of antimicrobial peptides. *Curr. Drug Targets* **13**, 1158-1172.

IF 2012: 3.8

Joana contributed significantly to the preparation of this review.

4.

Marques, J., Vilanova, E., Mourão, P.A.S., and Fernàndez-Busquets, X. Marine organism sulfated polysaccharides exhibiting significant antimalarial activity and inhibition of red blood cell invasion by *Plasmodium*.

Submitted to *PLOS Pathogens* (September 2015).

In this work, Joana has explored the capacity as antimalarials of heparin-like molecules derived from marine organisms. The polysaccharides assayed are significantly less anticoagulant than heparin and can substitute for it in future innovative antimalarial therapies.

Except for the initial purification of the marine polysaccharides, which was done by the Brazilian group with whom we have an ongoing collaboration, Joana performed all the main key experiments that ended up as figures in the final manuscript. She also participated in the experimental design and in the preparation of the manuscript draft.

5.

Marques, J., Valle-Delgado, J.J., Urbán, P., Baró, E., Prohens, R., Mayor, A., Cisteró, P., Delves, M., Sinden, R., Grandfils, C., Sevrin, C., de Paz, J.L., García-Salcedo, J.A., and Fernàndez-Busquets, X. Adaptation of targeted nanocarriers to changing requirements in antimalarial drug delivery.
In preparation for submission to *J. Control. Release*.

In this final paper of her PhD Thesis, Joana has made an impressive coordination effort in bringing together the expertise of several of our collaborators who have contributed different polysaccharide preparations. The objective of this work has been to explore the capacity of the liposome-heparin nanovectors developed by Joana during her PhD to be adapted to new cell targets, drug cargoes, nanocapsule structures, and targeting polysaccharides. Of particular relevance in this manuscript is the work done by Joana during her stay at the laboratory of Prof. Robert Sinden (Imperial College London).

Except for the initial preparation of some polysaccharides and the force spectroscopy assays, Joana performed all the main key experiments that ended up as figures in the final manuscript. She also participated in the experimental design and in the preparation of the manuscript draft.

Barcelona, September 8, 2015

XAVIER FERNÀNDEZ

Xavier Fernàndez Busquets

PhD Thesis advisor

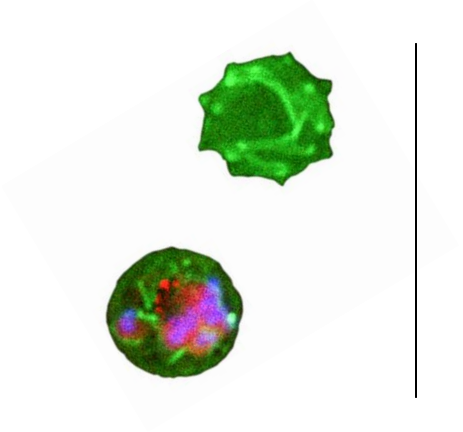

REFERENCES

REFERENCES

1. Carter, R. & Mendis, K. N. Evolutionary and Historical Aspects of the Burden of Malaria. *Clin. Microbiol. Rev.* **15,** 564–594 (2002).

2. Hauck, T. S., Giri, S., Gao, Y. & Chan, W. C. W. Nanotechnology diagnostics for infectious diseases prevalent in developing countries. *Advanced Drug Delivery Reviews* **62,** 438–448 (2010).

3. WHO. *Malaria*. **55,** (2014).

4. Garcia, L. S. Malaria. *Clin. Lab. Med.* **30,** 93–129 (2010).

5. Gething PW, Patil AP, Smith DL, Guerra CA, Elyazar IR, Johnston GL, Tatem AJ, H. S. A new world malaria map: *Plasmodium falciparum* endemicity in 2010. *Malar. J.* **10,** 378 (2011).

6. Rafael ME, Taylor T, Magill A, Lim YW, Girosi F, A. R. Reducing the burden of childhood malaria in Africa: the role of improved. *Nature* **444 Suppl,** 39–48 (2006).

7. Schantz-Dunn, J. & Nour, N. M. Malaria and pregnancy: a global health perspective. *Rev. Obstet. Gynecol.* **2,** 186–92 (2009).

8. Rodrigues, T., Prude, M., Moreira, R., Mota, M. M. & Lopes, F. Targeting the Liver Stage of Malaria Parasites: A Yet Unmet Goal. *J Med Chem* **55,** 995–1012 (2012).

9. Prudêncio, M., Rodriguez, A. & Mota, M. M. The silent path to thousands of merozoites: the *Plasmodium* liver stage. *Nat. Rev. Microbiol.* **4,** 849–856 (2006).

10. Cowman, A. F. & Crabb, B. S. Invasion of red blood cells by malaria parasites. *Cell* **124,** 755–766 (2006).

11. Radfar, A. *et al.* Synchronous culture of *Plasmodium falciparum* at high parasitemia levels. *Nat. Protoc.* **4,** 1899–1915 (2009).

12. Thabata Lopes Alberto Duque, Xênia Macedo Souto, Valter Viana de Andrade-Neto, V. E.-V. and R. F. S. M.-B. in *Immunology and Microbiology 'Autophagy - A Double-Edged Sword - Cell Survival or Death?'* (ed. Bailly, Y.) 289-319 (2013).

13. Griffith, K. S., Lewis, L. S., Mali, S. & Parise, M. E. Treatment of malaria in the United States: a systematic review. *JAMA* **297,** 2264-2277 (2007).

14. Sinden, R. E., Carter, R., Drakeley, C. & Leroy, D. The biology of sexual development of *Plasmodium*: the design and implementation of transmission-blocking strategies. *Malar. J.* **11,** 70 (2012).

15. Delves MJ, Ramakrishnan C, Blagborough AM, Leroy D, Wells TN, S. R. A high-throughput assay for the identification of malarial transmission-blocking drugs and vaccines. *Int. J. Parasitol.* **42,** 999-1006 (2012).

16. Delves, M. J. *Plasmodium* cell biology should inform strategies used in the development of antimalarial transmission-blocking drugs. *Future Med. Chem.* **4,** 2251-63 (2012).

17. Michael Delves, David Plouffe, Christian Scheurer, Stephan Meister, Sergio Wittlin, Elizabeth A. Winzeler, Robert E. Sinden, and D. L. The activities of current antimalarial drugs on the life cycle stages of *Plasmodium*: a comparative study with human and rodent parasites. *PLoS Med.* **9,** e1001169 (2012).

18. Marois, E. The multifaceted mosquito anti-*Plasmodium* response. *Curr. Opin. Microbiol.* **14,** 429-435 (2011).

19. Sinden, R. E. A biologist's perspective on malaria vaccine development. *Hum. Vaccin.* **6,** 3-11 (2010).

20. Leroy, D. *et al.* Defining the biology component of the drug discovery strategy for malaria eradication. *Trends Parasitol.* **30,** 478-490 (2014).

21. Burrows, J. N., van Huijsduijnen, R. H., Möhrle, J. J., Oeuvray, C. & Wells, T. N. C. Designing the next generation of medicines for malaria control and eradication. *Malar. J.* **12,** 187-207 (2013).

22. Kumar, S., Kumari, R. & Pandey, R. New insight-guided approaches to detect, cure, prevent and eliminate malaria. *Protoplasma* (2014). doi:10.1007/s00709-014-0697-x

23. Srinivasan, P. *et al.* Binding of *Plasmodium* merozoite proteins RON2 and AMA1 triggers commitment to invasion. *Proc. Natl. Acad. Sci. U. S. A.* **108,** 13275-80 (2011).

24. Trager, W. & Jensen, J. B. Human malaria parasites in continuous culture. *Science* **193,** 673-675 (1976).

25. Reddy, K. S. *et al.* Bacterially expressed full-length recombinant *Plasmodium falciparum* RH5 protein binds erythrocytes and elicits potent strain-transcending parasite-neutralizing antibodies. *Infect. Immun.* **82,** 152-164 (2014).

26. Huang, B. X. & Kim, H.-Y. Effective identification of Akt interacting proteins by two-step chemical crosslinking, co-immunoprecipitation and mass spectrometry. *PLoS One* **8,** e61430 (2013).

27. Bannister, L. H., Mitchell, G. H., Butcher, G. A., Dennis, E. D. & Cohen, S. Structure and development of the surface coat of erythrocytic merozoites of *Plasmodium knowlesi*. *Cell Tissue Res.* **245,** 281-290 (1986).

28. Cowman, A. F., Berry, D. & Baum, J. The cellular and molecular basis for malaria parasite invasion of the human red blood cell. *J. Cell Biol.* **198,** 961-971 (2012).

29. Dvorak, J. A., Miller, L. H., Whitehouse, W. C. & Shiroishi, T. Invasion of erythrocytes by malaria merozoites. *Science* **187,** 748-750 (1975).

30. Gilson, P. R. & Crabb, B. S. Morphology and kinetics of the three distinct phases of red blood cell invasion by *Plasmodium falciparum* merozoites. *Int. J. Parasitol.* **39,** 91-96 (2009).

31. Boyle, M. J., Richards, J. S., Gilson, P. R., Chai, W. & Beeson, J. G. Interactions with heparin-like molecules during erythrocyte invasion by *Plasmodium falciparum* merozoites. *Blood* **115,** 4559-68 (2010).

32. Goel, V. K. *et al.* Band 3 is a host receptor binding merozoite surface protein 1 during the *Plasmodium falciparum* invasion of erythrocytes. *Proc. Natl. Acad. Sci. U. S. A.* **100,** 5164–5169 (2003).

33. Li, X. *et al.* A Co-ligand Complex Anchors *Plasmodium falciparum* Merozoites to the Erythrocyte Invasion Receptor Band 3. *J. Biol. Chem.* **279,** 5765–5771 (2004).

34. McCormick, C. J., Tuckwell, D. S., Crisanti, A., Humphries, M. J. & Hollingdale, M. R. Identification of heparin as a ligand for the A-domain of *Plasmodium falciparum* thrombospondin-related adhesion protein. *Mol. Biochem. Parasitol.* **100,** 111-124 (1999).

35. Kobayashi, K. *et al.* Analyses of interactions between heparin and the apical surface proteins of *Plasmodium falciparum*. *Sci. Rep.* **3,** 3178 (2013).

36. Osier, F. H. *et al.* New antigens for a multicomponent blood-stage malaria vaccine. *Sci. Transl. Med.* **6,** 247ra102 (2014).

37. Wilson, D. W., Langer, C., Goodman, C. D., McFadden, G. I. & Beeson, J. G. Defining the timing of action of antimalarial drugs against *Plasmodium falciparum*. *Antimicrob. Agents Chemother.* **57,** 1455–1467 (2013).

38. Boyle, M. J., Wilson, D. W. & Beeson, J. G. New approaches to studying *Plasmodium falciparum* merozoite invasion and insights into invasion biology. *Int. J. Parasitol.* **43,** 1-10 (2013).

39. Boyle, M. J. *et al.* Sequential processing of merozoite surface proteins during and after erythrocyte invasion by *Plasmodium falciparum*. *Infect. Immun.* **82,** 924–936 (2014).

40. Valle-Delgado, J. J., Urbán, P. & Fernàndez-Busquets, X. Demonstration of specific binding of heparin to *Plasmodium falciparum*-infected vs. non-infected red blood cells by single-molecule force spectroscopy. *Nanoscale* **5,** 3673–80 (2013).

41. Idro, R., Jenkins, N. E. & Newton, C. R. J. C. Pathogenesis, clinical features, and neurological outcome of cerebral malaria. *Lancet Neurol.* **4,** 827–840 (2005).

42. Rowe, J. A., Claessens, A., Corrigan, R. A. & Arman, M. Adhesion of *Plasmodium falciparum*-infected erythrocytes to human cells: molecular mechanisms and therapeutic implications. *Expert Rev. Mol. Med.* **11,** e16 (2009).

43. Cooke, B. M., Wahlgren, M. & Coppel, R. L. Molecular Approaches to Malaria *Falciparum* Malaria : Sticking up , Standing out and Out-standing. *Parasitol. Today* **16,** 416-420 (2000).

44. Cooke, B. M., Mohandas, N. & Coppel, R. L. The malaria-infected red blood cell: structural and functional changes. *Adv. Parasitol.* **50,** 1-86 (2001).

45. Scherf, A., Lopez-Rubio, J. J. & Riviere, L. Antigenic variation in *Plasmodium falciparum*. *Annu. Rev. Microbiol.* **62,** 445-470 (2008).

46. Zilversmit, M. M. *et al.* Hypervariable antigen genes in malaria have ancient roots. *BMC Evol. Biol.* **13,** 110 (2013).

47. Su, X. Z. *et al.* The large diverse gene family var encodes proteins involved in cytoadherence and antigenic variation of *Plasmodium falciparum*-infected erythrocytes. *Cell* **82,** 89-100 (1995).

48. Smith, J. D. *et al.* Switches in expression of *Plasmodium falciparum* var genes correlate with changes in antigenic and cytoadherent phenotypes of infected erythrocytes. *Cell* **82,** 101-110 (1995).

49. Baruch, D. I. *et al.* Cloning the *P. falciparum* gene encoding PfEMP1, a malarial variant antigen and adherence receptor on the surface of parasitized human erythrocytes. *Cell* **82,** 77-87 (1995).

50. Pologe, L. G., Pavlovec, A., Shio, H. & Ravetch, J. V. Primary structure and subcellular localization of the knob-associated histidine-rich protein of *Plasmodium falciparum*. *Proc. Natl. Acad. Sci. U. S. A.* **84,** 7139-7143 (1987).

51. Culvenor, J. G. *et al.* *Plasmodium falciparum*: identification and localization of a knob protein antigen expressed by a cDNA clone. *Exp. Parasitol.* **63,** 58-67 (1987).

52. Ganguly, A. K., Ranjan, P., Kumar, A. & Bhavesh, N. S. Dynamic association of PfEMP1 and KAHRP in knobs mediates cytoadherence during *Plasmodium* invasion. *Sci. Rep.* **5,** 8617 (2015).

53. Maubert, B., Guilbert, L. J. & Deloron, P. Cytoadherence of *Plasmodium falciparum* to intercellular adhesion molecule 1 and chondroitin-4-sulfate expressed by the syncytiotrophoblast in the human placenta. *Infect. Immun.* **65,** 1251-1257 (1997).

54. MacPherson, G. G., Warrell, M. J., White, N. J., Looareesuwan, S. & Warrell, D. A. Human cerebral malaria. A quantitative ultrastructural analysis of parasitized erythrocyte sequestration. *Am. J. Pathol.* **119,** 385-401 (1985).

55. Cooke, B. M., Mohandas, N. & Coppel, R. L. Malaria and the red blood cell membrane. *Semin. Hematol.* **41,** 173-188 (2004).

56. Niang, M. *et al.* STEVOR is a *Plasmodium falciparum* erythrocyte binding protein that mediates merozoite invasion and rosetting. *Cell Host Microbe* **16,** 81-93 (2014).

57. Barragan, a *et al.* The duffy-binding-like domain 1 of *Plasmodium falciparum* erythrocyte membrane protein 1 (PfEMP1) is a heparan sulfate ligand that requires 12 mers for binding. *Blood* **95,** 3594-9 (2000).

58. Carlson, J. & Wahlgren, M. *Plasmodium falciparum* erythrocyte rosetting is mediated by promiscuous lectin-like interactions. *J. Exp. Med.* **176,** 1311-1317 (1992).

59. Angus, B. J., Thanikkul, K., Silamut, K., White, N. J. & Udomsangpetch, R. Short report: Rosette formation in *Plasmodium ovale* infection. *Am. J. Trop. Med. Hyg.* **55,** 560-561 (1996).

60. Chotivanich, K. T., Pukrittayakamee, S., Simpson, J. A., White, N. J. & Udomsangpetch, R. Characteristics of *Plasmodium vivax*-infected erythrocyte rosettes. *Am. J. Trop. Med. Hyg.* **59,** 73-76 (1998).

61. David, P. H., Handunnetti, S. M., Leech, J. H., Gamage, P. & Mendis, K. N. Rosetting: a new cytoadherence property of malaria-infected erythrocytes. *Am. J. Trop. Med. Hyg.* **38,** 289-297 (1988).

62. Mackinnon, M. J., Walker, P. R. & Rowe, J. A. *Plasmodium chabaudi*: rosetting in a rodent malaria model. *Exp. Parasitol.* **101,** 121-128

63. Udomsangpetch, R., Brown, A. E., Smith, C. D. & Webster, H. K. Rosette formation by *Plasmodium coatneyi*-infected red blood cells. *Am. J. Trop. Med. Hyg.* **44,** 399-401 (1991).

64. Rowe, A., Obeiro, J., Newbold, C. I. & Marsh, K. *Plasmodium falciparum* rosetting is associated with malaria severity in Kenya. *Infect. Immun.* **63,** 2323-2326 (1995).

65. Carlson, J. *et al.* Human cerebral malaria: association with erythrocyte rosetting and lack of anti-rosetting antibodies. *Lancet (London, England)* **336,** 1457-1460 (1990).

66. Vigan-Womas, I. *et al.* An *in vivo* and *in vitro* model of *Plasmodium falciparum* rosetting and autoagglutination mediated by varO, a group A var gene encoding a frequent serotype. *Infect. Immun.* **76,** 5565-5580 (2008).

67. Chen, Q. *et al.* The semiconserved head structure of *Plasmodium falciparum* erythrocyte membrane protein 1 mediates binding to multiple independent host receptors. *J. Exp. Med.* **192,** 1-10 (2000).

68. Rowe, J. A., Moulds, J. M., Newbold, C. I. & Miller, L. H. *P. falciparum* rosetting mediated by a parasite-variant erythrocyte membrane protein and complement-receptor 1. *Nature* **388,** 292-295 (1997).

69. Reyburn, H. *et al.* Rapid diagnostic tests compared with malaria microscopy for guiding outpatient treatment of febrile illness in Tanzania: randomised trial. *BMJ* **334,** 403 (2007).

70. Moody, A. Rapid diagnostic tests for malaria parasites. *Clinical Microbiology Reviews* **15,** 66-78 (2002).

71. Johnston, S. P. *et al.* PCR as a confirmatory technique for laboratory diagnosis of malaria. *J. Clin. Microbiol.* **44,** 1087-1089 (2006).

72. Miotto, O. *et al.* Multiple populations of artemisinin-resistant *Plasmodium falciparum* in Cambodia. *Nat. Genet.* **45,** 648-655 (2013).

73. Liu, N. Insecticide Resistance in Mosquitoes: Impact, Mechanisms, and Research Directions. *Annu. Rev. Entomol.* **60,** 537–559 (2015).

74. Bejon, P. *et al.* Efficacy of RTS,S malaria vaccines: individual-participant pooled analysis of phase 2 data. *Lancet. Infect. Dis.* **13,** 319–327 (2013).

75. Ockenhouse, C. F. *et al.* Ad35.CS.01 - RTS,S/AS01 Heterologous Prime Boost Vaccine Efficacy against Sporozoite Challenge in Healthy Malaria-Naïve Adults. *PLoS One* **10,** e0131571 (2015).

76. Cowman, A. F. & Crabb, B. S. Invasion of red blood cells by malaria parasites. *Cell* **124,** 755-66 (2006).

77. Farooq, U. & Mahajan, R. C. Drug resistance in malaria. *Journal of Vector Borne Diseases* **41,** 45–53 (2004).

78. World Health Organization. *Guidelines for the treatment of malaria, 2nd edition*. *WHO* (2010). doi:WHO Library Cataloguing-in-Publication Data

79. Winstanley, P. & Ward, S. Malaria Chemotherapy. *Advances in Parasitology* **61,** 47–76 (2006).

80. European Science Foundation. *Nanomedicine, an ESF-European Medical Research Councils (EMRC) Forward Look report*. (2015).

81. Urbán, P. *et al.* Nanotools for the Delivery of Antimicrobial Peptides. *Curr. Drug Targets* (2012).

82. Boisseau, P. & Loubaton, B. Nanomedicine, nanotechnology in medicine. *Comptes Rendus Phys.* **12,** 620–636 (2011).

83. Kamaly, N., Xiao, Z., Valencia, P. M., Radovic-Moreno, A. F. & Farokhzad, O. C. Targeted polymeric therapeutic nanoparticles: design, development and clinical translation. *Chemical Society Reviews* **41,** 2971–3010 (2012).

84. Santos-Magalhães, N. S. & Mosqueira, V. C. F. Nanotechnology applied to the treatment of malaria. *Adv. Drug Deliv. Rev.* **62,** 560–575 (2010).

85. Orive, G., Hernández, R. M., Gascón, A. R., Domínguez-Gil, A. & Pedraz, J. L. Drug delivery in biotechnology: Present and future. *Current Opinion in Biotechnology* **14,** 659-664 (2003).

86. White, N. J. Assessment of the pharmacodynamic properties of antimalarial drugs *in vivo*. *Antimicrob. Agents Chemother.* **41,** 1413-1422 (1997).

87. Rajakumar, G. *et al.* Antiplasmodial activity of eco-friendly synthesized palladium nanoparticles using Eclipta prostrata extract against Plasmodium berghei in Swiss albino mice. *Parasitol. Res.* **114,** 1397-1406 (2015).

88. Maurer, N., Fenske, D. B. & Cullis, P. R. Developments in liposomal drug delivery systems. *Expert Opin. Biol. Ther.* **1,** 923-947 (2001).

89. Fontaine, S. D. *et al.* Drug Delivery to the Malaria Parasite Using an Arterolane-Like Scaffold. *ChemMedChem* **10,** 47-51 (2015).

90. Urbán, P., Estelrich, J., Adeva, A., Cortés, A. & Fernàndez-Busquets, X. Study of the efficacy of antimalarial drugs delivered inside targeted immunoliposomal nanovectors. *Nanoscale Res. Lett.* **6,** 620 (2011).

91. Ogutu, B. *et al.* Preparation, characterization, and optimization of primaquine-loaded solid lipid nanoparticles. *Int. J. Nanomedicine* **9,** 3865-3874 (2014).

92. Murambiwa, P., Masola, B., Govender, T., Mukaratirwa, S. & Musabayane, C. T. Anti-malarial drug formulations and novel delivery systems: A review. *Acta Tropica* **118,** 71-79 (2011).

93. Fernàndez-Busquets, X. Heparin-functionalized nanocapsules: enabling targeted delivery of antimalarial drugs. *Future Med. Chem.* **5,** 737-739 (2013).

94. Immordino, M. L., Dosio, F. & Cattel, L. Stealth liposomes: review of the basic science, rationale, and clinical applications, existing and potential. *Int. J. Nanomedicine* **1,** 297-315 (2006).

95. Katyayani, M. and Sivasankar, T. Liposomes - The Future of Formulations. *Int. J. Res. Pharm. Chem.* **1,** 259-267 (2011).

96. Mufamadi, M. S. *et al.* A review on composite liposomal technologies for specialized drug delivery. *J. Drug Deliv.* **2011,** 1–19 (2011).

97. Yang, F. *et al.* Liposome based delivery systems in pancreatic cancer treatment: from bench to bedside. *Cancer Treat. Rev.* **37,** 633–642 (2011).

98. Jasmine, D. & Tushar, T. Role Of Liposomes In Nanotechnology And Drug Delivery. *Int. J. Drug Dev. Res.* **3,** 341–350 (2011).

99. Casals, E., Galán, A. M., Escolar, G., Gallardo, M. & Estelrich, J. Physical stability of liposomes bearing hemostatic activity. *Chem. Phys. Lipids* **125,** 139–146 (2003).

100. Tran, M. A., Watts, R. J. & Robertson, G. P. Use of liposomes as drug delivery vehicles for treatment of melanoma. *Pigment Cell and Melanoma Research* **22,** 388–399 (2009).

101. Damen, J., Regts, J. & Scherphof, G. Transfer and exchange of phospholipid between small unilamellar liposomes and rat plasma high density lipoproteins. Dependence on cholesterol content and phospholipid composition. *Biochim. Biophys. Acta* **665,** 538–345 (1981).

102. Čeh, B., Winterhalter, M., Frederik, P. M., Vallner, J. J. & Lasic, D. D. Stealth® liposomes: From theory to product. in *Advanced Drug Delivery Reviews* **24,** 165–177 (1997).

103. Bucior, I. & Burger, M. M. Carbohydrate–carbohydrate interactions in cell recognition. *Current Opinion in Structural Biology* **14,** 631–637 (2004).

104. Marques, J. *et al.* Application of heparin as a dual agent with antimalarial and liposome targeting activities toward *Plasmodium*-infected red blood cells. *Nanomedicine* **10,** 1719–1728 (2014).

105. Torchilin, V. P. Recent advances with liposomes as pharmaceutical carriers. *Nat. Rev. Drug Discov.* **4,** 145–160 (2005).

106. Mitchell, J. P., Roberts, K. D., Langley, J., Koentgen, F. & Lambert, J. N. A direct method for the formation of peptide and carbohydrate dendrimers. *Bioorganic Med. Chem. Lett.* **9,** 2785–2788 (1999).

107. Mishra, G. P., Bagui, M., Tamboli, V. & Mitra, A. K. Recent applications of liposomes in ophthalmic drug delivery. *J. Drug Deliv.* **2011**, 1–14 (2011).

108. Paleos, C. M., Tsiourvas, D., Sideratou, Z. & Tziveleka, L.-A. Drug delivery using multifunctional dendrimers and hyperbranched polymers. *Expert Opin. Drug Deliv.* **7**, 1387–1398 (2010).

109. Tiwari, A. K., Gajbhiye, V., Sharma, R. & Jain, N. K. Carrier mediated protein and peptide stabilization. *Drug Deliv.* **17**, 605–616 (2010).

110. Ferruti, P., Marchisio, M. a. & Duncan, R. Poly(amido-amine)s: Biomedical Applications. *Macromol. Rapid Commun.* **23**, 332–355 (2002).

111. Marchisio, M. A., Longo, T. & Ferruti, P. A selective de-heparinizer filter made of new cross-linked polymers of a poly-amido-amine structure. *Experientia* **29**, 93–95 (1973).

112. Duncan, R. The dawning era of polymer therapeutics. *Nat. Rev. Drug Discov.* **2**, 347–360 (2003).

113. Urban, P. & Fernandez-Busquets, X. Nanomedicine Against Malaria. *Curr. Med. Chem.* **21**, 605–629 (2014).

114. Khandare, J. & Minko, T. Polymer-drug conjugates: Progress in polymeric prodrugs. *Progress in Polymer Science (Oxford)* **31**, 359–397 (2006).

115. Urbán, P., Estelrich, J., Cortés, A. & Fernàndez-Busquets, X. A nanovector with complete discrimination for targeted delivery to *Plasmodium falciparum*-infected versus non-infected red blood cells *in vitro*. *J. Control. Release* **151**, 202–211 (2011).

116. Moles, E. *et al.* Immunoliposome-mediated drug delivery to *Plasmodium*-infected and non-infected red blood cells as a dual therapeutic/prophylactic antimalarial strategy. *J. Control. Release* **210**, 217–229 (2015).

117. Payal Agrawal, Umesh Gupta, N. K. J. Glycoconjugated peptide dendrimers-based nanoparticulate system for the delivery of chloroquine phosphate. *Biomaterials* **28**, 3349–3359 (2007).

118. Ganesan, S., Tekwani, B. L., Sahu, R., Tripathi, L. M. & Walker, L. a. Cytochrome P(450)-dependent toxic effects of primaquine on human erythrocytes. *Toxicol. Appl. Pharmacol.* **241,** 14–22 (2009).

119. Agrawal, A. K., Singhal, A. & Gupta, C. M. Functional drug targeting to erythrocytes *in vivo* using antibody bearing liposomes as drug vehicles. *Biochem. Biophys. Res. Commun.* **148,** 357–361 (1987).

120. Joshi, M., Pathak, S., Sharma, S. & Patravale, V. Design and *in vivo* pharmacodynamic evaluation of nanostructured lipid carriers for parenteral delivery of artemether: Nanoject. *Int. J. Pharm.* **364,** 119–126 (2008).

121. Urbán, P. *et al.* Use of poly(amidoamine) drug conjugates for the delivery of antimalarials to *Plasmodium*. *J. Control. Release* **177,** 84–95 (2014).

122. Glenister, F. K., Coppel, R. L., Cowman, A. F., Mohandas, N. & Cooke, B. M. Contribution of parasite proteins to altered mechanical properties of malaria-infected red blood cells. *Blood* **99,** 1060–1063 (2002).

123. Cooke, B. M., Stuart, J. & Nash, G. B. The cellular and molecular rheology of malaria. *Biorheology* **51,** 99–119 (2014).

124. Haldar, K. & Mohandas, N. Erythrocyte remodeling by malaria parasites. *Curr. Opin. Hematol.* **14,** 203–209 (2007).

125. Martin, R. E. & Kirk, K. Transport of the essential nutrient isoleucine in human erythrocytes infected with the malaria parasite *Plasmodium falciparum*. *Blood* **109,** 2217–2224 (2007).

126. Nakamura, K., Hasler, T., Morehead, K., Howard, R. J. & Aikawa, M. *Plasmodium falciparum*-infected erythrocyte receptor(s) for CD36 and thrombospondin are restricted to knobs on the erythrocyte surface. *J. Histochem. Cytochem.* **40,** 1419–1422 (1992).

127. Maier, A. G., Cooke, B. M., Cowman, A. F. & Tilley, L. Malaria parasite proteins that remodel the host erythrocyte. *Nat. Rev. Microbiol.* **7,** 341–354 (2009).

128. Marti, M., Baum, J., Rug, M., Tilley, L. & Cowman, A. F. Signal-mediated export of proteins from the malaria parasite to the host erythrocyte. *J. Cell Biol.* **171,** 587–592 (2005).

129. Goodyer, I. D., Pouvelle, B., Schneider, T. G., Trelka, D. P. & Taraschi, T. F. Characterization of macromolecular transport pathways in malaria-infected erythrocytes. *Mol. Biochem. Parasitol.* **87,** 13-28 (1997).

130. Lyon, J. A., Carter, J. M., Thomas, A. W. & Chulay, J. D. Merozoite surface protein-1 epitopes recognized by antibodies that inhibit *Plasmodium falciparum* merozoite dispersal. *Mol. Biochem. Parasitol.* **90,** 223-234 (1997).

131. Bergmann-Leitner, E. S., Duncan, E. H. & Angov, E. MSP-1p42-specific antibodies affect growth and development of intra-erythrocytic parasites of *Plasmodium falciparum*. *Malar. J.* **8,** 183 (2009).

132. Owais, M., Varshney, G. C., Choudhury, A., Chandra, S. & Gupta, C. M. Chloroquine encapsulated in malaria-infected erythrocyte-specific antibody-bearing liposomes effectively controls chloroquine-resistant *Plasmodium berghei* infections in mice. *Antimicrob. Agents Chemother.* **39,** 180-184 (1995).

133. Singhal, A. & Gupta, C. M. Antibody-mediated targeting of liposomes to red cells *in vivo*. *FEBS Lett.* **201,** 321-326 (1986).

134. Costa, L. S. *et al.* Biological activities of sulfated polysaccharides from tropical seaweeds. *Biomed. Pharmacother.* **64,** 21-28 (2010).

135. Pomin, V. H. Structural and functional insights into sulfated galactans: a systematic review. *Glycoconj. J.* **27,** 1-12 (2010).

136. Nader, H. B., Lopes, C. C., Rocha, H. A. O., Santos, E. A. & Dietrich, C. P. Heparins and heparinoids: occurrence, structure and mechanism of antithrombotic and hemorrhagic activities. *Curr. Pharm. Des.* **10,** 951-966 (2004).

137. Vogt, A. M. *et al.* Release of sequestered malaria parasites upon injection of a glycosaminoglycan. *PLoS Pathog.* **2,** e100 (2006).

138. Anna M. Vogt, Antonio Barragan, Qijun Chen, Fred Kironde, D. S. and M. W. Heparan sulfate on endothelial cells mediates the binding of P*lasmodium falciparum*-infected erythrocytes via the DBL1alpha domain of PfEMP1. *Blood* **101,** 2405-11 (2003).

139. Gemma, E., Meyer, O., Uhrín, D. & Hulme, A. N. Enabling methodology for the end functionalization of glycosaminoglycan oligosaccharides. *Mol. Biosyst.* **4,** 481-95 (2008).

140. Norman, R. 100 years. Looking back. Skill, drive and luck: the discovery and development of heparin. *CMAJ* **183,** 2139-40 (2011).

141. Martel-Pelletier, J., Farran, A., Montell, E., Vergés, J. & Pelletier, J.-P. Discrepancies in composition and biological effects of different formulations of chondroitin sulfate. *Molecules* **20,** 4277-4289 (2015).

142. Gainsford, G. J., Schwörer, R., Tyler, P. C. & Zubkova, O. V. Crystal packing in three related disaccharides: precursors to heparan sulfate oligosaccharides. *Acta Crystallogr. Sect. E, Crystallogr. Commun.* **71,** 582-587 (2015).

143. Goel, S. & Gowda, D. C. How specific is *Plasmodium falciparum* adherence to chondroitin 4-sulfate? *Trends Parasitol.* **27,** 375-381 (2011).

144. Higgins, M. K. The structure of a chondroitin sulfate-binding domain important in placental malaria. *J. Biol. Chem.* **283,** 21842-21846 (2008).

145. Ancsin, J. B. & Kisilevsky, R. A binding site for highly sulfated heparan sulfate is identified in the N terminus of the circumsporozoite protein: significance for malarial sporozoite attachment to hepatocytes. *J. Biol. Chem.* **279,** 21824-32 (2004).

146. Xiao, L., Yang, C., Patterson, P. S., Udhayakumar, V. & Lal, A. A. Sulfated polyanions inhibit invasion of erythrocytes by plasmodial merozoites and cytoadherence of endothelial cells to parasitized erythrocytes. *Infect. Immun.* **64,** 1373-1378 (1996).

147. Yan Zhang, Ning Jiang, Huijun Lu, Nan Hou, Xianyu Piao, Pengfei Cai, Jigang Yin, Mats Wahlgren, and Q. C. Proteomic Analysis of *Plasmodium falciparum* Schizonts Reveals Heparin-Binding Merozoite Proteins. *J. Proteome Res.* **12,** 2185-2193 (2013).

148. Kulane, A. *et al.* Effect of different fractions of heparin on *Plasmodium falciparum* merozoite invasion of red blood cells *in vitro*. *Am. J. Trop. Med. Hyg.* **46,** 589-94 (1992).

149. Xiao, L., Yang, C., Patterson, P. S., Udhayakumar, V. & Lal, A. A. Sulfated polyanions inhibit invasion of erythrocytes by plasmodial merozoites and cytoadherence of endothelial cells to parasitized erythrocytes. *Infect. Immun.* **64,** 1373-8 (1996).

150. Bastos, M. F. *et al.* Fucosylated chondroitin sulfate inhibits *Plasmodium falciparum* cytoadhesion and merozoite invasion. *Antimicrob. Agents Chemother.* **58,** 1862-1871 (2014).

151. Butcher, G. A., Parish, C. R. & Cowden, W. B. Inhibition of growth *in vitro* of *Plasmodium falciparum* by complex polysaccharides. *Trans. R. Soc. Trop. Med. Hyg.* **82,** 558-559 (1988).

152. Evans, S. G., Morrison, D., Kaneko, Y. & Havlik, I. The effect of curdlan sulphate on development *in vitro* of *Plasmodium falciparum*. *Trans. R. Soc. Trop. Med. Hyg.* **92,** 87-89

153. Clark, D. L., Su, S. & Davidson, E. A. Saccharide anions as inhibitors of the malaria parasite. *Glycoconj. J.* **14,** 473-479 (1997).

154. Chen, B. Q. *et al.* Identification of *Plasmodium falciparum* Erythrocyte Membrane Protein 1 (PfEMP1) as the Rosetting Ligand of the Malaria. *J. Exp. Med.* **187,** 15-23 (1998).

155. Rowe, A., Berendt, A. R., Marsh, K. & Newbold, C. I. *Plasmodium falciparum*: a family of sulphated glycoconjugates disrupts erythrocyte rosettes. *Exp. Parasitol.* **79,** 506-516 (1994).

156. Adams, Y. *et al.* Inhibition of *Plasmodium falciparum* growth *in vitro* and adhesion to chondroitin-4-sulfate by the heparan sulfate mimetic PI-88 and other sulfated oligosaccharides. *Antimicrob. Agents Chemother.* **50,** 2850-2 (2006).

157. Hirsh, J., Anand, S. S., Halperin, J. L. & Fuster, V. Guide to anticoagulant therapy: Heparin : a statement for healthcare professionals from the American Heart Association. *Circulation* **103,** 2994-3018 (2001).

158. Rampengan, T. H. Cerebral malaria in children. Comparative study between heparin, dexamethasone and placebo. *Paediatr. Indones.* **31,** 59-66

159. Leitgeb, A. M. *et al.* Low anticoagulant heparin disrupts *Plasmodium falciparum* rosettes in fresh clinical isolates. *Am. J. Trop. Med. Hyg.* **84,** 390-396 (2011).

160. Miura, Y., Aoyagi, S., Kusada, Y. & Miyamoto, K. The characteristics of anticoagulation by covalently immobilized heparin. *J. Biomed. Mater. Res.* **14,** 619-630 (1980).

161. Li, F. *et al. Plasmodium* ookinete-secreted proteins secreted through a common micronemal pathway are targets of blocking malaria transmission. *J. Biol. Chem.* **279,** 26635-44 (2004).

162. Dinglasan, R. R. *et al. Plasmodium falciparum* ookinetes require mosquito midgut chondroitin sulfate proteoglycans for cell invasion. *Proc. Natl. Acad. Sci. U. S. A.* **104,** 15882-7 (2007).

163. Mathias, D. K. *et al.* A small molecule glycosaminoglycan mimetic blocks *Plasmodium* invasion of the mosquito midgut. *PLoS Pathog.* **9,** e1003757 (2013).

164. Mourão, P. A. . *et al.* Inactivation of Thrombin by a Fucosylated Chondroitin Sulfate from Echinoderm. *Thromb. Res.* **102,** 167-176 (2001).

165. Mourao, P. A. S. *et al.* Structure and anticoagulant activity of a fucosylated chondroitin sulfate from echinoderm. Sulfated fucose branches on the polysaccharide account for its high anticoagulant action. *J. Biol. Chem.* **271,** 23973-23984 (1996).

166. Borsig, L. *et al.* Selectin blocking activity of a fucosylated chondroitin sulfate glycosaminoglycan from sea cucumber: Effect on tumor metastasis and neutrophil recruitment. *J. Biol. Chem.* **282,** 14984-14991 (2007).

167. Pomin, V. H. & Mourão, P. A. S. Structure, biology, evolution, and medical importance of sulfated fucans and galactans. *Glycobiology* **18,** 1016-27 (2008).

168. Pomin, V. H. & Mourão, P. A. S. Specific sulfation and glycosylation-a structural combination for the anticoagulation of marine carbohydrates. *Front. Cell. Infect. Microbiol.* **4,** 1-8 (2014).

169. Glauser, B. F., Pereira, M. S., Monteiro, R. Q. & Mourão, P. A. S. Serpin-independent anticoagulant activity of a fucosylated chondroitin sulfate. *Thromb. Haemost.* **100,** 420–428 (2008).

170. Pavão, M. S. G. Glycosaminoglycans analogs from marine invertebrates: structure, biological effects, and potential as new therapeutics. *Front. Cell. Infect. Microbiol.* **4,** 123 (2014).

171. Mourão, P. A. S. Perspective on the Use of Sulfated Polysaccharides from Marine Organisms as a Source of New Antithrombotic Drugs. *Mar. Drugs* **13,** 2770–2784 (2015).

172. Alonso, P. L. Malaria: Deploying a candidate vaccine (RTS,S/AS02A) for an old scourge of humankind. *International Microbiology* **9,** 83–93 (2006).

173. Daily, J. P. Antimalarial drug therapy: the role of parasite biology and drug resistance. *J. Clin. Pharmacol.* **46,** 1487–1497 (2006).

174. Alonso, P. L. & Tanner, M. Public health challenges and prospects for malaria control and elimination. *Nat. Med.* **19,** 150–155 (2013).

175. Marques, S. R. *et al.* An essential role of the basal body protein SAS-6 in *Plasmodium* male gamete development and malaria transmission. *Cell. Microbiol.* **17,** 191–206 (2015).

176. Kyes, S., Horrocks, P. & Newbold, C. Antigenic variation at the infected red cell surface in malaria. *Annu. Rev. Microbiol.* **55,** 673–707 (2001).

177. Miller, L. H., Baruch, D. I., Marsh, K. & Doumbo, O. K. The pathogenic basis of malaria. **415,** 673–679 (2002).

178. Robert, C. *et al.* Chondroitin-4-sulphate (proteoglycan) a receptor for *Plasmodium falciparum*-infected erythrocyte adherence on brain microvascular endothelial cells. *Res. Immunol.* **146,** 383–393 (1995).

179. Cooke, B. M., Rogerson, S. J., Brown, G. V & Coppel, R. L. Adhesion of malaria-infected red blood cells to chondroitin sulfate A under flow conditions. *Blood* **88,** 4040–4044 (1996).

180. Beeson, J. G. *et al.* Structural basis for binding of *Plasmodium falciparum* erythrocyte membrane protein 1 to chondroitin sulfate and placental tissue and the influence of protein polymorphisms on binding specificity. *J. Biol. Chem.* **282,** 22426–22436 (2007).

181. Andrews, K. T., Klatt, N., Adams, Y., Mischnick, P. & Schwartz-albiez, R. Inhibition of Chondroitin-4-Sulfate-Specific Adhesion of *Plasmodium falciparum*-Infected Erythrocytes by Sulfated Polysaccharides. **73,** 4288–4294 (2005).

182. Vogt, A. M. *et al.* Heparan sulfate on endothelial cells mediates the binding of *Plasmodium falciparum*-infected erythrocytes via the DBL1alpha domain of PfEMP1. *Blood* **101,** 2405–11 (2003).

183. Pancake, S. J., Holt, G. D., Mellouk, S. & Hoffman, S. L. Malaria sporozoites and circumsporozoite protein bind sulfated glycans: carbohydrate binding properties predicted from sequence homologies with other lectins. *Parassitologia* **35 Suppl,** 77–80 (1993).

184. Frevert, U. *et al.* Malaria circumsporozoite protein binds to heparan sulfate proteoglycans associated with the surface membrane of hepatocytes. *J. Exp. Med.* **177,** 1287–1298 (1993).

185. Capila, I. & Linhardt, R. J. Heparin-protein interactions. *Angew. Chem. Int. Ed. Engl.* **41,** 391–412 (2002).

186. Andrade, G. P. V *et al.* A heparin-like compound isolated from a marine crab rich in glucuronic acid 2-O-sulfate presents low anticoagulant activity. *Carbohydr. Polym.* **94,** 647–54 (2013).

187. Chen, Q. *et al.* Identification of *Plasmodium falciparum* erythrocyte membrane protein 1 (PfEMP1) as the rosetting ligand of the malaria parasite *P. falciparum*. *J. Exp. Med.* **187,** 15–23 (1998).

188. Juillerat, A. *et al.* Biochemical and biophysical characterisation of DBL1α1-varO, the rosetting domain of PfEMP1 from the VarO line of *Plasmodium falciparum*. *Mol. Biochem. Parasitol.* **170,** 84–92 (2010).

189. Juillerat, A. *et al.* Structure of a *Plasmodium falciparum* PfEMP1 rosetting domain reveals a role for the N-terminal segment in heparin-mediated rosette inhibition. *Proc. Natl. Acad. Sci. U. S. A.* **108,** 5243–5248 (2011).

190. Sheehy, T. W. Complications of *Falciparum* Malaria and Their Treatment. *Ann. Intern. Med.* **66,** 807 (1967).

191. Jaroonvesama, N. Intravascular coagulation in *falciparum* malaria. *Lancet (London, England)* **1,** 221–3 (1972).

192. Munir, M., Tjandra, H., Rampengan, T. H., Mustadjab, I. & Wulur, F. H. Heparin in the treatment of cerebral malaria. *Paediatr. Indones.* **20,** 47–50

193. Passirani, C., Barratt, G., Devissaguet, J. P. & Labarre, D. Interactions of nanoparticles bearing heparin or dextran covalently bound to poly(methyl methacrylate) with the complement system. *Life Sci.* **62,** 775–785 (1998).

194. Zhang, J. *et al.* Long-circulating heparin-functionalized magnetic nanoparticles for potential application as a protein drug delivery platform. *Mol. Pharm.* **10,** 3892–3902 (2013).

195. Pouvelle, B. *et al.* Direct access to serum macromolecules by intraerythrocytic malaria parasites. *Nature* **353,** 73–75 (1991).

196. Palivan, C. G., Beck, H. & Meier, W. Nanomimics of Host Cell Membranes Block Invasion and Expose Invasive. *ACS Nano* (2014).

197. Colliec-Jouault, S., Bavington, C. & Delbarre-Ladrat, C. Heparin-like entities from marine organisms. *Handb. Exp. Pharmacol.* **207,** 423–449 (2012).

198. Shanmugam, M. & Mody, K. H. Heparinoid-active sulphated polysaccharides from marine algae as potential blood anticoagulant agents. *Current Science* **79,** 1672–1683 (2000).

199. Quinderé, A. L. G. *et al.* Is the antithrombotic effect of sulfated galactans independent of serpin? *J. Thromb. Haemost.* **12,** 43–53 (2014).

200. Melo, F. R., Pereira, M. S., Foguel, D. & Mourão, P. A. S. Antithrombin-mediated anticoagulant activity of sulfated polysaccharides: Different

mechanisms for heparin and sulfated galactans. *J. Biol. Chem.* **279,** 20824-20835 (2004).

201. Recuenco, F. C. *et al.* Gellan sulfate inhibits *Plasmodium falciparum* growth and invasion of red blood cells *in vitro*. *Sci. Rep.* **4,** 4723 (2014).

202. Fernàndez-Busquets, X. Toy kit against malaria: magic bullets, LEGO, Trojan horses and Russian dolls. *Ther. Deliv.* **5,** 1049-1052 (2014).

203. Osmond, R. I. W., Kett, W. C., Skett, S. E. & Coombe, D. R. Protein-heparin interactions measured by BIAcore 2000 are affected by the method of heparin immobilization. *Anal. Biochem.* **310,** 199-207 (2002).

204. Looareesuwan, S. *et al.* Clinical studies of atovaquone, alone or in combination with other antimalarial drugs, for treatment of acute uncomplicated malaria in Thailand. *Am. J. Trop. Med. Hyg.* **54,** 62-66 (1996).

205. Press release - Dilaforette. (2015). at <http://www.dilaforette.se/arkiv/649>

206. Bricarello, D. A., Patel, M. A. & Parikh, A. N. Inhibiting host-pathogen interactions using membrane-based nanostructures. *Trends in Biotechnology* **30,** 323-330 (2012).

207. Rinaudo, M. Main properties and current applications of some polysaccharides as biomaterials. *Polym. Int.* **57,** 397-430 (2008).

208. Suh, J. K. & Matthew, H. W. Application of chitosan-based polysaccharide biomaterials in cartilage tissue engineering: a review. *Biomaterials* **21,** 258925-98 (2000).

209. Sivakumar, M. Preparation, characterization and in-vitro release of gentamicin from coralline hydroxyapatite-chitosan composite microspheres. *Carbohydr. Polym.* **49,** 281-288 (2002).

210. VandeVord, P. J. *et al.* Evaluation of the biocompatibility of a chitosan scaffold in mice. *J. Biomed. Mater. Res.* **59,** 585-590 (2002).

211. Khor, E. & Lim, L. Y. Implantable applications of chitin and chitosan. *Biomaterials* **24,** 2339-2349 (2003).

212. Sébastien, F., Stéphane, G., Copinet, A. & Coma, V. Novel biodegradable films made from chitosan and poly(lactic acid) with antifungal properties against mycotoxinogen strains. *Carbohydr. Polym.* **65,** 185–193 (2006).

213. Verma, D., Katti, K. S., Katti, D. R. & Mohanty, B. Mechanical response and multilevel structure of biomimetic hydroxyapatite/polygalacturonic/chitosan nanocomposites. *Mater. Sci. Eng. C* **28,** 399–405 (2008).

214. Katti, K. S., Katti, D. R. & Dash, R. Synthesis and characterization of a novel chitosan/montmorillonite/hydroxyapatite nanocomposite for bone tissue engineering. *Biomed. Mater.* **3,** 034122 (2008).

215. Kirk, K. Membrane Transport in the Malaria-Infected Erythrocyte. **81,** 495–537 (2001).

216. Greenwood, B. M. *et al.* Malaria: progress, perils, and prospects for eradication. *J. Clin. Invest.* **118,** 1266–1276 (2008).

217. White, N. J. *et al.* Malaria. *Lancet* **383,** 723–735 (2014).

218. Paaijmans, K. & Fernàndez-Busquets, X. Antimalarial drug delivery to the mosquito: an option worth exploring? *Future Microbiol.* **9,** 579–582 (2014).

219. Fried, M., Nosten, F., Brockman, A., Brabin, B. J. & Duffy, P. E. Maternal antibodies block malaria. *Nature* **395,** 851–852 (1998).

220. Ferruti P, Casini G, Tempesti F, Barbucci R, Mastacchi R, S. M. Heparinizable materials (III). Heparin retention power of a poly(amido-amine) either as crosslinked resin, or surface-grafted on PVC. *Biomaterials* **5,** 234–236 (1984).

221. WHO. *Antimalarial drug combination therapy.* (2001).

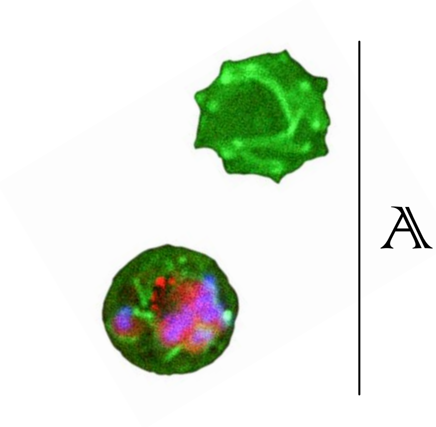

ACKNOWLEDGEMENTS

ACKNOWLEDGEMENTS

“One man may hit the mark, another blunder; but heed not these distinctions. Only from the alliance of the one, working with and through the other, are great things born.” - Antoine de Saint-Exupéry

Porque eu não seria nada nem ninguém sem a minha família da qual tanto me orgulho, um **muito obrigada** a todos. À minha **mãe**, o meu grande amor, a minha ídola, que me demonstra o verdadeiro valor da dedicação incondicional, a importância do aprender e de trabalharmos com toda a alma e coração; obrigada mãe por TUDO (que é imenso), por estar sempre comigo, por acreditar que sou sempre a melhor e por fazer-me sentir tão única! Ao meu **pai**, o menino dos meus olhos, o meu chão, a minha força, que me ensina a amar quem sou e tudo aquilo que faço; obrigada pai por estar sempre a meu lado não obstante a distância física e por compreender-me como se fôssemos um só! À minha **avó**, a minha mãe do coração, o meu exemplo de garra e de luta, a minha fiel defensora; jamais conseguirei dizer a palavra obrigada tantas vezes como as que mereces avó, infinitamente tua fã e admiradora. À minha **irmã**, a minha companheira, a minha mais-que-tudo, que me apoia sempre e me aconselha; obrigada Xuki por tudo o que vivemos sempre intensamente e por quem somos juntas! Ao meu **irmão**, o génio da família, o meu génio, o meu exemplo; obrigada Mike por estares sempre atento e protector mesmo quando nem dou por ela e por enriqueceres a nossa equipe com duas pessoas pelas quais sempre estarei agradecida e às quais também dedico um enorme obrigada, **Sofia** e o nosso bebé **Joãozinho**! *Last but not least*, à minha irmã do coração, **Carolina**, a minha alma-gémea, a minha professora, o meu guru; obrigada por seres quem és, por viveres as minhas batalhas e as minhas alegrias como se fossem tuas (porque o são) e por nunca, mas mesmo nunca, me faltares!

Porque para mí los NANO siempre ocuparán un lugar muy especial en mi corazón y porque sin vosotros jamás hubiese sido posible realizar esta tesis, **muchas gracias**! A ti, **Xavi**, gracias por confiar en mí y regalarme esta inolvidable oportunidad; fue un enorme reto de mi vida profesional y personal del que me

llevaré para siempre toneladas de aprendizaje y bonitas memorias. Mil gracias **Ernest**, mi hermano extranjero, por oírme, por ayudarme tantas y tantas veces, por ser mi gran apoyo en el laboratorio y por hacerme crecer profesionalmente! Gracias **Miriam** por siempre estar de mi lado y a mí lado, por entenderme, por escucharme y por tantos momentos de complicidad, amistad y apoyo. Muchas gracias por todo el conocimiento que habéis compartido conmigo **Juanjo** y **Patricia.** Y, por fin, gracias a los "pequeños gigantes" del grupo, **Cinta**, **Eli** y **Arnau.**

Porque aunque esté lejos de mi reino, me hacéis sentir en casa y me devolvisteis la alegría de tener un hogar, siempre os lo agradeceré con todo mi amor, **gracias**! *Grazie* **Eleonora** por ser mí maestra, por enseñarme el gusto por la investigación, por acogerme de brazos abiertos donde sea que estés y por miles de sonrisas, risas, birras, viajes y festivales (...) que compartimos! *Obrigada* a mis niñas, **Miriam**, **Marta** y **Ana** por tantos eventos juntas, por tantas experiencias, por tantos quilómetros y por todos los momentos gloriosos y peculiares; no los olvidaré jamás y me llevo un tatuaje vuestro en el corazón! *Moltes gràcies* a mi **Silveta** que siempre está dispuesta a ayudarme, a buscar solución para todo, a endulzarme con chocolate y a (en)cantarme; eres sin duda una de las personas *més boniques* que conozco! Muchas gracias **Sofia** por tantas confidencias entre muchas risas y unos cuantos brindis, por ser tan sincera y tan loca; tú sí que tienes una sonrisa preciosa! Gracias **Aida** por todo, por siempre "abrir la puerta para ver salir el sol" y porque siempre tienes una *vibe* tan positiva para compartir con los demás! Um super obrigada **Armando** por teres chegado de braços abertos pronto a acolher todos no teu eu e por teres contribuído tanto para a união no laboratório!

Porque hacéis que el trabajo y todos los experimentos se vuelvan más leves y alegres, **muchas gracias** a todos; me siento muy afortunada de haber formado parte de la **Planta 1**. Gracias por soportar mi mal humor y/o mis risas de elevados decibeles especialmente a los grupos más cercanos: **Vivax** & **Glyco**! Gracias también al gran motor de la planta **Cristina Canaleta**, la jefa!

Because thanks to you my time in London was absolutely unforgettable in professional matters and also personally; **thank you Professor Robert Sinden** for the opportunity and all the great discussions. **Many thanks** to **Michael** and **Ursula** for all the technical and experimental support and for your patience; I learnt so much with you! **Thanks** to **XARXA Eurolife** from UB for funding this project.

Porque algunos experimentos parecen auténticas batallas, **muchas gracias** a todas las personas de los **Centros Científicos y Tecnológicos de la UB** que me ayudaron a cumplir estos pequeños grandes retos.

Porque llegar a casa es siempre un placer y habéis transformado el piso en un lugar donde me siento tan bien acogida, **mil gracias Silvia y Isabel**; por todas las notas de apoyo, por escuchar mis desahogos, por tantos mimos y por compartir conmigo mis alegrías!

Porque é também graças a vocês que me sinto tão bem no Porto, como se nunca tivesse estado ausente, como se fosse parte do vosso dia-a-dia *always*, **obrigada Marta**, **Maria**, **Carlota**, **João**, **António**, **Marta Maria**; há sempre e para sempre um pedacinho de mim com vocês e um pedacinho de vocês comigo! Adoro-vos milhões.

Porque és um enorme motivo para sorrir *nonstop* e o “de repente” mais afortunado de sempre, um **super obrigada Guilherme**; “você me apareceu e fez o nada virar tudo”.

Muito obrigada!